Department of Biotechnology

Graduate School for Health and Life Sciences

Doctoral Program in Molecular, Industrial and Environmental Biotechnology

Cycle XXXI – Year 2018

Functional analysis of *AtZIP4*, *AtZIP6* and *AtZIP9* metal transporters of *Arabidopsis thaliana.*

and

Expression of *Saccharomyces cerevisiae* ZRC1 in different plant species.

S.S.D. AGR/07

Coordinator: Prof. Matteo Ballottari

Tutor: Prof.ssa Antonella Furini

Doctoral Student: Dott. Flavio Martini

CONTENTS

CONTENTS II

ABSTRACT V

Chapter 1: Functional analysis of *AtZIP4*, *AtZIP6* and *AtZIP9* metal transporters of *Arabidopsis thaliana.* V

Chapter 2: Expression of *Saccharomyces cerevisiae* ZRC1 in different plant species. VI

SOMMARIO VIII

Capitolo 1: Analisi funzionale di tre trasportatori di metalli di *Arabidopsis thaliana*: *AtZIP4*, *AtZIP6* and *AtZIP9*. VIII

Capitolo 2: Espressione del trasportatore ZRC1, derivato da *Saccharomyces cerevisiae,* in diverse specie vegetali. IX

List of abbreviations: XII

Chapter 1: 1

Functional analysis of *AtZIP4*, *AtZIP6* and *AtZIP9* metal transporters of *Arabidopsis thaliana.* 1

1. INTRODUCTION 2

1.1ESSENTIAL ELEMENTS AND THE MECHANISMS OF NUTRIENT UPTAKE: 2

1.2 METALS AS ESSENTIAL AND NON-ESSENTIAL ELEMENTS: 3

1.2.1 Fe: 4

1.2.2 Mn: 5

1.2.3 Zn: 6

1.3 METALLOPHYTE AND HYPERACCUMULATOR PLANTS: 6

1.4 METAL TRANSPORTERS: 8

1.4.1 CDF transporters: 8

1.4.2 HMA transporters: 9

1.4.3 NRAMP transporters: 10

1.4.4 CAX transporters: 10

1.4.5 YSL transporters: 11

1.4.6 COPT transporters: 12

1.4.7 CCC1 trasporters: 12

1.4.8 IREG transporters: 13

1.4.9 ABC transporters: 13

1.4.10 ZIP FAMILY: 14

1.5 *AtZIP4*, *AtZIP6* and *AtZIP9*: 18

1.6 ZIP GENES IN VARIOUS PLANT SPECIES: 20

1.7 METAL TRANSPORT MECHANISMS: 22

2. AIM OF THE WORK 25

3. MATERIALS AND METHODS 27

3.1 PLANT MATERIAL AND GROWTH CONDITIONS: 27

3.2 GENOMIC DNA EXTRACTION: 27

3.3 RNA EXTRACTION AND cDNA SYNTHESIS: 27

3.4 PCR (POLYMERASE CHAIN REACTION): 28

3.5 REAL TIME PCR: 28

3.6 SINGLE DOUBLE AND TRIPLE KNOCK-OUT MUTANTS: 28
3.7 PHENOTYPIC CHARACTERIZATION OF SINGLE KNOCK-OUT MUTANTS: 29
3.8 ANALYSIS OF METAL CONTENT: 30
3.9 LOCALIZATION OF *AtZIP4*, *AtZIP6* AND *AtZIP9* EXPRESSION THROUGH HISTOCHEMICAL GUS ASSAY: 30
3.10 TRANSFORMATION OF *A. thaliana* BY FLORAL DIPPING: 31
3.11 GUS HISTOCHEMICAL ASSAY: 31
3.12 PREPARATION OF THE CONSTRUCTS FOR THE SUBCELLULAR LOCALIZATION OF *AtZIP4*, *AtZIP6* AND *AtZIP9*: 32
3.13 PROTOPLAST ISOLATION AND TRANSFECTION WITH THE CONSTRUCTS FOR THE SUBCELLULAR LOCALIZATION OF *AtZIP4*, *AtZIP6* AND *AtZIP9*: 32
3.14 YEAST TRANSFORMATION AND COMPLEMENTATION: 34
3.15 LOCALIZATION OF *AtZIP4*, *AtZIP6* AND *AtZIP9* EXPRESSION THROUGH GFP REPORTER LINES: 35
3.16 *AtZIP4*, *AtZIP6* AND *AtZIP9* OVEREXPRESSING LINES AND THEIR PHENOTYPIC CHARACTERIZATION: 36
3.17 STATISTICAL ANALYSIS: 37
3.18 ZINPYR-1 STAINING: 37
3.19 CRYO-SECTIONING AND X-RAY SPECTROMICROSCOPY: 37

4. RESULTS AND DISCUSSION 39
4.1 STUDY OF *AtZIP4*, *AtZIP6* AND *AtZIP9* EXPRESSION: 39
4.2 SINGLE *AtZIP4*, *AtZIP6* AND *AtZIP9* KNOCK-OUT MUTANTS: 41
4.3 PHENOTYPIC ANALYSIS of *AtZIP4*, *AtZIP6* AND *AtZIP9* SINGLE KNOCK-OUT MUTANTS: 43
4.4 *AtZIP4*, *AtZIP6* AND *AtZIP9* OVER-EXPRESSING LINES: 49
4.5 DOUBLE AND TRIPLE KNOCK-OUT MUTANTS: 55
4.6 ANALYSIS OF METAL CONTENT: 56
4.7 TISSUE LOCALIZATION of *AtZIP4*, *AtZIP6* AND *AtZIP9*: 61
4.8 SUBCELLULAR LOCALIZATION of *AtZIP4*, *AtZIP6* AND *AtZIP9*: 67
4.9 COMPLEMENTATION OF YEAST METAL UPTAKE MUTANTS: 69
4.10 Zinpyr-1 STAINING: 72
4.11 TwinMic X-Ray SPECTROMICROSCOPE: 75

5. CONCLUSIONS 78

6. SUPPLEMENTARY DATA 83

7. REFERENCES 94

Chapter 2: 106

Expression of *Saccharomyces cerevisiae* ZRC1 in different plant species. 106

1. INTRODUCTION 107
1.1 BIOFORTIFICATION AND PHYTOREMEDIATION: 107
1.1.1BIOFORTIFICATION: 107
1.1.2 PHYTOREMEDIATION: 108
1.2 TRANSGENIC POPLAR PLANTS AND PHYTOREMEDIATION: 109
1.3 THE ZINC HOMEOSTASIS IN *Saccharomyces cerevisiae*: 111

3. AIM OF THE WORK 113

3. MATERIALS AND METHODS 114
3.1 PLANT MATERIAL AND GROWTH CONDITIONS: 114
3.2 AMPLIFICATION OF *ScZRC1* AND THE PROMOTER OF THE SMALL SUBUNIT OF RUBISCO (prbcS): 114

3.3 POPLAR TRANSFORMATION: 115
3.4 EVALUATION OF TRANSGENIC LINES: 115
3.5 ANALYSIS OF METALS CONTENT: 115
3.7 SUBCELLULAR LOCALIZATION OF *ScZRC1* IN *A. thaliana* PROTOPLASTS: 116
3.8 STATISTICAL ANALYSIS: 116

4. RESULTS AND DISCUSSION 117
4.1 AMPLIFICATION of *ScZRC1* AND THE PROMOTER OF THE SMALL SUBUNIT OF RUBISCO: 117
4.2 SUBCELLULAR LOCALIZATION OF *ScZRC1* IN *A. thaliana* PROTOPLAST: 119
4.3 TRANSGENIC *ScZRC1 A. thaliana* LINES: 120
4.4 ACCUMULATION ANALYSIS ON *ScZRC1* TRANSGENIC *A. thaliana* LINES: 120
4.5 TRANSGENIC *ScZRC1* POPLAR LINES AND ACCUMULATION ANALYSIS: 122

5. CONCLUSIONS 127

6. REFERENCES 129

AKNOWLEDGEMENTS: 133

ABSTRACT

Chapter 1: Functional analysis of *AtZIP4*, *AtZIP6* and *AtZIP9* metal transporters of *Arabidopsis thaliana.*

Plants have developed a variety of adaptive strategies to take up sufficient quantities of essential macro- and micro-nutrients and avoid their excessive accumulation, which could be toxic. Furthermore, plants have to deal with non-essential elements that may be potentially harmful. Metal transporters play an essential role in this homeostatic network by controlling the metal efflux across cellular membranes and compartments. The ZIP (ZRT IRT1-like Proteins: Zinc-regulated transporter Iron-regulated transporter 1-like protein) family of metal transporter is involved in this complex network. Fifteen members of the ZIP family have been identified in *A. thaliana,* which can be clustered into four main groups that share a 38 to 85% sequence similarity (Maser *et al.,* 2001). This project focuses on three ZIP-family members: *AtZIP4*, *AtZIP6* and *AtZIP9,* for which very little information is available. *AtZIP4* has been partly investigated (Assunção *et al.,* 2010), with Lin *et al.* (2016) performing the analysis of its promoter. *AtZIP4* and *AtZIP9* share a 77% similarity at amino acid sequence level, and both are up-regulated upon Zn-deficiency in roots and shoots. On the other hand, the expression of *AtZIP6*, which is not included in any of the four groups mentioned previously, does not appear to be modulated by variations in either Zn or Fe concentrations (Wintz *et al.,* 2003).

The characterization of these three genes was investigated by a variety of approaches. At first, single *AtZIP4, AtZIP6* and *AtZIP9* knockout mutants were taken into consideration, testing the effect of various Zn, Fe and Mn concentrations on their growth, and coupling excess Zn with Fe deficiency or vice versa. The primary root length of the single *zip4.1* knockout mutant was significantly reduced only under conditions of excess Fe, whereas the single *zip9.1* knockout mutant displayed shorter roots at high and low concentrations of both Zn and Fe. On the other hand, the knockout mutant for *AtZIP6* seemed to grow better in excess of Zn. To investigate the possibility of a functional redundancy between these genes, double *zip4/zip6*, *zip4/zip9*, *zip6/zip9* mutants, as well as triple *zip4/zip6/zip9* mutants were obtained by traditional crossing procedures, and their ionomic profile was analyzed in comparison to that of wild-types and single knock-out mutants. The plants' ionome was investigated during my stay at the University of Nottingham under the supervision of Prof. David Salt, and revealed a reduced Zn accumulation in the shoots of double *zip4/zip6, zip6/zip9* and triple *zip4/zip6/zip9* knockout mutants, as compared to the wild-types, under conditions of excess Zn. The ionome profile also showed differences in Fe, S and P accumulation

among the mutant lines. Moreover, constructs were prepared for plant transformation harboring the strong promoter CaMV35S fused upstream the coding sequence of the three genes, and upon introduction into *A. thaliana,* produced various over-expressing lines that were phenotypically tested under different Zn and Fe conditions. The analysis of subcellular protein localization was performed on protoplasts transfected with fusion proteins of each transporter and the eGFP marker protein, and revealed that ZIP4 and ZIP9 were located at the plasma membrane and tonoplast, respectively. ZIP6 localization was not as clear, so we performed a co-localization analysis with different membrane reporters to confirm ZIP4 and ZIP9 and better investigate the ZIP6 localization. To promote correct eGFP folding we removed the last transmembrane domain of each transporter because its fusion on the N- and C- terminus of the complete coding sequence did not give any result. We were subsequently able to identify the tissue-specific localization using transgenic plants harboring each ZIP promoter controlling the GUS marker gene. GUS localization was analyzed both in plants cultured under standard conditions and in ones subjected to various metal treatments. The expression pattern of *AtZIP6* and *AtZIP9* revealed a different tissue localization at root level. *AtZIP9* expression is localized in the endodermis, cortex and epidermis, while *AtZIP6* only in the vascular tissues of the roots. The tissue localization of ZIP4 was previously observed in the root stele and endodermis, as reported by Lin *et al.* (2016). The Zn distribution in the single *zip4.1, zip6.1*, *zip9.1*, double *zip4/zip6, zip4/zip9, zip6/zip9* and the triple *zip4/zip6/zip9* knockout mutant roots was tested using Zinpyr-1, a Zn-specific fluorescent probe, as described by Sinclair *et al.* (2007), to clarify whether the absence of these transporters affects the localization of Zn. Given the need for an alternative technique, independent of a fluorescent and diffusing mobile dye, we applied for the use of the TwinMic X-ray spectromicroscope at the synchrotron of Trieste with the kind collaboration of Dr. Alessandra Gianoncelli to analyze root cross-sections of the single, double and triple knockout mutants prepared at the University of Ljubljana under the supervision of Prof. Katarina Vogel Mikus.

Chapter 2: Expression of *Saccharomyces cerevisiae* ZRC1 in different plant species.

In recent decades, the biosphere has been affected by anthropic activities that have raised the levels of toxic elements (Gisbert *et al.,* 2003). Of particular concern are trace elements, especially those referred to as heavy metal(loid)s such as As, Hg, Pb, Cd and Zn, which can be taken up by plants and can be toxic for all the organisms that are part of the food chain. Throughout time, plants have evolved specific strategies to survive on contaminated soils, and thanks to this, they can be exploited for the remediation of polluted soils. This emerging approach, known as

phytoremediation, improves the biological and physical aspects of the environment, is non-invasive and cheaper than other strategies (Pilon-Smith, 2005). The ability to tolerate and accumulate high levels of toxic elements in their tissues above ground level is one of the key aspects that characterize the ideal plant; other important factors are great biomass production and rapid growth (Kärenlampi *et al.*, 2000). Hyperaccumulator plants absorb large amounts of heavy metals from the soil, storing them in the aerial parts (Brown *et al.,* 1995). Although given their reduced biomass, hyperaccumulator plants are not ideal for phytoremediation (Kärenlampi *et al.*, 2000), the mechanisms that are involved in the hyper-accumulator trait are essential to improve more appropriate plant species. Poplar has been suggested as an excellent candidate for phytoremediation (Dix *et al.,* 1997) since it possesses an extended root system, produces large amounts of biomass, grows rapidly, and can be easily transformed and propagated (Confalonieri *et al.,* 2003). The exogenous introduction of yeast transporters into the poplar background could improve the plant's ability to accumulate heavy metals; indeed, transgenic poplars harboring the *Saccharomyces cerevisiae* vacuolar Cd transporter *ScYCF1* accumulated more Cd than the wild-type (Shim *et al.,* 2013). In this work, ZRC1 was selected as the candidate gene to improve metal accumulation and tolerance in model plant species since it induces Zn/Cd resistance in *S. cerevisiae.* Furthermore, *ScZRC1* is a vacuolar transporter that mediates the detoxification of excess Zn by storing it into the vacuole (MacDiarmid *et al.,* 2003); it belongs to the CDF transporter family and is believed to play a putative role in Cd detoxification. The coding sequence of *ScZRC1* was amplified from *S. cerevisiae* genome and cloned into two distinct expression vectors: 1) under the control of the CaMV35S constitutive promoter and 2) upstream of the light inducible Rubisco promoter (*prbcS*), so as to drive the accumulation of this metal across the entire plant and only in the shoots, respectively. These constructs were used for plant transformation, and several *Arabidopsis* and *Populus alba* (cv. Villafranca) *p35S::ScZRC1* and *prbcS::ZRC1* transgenic lines were thus obtained. Zn and Fe accumulation in *Arabidopsis* and poplar transgenic lines for both constructs were tested in hydroponics at different Zn concentration, and the results revealed that their shoots contained more Zn than those of the wild-types. Moreover, in order to clarify whether in these plants the heterologous ZRC1 was localized at the tonoplast, reporter lines were obtained by fusing the eGFP protein at the C- terminus of ZRC1. The subcellular localization of *ScZRC1::eGFP* protein was thus tested on *Arabidopsis* protoplasts, and the results confirmed the localization across the vacuole membrane.

SOMMARIO

Capitolo 1: Analisi funzionale di tre trasportatori di metalli di *Arabidopsis thaliana*: *AtZIP4*, *AtZIP6* and *AtZIP9.*

Le piante superiori hanno sviluppato diverse strategie per assorbire sufficienti quantità di macro- e micro- nutrienti regolandone il trasporto (Williams and Salt, 2009), evitando così un eccessivo accumulo di elementi non essenziali come As, Cd, Pb, Hg e Cr che potrebbero risultare tossici. La famiglia dei trasportatori ZIP (ZRT IRT1-like Proteins) rappresenta una delle principali famiglie coinvolte nella regolazione di questo complesso flusso di ioni metallici. Quindici membri appartenenti a questa famiglia sono stati individuati in *A. thaliana*. Questi trasportatori sono stati suddivisi in quattro gruppi attraverso una analisi filogenetica condotta da Maser *et al.,* (2001), che ha inoltre evidenziato una similarità tra le diverse sequenze che spazia tra il 38 e 85%. Durante il mio progetto di dottorato mi sono quindi interessato a 3 membri di questa famiglia di trasportatori: *AtZIP4*, *AtZIP6* and *AtZIP9*. Il trasportatore *AtZIP4* è stato in parte studiato da Assunção *et al.,* (2010), mentre lo studio del suo promotore è stato condotto da Lin et al., nel 2016. *AtZIP4* e *AtZIP9* presentano una similarità di sequenza amminoacidica del 77% e l'espressione di questi geni viene indotta in condizioni di carenza di Zn sia nelle radici che nelle foglie. *AtZIP6* non rientra nei quattro gruppi filogenetici descritti d Maser *et al.,* (2001), inoltre non presenta nessuna modulazione di espressione a diverse concentrazioni di Zn e Fe (Wintz *et al.,* 2003). Lo studio della funzione di questi tre geni è stata condotta utilizzando diverse strategie. Inizialmente sono stati ottenuti dei singoli mutanti inserzionali per *AtZIP4, AtZIP6* and *AtZIP9* che sono stati fatti crescere a diverse concentrazioni di Zn, Fe e Mn, accoppiando anche un eccesso di Zn con una carenza di Fe e viceversa, per analizzare variazioni della crescita rispetto al controllo. La lunghezza della radice primaria del mutante *zip4* risulta essere più corta in condizioni di eccesso di Fe mentre quella del mutante *zip9* viene ridotta in condizioni di eccesso e carenza di Zn e Fe. Il mutante inserzionale di *AtZIP6* presenta invece una crescita migliore in eccesso di Zn. Abbiamo inoltre ottenuto dei doppi mutanti *zip4/zip6*, *zip4/zip9*, *zip6/zip9,* e un triplo mutante *zip4/zip6/zip9* tramite incrocio per investigare la presenza di una possibile funzione complementare tra questi trasportatori. L'accumulo di metalli di queste linee mutanti è stato analizzato a diverse concentrazioni di Zn durante il mio periodo di internazionalizzazione presso l'università di Nottingham, sotto la supervisione del Professor David Salt. I doppi mutanti *zip4/zip6, zip6/zip9* e il triplo mutante *zip4/zip6/zip9* presentano un ridotto contenuto di Zn rispetto alle altre linee in condizioni di eccesso di Zn. Il profilo ionomico presenta inoltre delle differenze di accumulo di Fe, S e P tra le diverse

linee. Un'altra strategia utilizzata per lo studio di questi trasportatori prevede l'induzione costitutiva dell'espressione di questi tre trasportatori attraverso l'utilizzo del promotore CaMV35S ottenendo quindi delle linee sovra- esprimenti che sono state testate a diverse concentrazioni di Zn e Fe. Determinare la localizzazione subcellulare di questi trasportatori è essenziale per conoscere la loro funzione. Sono stati quindi creati dei costrutti reporter fondendo una proteina fluorescente (eGFP) all'estremità C-terminale dei tre diversi trasportatori per determinarne la localizzazione tramite la trasfezione di protoplasti di Arabidopsis. ZIP4 sembra localizzato a livello della membrana plasmatica e ZIP9 nel tonoplasto mentre la localizzazione di ZIP6 non risulta ancora chiara, quindi per investigare nel dettaglio la localizzazione di ZIP6 e confermare gli altri due trasportatori abbiamo condotto un esperimento di co-localizzazione con alcuni marcatori delle membrane cellulari. Successivamente, l'espressione e l'attività dei promotori sono state investigate fondendo le sequenze promotrici con il gene reporter GUS. A livello della radice *AtZIP6* e *AtZIP9* vengono espressi in tessuti differenti: *AtZIP6* principalmente nei fasci vascolari della radice mentre *AtZIP9* nell'epidermide, nella corteccia e nell'endodermide. La localizzazione tissutale del gene *AtZIP4* all'interno del periciclo e dell'endodermide è stata precedentemente determinata (Lin *et al.,* 2016). La localizzazione dello Zn nei singoli mutanti *zip4, zip6*, *zip9*, nei doppi mutanti *zip4/zip6, zip4/zip9, zip6/zip9* e nel triplo mutante *zip4/zip6/zip9* è stata inoltre analizzata attraverso l'utilizzo dello Zinpyr-1, una sonda fluorescente che si lega specificatamente allo Zn intra-cellulare, seguendo il protocollo fornito da Sinclair *et al.,* (2007). Per analizzare quindi la distribuzione dello Zn all'interno della radice attraverso una tecnica alternativa alle sonde fluorescenti, abbiamo scritto un progetto per l'utilizzo della spettromicroscopia ai raggi-X, in collaborazione con la Dott.ssa Alessandra Gianoncelli del Sincrotrone di Trieste e con la Prof.ssa Katarina Vogel Mikus dell'università di Lubiana.

Capitolo 2: Espressione del trasportatore ZRC1, derivato da *Saccharomyces cerevisiae,* in diverse specie vegetali.

Negli ultimi decenni, le attività antropiche hanno innalzato eccessivamente i livelli di elementi inorganici tossici nella biosfera (Gisbert *et al.,* 2003). La preoccupazione maggiore risiede in quei metalli come As, Hg, Pb, Zn e metalloidi come il Cd che risultano molto persistenti nel terreno e possono quindi essere assorbiti in grandi quantità dalle piante ed entrare facilmente nella catena alimentare. Le piante superiori durante l'evoluzione hanno sviluppato diverse strategie per l'accumulo di grandi quantità di metalli pesanti, suggerendo la possibilità di utilizzarle per la

bonifica di terreni contaminati come una strategia emergente conosciuta come fitobonifica. Questo approccio migliora notevolmente l'aspetto fisico e biologico dell'ambiente risultando non invasivo e meno costoso di altre metodologie (Pilon-Smith, 2005). L'abilità di una pianta di accumulare grandi quantità di metalli nella parte epigea è una caratteristica fondamentale che identifica le specie ideali per il fitorimedio, accoppiata alla capacità di crescere velocemente producendo una estesa biomassa (Kärenlampi *et al.*, 2000). Le specie iper-accumulatrici possiedono la capacità di assorbire alti livelli di metalli e di immagazzinarli nei germogli, raggiungendo quantità tali da risultare tossiche per altre specie vegetali (Brown *et al.,* 1995). Queste piante spesso non vengono considerate dei modelli ideali per la fitobonifica perché sono di solito di piccole dimensioni e non possiedono la capacità di produrre una grande quantità di biomassa (Kärenlampi *et al.*, 2000) ma i meccanismi genetici che determinano il tratto di iper-accumulo possono essere utilizzati per migliorare piante più adatte al fitorimedio. Il pioppo (*Populus alba*) viene considerato una eccellente specie vegetale ideale per la fitobonifica (Dix *et al.,* 1997), infatti produce un sistema radicale molto esteso ed approfondito, un fusto e un apparato vegetativo considerevole, cresce velocemente, e può essere inoltre ingegnerizzato e propagato facilmente *in vitro* (Confalonieri *et al.,* 2003). La modificazione e l'introduzione nel suo genoma di trasportatori esogeni di lievito, può notevolmente migliorare la capacità di questa specie di accumulare metalli non essenziali. Shim *et al.,* (2013) hanno dimostrato per esempio che introducendo il trasportatore *ScYCF1* di *Saccharomyces cerevisiae* veniva indotto un maggiore accumulo di Cd nelle linee di pioppo transgeniche rispetto al controllo. In questo progetto di dottorato è stato ingegnerizzato *Populus alba* (cv. Villafranca) e come specie modello *Arabidopsis*, introducendo il trasportatore ZRC1, un trasportatore vacuolare di lievito (MacDiarmid et al., 2003) appartenente alla famiglia di trasportatori CDF, coinvolto nel trasporto dello Zn con un possibile ruolo putativo anche nel trasporto del Cd. La sequenza codificante di *ScZRC1* è stata amplificata dal genoma di lievito e clonata in due diversi vettori di espressione: 1) controllata dal promotore costitutivo CaMV35S e 2) controllata dal promotore luce-inducibile della piccola sub-unità della Rubisco (*prbcS*) per indurre l'espressione in tutta la pianta nel primo caso o solo nella parte aerea con il secondo costrutto. Questi vettori sono stati utilizzati per la trasformazione di *Arabidopsis* e *Populus alba* (cv. Villafranca) ottenendo diverse linee transgeniche per i geni *p35S::ScZRC1* e *prbcS::ZRC1*. L'accumulo di Zn e Fe delle linee transgeniche di *Arabidopsis* e pioppo è stato analizzato preparando delle idroponiche a diverse concentrazioni di Zn. Per essere certi che l'espressione eterologa di questo trasportatore di lievito in pianta mantenesse la localizzazione a livello del tonoplasto abbiamo preparato un costrutto reporter fondendo una proteina fluorescente al C-terminale della sua sequenza codificante. La localizzazione sub-cellulare della proteina

ScZRC1::eGFP è stata quindi testata su protoplasti di *Arabidopsis* confermando la localizzazione nella membrana vacuolare.

List of abbreviations:

35S CaMV	35S Cauliflower Mosaic Virus promoter
ANOVA	Analysis of variance
bp	Base pairs
CaCa	Ca2+/Cation Antiporter
CAX	Cation exchanger
CDF	Cation diffusion facilitator
cDNA	complementary deoxyribonucleic acid
DNA	deoxyribonucleic acid
DTT	dithiothreitole
EDTA	Ethylenediamine tetraacetic acid
GFP	green fluorescent protein
GSH	glutathione
GST	glutathione-S-transferase
GUS	β-glucuronidase
HMA	Heavy Metal P-type ATPase
hyg	hygromycin
IRT	Iron Regulated Transporter
IPTG	isopropyl-β-D-1-thiogalactopyranoside
Kan	kanamycin
kb	kilobase
IAA	indole-3-acetic acid
LB	left border
MRE	Metal Response Element
MS	Murashige and Skoog
MT	metallothionein
MTP	Metal Tolerance Protein
NA	nicotianamine
NAS	nicotianamine synthase
NRAMP	Natural Resistance-Associated Macrophage Protein
ORF	open reading frame
PC	phytochelatin
PCI	phenol:chloroform:isoamyl alcohol
PCR	Polymerase Chain Reaction

PCS	phytochelatin synthase
PI	Propidium iodide
RB	Right border
RNA	ribonucleic acid
RNAi	RNA interference
ROS	reactive oxygen species
rpm	rotation per minute
RT	reverse transcription
RE	endoplasmic reticulum
SDS	sodium dodecyl sulphate
Ta	annealing temperature
TAE	Tris-acetate-EDTA
TAIR	The Arabidopsis Information Resource
TF	transcription factor
Tm	melting temperature
TMD	trans-membrane domain
UTR	untraslated region
wt	wild type
X-Gal	5-bromo-4-chloro-3-indolyl-β-D-galactopyranoside
X-Gluc	5-bromo-4-chloro-3-indolyl-β-D-glucuronic acid
YEB	Yeast Extract Broth
YSL	Yellow Stripe-like protein
ZIP	ZRT, IRT-like protein
ZRT	Zinc Regulated Transporter

Chapter 1:

Functional analysis of *AtZIP4*, *AtZIP6* and *AtZIP9* metal transporters of *Arabidopsis thaliana*.

1. INTRODUCTION

1.1ESSENTIAL ELEMENTS AND THE MECHANISMS OF NUTRIENT UPTAKE:

All organisms need essential elements for their growth and development (Epstein, 1972). The root system plays a key role in the uptake and distribution of these elements across the entire plant, regulating their homeostasis among the various tissues and their transport into the vascular tissues. Seventeen essential elements can be grouped into macronutrients (C, H, O, N, P, K, S, Ca, Mg), required in large amounts, and micronutrients (Cu, Fe, Mn, Zn, B, Mo, Cl, Ni), which are only required in traces (Epstein, 1972). Terrestrial plants take up O, H and C mainly from air, and water, carbon dioxide and all the other nutrients they need from the soil (Epstein, 1972). Insufficient amounts of any of these essential elements can hinder plant growth and development, and may also impact its yield and productivity. Soil is a heterogeneous material, mainly composed of solid, liquid and gaseous phases that influence nutrient availability and their transport towards the roots (Mengel *el al.,* 2001). The solid phase is the main source of essential elements such as Na, Mg, K, Fe, Mn, Ca, Zn, and Cu, and its organic fraction is the main source of N, which reaches the soil dissolved in raindrops, and is then fixed by N_2-fixing bacteria; it is also the key source of S and P (Mengel *el al.,* 2001). The liquid phase plays a fundamental role in the transport of these nutrients (Mengel *el al.,* 2001). Only a small amount of nutrients is present as free molecules and is directly available for uptake: most trace elements are bound to the solid soil fraction in various ways, forming complexes with the organic matter, hydrated oxides, carbonates, etc. (Kabata-Pendias and Pendias, 1984). Their availability depends on several soil properties, i.e. pH, mineral composition, redox potential, aeration, structure, texture, water status, and microbial activity (Epstein, 1972).

Plants have evolved a variety of mechanisms to improve the bioavailability of essential elements and overcome the risk of nutrient deficiency, inducing changes in the soil composition, promoting the growth of other organisms and producing chelating agents to increase nutrient availability (Robinson *et al.,* 2006). Roots are an essential plant organ that plays a key role in many processes, ranging from water and nutrient uptake to providing mechanical support for plants (Smith and De Smet, 2012). They have storage functions and interact symbiotically with bacteria and fungi to improve the availability of soil minerals, and are in brief a fundamental interface between plants and the soil, considered in all its biotic and abiotic aspects (Smith and De Smet, 2012). Transport across the plasma membrane occurs through two different mechanisms: passive and active transport. Passive transport takes place when an element diffuses across a membrane according to

its concentration gradient without the need for energy, either directly by diffusion or through specific channel proteins. Active transport on the other hand requires energy to transport an element against its gradient and usually involves elements that are present in the soil solution at very low concentrations. Active transport mechanisms can in turn classified as primary and secondary ones. Primary active transport is mediated by proteins that can directly hydrolyze ATP whereas secondary transport by proteins exploiting the potential energy generated by an electrochemical gradient (Chrispeels *et al.,* 1999). The expression of different transporters is mediated by the presence or absence of a particular element and the affinity of the transporters for its substrate depends on its chemical nature. Usually, transporters can be classified as high- or low-affinity transporters depending on their affinity for their substrates. High-affinity transporters are mostly involved in the uptake of nutrients that are present at very low concentrations in the soil, often referred to as trace elements (Clemens *et al.,* 2002).

1.2 METALS AS ESSENTIAL AND NON-ESSENTIAL ELEMENTS:

A high percentage of the key nutrients is represented by metals, which are necessary for plant development and metabolism. Metals differ from nonmetallic elements for many physical properties (Appenroth, 2010). The former elements have a lustrous appearance, are malleable, ductile and can conduct heat and electricity. These features, and electrical conductivity in particular, which is temperature dependent, allow us to better categorize metals from metalloids and nonmetals (Appenroth, 2010). Metals are unavailable for plants in their elemental state but can only be taken up when they are solubilized, thanks to the interaction with other elements. From a chemical point of view, plants encounter a variety of metal ions and metalloids, which can be either essential (Cu, Fe, Mn, Zn, Ni, Mo) or non-essential (As, Cd, Pb, Hg, Cr). Usually, excess concentrations of both essential and non-essential metals, are poisonous to plants (Salt *et al.,* 1995). Metals that induce toxicity are often referred to in literature as “heavy metals” (Appenroth, 2010). Metal toxicity is concentration-dependent and various heavy metals are essential for plant cells, at low levels. There is no clear definition of what a heavy metal is in the literature, and in the past, many authors attempted to classify them on the grounds of their density, which would range from 3.5 to 7 g cm^{-3} (Duffus, 2002). Despite these limitations, the definition “heavy metals” is widely used in the scientific world, hence a better way to describe them needs to be found (Appenroth, 2010). Micronutrients play a key role in plant growth, biosynthesis of secondary metabolites and development. This research is mainly focused on transport proteins that appear to regulate the transport of three major metal micronutrients: Fe, Mn and Zn

1.2.1 Fe:

Fe is the fourth most abundant element on Earth, forming much of our planet's outer and inner core. Fe solubility is pH dependent: it is more soluble in acidic soils, but because one third of our arable land lies on calcareous soils, its availability for plant nutrition is often very low (Marschner, 1995). Fe is considered an essential element since it is involved in a wide range of cell mechanisms, such as respiration, photosynthesis and chlorophyll biosynthesis (Kobayashi and Nishizawa, 2012). Moreover, Fe is found in two redox states and the transition between them, requiring the exchange of an electron, makes it a key element in heme-complexes and sulfur clusters involved in many reactions such as nucleotide synthesis and the photosynthesis electron transport chain (Roschzttardtz *et al.,* 2013). Plants possess two different strategies for Fe acquisition: Strategy I is used by all higher nongraminaceous plants and Strategy II is specific to graminaceous plants (Figure 1.1). In Strategy I, Fe deficiency induces the expression of the AHA H^+-ATPase gene and protons are extruded into the soil reducing the pH at the rhizosphere (Morrissey and Guerinot, 2009). In *A. thaliana* AHA1, AHA2, and AHA7 are all up-regulated under low Fe conditions but AHA2 seems to be the most critical for rhizosphere acidification (Santi and Schmidt, 2009).

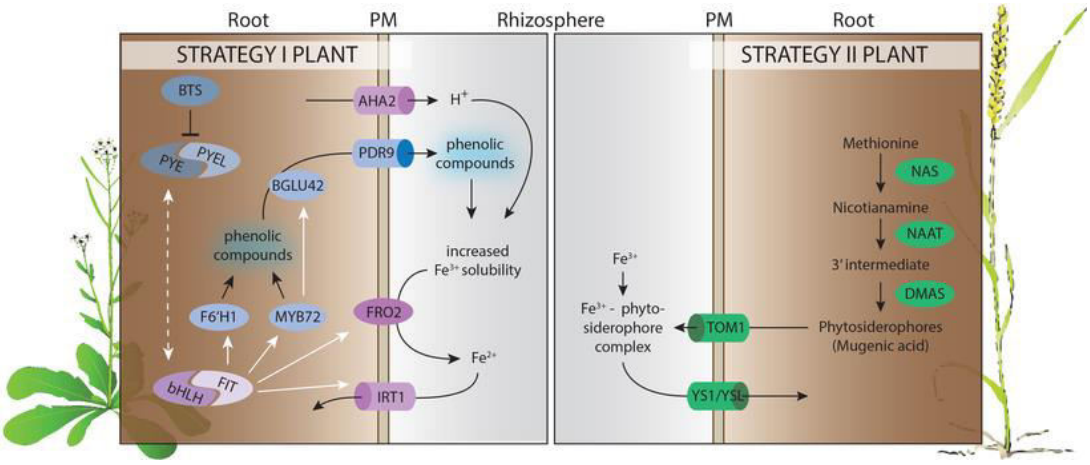

Figure 1.1: Strategies for Fe uptake from soils in nongraminaceous and graminaceous plants (from Verbon *et al.,* 2017).

A reduction in the pH enhances Fe bioavailability since the Fe (III) form is reduced to Fe(II) by the ferric chelate reductase *AtFRO2* and is subsequently transported into the root by the high affinity ZIP transporter *AtIRT1* (Henriques *et al.,* 2002; Varotto *et al.,* 2002). In Strategy II, graminaceous plants secrete phytosiderophores, a class of mugeinic acids (MAs) produced starting from L-methionine, which are capable of chelating Fe(III) (Kobayashi and Nishizawa, 2012). The Fe(III)-phytosiderophore complex is than taken up by YELLOW STRIPE 1-like (YSL) transporters, the most characterized of which is maize YS1 (Curie *et al.,* 2001). Even though Fe is a fundamental

element, its homeostasis must to be regulated to prevent the formation of reactive oxygen species (ROS), as a consequence of its redox activity in the presence of oxygen (Thomine and Lanquar, 2011).

1.2.2 Mn:

Manganese is an essential element for plant metabolism, and even though it is the second most abundant element in the Earth's crust, it is only required in trace amounts (Yang *et al.,* 2008). Its oxidation state is very crucial for its bioavailability: plants are only able to take up the divalent cation Mn^{2+} instead of its oxidized form Mn(III) and Mn(IV) found in high-pH soils or high-organic matter soils. In plants, Mn takes part in various biological functions as a cofactor or an activator interacting with numerous enzymes, such as RNA polymerases, PEP carboxykinase during gluconeogenesis, enzymes of the citric acid cycle such as isocitrate dehydrogenase and manganese superoxide dismutase (MnSOD), an essential antioxidant enzyme (Marschner, 1995). Moreover, Mn forms a fundamental complex in photosystem II for the light-driven catalytic water splitting reaction where water is oxidized to oxygen. Recently, investigations on various metal transporters have shed light on the Mn uptake pathway from the soil. IRT1, a member of ZIP transporters family, is a plasma membrane protein mainly involved in Fe uptake, although the characterization of IRT1 knockout mutants has revealed that it also plays a putative role in Mn uptake (Vert *et al.,* 2002). Cailliatte *et al.* (2010) found that *AtNRAMP1* is required for high-affinity Mn transport into the root under Mn deficiency conditions. It has been suggested that the presence in *A. thaliana* of a possible YSL-like transporter could transport a nicotianamine-Mn complex such as that observed for *OsYSL2* (Koike *et al.,* 2004). It is believed that other members of ZIP family, like *AtZIP1*, *AtZIP2*, *AtZIP5*, *AtZIP6*, *AtZIP7*, and *AtZIP9* could transport Mn through a yeast mutant complementation assay, but additional investigations are necessary (Milner *et al.,* 2013). The cation diffusion facilitator (CDF) family also includes a Mn-CDF subgroup (*AtMTP8*, *AtMTP9*, *AtMTP10* and *AtMTP11*) that seems to be involved in Mn tolerance within plant tissues (Peiter *et al.,* 2007). *AtMTP11* is the most functionally characterized member (Peiter *et al.,* 2007), though more recently a yeast complementation study was performed on the other members which revealed the key role for AtMTP8 in the distribution of Mn and Fe in seeds (Chu *et al.,* 2017).

1.2.3 Zn:

Zinc is the second most abundant transition metal present in organisms after Fe (Auld *et al.,* 2001) and the 23rd most abundant element on Earth. Zn is an essential element involved in numerous metabolic processes as a component of different proteins, and indeed, is present in all enzyme classes (oxidoreductases, lyases, hydrolases, transferases, ligases, isomerases) (Broadley *et al.,* 2007). Zn interacts with several enzymes that are involved in processes ranging from carbohydrate metabolism to the maintenance of the integrity of cell membranes, from protein synthesis to pollen formation and the regulation of auxin synthesis (Noulas *et al.,* 2018). The presence of Zn is necessary for the activity of several enzymes such as alcohol dehydrogenases, protein kinases, carbonic anhydrases, superoxide dismutases and the stability of ribosomes (Hafeez *et al.,* 2013). Enzyme activity depends on the Zn-complex binding properties but also the presence of three different Zn-binding sites: catalytic, cocatalytic and structural where Zn has a folding, catalytic and regulatory/structural function, respectively (Broadley *et al.,* 2007; Auld *et al.,* 2001). Different Zn-binding proteins possess zinc finger domains that allow the binding with DNA, RNA and proteins regulating directly the transcription, or indirectly through the regulation of chromatin (Englbrecht *et al.,* 2004). The most common oxidation state in solution is Zn^{2+}, which unlike other elements such as Fe, is stable under physiological conditions. Approximately 90% of Zn in the soil is insoluble, complexed in minerals or adsorbed by clay and humic compounds, and is therefore unavailable to plant (Broadley *et al.,* 2007). Zn bioavailability is reduced at high pH levels, in calcareous and saline soils, the particles of which act as cation exchange sites for its adsorption (Broadley *et al.,* 2007). Zn is taken up from the soil solution by means of various transporters, and once inside the symplast, it can cross the Casparian strip through the plasmodesmata, reaching the inner root cells from where they are actively transported into the xylem (Palmer and Guerinot, 2009). It can also enter into the stele apoplast when the Casparian strip is not completely formed (White *et al.,* 2002). Zn toxicity occurs especially in low-pH soils contaminated by anthropic activities such as mining and smelting processes, applications of sewage sludge, pesticides and fertilizers (Broadley *et al.,* 2007).

1.3 METALLOPHYTE AND HYPERACCUMULATOR PLANTS:

The performance of all species is optimal under ideal conditions and is influenced by the selection pressure of the surrounding environment. Metalliferous soils were a strong source of pressure leading to the selection of a variety of metal-tolerant genotypes from non-metalliferous populations (Baker *et al.,* 2010). For most plants, non-essential metals are toxic at extremely low levels but

several species exist that can tolerate the presence of heavy metals (Salt *et al.,* 1995). Plants that are able to survive in soils contaminated by high levels of toxic metals are referred as metallophytes (Baker *et al.,* 2010). Metallophytes can be classified as obligate or facultative according to whether they need or not toxic metals in the soil to survive (Baker *et al.,* 2010). Obligate metallophytes are endemic species, strictly localized in contaminated areas whereas facultative plants are usually specific ecotypes from a common species that have adapted to the presence of a specific metal but are also able to survive in uncontaminated areas. Metallophytes can also be grouped into three different categories according to the ratio between the concentration of metals in the soil and in their tissues (Baker, 1981):

1) **Accumulators** store high levels of metals in their shoots regardless of the amount present in the soil. Various species of the *Noccaea* and *Alyssum* genera possess this hyperaccumulating ability, and display an increased translocation factor between roots and shoots.
2) **Indicators** such as *Brassica napus* (Lehn and Bopp, 1987), in which there is a correlation between the amount of metal accumulated and that present in the soil.
3) **Excluders** like *Silene maritima* (Baker, 1987) have very low levels of metals in their shoots but accumulate them in large amounts in their roots.

The first example of Ni hyperaccumulation was observed in *Alyssum bertolonii,* a member of the brassicaceae family, and was described by Minguzzi and Vergnano in 1948, but already in 1865 Sachs had observed that *N. caerulescens* acts as a Zn hyperaccumulator. The term hyperaccumulators was first introduced to describe plants with levels of Ni greater than 0.1% (1.000 μg g^{-1}d.m.) of their dry weight (Brooks *et al.*, 1977); only later it was extended to other metals. The threshold level is specific for each metal, for example Mn and Zn hyperaccumulator plants are those accumulating more than 1% (10.000 μg g^{-1}) of metal on the shoots dry weight whereas in the case of Cd the threshold is of 0.01% (100 μg g^{-1}) (Baker and Walker, 1990; Baker *et al.,* 1994).

A. halleri and *Noccaea caerulescens* are two Brassicaceae species that are phylogenetically very close to *A. thaliana,* sharing a 94% and 88% nucleotide identity with its coding sequence respectively (Becher *et al.,* 2004, Assunção *et al.,* 2001). Talke *et al.* (2006) suggested that *A. halleri* diverged from *A. thaliana* about 3.5-5.8 million years ago, whereas *N. caerulescens* about 20 million years ago. The sequence conservation with *A. thaliana* has allowed the molecular characterization of these two-model plant species for metal accumulation. The transcriptomic

analysis of *A. halleri* and *Noccaea caerulescens* hyperaccumulators plants and comparison with non-accumulating species suggests various metal transporters, often present in multiple copies, as a possible answer to the hyperaccumulation trait (Talke *et al.,* 2006; Becher *et al.,* 2004; van de Mortel *et al.,* 2006; Weber *et al.,* 2004).

1.4 METAL TRANSPORTERS:

Metal transporters play a key role in the uptake, homeostasis and transport of metals across the cell membranes, and are present in every step of their long-distance translocation from roots to shoots. According to their phylogenic relationships, metal transporters can be grouped into the following families: the ZIP (ZRT IRT1-like Proteins: Zinc-regulated transporter Iron-regulated transporter 1-like proteins) gene family, the CDF (Cation Diffusion Facilitator) family, the HMA (Heavy Metals P_{1B}-type ATPases) family, the NRAMP (Naturally Resistant Associated Macrophage Proteins) family, the CAX (Cation exchanger) family, the YSL (Yellow-Stripe 1-Like) transporters that are part of the OPT (Oligoeptide Transporter) superfamily, the COPT (Copper Transporters) family, the CCC1 (Ca^{2+}-sensitive Cross Complementer 1) family, the IREG (Iron-Regulated protein) family and the ABC (ATP-binding Cassette transporter) family which among others, includes the following three subfamilies: MRP (multidrug resistance-associated proteins), ATM (ABC transporters of the mitochondria) and PDR (pleiotropic drug resistance) transporters (Krämer *et al.,* 2007).

1.4.1 CDF transporters:

CDF transporters play a key role in the transport of divalent cations, whether with the translocation into internal compartments or extracellular space (Gustin *et al.,* 2011). The members of this family exhibit six transmembrane domains (TMs) with a cytoplasm-protruding, histidine-rich region between the IV and V TM (Paulsen and Saier, 1997). CDFs share a signature sequence at the N-terminus and a cation efflux domain at the C-terminus (Paulsen and Saier, 1997). Twelve CDF members have been identified in *A. thaliana* that are referred to as MTPs (metal tolerance proteins). These transporters can translocate a variety of divalent cations, such as Fe, Co, Zn, Mn and Cd, and can therefore be classified into three groups according to their metal specificity: Zn-CDFs, Fe/Zn-CDFs, and Mn-CDFs (Montanini *et al.,* 2007; Gustin *et al.,* 2011). The most characterized transporter of this family is MTP1, a vacuole Zn^{2+}/H^{+} antiporter involved in Zn tolerance, which accumulates Zn into the vacuole (Desbrosses-Fonrouge *et al.,* 2005). MTP1 is highly expressed in

hyperaccumulator plants such as *A. halleri* and *T. caerulescens,* and indeed, the genome of the former species exhibits three different MTP1 gene copies (Dräger *et al.,* 2004; Krämer *et al.,* 2007; Fasani *et al.,* 2017). MTP3 is localized at the vacuole and its ectopic expression results in greater Zn accumulation in both the roots and shoots of *A. thaliana* (Arrivault *et al.,* 2006). The Mn-CDFs group has four members classified into two subgroups, i.e. *AtMTP8,* belonging to group 8 and *AtMTP9*/*AtMTP10*/ *AtMTP11,* which are included in group 9 (Gustin *et al.,* 2011). As regards the members of this latter group, only the functions of *AtMTP11* has been identified, revealing a Golgi-associated compartment localization and a key role in manganese tolerance (Delhaize *et al.,* 2007; Peiter *et al.,* 2007).

1.4.2 HMA transporters:

The Heavy Metals P_{1B}-type ATPases (HMA) transporters contribute to the diffusion of cations out of the cytoplasm by hydrolyzing ATP. These proteins are characterized by eight transmembrane domains with a short C-terminus and a large N-terminal region, which contains a HMA (heavy metal-associated) domain (Axelsen *et al.,* 2001). The HMA domain is 31 aa long and exhibits a GMTCxxC motif involved in metal binding, which has also been suggested to have a role as a sensor for heavy metals. The members of this family have been classified into two groups, according to their specificity for the metals they transport, hence we have the Cu/Ag group, also known as group IB-1 and the Zn/Co/Cd/Pb group, referred as group IB-2 (Axelsen *et al.,* 2001; Argüello, 2003; Cobbett *et al.,* 2003; Williams and Mills, 2005). In *A. thaliana,* there are eight HMA transporters and the first four members (*AtHMA1*, *AtHMA2*, *AtHMA3*, *AtHMA4*) belong to the second group. Kim *et al.* (2009) have shown a chloroplast envelope localization for *AtHMA1* which is involved in the Zn detoxification of plastids. *AtHMA3* on the other hand seems to be involved in the detoxification of Zn/Cd/Co and Pb, regulating their sequestration into the vacuole (Morel *et al.,* 2009). *AtHMA2* and *AtHMA4* are plasma membrane transporters expressed in vascular tissues, and are involved in Zn translocation from roots to shoots via xylem loading (Mills *et al.,* 2003; Hussain *et al.,* 2004; Verret *et al.,* 2004). The expression of HMA4 is higher in hyperaccumulator plants such as *A. halleri* and *Noccaea caerulescens* due to the presence of more gene copies (Talke *et al.,* 2006; Ó Lochlainn *et al.,* 2011), thus the expression seems to be constitutively higher in *A. halleri* and induced by high Zn and Cd concentrations in *N. caerulescens* (Talke *et al.,* 2006; Papoyan and Kochien, 2004). *AtHMA5* through AtHMA8 belong to the IB-1 group involved in the Cu/Ag transport (Argüello, 2003; Cobbett *et al.,* 2003; Williams and Mills, 2005). *AtHMA5* seems to have a role in the root-to-shoot transport of Cu and in its detoxification at

the root level (Andrés-Colás *et al.,* 2005). *AtHMA6* (PAA1) and *AtHMA8* (PAA2) present a role in the Cu transport into chloroplasts carrying Cu across the envelope and the thylakoid membrane, respectively (Shikanai *et al.,* 2002; Abdel-Ghany *et al.,* 2005). *AtHMA7* (RAN1) seems instead to transport Cu into Golgi to deliver this cofactor to ethylene receptor (Hirayama *et al.,* 1999; Woeste and Kieber, 2000).

1.4.3 NRAMP transporters:

The Naturally Resistant Associated Macrophage Proteins (NRAMPs) family of metal transporters is highly conserved in many organisms from bacteria to animals and is involved in the transport of multiple metal ions across the membranes (Hall and Williams, 2003). Most members of this family possess 12 transmembrane domains with a predicted transport motif between the VIII and IX TM (Williams *et al.,* 2000). Six members of this family have been identified in *A. thaliana,* which have been grouped into two sub-families: *AtNRAMP1* and *AtNRAMP6* belong to one, and *AtNRAMP2-5* to the other (Williams *et al.,* 2000; Thomine *et al.,* 2000; Maser *et al.,* 2001). Furthermore, the ethylene insensitivity gene (EIN2) involved in the ethylene signaling presents a NRAMP homologous domain (Alonso *et al.,* 1999), even if seems not to have a metal transport activity. *AtNRAMP1* is able to complement Fe and Mn transport in yeast metal uptake mutants (Curie *et al.,* 2000; Thomine *et al.,* 2000). This transporter is localized at the plasma membrane, and has been observed to be involved in high-affinity Mn uptake from the soil (Cailliatte, 2010). Moreover, *AtNRAMP2* seems to be not involved in Fe transport (Curie *et al.,* 2000). Thomine *et al.* (2000) proved that *AtNRAMP3* and *AtNRAMP4* are able to transport Fe and Mn, and could restore the uptake ability of yeast mutants defective in the transport of these two elements. *AtNRAMP3* and *AtNRAMP4* on the other hand are localized at the tonoplast, and seem to play a key role in Fe mobilization during germination and early developmental stages (Lanquar *et al.,* 2005).

1.4.4 CAX transporters:

Calcium (Ca) is an important element that regulates many enzymes and reactions either by influencing signal transduction or acting as a second messenger. It is accumulated into the vacuole and the gradient can be directly modulated by various H^+/Ca^{2+}exchangers. These Ca^{2+} (CAX) transporters were discovered through the complementation of a yeast mutant, unable to transport Ca into the vacuole (Hirschi *et al.,* 1996). The CAX family is part of the Ca^{2+}/Cation Antiporter (CaCA) superfamily (Pitman and Hirschi, 2016). Their structure, highly conserved among all

members of the superfamily, is characterized by ten membrane-spanning domains with repeat cation binding regions: α1, between transmembrane domain II and III, and α2, between transmembrane domain VII and VIII (Pitman and Hirschi, 2016). *A. thaliana* possesses six different CAX transporters (Maser *et al.,* 2001), most of which have already been characterized. CAX1 and CAX3 are vacuolar H^+/Ca^{2+}exchangers, and CAX1 knockout mutants shows a marked reduction in their tonoplast antiporter activity (Cheng *et al.,* 2003; 2005). CAX2 has a low affinity for Ca^{2+} but Pittman *et al.* (2004) observed that it that can transport other metals too, including Cd^{2+} and Mn^{2+}. CAX4 seems to be specifically expressed in Ca^{2+}-deficient roots and at excess levels of $Ni^{2+}$and Mn^{2+} (Mei *et al.,* 2009), suggesting a role in root development under conditions of metal stress.

1.4.5 YSL transporters:

Yellow Stripe 1-like (YSL) transporters belong to the oligopeptide transporter (OPT) family, involved in the transport of peptides and amino acid derivatives (Curie *et al.,* 2009). YS1 of maize is the founding member of this family that transports, like its orthologs, a FeIII-phytosiderophore complex preventing physiological Fe deficiency (Curie *et al.,* 2001). Eight different YSL transporters have been identified in *A. thaliana,* whose topology reveals the presence of 15 transmembrane domains with a variable extra-membranous region between by the VII and VIII TM and a very similar N terminal sequence (DiDonato *et al.,* 2004). *AtYSL1* and *AtYSL3* are plasma membrane transporters greatly expressed at leaf parenchyma level, but expression decreases under scarce Fe conditions (DiDonato *et al.,* 2004; Waters *et al.,* 2006; Chu *et al.,* 2010). DiDonato *et al.,* (2004) observed that *AtYSL2* is expressed at the lateral membranes of pericycle cells, suggesting a role in the movement of metals into the vascular tissues. Furthermore, the *AtYSL2* expression was down-regulated under low Zn and Fe (Schaff *et al.,* 2005). Conte *et al.,* (2013) suggested a tonoplast and ER localization for *AtYSL4* and *AtYSL6* confirming a proteomic analysis of the tonoplast proteome (Jaquinod *et al.,* 2007). On the contrary, the localization of *AtYSL4* and *AtYSL6* was also observed at the chloroplast level and their ectopic expression mediates a reduction in chloroplast Fe (Divol *et al.,* 2013).

1.4.6 COPT transporters:

The high-affinity copper (Cu) transporter family CTR/COPT is involved in the acquisition of Cu by cells. The expression of these proteins, coupled with the expression of Cu^{2+} reductases such as FRO4 and FRO5, is activated by SPL7 (SQUAMOSA promoter-binding protein-like 7) under conditions of Cu deficiency (Yamasaki *et al.,* 2009; Bernal *et al.,* 2012). As regards their structure, COPTs usually possess three transmembrane domains with a Mx3Mx12Gx3G motif between TMII and TMIII and a methionine or histidine-rich N-terminal domain (Puig *et al.,* 2002; Aller *et al.,* 2004). Six COPT members have been identified in *A. thaliana,* with different subcellular localizations: COPT1, COPT2 and COPT6 are localized at the plasma membrane whereas COPT3 and COPT5 on intracellular membranes (Sancenón *et al.,* 2004; Jung *et al.,* 2012). COPT1 was the first member to be characterized and together with COPT2 was observed to be strongly expressed both in root tips and along the entire root (Sancenón *et al.,* 2003, 2004; Perea-García *et al.,* 2013). Moreover, COPT1 and COPT2 are able to complement the respiratory defect of the yeast *ctr1*Δ*ctr3*Δ mutant whereas COPT3 and COPT5 can complement it only partially (Kampfenkel *et al.,* 1995; Sancenón *et al.,* 2003). The COPT4 protein expression seems to be toxic for the yeast cells (Sancenón *et al.,* 2003). COPT5 is expressed in root and shoot vascular tissues, and has a pre-vacuolar and tonoplast localization (Garcia-Molina *et al.,* 2011). Jung *et al.* (2012) showed that COPT6 was able to complement the Cu uptake deficiency of the *ctr1*Δ*ctr2*Δ*ctr3*Δ yeast mutant independently from the interaction with COPT1.

1.4.7 CCC1 trasporters:

The Ca^{2+}-sensitive cross complementer 1 (CCC1) family of transporters was first discovered in yeast (Li *et al.,* 2001) and its members are involved in Fe/Mn translocation into the vacuole (Gollhofer *et al.,* 2011). In *A. thaliana*, there are six orthologs of yeast CCC1 exhibiting five predicted transmembrane domains (Gollhofer *et al.,* 2011). *AtVIT1* (Vacuolar Iron Transporter1), the most characterized to date, is a vacuolar transporter involved in Fe sequestration (Kim *et al.,* 2006). Furthermore, three homologous proteins of *AtVIT1*, *AtVTL1* (Vacuolar Iron Transporter-Like1; At1g21140), *AtVTL2* (At1g76800) and *AtVTL5* (At3g25190) were able to complement the iron yeast *Δccc1* mutant, restoring the root grown in *nramp3/nramp4* and *vit1-1* mutants (Gollhofer *et al.,* 2014).

1.4.8 IREG transporters:

The IREG (iron-regulated protein) family in *A. thaliana* is composed of three members that seem to be involved in the metal long distance transport (Kramer *et al.,* 2007). IREG proteins are homologous to mammalian Ferroportin 1, a Fe transporter (McKie *et al.,* 2000) with ten predicted transmembrane domains. The topology of rat IREG1 shows 11 TM domains with an extra cytosolic loop between the V and VI TM (Yeh *et al.,* 2011). Iron Regulated 1 (IREG1/FPN1) and IREG2/FPN2 are localized to the plasma membrane and in the tonoplast, respectively (Morrissey *et al.,* 2009). IREG1 was expressed in the vascular tissues suggesting a role in the root-to-shoot Fe transport whereas IREG2, in the epidermis and cortex layers suggesting a role in the Fe homeostasis under low Fe conditions (Morrissey *et al.,* 2009). Both seems also to be involved in Co transport (Morrissey *et al.,* 2009). In a previous work, was observed that even though *AtIREG2* is co-regulated with *AtIRT1,* it did not seem to be involved in Fe transport but displayed instead a substrate specificity for Ni (Schaaf *et al.,* 2006). Conte *et al.* (2009) showed that a mutation in the *A. thaliana* locus *Multiple Antibiotic Resistance1* (*MAR1*), in the 10th exon of the At5g26820 gene referred as *AtIREG3* (Schaff *et al.,* 2006) or RTS3 (Aufsatz *et al.,* 2009), conferred a higher tolerance to antibiotics. MAR1 seems to be a plastid transporter involved in the Fe homeostasis at the chloroplast level (Conte *et al.,* 2009).

1.4.9 ABC transporters:

ATP-Binding Cassette (ABC) proteins are members of a very large family of transporters involved in many biological processes ranging from pathogen response to phytohormone transport across various membranes by means of ATP hydrolysis (Kang *et al.,* 2011). ABC proteins are divided into 13 subfamilies according to their protein organization, size and orientation, and usually exhibit two transmembrane domains (TMD) and two nucleotide-binding domains (NBD) that contain the Walker A and B ATP-binding motifs separated by the ABC signature motif ([LIVMFY]S[SG]GX3[RKA][LIVMYA]-X[LIVFM][AG] (Rea, 2007). In *A. thaliana,* 130 ABC transporters have been identified, few of which however have been fully characterized. Among the various ABC subfamilies, those involved in metal transport appear to be MRP (multidrug resistance-associated proteins), ATM (ABC transporters of the mitochondria) and PDR (pleiotropic drug resistance) (Krämer *et al.,* 2007). The ABCC/MRP subfamily presents 15 members that are characterized by an additional transmembrane domain (TMD0) at the N-terminus (Klein *et al.,* 2006). *AtABCC1* and *AtABCC2*, two MRP proteins, seem to be involved in vacuole arsenic sequestration mediated by phytochelatins (PCs) (Song *et al.,* 2010) conferring also tolerance to Cd

and Hg (Park et al., 2012). The heterologous expression of *AtABCC3*, *AtABCC4* and *AtABCC7* was able to complement in part the yeast *Δycf1* mutant, defecting in the Cd transport into the tonoplast (Klein et al., 2006). In addition, Brunetti *et al.,* (2015) showed that *AtABCC3* could be involved in PC-dependent Cd detoxification. Kim *et al.* (2007) observed that a member of PDR subfamily, *AtPDR8*, displays efflux Cd activity at plasma membrane level. Moreover, *AtATM3* is a mitochondrial ATM protein playing a role in iron homeostasis, and also seems to be involved in Cd resistance (Kim *et al.,* 2006).

1.4.10 ZIP FAMILY:

The ZIP (ZRT IRT1-like Proteins: Zinc-regulated transporter Iron-regulated transporter 1-like protein) family of metal transporters was first identified in plants (Guerinot, 2000). Its name originates from the first members to be characterized: IRT1 (iron-regulated transporter) by Eide et al., (1996) in *A. thaliana* whereas ZRT1and ZRT2 (zinc regulated transporter) identified in in *S. cerevisiae* by Zhao et al., 1996a and 1996b respectively. ZRT1 belongs to the high-affinity system involved in zinc uptake, and is induced by shortage of its substrate (Zhao and Eide, 1996a) whereas ZRT2 has been characterized as a low-affinity transporter protein (Zhao and Eide, 1996b). Fifteen members of ZIP family have been identified in *A. thaliana*, which can be clustered into four groups sharing a sequence similarity between 38% and 85% (Maser *et al.,* 2001) (Figure 1.2A). Most members of the ZIP family fold into eight transmembrane domains spaced by a variable metal-binding region located between transmembrane domain III and IV, with the N- and C-terminus of the sequence located on the extracellular side of the membrane. The sequence of ZIP transporters ranges from 309 to 476 amino acids, depending on the length of the variable metal-binding region. Moreover, the potential metal-binding domain, rich in histidine residues, seems to have a cytoplasmic localization (Guerinot, 2000) (Figure 1.2B). The presence of a conserved metal-binding motif with multiple histidine residues has been observed in different members of this family, such as IRT1, IRT2, ZIP1, ZIP4, ZRT1 and ZRT2 (Grotz *et al.,* 1998; Eng *et al.,* 1998). IRT1 exhibits, together with ZRT1 and ZRT2, a $(HX)_n$ repeated motif that has also been observed between the IV and V transmembrane domains of members of the cation diffusion facilitator (CDF) family (Eng *et al.,* 1998). Conversely, ZIP2 and ZIP3 only have a single histidine residue in their variable region. A single Hys residue conserved among the members of ZIP family has been also predicted inside the II, IV and V transmembrane domains (Grotz *et al.,* 1998). The substitution of the conserved single glutamic acid residue of IRT1 in the II transmembrane domain at position 103, adjacent to the Hys residue, eliminated its ability to transport Zn, whereas when the aspartic acid

residues either at position 100 and 136 were removed, both Fe and Mn transport mechanisms were stalled (Rogers *et al.,* 2000). The function of ZIP proteins in plants, clarified in only a few cases, is a matter of research, although it is known that they are involved in Zn and divalent cations uptake, distribution and translocation to shoots and seeds (Grotz *et al.,* 1998; Waters and Sankaran, 2011; White and Broadley, 2011; Olsen and Palmgren, 2014). ZIP proteins are ubiquitous Zn transporters (Grotz *et al.,* 1998; Lin *et al.,* 2009; Assunção *et al.,* 2010; Mizuno *et al.,* 2005; Milner *et al.,* 2012; Milner *et al.,* 2013), Fe (Vert *et al.,* 2001; Vert *et al.,* 2002; Vert *et al.,* 2009; Milner *et al.,* 2013; Lin *et al.,* 2016), Mn (Mizuno *et al.,* 2005; Milner *et al.,* 2012; Milner *et al.,* 2013), Cu (Wintz *et al.,* 2003; Milner *et al.,* 2012), Cd (Cohen *et al.,* 1998; Mizuno *et al.,* 2005; Lin *et al.,* 2016) and Ni (Nishida *et al.,* 2011; Nishida *et al.,* 2015).

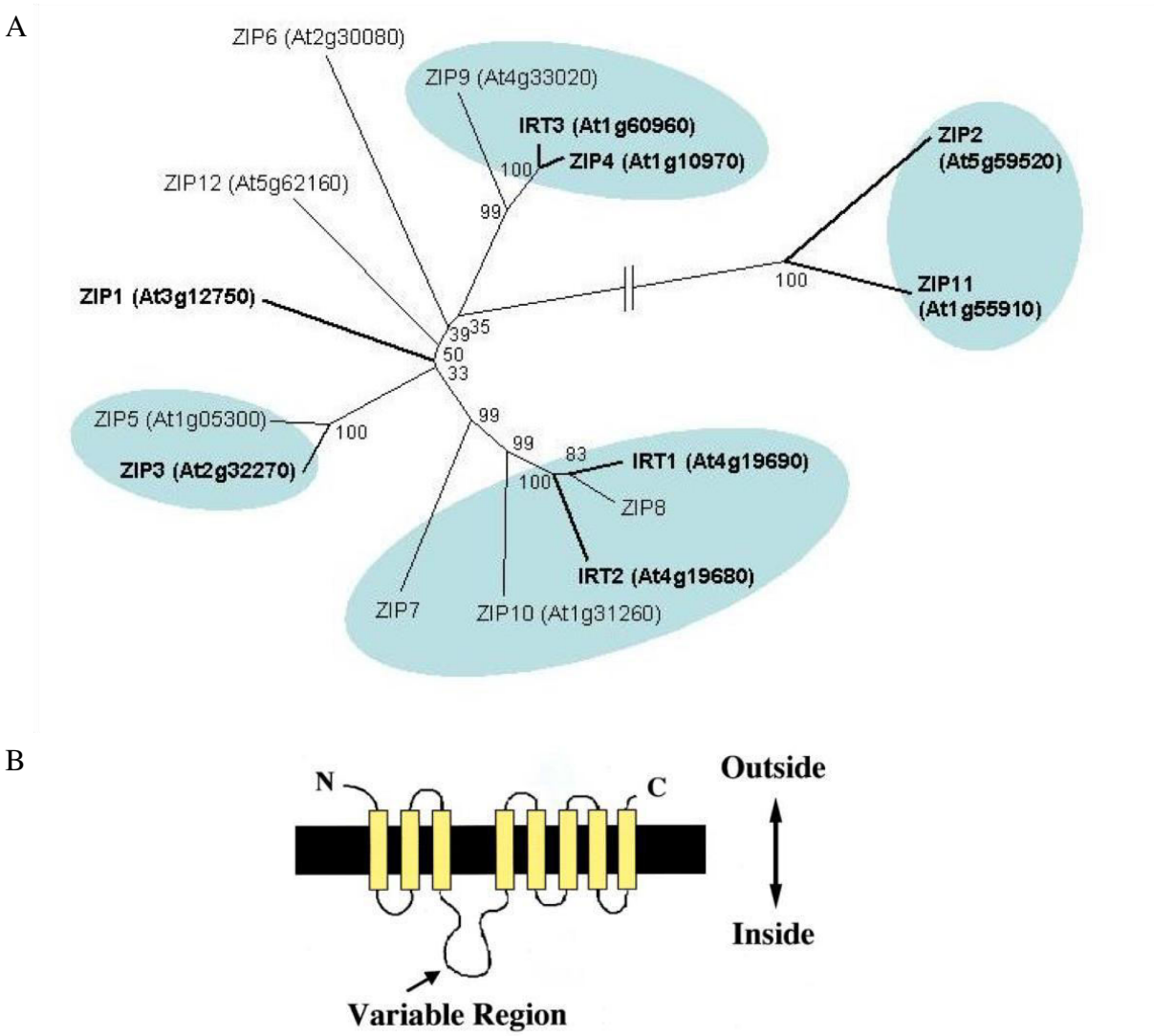

Figure 1.2: A) Phylogenetic tree of *Arabidopsis* ZIP transporters (Maser *et al.,* 2001) and B) predicted membrane topology of a ZIP family member (Guerinot, 2000).

Only few members, such as *AtIRT1*, *AtIRT2* and *AtIRT3* have been well characterized, and to date, little is known about the others. *AtIRT1*, the first member of the ZIP family to be identified, is an Fe(II) transporter that takes up iron from the soil. In *A. thaliana*, *AtIRT1* mRNA is expressed in roots upon iron deficiency (Eide *et al.,* 1996). *AtIRT1* is localized at the plasma membrane and is expressed in the epidermis and root hairs (Vert *et al.,* 2002). *AtIRT1* knockout mutants display severe chlorosis, a small number of thylakoids and low biomass production, i.e. all the typical symptoms of Fe deficiency (Henriques *et al.,* 2002). *AtZIP1* and *AtIRT2* expression is induced in the shoots and roots of the *irt1* insertional mutant, respectively, whereas *AtZIP2* is reduced at root level. Moreover, Fe-starved *irt1* mutants accumulate less Ni and Mn and under the same conditions, *AtIRT1* over-expressing lines less Zn and Cd, suggesting a role in the transport of these target metals (Vert *et al.,* 2002; Connolly *et al.,* 2002; Nishida *et al.,* 2011). The expression of *AtIRT2* is very similar to that of *AtIRT1,* is induced under Fe-limited conditions and localized in the outer layers of the roots; furthermore, it only complements yeast mutants defective in the transport of Zn and Fe and not in the transport of Cd and Mn (Vert *et al.,* 2001). The levels of *AtIRT2* mRNA are increased in *AtIRT1* knockout mutants but the overexpression of IRT1 doesn't complement the phenotype of the insertional *AtIRT2* mutant, indicating a different function than that of IRT1. *AtIRT2* is localized on intracellular vesicles, suggesting that it plays a detoxification role of the epidermal layer rather than being involved in Fe uptake from the soil (Vert *et al.,* 2009). Lin *et al.* (2009) observed that *AtIRT3* is localized at the plasma membrane and is able to complement yeast mutants for the uptake of Zn and Fe; moreover, promoter activity seems to be ubiquitous, and is very clear at root stele level. The expression of *AtIRT3* is induced by Zn deficiency and its over-expression in *A. thaliana* results in greater Zn accumulation in the shoots and a higher level of Fe in the roots (Lin *et al.,* 2009). When over-expressed in Fe-starved *irt1* mutants, it can restore the wild-type phenotype and may be involved in Zn and Fe translocation (Shanmugam *et al.,* 2011). In recent years, other members of the ZIP family have been investigated. In *A. thaliana* roots, ZIP1, ZIP3 and ZIP4 are induced under conditions of Zn deficiency (Grotz *et al.,* 1998), suggesting a role in Zn uptake from the soil. Jain *et al.* (2013) observed that ZIP2, ZIP3, ZIP4, ZIP5, ZIP8, ZIP9 and ZIP12 are 2-fold up-regulated in both roots and shoots at low Zn availability, whereas ZIP7 and ZIP1 are induced in the roots and shoots, respectively. The expression of ZIP6, ZIP10 and ZIP11 does not appear to be induced by lack of Zn, and it similar to that measured under standard growth conditions (Jain *et al.,* 2013). Milner *et al.* (2013) showed that several members of ZIP family can complement yeast mutants deficient in Fe, Zn, Mn and Cu uptake mechanisms (Figure 1.3). ZIP1, ZIP2, ZIP3, ZIP7, ZIP11, and ZIP12 seems to complement the *zrt1/zrt2* yeast mutant defective in the Zn uptake system whereas ZIP1, ZIP2, ZIP5, ZIP6, ZIP7, and ZIP9 also seem to complement

the Mn uptake mutant (Milner *et al.,* 2013). Only ZIP7 seems to partially complement the iron *fet3/fet4* yeast mutant. *AtZIP1* is located in vacuolar membranes and is chiefly expressed in the leaf vasculature, the pericycle and in the vascular tissues of the roots (Milner *et al.,* 2013). Although, as mentioned previously, ZIP1 can complement the uptake in yeast mutants lacking Zn and Mn transporters (Figure 1.3), the roots of the single *AtZIP1* knockout mutant appears to have higher amounts of Mn, but not Zn, than the wild-type, suggesting a role in Mn distribution into the xylem parenchyma (Milner *et al.,* 2013). Grotz *et al.* (1998) suggest that Cu may be also a substrate of ZIP1, although it is incapable of complementing the *ctr1/ctr3* yeast mutant for the uptake of Cu (Milner *et al.,* 2013). On the other hand, *AtZIP2* is located at the plasma membrane and like *AtZIP1* seems to be involved in Zn and Mn transport (Figure 1.3; Milner *et al.,* 2013). Both are expressed at root stele level and have been suggested to play a key role in Mn and Zn root to shoot transport, even though ZIP2 may be more involved in uptake and xylem loading than Zn/Mn distribution (Milner *et al.,* 2013). Another ZIP transporter that is thought to be involved in Zn transport is *AtZIP3* (Grotz *et al.,* 1998). Its expression appears to be up-regulated under Zn-limiting conditions and given its ability to complement the *zrt1/zrt2* yeast mutant, it may be involved in Zn transport, although more information is needed to confirm this assumption (Grotz *et al.,* 1998).

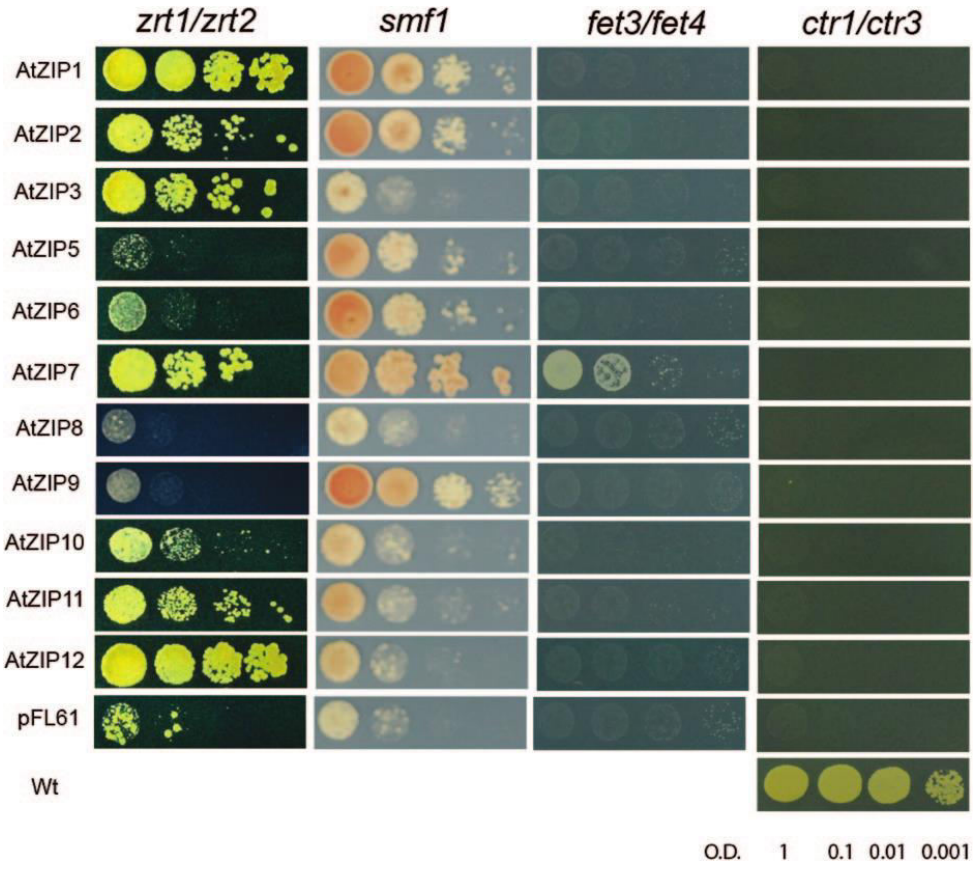

Figure 1.3: Metal uptake complementation of yeast mutants for the uptake of Zn (*zrt1/zrt2*), Mn (*smf1*), Fe (*fet3/fet4*) and Cu(*ctr1/ctr3*) with *AtZIP* genes. pFL61 are the transformed mutants containing the empty vector (Milner *et al.,* 2013).

1.5 *AtZIP4*, *AtZIP6* and *AtZIP9*:

The project focuses on three ZIP-family members: *AtZIP4*, *AtZIP6* and *AtZIP9*, for which little information is available. These three transporters were chosen because it is believed that the latter two transporters play a key role in root uptake and vascular tissue unloading, respectively, whereas *AtZIP4* is involved in both processes (Figure 1.4). *AtZIP4* has already been partially characterized (Assunção *et al.,* 2010; Lin *et al.,* 2016), and has been observed to share an 82% identity and 78% similarity with the amino acid sequence of *AtIRT3*. Furthermore, *AtZIP4* falls into the phylogenic group of *AtZIP9* (Figure 1.2A; Maser *et al.* 2001), with whom it shares a 63% identity and a 77% similarity at protein level. Wintz *et al.* (2003) observed that in *A. thaliana* both *AtZIP4* and *AtZIP9* are up-regulated in roots and shoots under conditions of Zn deficiency.

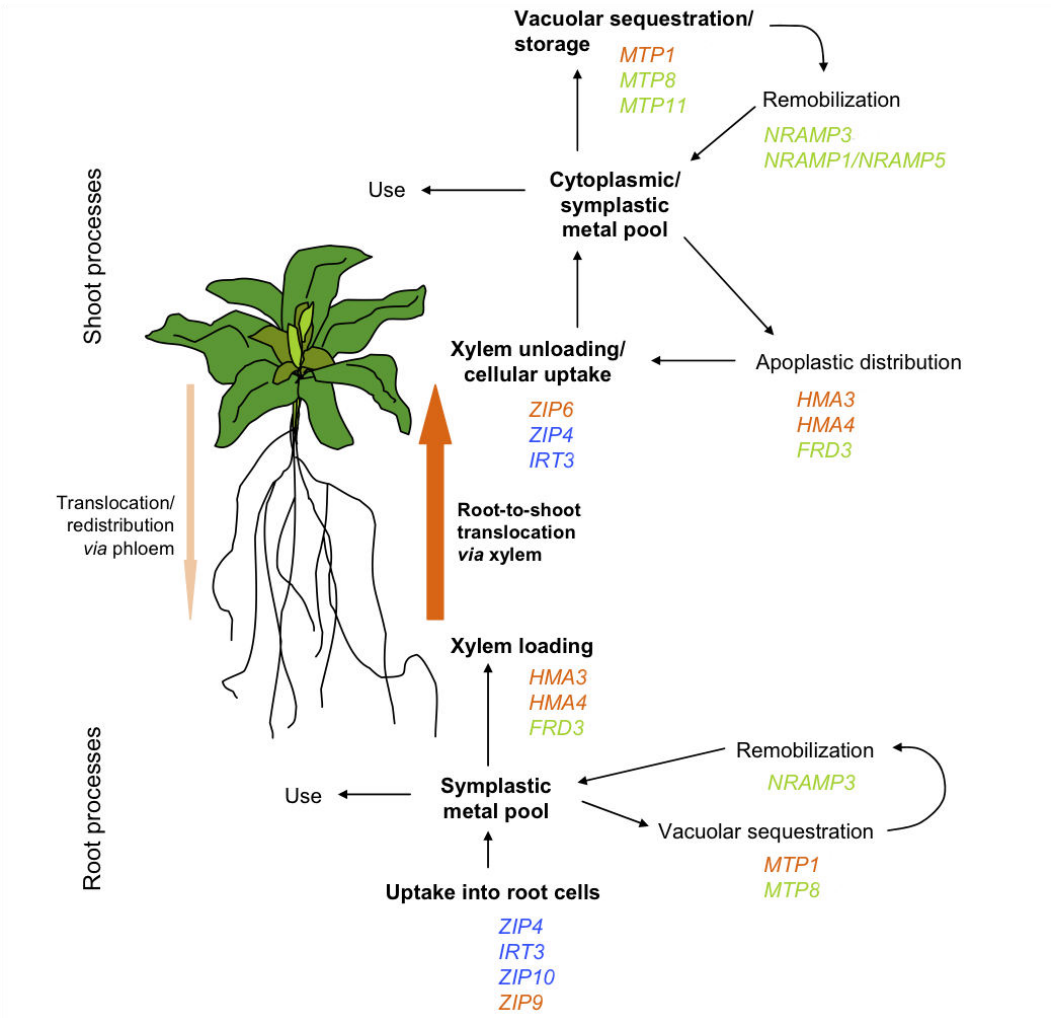

Figure 1.4: Model of the transition metal transporters of the hyperaccumulating species *A. halleri* and *T. caerulescens* (Krämer *et al.* 2007).

AtZIP4 has been partially studied by Assunção *et al.* (2010) who observed its ability to complement *Saccharomyces cerevisiae zrt1/zrt2* mutants, and using a yeast one-hybrid assay, found that two bZIP family transcription factors, *bZIP19* and *bZIP23,* respond to Zn deficiency by regulating the transcription of *AtZIP4* binding specific Zinc Deficiency Response Elements (ZDRE).

Moreover, Lin *et al.* (2016) analyzed the promoter activity of this gene, and observed its expression in the endodermis/pericycle at root level and at the leaf edges and in the trichomes of the shoots. Milner and Kochian (2008) previously suggested a different cell-specific expression located in the root stele and not in the endodermis. *AtZIP4* is also up-regulated under conditions of Cu deficiency; this, together with the fact that it can complement the *ctr1* yeast mutant that lacking Cu transport systems, suggests that *AtZIP4* could also be involved in Cu transport (Wintz *et al.* 2003).

On the other hand, the expression of *AtZIP6*, which is not included in any of the four groups mentioned previously (Maser *et al*., 2001), does not appear to be modulated by changes in Zn or Fe concentrations (Wintz *et al.,* 2003) but increases in roots during senescence (Milner *et al.,* 2013). Very little information is available for *AtZIP6,* but it has been suggested to be one of the candidates for the hyperaccumulator trait displayed by *A. halleri* and *T. caerulescens* (Becher *et al.,* 2004; Hammond *et al.,* 2006). *AhZIP6* is constitutively more highly expressed both in the roots and shoots of *A. halleri* ssp. *halleri,* a Zn hyperaccumulator species, than in those of non-accumulators (Becher *et al.,* 2004; Weber *et al.,* 2004). Two copies of *AhZIP6* seem to be present in *A. halleri* genome, which are highly expressed and whose regulation does not appear to be metal-dependent (Talke *et al*., 2006).

AtZIP9 falls in the same phylogenetic group as *AtZIP4* and, like other ZIP members, is up-regulated in both roots and shoots under Zn deficient conditions (Wintz *et al.,* 2003; Weber *et al.,* 2004; Jain *et al.,* 2013). In *A. halleri*, ZIP9 is encoded by two gene copies and is highly expressed in the roots at low Zn availability, although it seems that the ability to respond to different concentrations of Zn has been partially lost in hyperaccumulator plants such as *T. caerulescens* (Weber *et al.,* 2004; Talke *et al*., 2006; van de Mortel *et al.,* 2006). The expression of *AhZIP9* is only visible in shoots under conditions of Zn deficiency (Talke *et al*., 2006). Moreover, *AtZIP9* expression seems to be mediated by *bZIP19*, a basic-region leucine-zipper transcription factor (Inaba *et al.,* 2015). A proteomic analysis on microsomal proteins from *bZIP19* mutants failed to reveal any induction of ZIP9 and ZIP3 brought about by Zn deficiency; gene expression analysis revealed the same pattern for ZIP4 and ZIP5 (Inaba *et al.,* 2015).

1.6 ZIP GENES IN VARIOUS PLANT SPECIES:

The function of ZIP proteins has only been clarified for just a few members of the family, even in plant species other than *Arabidopsis*, ranging from hyper-accumulator plants such as *Noccaea caerulescens* (Pence *et al.,* 2000; Milner *et al.,* 2012), *Arabidopsis halleri* (Weber *et al.,* 2004; Talke *et al.,* 2006, Lin *et al.,* 2009), *Thlaspi japonicum* (Mizuno *et al.,* 2005; Nishida *et al.,* 2008; Nishida *et al.,* 2011) and *Chengiopanax sciadophylloides* (Mizuno *et al.,* 2008), to other plant models such as rice (Bughio *et al.,* 2002; Ishimaru *et al.,* 2005; Ishimaru *et al.,* 2006; Yang *et al.,* 2009; Lee *et al.,* 2010; Suzuki *et al.,* 2012; Sasaki *et al.,* 2015), maize (Li *et al.,* 2013), barley (Pedas *et al.,* 2008; Pedas *et al.,* 2009; Tiong *et al.,* 2015), tomato (Eckhardt *et al.,* 2001), *Pisum sativum* (Cohen *et al.,* 2004), *Medicago trucatula* (López-Millán *et al.,* 2004), poplar (Huang and Dai, 2015) and trifoliate orange (Fu *et al.,* 2017).

NcZNT1 was the first member of this family to be studied in hyperaccumulator plants. Yeast complementation studies performed by Pence *et al.* (2000) seemed to indicate a role in Zn high- and Cd low-affinity transport, but more recent investigations revealed that it only mediates Zn transport and not that of Cd, Fe, Mn or Cu (Milner *et al.,* 2012). *NcZNT1* is a plasma membrane transporter involved in the long-distance transport of Zn, and is mainly expressed in the epidermis and vascular tissues of both roots and shoots (Milner *et al.,* 2012). *A. halleri* is a model plant for the hyperaccumulation of Zn and Cd. Weber *et al.* (2004) showed by means of a comparative microarray analysis that various ZIP members such as *AhZIP3*, *AhZIP6*, *AhZIP12* and *AhIRT3* are highly expressed in both the roots and shoots of *A. halleri* whereas *AhZIP9* only in the roots, thus they can be at least partly responsible for the hyperaccumulator trait. *AhIRT3,* located at the plasma membrane, is able to complement the double *zrt1/zrt2* and *fet3/fet4* mutant defective in Zn and Fe uptake respectively but cannot mediate Mn transport (Lin *et al.,* 2009). The ZIP transporters best investigated in *Thlaspi japonicum,* a Ni hyperaccumulator plant model, are *TjZNT1* and *TjZNT2. TjZNT1* shares a 77% similarity with the amino acid sequence of *TjZNT2:* both are able to transport Zn and Mn but *TjZNT1* can also transport Cd (Mizuno *et al.,* 2005). Unlike other ZIP transporters, *TjZNT1* and *TjZNT2* possess two histidine-rich domains (HRDs) between the III and IV transmembrane domains. A deletion of HDR2 resulted in the plant losing its ability to transport Zn, but the removal of HDR1 or both HDR1-2 did not affect this process (Nishida *et al.,* 2008). Moreover, the subcellular localization of *TjZNT1* was found to be at the plasma and vacuolar membranes level, and the loss of HDRs has no effects on localization (Nishida *et al.,* 2008). *Chengiopanax sciadophylloides* is a hyperaccumulating tree species specific for Mn. Mizuno *et al.* (2008) were able to isolate its *CsZIP1* transporter, similar to *TjZNT1,* the expression of which is up-regulated in the plant's callus under Mn deficiency conditions; however, this protein seems to be

more involved in Cd transport than in that of Mn. Seventeen members of the ZIP family have been reported in rice (Bughio *et al.,* 2002) and several members have been widely characterized. The homologous of *Arabidopsis* IRT1, *OsIRT1,* is induced at low Fe availability and its over-expression in rice results in higher levels of Fe and Zn in roots, leaves and seeds (Ishimaru *et al.,* 2006). Zn-deficiency conditions raise the transcript level of different plasma membrane ZIP members such as *OsZIP1*, *OsZIP3*, *OsZIP4*, *OsZIP5* and *OsZIP8* (Ishimaru *et al.,* 2005; Yang *et al.,* 2009; Suzuki *et al.,* 2012). *OsZIP1* is up-regulated by a scarcity of either Zn or Cu, the expression of *OsZIP3* instead does not appear to be modulated by Zn availability although both can complement the defective Zn-uptake yeast mutant (Ishimaru *et al.,* 2005; Sasaki *et al.,* 2015). The expression of *OsZIP3* is localized in the xylem parenchyma cells and nodes, furthermore RNA interferance of *OsZIP3* resulted in a reduced Zn distribution along the shoot elongation zone but not in the lower leaves where it seems more equally distributed, suggesting a role in xylem unloading and Zn distribution during tissue development (Sasaki *et al.,* 2015). Ishimaru *et al.* (2005) investigated the expression pattern of *OsZIP4*, *OsZIP5*, *OsZIP6* and *OsZIP7*, members similar to *OsIRT1,* and found an induction of *OsZIP5* and *OsZIP7* in shoots and *OsZIP4* both in roots and shoots under conditions of low Zn availability. *OsZIP6* is activated in both roots and shoots in response to Zn, Fe and Mn starvation but the heterologous expression in the oocytes of *Xenopus laevis* shows that it also mediates the transport of Fe, Co and Cd (Kavitha *et al.,* 2015). *OsZIP4* expression is located in the vascular bundles of the whole plant and together with *OsZIP8* complement the *zrt1/zrt2* yeast mutant (Ishimaru *et al.,* 2005; Lee *et al.,* 2010). The over-expression of both these genes results in a higher Zn content in roots instead of the shoots and seeds where the Zn level is lower than in the wild-type (Ishimaru *et al.,* 2007; Lee *et al.,* 2010). Nine ZIP-coding genes have been identified in the maize genome and all seem to be localized at the plasma membrane and endoplasmic reticulum (ER) (Li *et al.,* 2013). These transporters share a conserved transmembrane domain and like *A. thaliana* exhibit a variable region between the III and the IV transmembrane domains. The expression of these proteins varies during the different stages of embryo development, for example *ZmZIP4* is up-regulated in the early stages whereas the amount of *ZmIRT1* and *ZmZIP6* mRNA increases later (Li *et al.,* 2013). An ectopic over-expression of *ZmZIP3* and *ZmIRT1* was performed in *A. thaliana,* resulting in a greater accumulation of Zn and Fe in *ZmIRT1* transgenic lines and of Zn alone in *ZmZIP3* transgenic lines, both at root level and in the seeds (Li *et al.,* 2015). Several ZIP proteins have also been characterized in barley, the first of which was the plasma membrane localized *HvIRT1,* a Mn transporter similar to *OsIRT1* (Pedas *et al.,* 2008). ICP-MS and yeast uptake assays have revealed that *HvIRT1* is also involved in the transport of Fe, Zn and Cd. Pedas *et al.* (2009) isolated other three members of this family, namely *HvZIP3*, *HvZIP5* and *HvZIP8,*

screening and expressing a cDNA library in the *zrt1/zrt2* yeast mutant. *HvZIP3* and *HvZIP5* are up-regulated by low concentrations of Zn in the plant tissues while *HvZIP8* seems to be constitutively expressed in the roots (Pedas *et al.,* 2009). *HvZIP3*, *HvZIP5*, *HvZIP8, HvZIP10 and HvZIP13* are located at the plasma membrane, and their levels of mRNA increase under Zn-deficiency conditions (Tiong *et al.,* 2015). Two ZIP proteins were isolated from a cDNA library constructed from roots of iron-deficient tomato plants: *LeIRT1* and *LeIRT2* (Eckhardt *et al.,* 2001). Both *LeIRT1* and *LeIRT2* complement a Fe-uptake-deficient yeast mutant, although only *LeIRT1* is up-regulated in the absence on Fe in the soil solution (Eckhardt *et al.,* 2001). The kinetic properties of an *Arabidopsis* IRT1 homolog were investigated in *Pisum sativum* by Cohen *et al.* (2004), and the results confirmed its primary role in high-affinity Fe transport. Six members of the ZIP protein family, *MtZIP1*, *MtZIP3*, *MtZIP4*, *MtZIP5*, *MtZIP6*, and *MtZIP7*, were identified in *Medicago truncatula,* a model plant species of the legume family (López-Millán *et al.,* 2004). Their topological structure is similar to that of *Arabidopsis* members. *MtZIP5* and *MtZIP6* mediate the transport of both Zn and Fe, *MtZIP1* and *MtZIP3* of Zn and Fe only, respectively, whereas *MtZIP4* and *MtZIP7* can restore yeast growth on Mn-limited media (López-Millán *et al.,* 2004). Two ZIP transporters have been isolated in poplar: *PtIRT1* and *PtIRT3* (Huang and Dai, 2015). Both *PtIRT1* and *PtIRT3* can restore Fe uptake in *fet3/fet4* yeast mutants and their expression is up-regulated under conditions of Fe-deficiency (Huang and Dai, 2015). The ZIP family of a perennial rootstock, trifoliate orange (*Poncirus trifoliata* L. Raf.) was also recently analyzed, and investigations revealed the presence of 12 different transporters (Fu *et al.,* 2017). A yeast complementation analysis was performed, showing that *PtIRT1* and *PtZIP7* can restore yeast growth on Fe-limited media; *PtIRT1*, *PtZIP1*, *PtZIP2*, *PtZIP3*, and *PtZIP12* can restore yeast growth on Zn-limited media and *PtIRT1* is also able to complement Mn-uptake-deficient yeast mutants (Fu *et al.,* 2017).

1.7 METAL TRANSPORT MECHANISMS:

Metal transporters mediate the transport of transition metals across cell membranes when they are in the proper oxidative state or complexed with the right metallophore (González-Guerrero *et al.,* 2016). Metal transporter families can be divided into two categories, according to the direction of transport: those involved in the uptake of metals, such as the ZIP, Nramp, YSL and COPT families, and transporters that release metals out of the compartments such as the CDF and P_{1B}-type ATPases families (Figure 1.5) (González-Guerrero *et al.,* 2016).

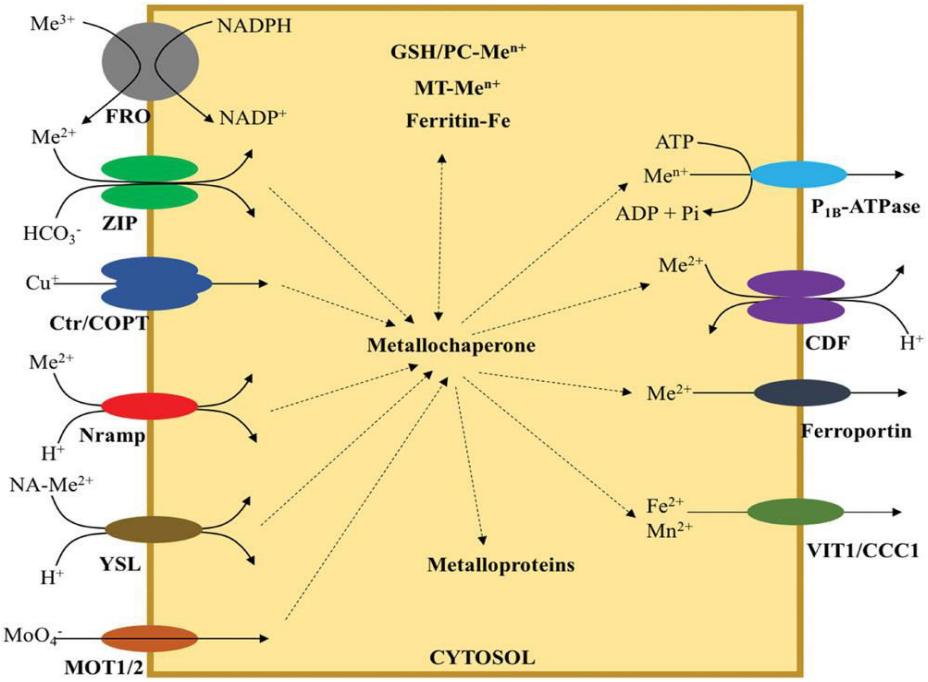

Figure 1.5: Model of the metal transport mechanisms (González-Guerrero *et al.,* 2016).

- ZIP transporters: Computational analyses suggest that ZIP proteins form homodimers, but the structure of these proteins has not been solved (González-Guerrero *et al.,* 2016). Lin *et al.* (2010) believe that these transporters work like channels, but other authors suggest a HCO_3^--symport activity (Gaither and Eide, 2000; Liu *et al.,* 2008).
- NRAMP transporters: These monomeric transporters are H^+symporters (Gunshin *et al.,* 1997). The metal-binding site consists of a methionine residue on the VI transmembrane domain (TM6), two aspartic acid residues on TM1 and a backbone carbonyl from TM6 (Ehrnstorfer *et al.,* 2010).
- YSL transporters: YSL proteins are involved in the transport of complexes between metals and chelating agents such as nicotianamine (NA) (Curie *et al.,* 2008). The mechanism is energized by a H^+-symport, as demonstrated by electrophysiological analyses on oocytes (Schaaf *et al.,* 2004).
- COPT transporters: These transporters form a Cu-specific channel operating as a homotrimer (Aller and Unger, 2006; Nose *et al.,* 2006).
- CDF transporters: CDF proteins form a homodimer energized by a H^+-antiport (Lu and Fu, 2007). These transporters possess three regions involved in the binding of the metal, referred to as site 1, 2 and 3, located in the TM region, the membrane-cytosol interface and the C-terminus region, respectively (Lu and Fu, 2007). Site 3 mediates dimerization whereas two aspartic acid residues (Asp) on TM2 and both an Asp and a histidine (His) residue on TM5 are thought ot mediate metal binding (Ricachenevsky *et al.,* 2013).

P_{1B}-type ATPases transporters: These transporters are monomers having two cytosol loops at the C-terminus region that form the ATPase domain. Metal binding is mediated by various amino acids present on the last three TMs and by metal-binding domains at the N- and C- termini (González-Guerrero and Argüello, 2008).

2. AIM OF THE WORK

Plants have developed a variety of mechanisms to maintain the cellular concentration of essential metals within physiological limits. A complex homeostatic network controls the uptake, chelation and transport of metal ions to ensure healthy amounts of essential elements, and avoid an excess of non-essential ones (Williams and Salt, 2009). Metal transporters play a key role in metal uptake from the soil, metal homeostasis and metal transport across the cell membranes. The ZIP (ZRT IRT1-like Proteins: Zinc-regulated transporter Iron-regulated transporter 1-like protein) family of metal transporters is involved in this complex network. Fifteen members of this family have been identified in *Arabidopsis thaliana,* which can be clustered into four main groups that share a sequence similarity between 38 and 85%. To better understand the role of these metal transporters we focused on *AtZIP4*, *AtZIP6* and *AtZIP9*, members of ZIP family. To date, neither *AtZIP6* or *AtZIP9* have been characterized, although a possible role in micronutrients vascular system uploading and root uptake has been hypothesized (Krämer *et al.,* 2007). Wintz *et al.* (2003) observed that both *AtZIP4* and *AtZIP9* are up-regulated in the roots and shoots of *A. thaliana* when Zn availability is scarce. *AtZIP6* does not belong to any of the four groups mentioned previously and Milner *et al.* (2013) revealed that it more highly expressed in the roots than the shoots, and does not appear to be modulated by changes in Zn or Fe concentrations (Wintz *et al.,* 2003). The aim of this project is to functionally characterize *AtZIP4, AtZIP6* and *AtZIP9,* and understand their role in metal homeostasis in *A. thaliana*. The promoter analysis for *AtZIP6* and *AtZIP9* was performed on transgenic *A. thaliana* lines carrying the promoter sequence fused to the GUS reporter gene whereas the promoter analysis of *AtZIP4* had already partly been carried out (Milner and Kochian, 2008; Lin *et al.,* 2016). The expression pattern of *AtZIP6* and *AtZIP9* revealed different tissue localizations. *AtZIP9* expression is present in the stomata of leaves, and in the root endodermis, cortex and epidermis, while *AtZIP6* is expressed in the vascular tissues of both roots and shoots. For this work, we analized single *AtZIP4, AtZIP6* and *AtZIP9* knockout mutants, *zip4/zip9*, *zip4/zip6*, *zip6/zip9* double mutants and *zip4/zip6/zip9* triple mutant obtained by crossing single homozygous mutant plants. These mutants were grown at different Zn, Fe and Mn concentrations, and ionomic analysis at different Zn concentrations was performed to detect differences in the accumulation of these elements. To analyze the effect of the overexpression of *ZIP4*, *ZIP6* and *ZIP9*, the coding sequences of these three genes was cloned downstream of the strong promoter CaMV35S. The constructs were introduced into *A. thaliana* obtaining different over-expressing lines. Furthermore, the subcellular protein localization was characterized in protoplasts transfected with genes encoding fusion proteins

of ZIP4 and ZIP9 with GFP, and GFP was observed at both the plasma membrane and the tonoplast.

3. MATERIALS AND METHODS

3.1 PLANT MATERIAL AND GROWTH CONDITIONS:

A. thaliana ecotype Columbia (Col-0) was used as a control for the experiments here described and the following ZIP knockout lines were taken into consideration:

- *zip4.1*; SALK_ 145371C - NASC ID: N664252
- *zip6.1*; SALK_116013 - NASC ID: N616013
- *zip6*.2; WiscDsLox233237_03O – NASC ID: N849271
- *zip9.1*; SALK_ 090000 - NASC ID: N590000
- *zip9*.2; SALK_090345 – NASC ID: N590345

For *in vitro* experiments, the surface of the seeds was sterilized for 1 min with 70% ethanol and for 13 min with 20% sodium hypochlorite and 0.03% Triton X-100, then rinsed three times with sterile water. They were therefore cultured on MS medium (Murashige and Skoog, 1962) at a 16-h light/8-h dark regime at 22 °C/18 °C (light intensity of 80 to 120 μmol $m^{-2}s^{-1}$). Alternatively, plants were grown in hydroponics or in the soil, and kept in greenhouse, under controlled conditions. The growth conditions for each experiment will be described in further detail in the following pages.

3.2 GENOMIC DNA EXTRACTION:

Plant genomic DNA was extracted by grinding 100 mg of fresh material in Extraction Buffer (200 mM Tris-HCl pH 8.0, 250 mM NaCl, 25 mM EDTA pH 8.0, 0.5% SDS), followed by a PCI (UltraPureTM Phenol:Chloroform:Isoamyl alcohol, Life Technologies, Löhne, Germany) purification and a 2-propanol precipitation step, according to standard protocols (Sambrook and Russell, 2001).

3.3 RNA EXTRACTION AND cDNA SYNTHESIS:

In order to verify gene expression, total RNA was isolated from fresh roots and leaves using TRIzol® reagent (Life Technologies, Carlsbad, CA, USA) following the manufacturer's instructions. Genomic DNA contaminations were removed using a RQ1 RNase-Free DNase (Promega, Madison, WI, USA) and the first-strand cDNA synthesis was performed by means of the Superscript® III Reverse Transcriptase (Life Technologies), following the instructions. A RNase H

(Life Technologies) treatment was performed to remove RNA from the hybrid cDNA-RNA filament.

3.4 PCR (POLYMERASE CHAIN REACTION):

The screening of transformed plants, mutants and colony PCR was carried out using GoTaq® DNA Polymerase (Promega) whereas high-fidelity amplification was performed using the High Fidelity Platinum® *Pfx* DNA Polymerase (Thermo Fisher Scientific), following the manufacturer's instructions.

3.5 REAL TIME PCR:

Real-Time PCR analysis was performed in triplicate on cDNA to analyze gene expression, using specific primers (Table 3.1) by means of the ABI PRISM® 7000 Sequence Detection System (Life Technologies) and KAPA SYBR® FAST qPCR Kits (Kapa Biosystems, Boston, USA). PCR amplification was conducted on the cDNA that was retro-transcribed from the RNA extracted from transgenic plants for 40 cycles, each comprising a 30-s step at 95°C, followed by a 30-s step at 55°C and one of equal duration at 72°C. Primers for the endogenous reference gene were designed on the two *Actin* isotype *ACT2* (*ACTIN2*; At3g18780) and *ACT8* (*ACTIN8*; At1g49240). The expression data were analyzed using the $2^{-\Delta\Delta CT}$ method (Livak and Schmittgen, 2001).

Table 3.1

Gene	Primer Name	Primer Sequence	Tm(°C)	Length(bp)
ZIP4	ZIP4-RT-For ZIP4-RT-Rev	5'-AGCTGATTTTCTGAGTAAGAGG-3' 5'-CAAATGGCGAGAGCAGACATA-3'	60 60	22 21
ZIP6	ZIP6-RT-For ZIP6-RT-Rev	5'- ATGTGCTTAATGTTCGCGGTA-3' 5'-GTTCGGGTTCTGATCATCGT -3'	60 60	21 20
ZIP9	ZIP9-RT-For ZIP9-RT-Rev	5'- ATTTGATCGCTGCGGATTT -3' 5'- TCATCCCAGCTCCAAGAAAC -3'	54 62	19 20
Actin	AtACT-RT-For AtACT-RT-Rev	5'-GAACTACGAGCTACCTGATG-3' 5'-CTTCCATTCCGATGAGCGAT-3'	60 60	20 20

3.6 SINGLE DOUBLE AND TRIPLE KNOCK-OUT MUTANTS:

Homozygous single knock-out mutants were screened by PCR using various primer pairs, designed to amplify the entire coding sequence and check the presence of the insertion using a primer that was specific for the T-DNA left border sequence (LBa1). The single knock-out mutants taken into consideration were:

- *zip4.1*: SALK_ 145371C - NASC ID: N664252
- *zip6.1*: SALK_116013 - NASC ID: N616013
- *zip6.2*: WiscDsLox233237_03O – NASC ID: N849271
- *zip9.1*: SALK_ 090000 - NASC ID: N590000
- *zip9.2*: SALK_090345 – NASC ID: N590345 (Inaba *et al.,* 2015).

To screen different *zip4.1* single knockout mutant plants, a ZIP4Int458-For primer was used, specific for an internal region of *AtZIP4* (Table 3.2). Double *zip4/zip6, zip4/zip9* and *zip6/zip9* knockout mutants were obtained by traditional crossing of the single homozygous *zip4.1, zip6.1* and *zip9.1* mutants and the triple *zip4/zip6/zip9* knockout mutant was obtained by crossing the double *zip6/zip9* and the single *zip4.1* mutants. The double and triple knockout mutants were confirmed by PCR using the primers listed in Table 3.2.

Table 3.2

Gene	Primer Name	Primer Sequence	Tm(°C)	Length(bp)
ZIP4	ZIP4Int458-For XhoI-ZIP4-Rev	5'-TGGATTTCATGGGGACACAGTACTA-3' 5'-CTCGAGCTAAGCCCAAATGGCGAGAG-3'	72	25
ZIP6	XbaI-ZIP6-For SacI-ZIP6-Rev	5'- TCTAGAATGGCTTCTTGCGTCACCGGA -3' 5'- GAGCTCCTAAGCCCAAAGAGCAAGTAG -3'	62 62	21 21
ZIP9	XbaI-ZIP9-For SacI-ZIP9-Rev	5'-TCTAGAATGGCGTCGATCCTTATCTC-3' 5'-GAGCTCTCAAGCCCAAATTGCAAGAGC -3'	60 62	21 21
T-DNA	LBa1	5'-TGGTTCACGTAGTGGGCCATCG-3'	70	22

3.7 PHENOTYPIC CHARACTERIZATION OF SINGLE KNOCK-OUT MUTANTS:

Single *zip4.1, zip6.1*, *zip9.1* knock out mutants were grown vertically in solid 1X Hoagland medium (1 mM KH_2PO_4, 2 mM $MgSO_4 \cdot 7H_2O$, 5 mM $Ca(NO_3)_2 \cdot 4H_2O$, 5 mM KNO_3, 46 µM H_3BO_3, 0.3 µM $CuSO_4$, 0.011 µM $NH_4MoO_4 4H_2O$, 1% Sucrose, 1% Agarose type A, pH 5.7) at different Zn, Fe and Mn concentrations:

- Zn: 0, 0.7 and 25 µM $ZnSO_4$
- Fe: 0, 24 and 150 µM FeNaEDTA
- Mn: 0, 9 and 100 µM $MnSO_4$

The primary root length and the dry weight of shoots were measured after 10 days.

3.8 ANALYSIS OF METAL CONTENT:

Accumulation analysis was performed on single *zip4.1, zip6.1*, *zip9.1*, double *zip4/zip6, zip4/zip9, zip6/zip9* and triple *zip4/zip6/zip9* knockout lines and the Col-0 control using two different systems: *in vitro* on plates and *in vivo* on hydroponic culture. For the *in vitro* experiments, seeds were surfaced-sterilized as described previously and plants were grown vertically for 2 weeks on solid 1/10 modified Hoagland medium (100 µM $NH_4H_2PO_4$, 200 µM $MgSO_4$, 400 µM $Ca(NO_3)_2$, 600 µM KNO_3, 5 µM Fe-HBED, 4.63 µM H_3BO_3, 0.032 µM $CuSO_4$, 0.915 µM $MnCl_2$, 0.011 µM MoO_3, 1% Sucrose, 1% Agarose type A, pH 5.7) at 4 different Zn concentrations: 0, 0.07, 5, 50 µM $ZnSO_4$. For the hydroponic treatment, seeds were vernalized and germinated in 1/10 Hoagland 0.5% (w/v) agar-filled tubes cut at the bottom and placed in liquid 1/10 Hoagland medium without sucrose and MES for 2 weeks. The solution was replaced every week. Subsequently the plants were treated for 2 weeks in liquid 1/10 Hoagland with three different Zn concentrations: 0, 2, 10 µM $ZnSO_4$. Plants were grown in a climate-controlled chamber (10-h light/14-h dark regime at 22 °C/18 °C, light intensity of 80 to 120 µmol $m^{-2}s^{-1}$, relative humidity 40-65%). Three and five replicates were used for the *in vitro* and hydroponics experiment, respectively. Roots were harvested and rinsed with 10 mM $CaCl_2$ and deionized sterile water, whereas the shoots were only rinsed with deionized water. They were then blot dried, placed on the bottom of Pyrex tubes and air-dried for 48 h in a hot air oven at 60°C. The samples were digested with 1 mL HNO_3 Primar Plus™ (Fisher Chemical, Thermo Fisher Scientific) spiked with indium internal standard for 4 h at 115°C using a DigiPREP MS block digestion system (SCP Science; QMX Laboratories, Essex, UK). The sample were diluted to 10 mL with sterile deionized water and analyzed using an inductively coupled plasma-mass spectrometry (ICP-MS), PerkinElmer NexION 2000 equipped with Elemental Scientific Inc. autosampler, in the collision mode (He). Calibration standards were prepared using single-element standard solutions (Inorganic Ventures; Essex Scientific Laboratory Supplies Ltd, Essex, UK).

3.9 LOCALIZATION OF *AtZIP4*, *AtZIP6* AND *AtZIP9* EXPRESSION THROUGH HISTOCHEMICAL GUS ASSAY:

The putative promoters of *AtZIP4, AtZIP6* and *AtZIP9*, pZIP4 (corresponding to 2000 bp, TAIR Accession: Locus: 2197459), pZIP6 (corresponding to 1971 bp, TAIR Accession: Locus:2045634) and pZIP9 (corresponding to 2002 bp, TAIR Accession: Locus:2123787) were amplified by means of a *Pfx* DNA polymerase (Thermo Fisher Scientific) from the genomic DNA of *A. thaliana* Col-0

extracted from its leaves, using primers designed on the regions corresponding to the recognition sequences for the restriction enzymes HindIII (at the 5'-end) and BamHI (at the 3'-end) and described in Table 3.3.

Table 3.3

Gene	Primer Name	Primer Sequence	Tm(°C)	Length(bp)
pZIP4	HindIII-pZIP4-For BamHI-pZIP4-Rev	5'-AAGCTTGGAAGAACAGAGGTGGCTAT-3' 5'-GGATCCGGGAACAAGAGTTTATTCTTCT-3'	60 60	20 21
pZIP6	HindIII-pZIP6-For BamHI-pZIP6-Rev	5'-AAGCTTCTTGGTTACAAAGTAGCTCCATC-3' 5'-GGATCCTTGTGGAAGAAGAAGAAAGAGAG-3'	66 64	23 23
pZIP9	HindIII-pZIP9-For BamHI-pZIP9-Rev	5'-AAGCTTGGGTGGTGCTTGTTGGGTTAT-3' 5'-GGATCCAGCTGCGAACTTGAGGGTAAG-3'	64 64	21 21

The three promoters were inserted into the pGEM® T-Easy vector (Promega) and checked by sequencing using specific primers designed on the internal sequence of the amplicons to cover the full length of the sequences (Table 3.4) and then cloned into the binary plasmid pBI121 (Clontech, Mountain View, CA-USA) upstream of the GUS reporter gene.

Table 3.4

Gene	Primer Name	Primer Sequence	Tm(°C)	Length(bp)
pZIP4	Int-pZIP4-forward	5'-GTTTGCAACTGTGCTTGTAATC-3'	62	22
pZIP6	Int-pZIP6-forward Int-pZIP6-reverse	5'-GGCACTATCCAACATATGTTAGC-3' 5'-GCTAACATATGTTGGATAGTGCC-3'	66 66	25 24
pZIP9	Int-pZIP9-forward Int-pZIP9-reverse	5'-CATTACTAGTATTTCGCATTGTAAT-3' 5'-CGAAATACTAGTAATGTTTTGCGT-3'	64 64	19 21

3.10 TRANSFORMATION OF *A. thaliana* BY FLORAL DIPPING:

A. thaliana ecotype Columbia (Col-0) plants were transformed by floral dipping (Clough and Bent, 1998). The aerial parts of *A. thaliana* plants were dipped into an Agrobacterium suspension for 2 min with gentle agitation and were then transferred to the greenhouse (Zhang *et al.,* 2006).

3.11 GUS HISTOCHEMICAL ASSAY:

pZIP4::GUS, pZIP6::GUS and pZIP9::GUS lines were grown vertically on 1/2 strength Hoagland medium for 7 days. Plants were incubated overnight at 37°C with the GUS reaction buffer (100 mM sodium phosphate buffer, pH 7.0, 1 mM EDTA, pH 8.0, 2 mM potassium ferrocyanide, 2 mM potassium ferricyanide,1% Triton X-100, 500 mg/L 5-bromo-4-chloro-3-indolyl β-D-glucuronide in dimethylformamide) to detect GUS expression (Basu *et al.,* 2003). The plants were then incubated in 70% ethanol at 70°C for 10 min to remove the chlorophyll. Roots were also fixed in 0.1% glutaraldehyde and 4% paraformaldehyde in a 100 mM sodium phosphate buffer, pH 7.2, followed

by a dehydration step in increasing concentrations of ethanol. Roots were included in Paraplast® (Sigma Aldrich), after which ethanol was gradually substituted by xylene, as previously described (Ruzin, 1999). Cross-sections were obtained using the Leica RM2125 RTS (Leica Biosystems) microtome and the images were taken using a Leica MZ16 F stereomicroscope (Leica Microsystem GmbH, Wetzlar, Germany) and a Leica DM RB microscope (Leica Microsystem GmbH).

3.12 PREPARATION OF THE CONSTRUCTS FOR THE SUBCELLULAR LOCALIZATION OF *AtZIP4*, *AtZIP6* AND *AtZIP9*:

The coding sequences of *AtZIP4*, *AtZIP6* and *AtZIP9* were fused separately to the N- and C-terminus of the coding sequence of the green fluorescent protein (eGFP). The three genes were amplified using primers with specific restriction sites (Table 3.5) to allow the cloning of the fusion genes into the pMD1 expression vector downstream of the sequence of the CaMV35S promoter. The fusion constructs thus obtained, i.e. pMD1-eGFP::*AtZIP4* and pMD1-eGFP::*AtZIP9,* were introduced into competent *Agrobacterium tumefaciens* (strain EHA105) cells. *A. thaliana* cv. Col-0 plants were therefore stably transformed by floral dipping and the presence of the transgene checked by PCR on the genomic DNA of selected lines. The eGFP reporter protein was also fused to the C- terminus of ZIP4, ZIP6 and ZIP9, obtaining the pMD1-*AtZIP4*:: eGFP, pMD1- *AtZIP6*:: eGFP and pMD1- *AtZIP9*:: eGFP constructs, respectively. Moreover, ZIP4, ZIP6 and ZIP9 deprived of the last transmembrane domain were cloned into the pMD1 expression vector in frame with the N-terminus of eGFP, obtaining the *AtZIP4*noUTM::eGFP, *AtZIP6* noUTM:: eGFP and *AtZIP9* noUTM:: eGFP genes. These constructs were used for experiments of transient expression in *A. thaliana* protoplasts (Section 3.13).

3.13 PROTOPLAST ISOLATION AND TRANSFECTION WITH THE CONSTRUCTS FOR THE SUBCELLULAR LOCALIZATION OF *AtZIP4*, *AtZIP6* AND *AtZIP9*:

Leaves were collected from 3-4 week-old *A. thaliana* ecotype Columbia (Col-0) plants grown under short photoperiod conditions (10-h light/14-h dark regime at 22 °C/18 °C, light intensity of 80 to 120 µmol $m^{-2}s^{-1}$, relative humidity 40-65%). The cell layer of the lower epidermal surface was peeled off using a specific tape (Shamrock Labels) and incubated for 3 h in an enzymatic solution (20 mM MES, 1.5% cellulose R10, 0.4% macerozyme R10, 0.4 M mannitol, 20 mM KCl, 10 mM

$CaCl_2$ and 0.1% BSA, pH 5.7) as described by Yoo *et al.* (2007). The enzyme/protoplast solution was diluted with an equal volume of W5 solution (2 mM MES, 154 mM NaCl, 125 mM $CaCl_2$ and 5 mM KCl, pH 5.7) and filtered with a 75-µm nylon mesh. After a centrifugation at 100*g* for 1 min the pellet was re-suspended in W5 at 2 X 10^5 mL^{-1}, stored on ice for 30 min and the pellet obtained from precipitation was re-suspended at 2 X 10^5 mL^{-1} in MMG (4 mM MES, 0.4 M mannitol and 15 mM $MgCl_2$, pH 5.7). The transfection was performed adding 110 µL of PEG (40% PEG4000, 0.2 M mannitol and 100 mM $CaCl_2$) solution to 10 µL (10-20 µg of plasmid DNA) and 100 µL of protoplast for 5 min. The transfection was performed by adding 110 µL PEG solution (40% PEG4000, 0.2 M mannitol and 100 mM $CaCl_2$) to 10 µL (10-20 µg of plasmid DNA) and 100 µL of protoplast suspension and leaving it to incubate for 5 min.

Table 3.5

Gene	Primer Name	Primer Sequence	Tm(°C)	Length(bp)
eGFP::*AtZIP4*, eGFP::*AtZIP6* and eGFP::*AtZIP9*				
ZIP4	BamHI-ZIP4-For XhoI-ZIP4-Rev	5'-GGATCCATCTTCGTCGATGTTCTTTGGA-3' 5'-CTCGAGCTAAGCCCAAATGGCGAGAGC-3'	62 66	22 21
ZIP6	SalI-ZIP6-For SacI-ZIP6-Rev	5'-GTCGACGCTTCTTGCGTCACCGGAAC-3' 5'-GAGCTCCTAAGCCCAAAGAGCAAGTAG-3'	64 62	20 21
ZIP9	SalI-ZIP9-For SacI-ZIP9-Rev	5'-GTCGACGCGTCGATCCTTATCTCCGG-3' 5'-GAGCTCTCAAGCCCAAATTGCAAGAGC-3'	64 62	20 21
GFP	XbaI-GFP-For BamHI-GFP4-Rev SalI-GFP6/9- Rev	5'-TCTAGAATGGTGAGCAAGGGCGAGGA-3' 5'-GGATCCCTTGTACAGCTCGTCCATGC-3' 5'-GTCGACCTTGTACAGCTCGTCCATGC-3'	64 62 62	20 20 20
***AtZIP4*::eGFP, *AtZIP6*:: eGFP and *AtZIP9*:: eGFP**				
ZIP4	XbaI-ZIP4C-For SalI-ZIP4C-Rev	5'-TCTAGAATGATCTTCGTCGATGTTCTTTG-3' 5'-GTCGACAGCCCAAATGGCGAGAGCAG-3'	64 62	23 20
ZIP6	XbaI-ZIP6-For SalI-ZIP6C-Rev	5'-TCTAGAATGGCTTCTTGCGTCACCGGA-3' 5'-GTCGACAGCCCAAAGAGCAAGTAGTG-3'	62 60	21 20
ZIP9	XbaI-ZIP9-For SalI-ZIP9C-Rev	5'-TCTAGAATGGCGTCGATCCTTATCTC-3' 5'-GTCGACAGCCCAAATTGCAAGAGCAG-3'	60 60	20 20
GFP	SalI-GFP-For SacI-GFP-Rev	5'-GTCGACGTGAGCAAGGGCGAGGAGC-3' 5'-GAGCTCTTACTTGTACAGCTCGTCCATG-3'	64 64	25 28
***AtZIP4*noUTM::eGFP, *AtZIP6*noUTM::eGFP and *AtZIP9*noUTM::eGFP**				
ZIP4noUTM	XbaI-ZIP4C-For SalI-4noUTM-Rev	5'-TCTAGAATGATCTTCGTCGATGTTCTTTG-3' 5'-GTCGACTTCAGCCCTCAAATTACAAC TCATCCTC -3'	64 62	23 28
ZIP6noUTM	XbaI-ZIP6-For SalI-6noUTM-Rev	5'-TCTAGAATGGCTTCTTGCGTCACCGGA-3' 5'-GTCGACTTCAGCGAGGCGAGAACCCGATTC -3'	62 58	21 24
ZIP9noUTM	XbaI-ZIP9-For SalI-9noUTM-Rev	5'-TCTAGAATGGCTTCTTGCGTCACCGGA-3' 5'-GTCGACTTCAGCTCTGAAATCAACACTCATCTTC -3'	62 60	21 28
GFP	SalI-GFP-For SacI-GFP-Rev	5'-GTCGACGTGAGCAAGGGCGAGGAGC-3' 5'-GAGCTCTTACTTGTACAGCTCGTCCATG-3'	64 64	19 22

The transfection mixture was then diluted with 440 µL of W5 solution and after a 2-min centrifugation at 100*g,* the protoplast pellet was re-suspended in 1 mL of WI (4 mM MES, 0.5 M

mannitol and 20 mM KCl, pH 5.7) solution and incubated for 18 h at room temperature (20-25 °C). Images were taken with a Leica TCS SP5 confocal microscope using a 488-nm argon laser for the detection of GFP in the lambda range of 496- to 555-nm, and both 488-nm and 561- nm lasers for the chloroplast auto-fluorescence detection at 651 to 800 nm.

3.14 YEAST TRANSFORMATION AND COMPLEMENTATION:

AtZIP4 and *AtZIP9* were tested for their ability to complement various metal uptake-deficient yeast mutants and determine their transport specificity. Different yeast lines defective in the plasma membrane uptake mechanisms for Zn (*zrt1/zrt2Δ*), Fe (*fet3/ fet4Δ*), Mn (*smf1Δ*), the vacuolar uptake of Zn (*zrc1/cot1 Δ*), export of Zn across the tonoplast *(zrt3Δ*), as well as the control (DY1457) were transformed and analyzed. The *S. cerevisiae* lines used were:

- ***zrt1zrt2*** (MATalfa, *ade6, can1, his3, leu2, trp1, ura3, zrt1::*LEU2, *zrt2::*HIS)
- ***fet3fet4*** (MATalfa, *ade6, can1, his3, leu2, trp1, ura3, fet3::*HIS3, *fet4::*LEU2)
- ***smf1*** (MATalfa, *ura3*, *lys2*, *leu2*, *his3*, *smf1*-KAN^R)
- ***zrc1cot1*** (MATalfa, *can1-100oc, his3, leu2, trp1, ura3-52, zrc1::*HIS3, *cot1::*URA3)
- ***zrt3*** (MATalfa, *can1-100oc, his3, leu2, trp1, ura3-52, zrt3*-KAN^R)
- **DY1457** (MATalfa, *ade6*, *can1*, *his3, leu2*, *trp1, ura3*)

For the transformation of *S. cerevisiae,* the strains were grown in liquid SD (7 g/L Yeast Nitrogen Base w/o amino acids and complete CSM medium) overnight at 30°C, stirring continuously, and transferred to 50 mL of SD medium to reach an OD_{600} of 0.7-0.8. Subsequently, 1 mL of the culture was centrifuged at 1000x *g* for 5 min, re-suspended in sterile water and after another centrifugation, in 10 µL of 100 mM LiAc. 0,1 µg of the plasmid suspension was added to 300 µL of PEG (40% PEG4000, 100 mM LiAc and 0.3 mg/mL Salmon Sperm DNA) solution and, after 30 min at 30 °C and 15 min at 42°C, was resuspended in 500 µL of water and 50 µL were plated on a SD (7 g/L Yeast Nitrogen Base w/o amino acids, 20 g/L Microagar and CSM medium “dropped out” of specific amino acids) selective medium. The primers used to amplify *AtZIP4* and *AtZIP9* are listed in Table 3.6. *AtZIP9* was introduced into the yeast expression vector pADSL to complement *zrc1/cot1Δ* and *zrt3Δ* mutants, whereas *AtZIP4* was cloned into the pADSL vector to complement *zrt1/zrt2Δ* and *fet3/ fet4Δ* and into the yeast expression vector pNEV-N to complement the *smf1Δ* strain.

Table 3.6

Gene	Primer Name	Primer Sequence	Tm(°C)	Length(bp)
ZIP4	BamHI-YeastZIP4-For	5'-GGATCCATGATCTTCGTCGATGTTCTTTG-3'	64	23
	SalI-ZIP4yeast-Rev	5'-GTCGACCTAAGCCCAAATGGCGAGAGC-3'	62	21
	NotI-YeastZIP4-For	5'-GCGGCCGCATGATCTTCGTCGATGTTCTTTG-3'	64	23
	NotI-YeastZIP4-Rev	5'-GCGGCCGCCTAAGCCCAAATGGCGAGAGC-3'	64	21
ZIP9	SmaI-YeastZIP9-For	5'-CCCGGGATGGCGTCGATCCTTATCTC-3'	60	20
	SalI-ZIP9yeast-Rev	5'GTCGACTTCAGCTCTGAAATCAACACTCATCTTC3'	60	28

Yeast mutants were grown in a selective liquid SD medium to an OD of 1, then serially diluted 10- and 100-fold and 5 µl were plated on a solid selective SD medium containing:

- 1 mM EDTA and 500 µM $ZnCl_2$ to create Zn-limiting conditions for the *zrt1/zrt2Δ* mutant (Pence *et al.,* 2000);
- 80 µM bathophenanthroline disulphonate (BPS) to create Fe-limiting conditions for the *fet3/fet4Δ* mutant (Eide *et al.,* 1996).
- 0, 0.2, 5, 10, 15 µM $ZnSO_4$ for the *zrc1/cot1Δ* mutant (Kawachi *et al.,* 2008).

3.15 LOCALIZATION OF *AtZIP4*, *AtZIP6* AND *AtZIP9* EXPRESSION THROUGH GFP REPORTER LINES:

The putative promoters of *AtZIP4, AtZIP6* and *AtZIP9* were amplified using the primer pairs listed in Table 5, to obtain eGFP reporter lines driven by the native promoter. The primers were designed on selected regions corresponding to the recognition sequences for the restriction enzymes HindIII (at the 5'-end) and XbaI (at the 3'-end), to replace the sequence of the CaMV35S promoter of the pMD1-*AtZIP4*noUTM::eGFP, pMD1- *AtZIP6* noUTM:: eGFP and pMD1- *AtZIP9* noUTM:: eGFP lines obtained previously (Table 3.7).

Table 3.7

Gene	Primer Name	Primer Sequence	Tm(°C)	Length(bp)
pZIP4	HindIII-pZIP4-For	5'-AAGCTTGGAAGAACAGAGGTGGCTAT-3'	60	20
	XbaI-pZIP4-Rev	5'-TCTAGAGGGAACAAGAGTTTATTCTTCT-3'	60	22
pZIP6	HindIII-pZIP6-For	5'-AAGCTTCTTGGTTACAAAGTAGCTCCATC-3'	66	23
	XbaI-pZIP6-Rev	5'-TCTAGATTGTGGAAGAAGAAGAAAGAGAG-3'	64	23
pZIP9	HindIII-pZIP9-For	5'-AAGCTTGGGTGGTGCTTGTTGGGTTA-3'	62	21
	XbaI-pZIP9-Rev	5'-TCTAGAAGCTGCGAACTTGAGGGTAAG-3'	64	21

3.16 *AtZIP4*, *AtZIP6* AND *AtZIP9* OVEREXPRESSING LINES AND THEIR PHENOTYPIC CHARACTERIZATION:

To obtain lines over-expressing *AtZIP4*, *AtZIP6* and *AtZIP9,* the coding sequence of each gene was amplified using the primers reported in Table 3.8 and introduced into the plant pMD1 expression vector down-stream of the CaMV35S promoter. The pMD1-35S::*AtZIP4,* pMD1-35S::*AtZIP6* and pMD1- 35S::*AtZIP9* vectors were introduced into *A. tumefaciens* strain EHA105 for the transformation of *A. thaliana* by floral dipping (Section 3.10). *AtZIP4*, *AtZIP6* and *AtZIP9* were also cloned in the plant pH2GW7 over-expressing vector, which is endowed with a hygromycin-resistance gene. Three single copy homozygous lines of *AtZIP4* (*AtZIP4*ox) and *AtZIP6* (*AtZIP6*ox) were selected and grown vertically for 10 days in solid 1X Hoagland medium (1 mM KH_2PO_4, 2 mM $MgSO_4 \cdot 7H_2O$, 5 mM $Ca(NO_3)_2 \cdot 4H_2O$, 5 mM KNO_3, 46 µM H_3BO_3, 0.3 µM $CuSO_4$, 0.011 µM $NH_4MoO_4 4H_2O$, 1% Sucrose, 1% Agarose type A, pH 5.7) at the following Zn and Fe concentrations:

- Zn: 0, 0.7 and 25 µM $ZnSO_4$
- Fe: 0, 24 and 150 µM FeNaEDTA

Table 3.8

Gene	Primer Name	Primer Sequence	Tm(°C)	Length(bp)
pMD1-35S::*AtZIP4* and pH2GW7- 35S:: *AtZIP4*				
ZIP4	BamHI-ZIP4-For	5'-GGATCCATGATCTTCGTCGATGTTCTTTG-3'	64	23
	XhoI-ZIP4-Rev	5'-CTCGAGCTAAGCCCAAATGGCGAGAG-3'	62	20
	SpeI-ZIP4-For	5'-ACTAGTATGATCTTCGTCGATGTTCTTTG-3'	64	23
	BamHI-ZIP4-Rev	5'-GGATCCCTAAGCCCAAATGGCGAGAGC-3'	66	21
pMD1-35S::*AtZIP6* and pH2GW7- 35S:: *AtZIP6*				
ZIP6	XbaI-ZIP6-For	5'- TCTAGAATGGCTTCTTGCGTCACCGGA -3'	62	21
	SacI-ZIP6-Rev	5'- GAGCTCCTAAGCCCAAAGAGCAAGTAG -3'	62	21
	SpeI-ZIP6-For	5'-ACTAGTATGGCTTCTTGCGTCACCG-3'	60	19
	SmaI-Zip6-Rev	5'-CCCGGGCTAAGCCCAAAGAGCAAGTAG-3'	62	21
pMD1-35S::*AtZIP9* and pH2GW7- 35S:: *AtZIP9*				
ZIP9	XbaI-ZIP9-For	5'-TCTAGAATGGCGTCGATCCTTATCTC-3'	60	21
	SacI-ZIP9-Rev	5'-GAGCTCTCAAGCCCAAATTGCAAGAGC -3'	62	21
	SpeI-ZIP9-For	5'-ACTAGTATGGCGTCGATCCTTATCTC-3'	60	20
	SmaI-ZIP9-Rev	5'-CCCGGGTCAAGCCCAAATTGCAAGAGC-3'	62	21

3.17 STATISTICAL ANALYSIS:

Data regarding the relative expression of *AtZIP4*, *AtZIP6* and *AtZIP9*, the phenotypic analysis of single knock out and over-expressing lines, and the analysis of metal content of single, double and triple knock-mutant mutants are reported in histograms as mean ± SEM. Statistical analysis of data was performed using the one-way analysis of variance (ANOVA) followed by a post hoc Tukey's test using the GraphPad Prism 7 (GraphPad Software). Statistical significant variations are marked by asterisks (*P<0.05; **P<0.01; ***P<0,001; ****P<0,0001).

3.18 ZINPYR-1 STAINING:

A 5 µM working solution of Zinpyr-1 in 0.9% saline was prepared by diluting a 1 mM stock made up in dimethyl sulphoxide (DMSO), as described by Sinclair *et al.* (2007). Seven day-old *A. thaliana* seedlings were washed with deionized water and incubated in the Zinpyr-1 working solution in the dark and at room temperature for 3 h. Samples were immersed in water and then stained with 75 µM propidium iodide (PI). Images were taken with a Leica TCS SP5 confocal microscope using a 488-nm argon laser for the detection of Zinpyr-1 in the lambda range of 500- to 540-nm, and 561- nm lasers for PI detection at 600 to 670 nm. The cross-sections of the roots were obtained by dipping the roots in a melted 4% agarose gel and then left to solidify. The slides were obtained using a Leica VT1000 S (Leica, Bensheim, Germany) vibratome.

3.19 CRYO-SECTIONING AND X-RAY SPECTROMICROSCOPY:

Seeds of the single *zip4.1, zip6.1*, *zip9.1*, *hma4* (used as control), double *zip4/zip6, zip4/zip9, zip6/zip9,* triple *zip4/zip6/zip9* knockout mutants and Col-0 lines were grown vertically on plates on solid 1/10 modified Hoagland medium (100 µM $NH_4H_2PO_4$, 200 µM $MgSO_4$, 400 µM $Ca(NO_3)_2$, 600 µM KNO_3, 5 µM Fe-HBED, 4.63 µM H_3BO_3, 0.032 µM $CuSO_4$, 0.915 µM $MnCl_2$, 0.011 µM MoO_3, 1 µM $ZnSO_4$, 1% Sucrose, 1% Agarose type A, pH 5.7) for 1 week in a climate-controlled chamber (10-h light/14-h dark regime at 22 °C/18 °C, light intensity of 80 to 120 µmol , relative humidity 40-65%). Six primary roots for each genotype were cut into 8-10 mm-long pieces, dipped and aligned in a tissue freezing medium (Leica) and frozen in liquid propane first and then in liquid nitrogen. The root pieces were sectioned with a Leica CM3050 cryo-microtome (Leica, Bensheim, Germany) with a thickness of 40 µm and the section were freeze-dried using an Alpha 2-4 freeze dryer (Martin Christ, Osterode am Harz, Germany). 10-20 sections were obtained for each

root and the LEXRF measurements were performed using the TwinMic Beamline at the Elettra Synchrotron of Trieste (http://www.elettra.trieste.it), (BL 1.1L). Three different scans of 80 x 80 μm were performed at micrometric resolution for each genotype.

4. RESULTS AND DISCUSSION

4.1 STUDY OF *AtZIP4*, *AtZIP6* AND *AtZIP9* EXPRESSION:

The expression of the ZIP family members has been well investigated in recent works, although the specific role of these transporters is still a matter of study. Wintz *et al.* (2003) for example showed that in *A. thaliana* both *AtZIP4* and *AtZIP9* are up-regulated in shoots and roots under Zn starvation conditions, whereas *AtZIP6* does not seem to be regulated by variations in Zn and Fe concentrations. Jain *et al.* (2013) confirmed that both *AtZIP4* and *AtZIP9* are induced by low Zn availability and observed a significant reduction in the expression of these two genes at excess levels of Zn in the roots and shoots. These results were also confirmed at root level by Inaba *et al.* (2015). The expression profile of these genes was mainly tested under different Zn, Cu and low-Fe conditions (Wintz *et al.,* 2003; Jain *et al.,* 2013; Inaba *et al.,* 2015). In this work, we analyzed the expression of *AtZIP4*, *AtZIP6* and *AtZIP9* by Real Time PCR on *A. thaliana* cv. Col-0 at various levels of Fe, Mn and Zn and in their absence (Figure 4.1). *AtZIP4* is highly induced under low Zn conditions in both roots and shoots but its expression is reduced when Zn is present in excess, as reported previously (Wintz *et al.,* 2003; Jain *et al.,* 2013). Under Fe deficiency conditions, *AtZIP4* is significant down-regulated in the roots, as observed by Wintz *et al.* (2003) and a similar trend was also observed at high levels of Fe. No significant differences were observed in roots growing in excess Mn and in shoots at different concentration of Fe and Mn. These results suggest that *AtZIP4* may have a high affinity for Zn, and a low affinity for Fe. Moreover, the down-regulation of *AtZIP4* at low Fe availability suggests that under these conditions plants suffer from excess Zn, and display the same regulation mechanisms observed in the presence of high levels of this metal. In the shoots, *AtZIP6* expression seems unaffected by excess or absence of Zn and also by changes in the concentrations of Fe and Mn (Figure 4.1). With regard to the roots, we observed that *AtZIP6* is not modulated either by the lack or excess of Zn, Fe and Mn, confirming the pattern of expression obtained by both Wintz *et al.* (2003) and Jain *et al.* (2013). Our results concerning *AtZIP6* expression in roots and shoots suggest that it may either be constitutively expressed or uninvolved in the transport of these metals.

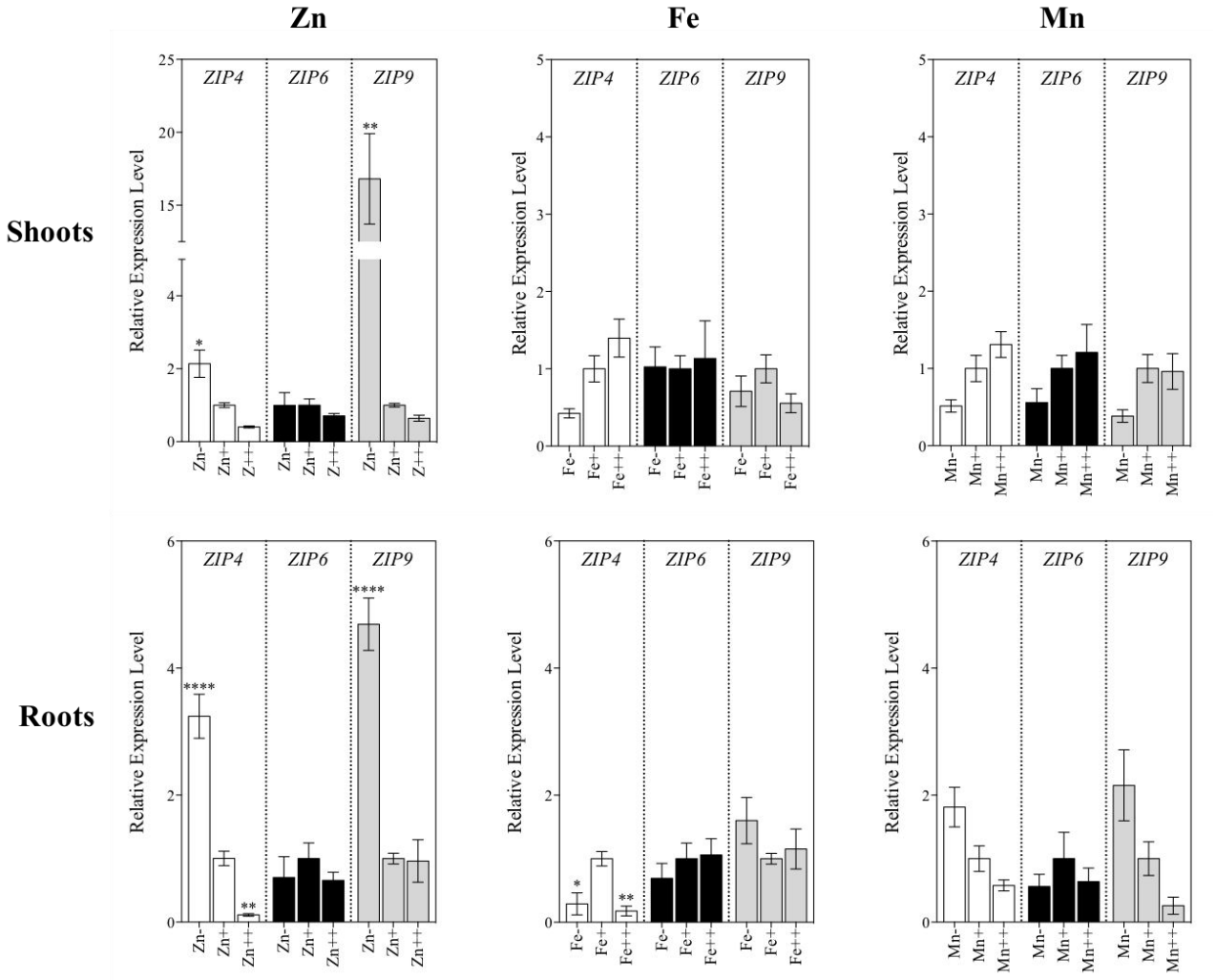

Figure 4.1: Relative amounts of *AtZIP4*, *AtZIP6* and *AtZIP9* in root and shoot tissues of *A. thaliana* cv. Col-0 plants grown at different Zn, Fe and Mn concentrations. Zn-, Zn+ and Zn++ refer to 0, 0.7 and 25 µM $ZnSO_4$, Fe-, Fe+ and Fe++ refer to 0, 24 and 150 µM FeNaEDTA whereas Mn-, Mn+ and Mn++ refer to 0, 9 and 100 µM $MnSO_4$, respectively. The expression under Zn+, Fe+ and Mn+ conditions was set to 1 as the frame of reference.

Conversely, *AtZIP9* is greatly induced under low Zn condition in both roots and shoots, confirming the results reported in the literature (Wintz *et al.,* 2003; Jain *et al.,* 2013; Inaba *et al.,* 2015). Surprisingly, it does not appear to be down-regulated in roots at excess Zn levels, unlike what reported by Jain *et al.* (2013) and Inaba *et al.* (2015), although this analysis was performed in two independent experiments. Different amounts of Fe did not affect *AtZIP9* expression either in roots or shoots (Figure 4.1). Unlike the shoots, *AtZIP9* expression in the roots seems to be slightly up-regulated at low Mn availability, suggesting a possible role in Mn transport, although the differences are no significant, and certainly not as strong as the induction observed under low Zn conditions.

4.2 SINGLE *AtZIP4*, *AtZIP6* AND *AtZIP9* KNOCK-OUT MUTANTS:

Single *AtZIP4* (*zip4.1*), *AtZIP6* (*zip6.1*) and *AtZIP9* (*zip9.1*) knockout mutants were screened by PCR to verify that the mutations had actually occurred (Figure 4.2). Furthermore, another mutant for both *AtZIP6* (*zip6.2*) and *AtZIP9* (*zip9.2*) was selected to better investigate the function of these genes and will be used to confirm the results obtained with the first single knockout mutants (data not shown). The *zip4.1* knockout mutant exhibits the T-DNA insertion in the fourth exon, whereas *zip6.1* and *zip9.1* mutants are both interrupted in the central intron. To confirm the lack of gene expression, Real Time PCR on *AtZIP4, AtZIP6* and *AtZIP9* in the respective insertional lines were performed on plants grown under Zn-deficiency conditions and their controls (Figure 4.3).

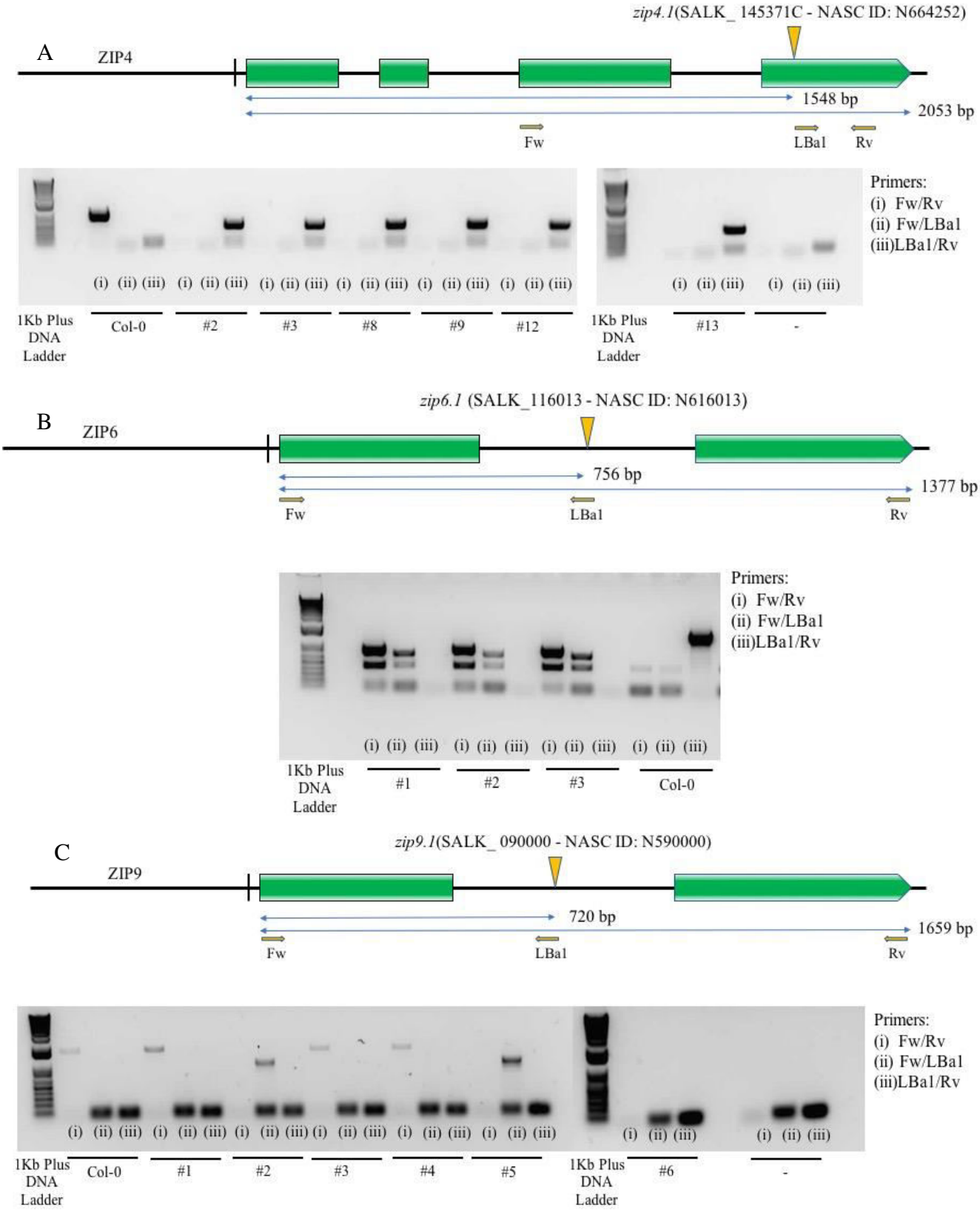

Figure 4.2: Screening of homozygous lines for the single A) *zip4.1*(SALK_ 145371C), B) *zip6.1* (SALK_116013) and C) *zip9.1* (SALK_ 090000) knockout mutants. Green boxes are the exons separated by a black line (the introns), and the yellow triangle is where the T-DNA insertion is located. Each mutant was checked by PCR using different primer pairs: (i) Fw/Rv to amplify the entire gene, (ii) Fw/LBa1 and (iii) LBa1/Rv to verify the presence of the T-DNA insertion.

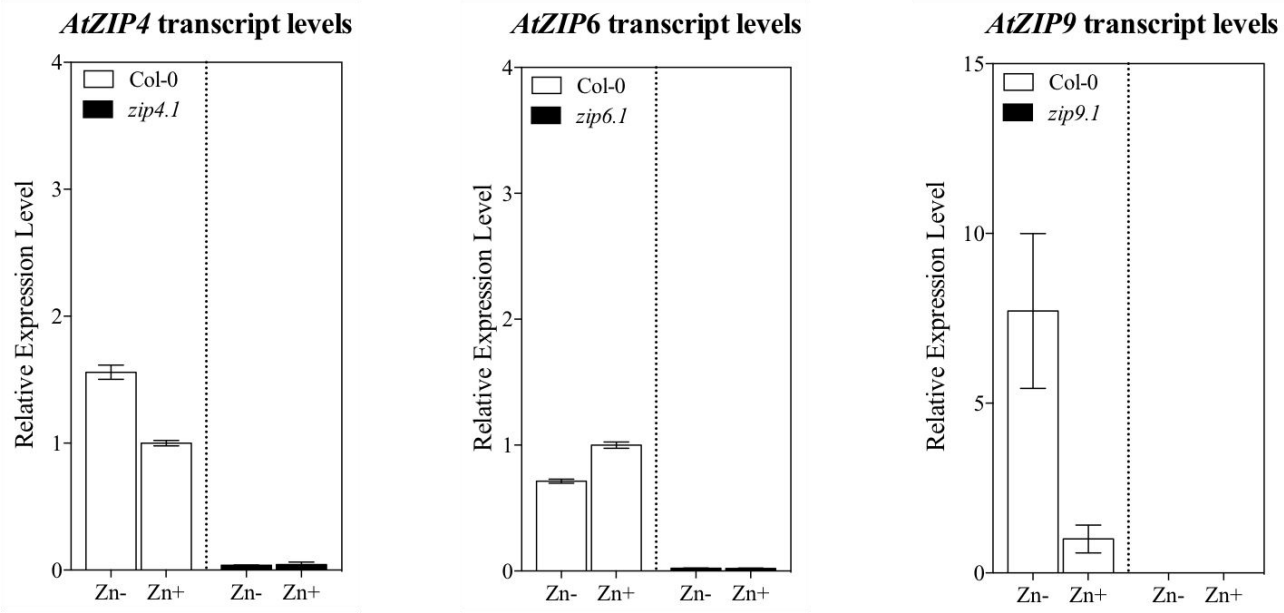

Figure 4.3: Relative expression of A) *AtZIP4,* B) *AtZIP6* and C) *AtZIP9* in wt, *zip4.1*, *zip6.1* and *zip9.1* single knockout mutants, respectively, at different concentrations of Zn, determined by Real Time PCR. Bars correspond to standard error. Zn- refers to 0 µM whereas Zn+ refers to 30 µM of $ZnSO_4$. The expression under Zn+ condition was set to 1 as the frame of reference.

4.3 PHENOTYPIC ANALYSIS of *AtZIP4*, *AtZIP6* AND *AtZIP9* SINGLE KNOCK-OUT MUTANTS:

A phenotypic characterization was performed on *zip4.1*, *zip6.1* and *zip9.1* single knockout mutants and wild-type (Col-0) controls, measuring the length of the primary root in plants grown on different concentrations of Zn, Fe, and Mn (Figure 4.4-4.6). Moreover, to verify the effect of multiple concentrations of the two metals, we also tried to stress these lines with low Zn availability coupled with high Fe levels and *vice versa* (Figure 4.8A). Different medium compositions and methods were tested (data not shown) for the phenotypic characterization of these mutants, and we found that the best way was to use a medium with a lower nutrient content (Hoagland's medium 1X) and grow the plants on Petri dishes, vertically. Under these conditions, *zip4.1* does not display any differences in primary root length at different concentrations of Zn and Mn, which however is shorter upon excess Fe, suggesting a role in preserving Fe homeostasis (Figure 4.4). Furthermore, the difference in primary root length is greater under low Fe conditions coupled with excess Zn availability than when the plants are only Fe-starved, hence it is plausible that it also plays a role in Zn transport (Figure 4.8A). The single *zip6.1* knockout mutant does not appear significantly different from the wild-type plants when grown at different Fe and Mn concentrations, but when Zn levels are excessive, the length of its primary root is greater. The primary root of *zip6.1* is also longer under low Zn conditions, although not significantly (Figure 4.5).

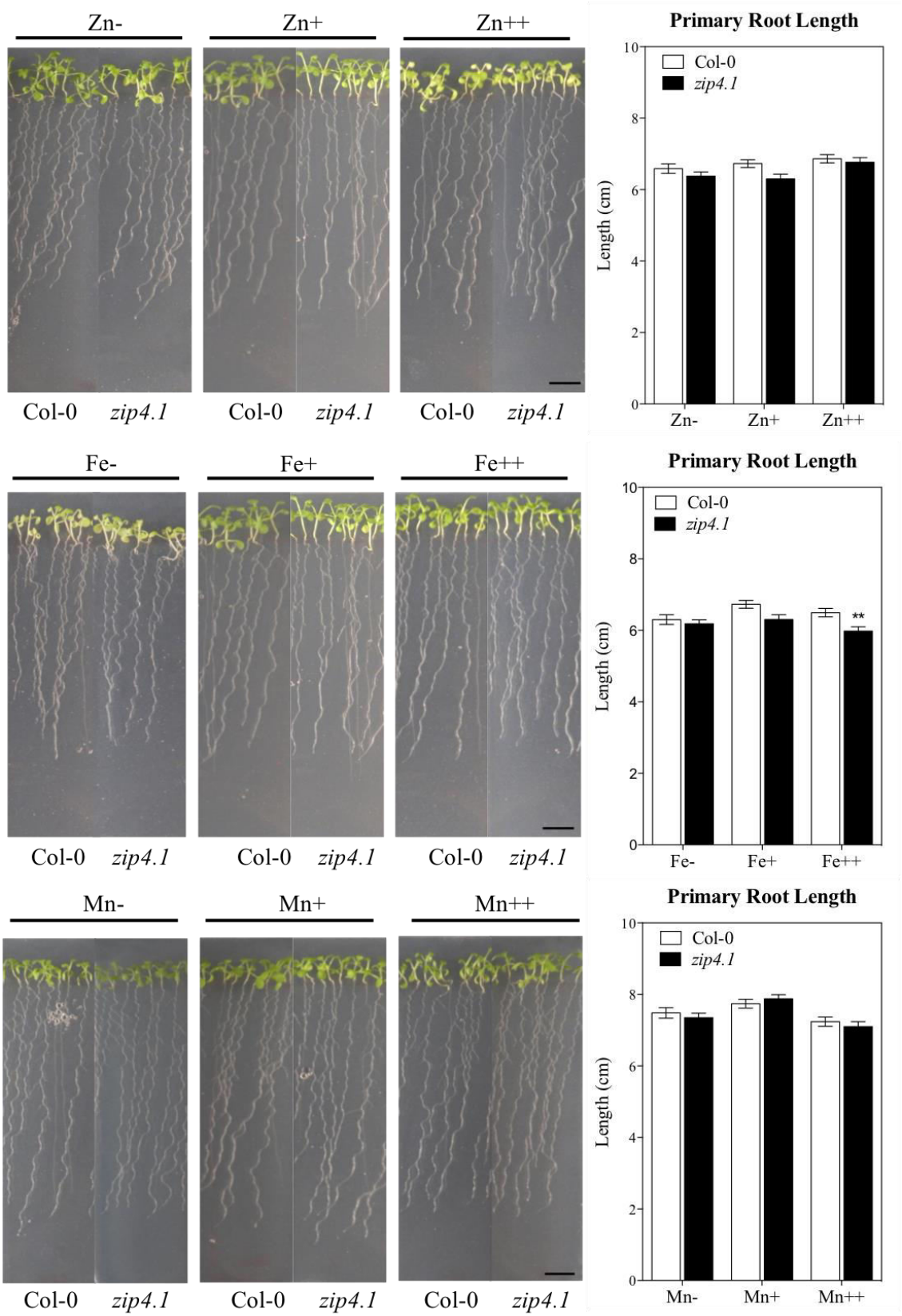

Figure 4.4: Primary root length differences between *zip4.1* knockout mutant lines and wild-types at different Zn, Fe and Mn concentrations. Values are means ± SEM (n=45). Scale bars = 1 cm.

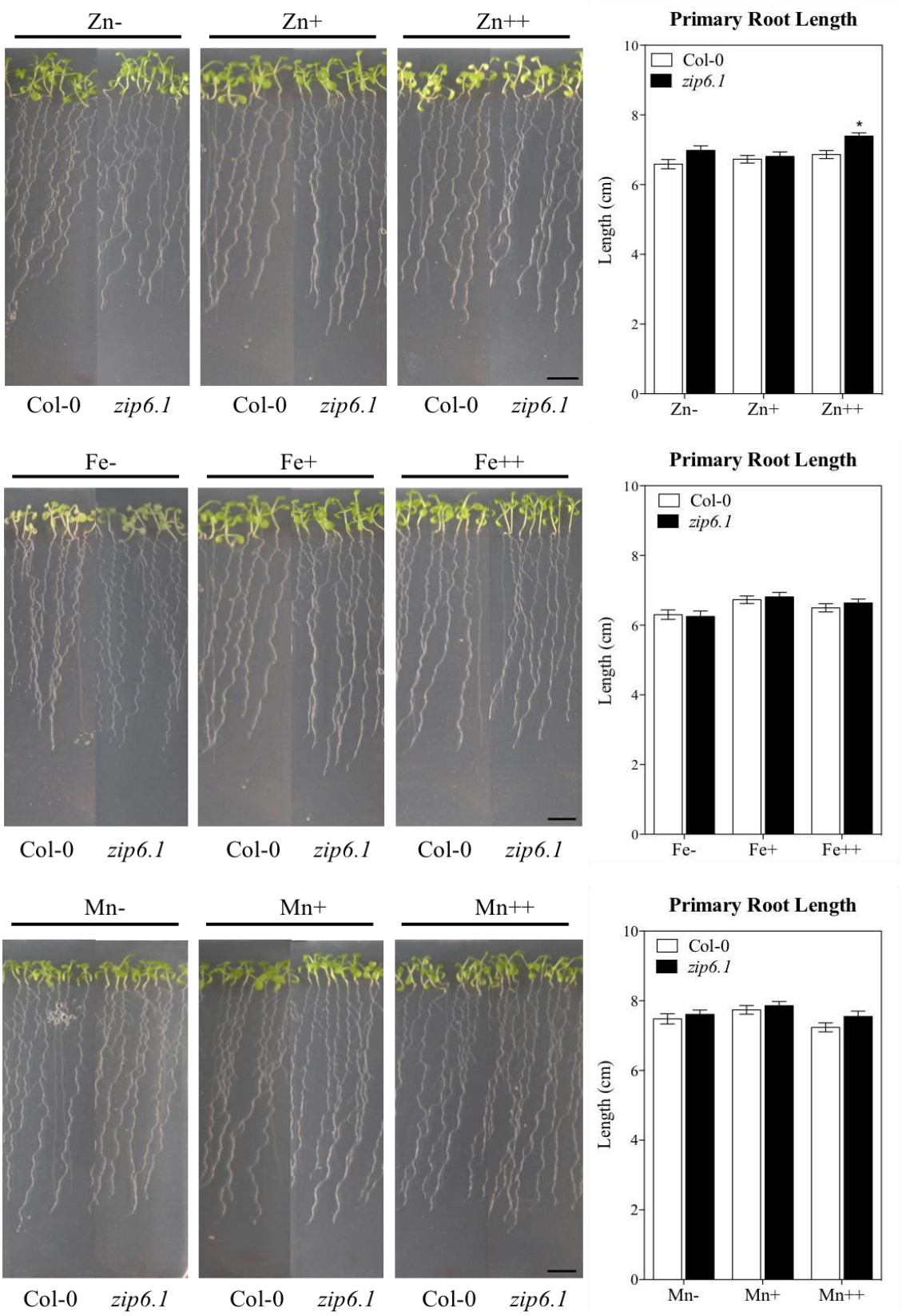

Figure 4.5: Primary root length differences between *zip6.1* knockout mutant lines and wild-types at different Zn, Fe and Mn concentrations. Values are means ± SEM (n=45). Scale bars = 1 cm.

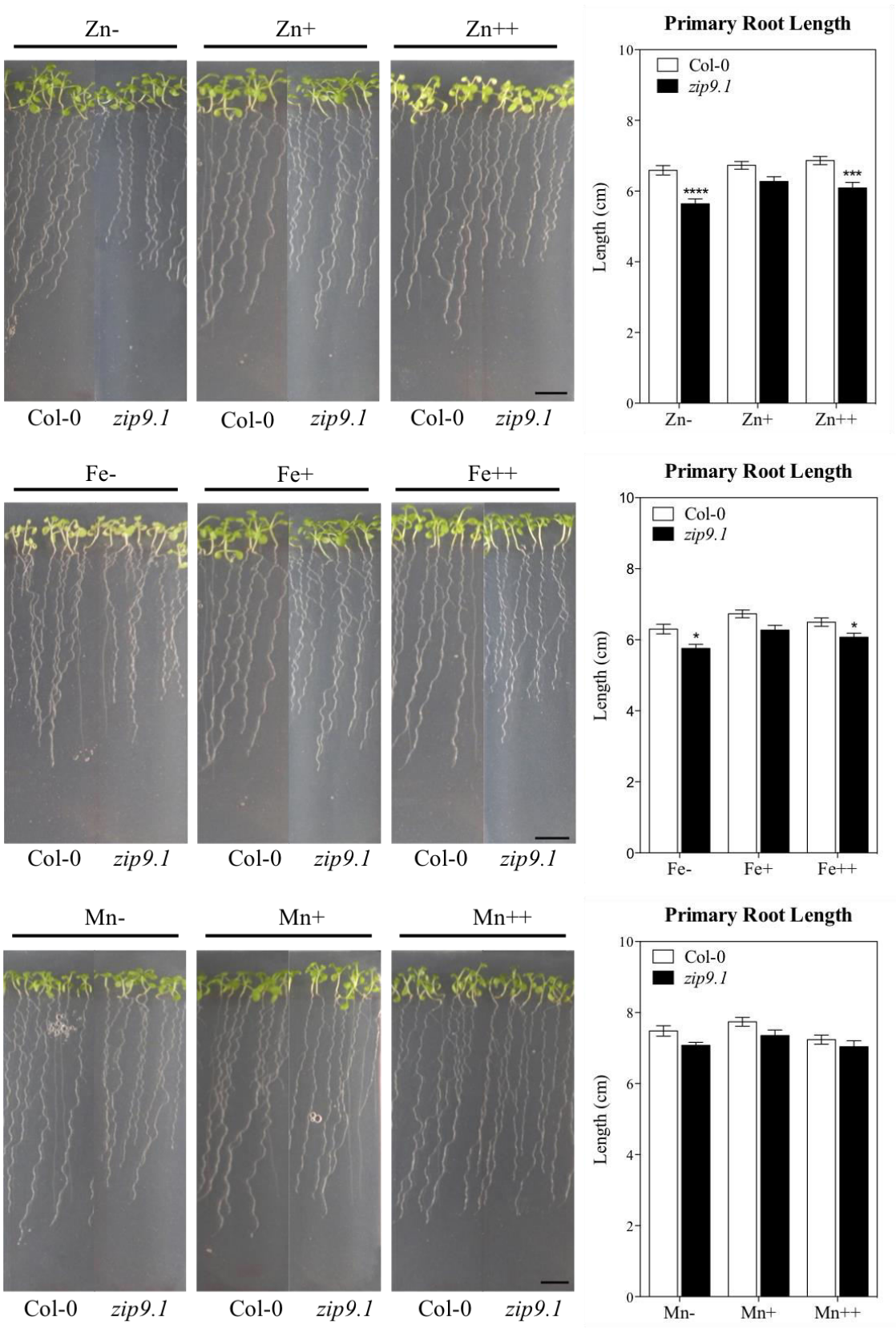

Figure 4.6: Primary root length differences between *zip9.1* knockout mutant lines and wild-types at different Zn, Fe and Mn concentrations. Values are means ± SEM (n=45). Scale bars = 1 cm.

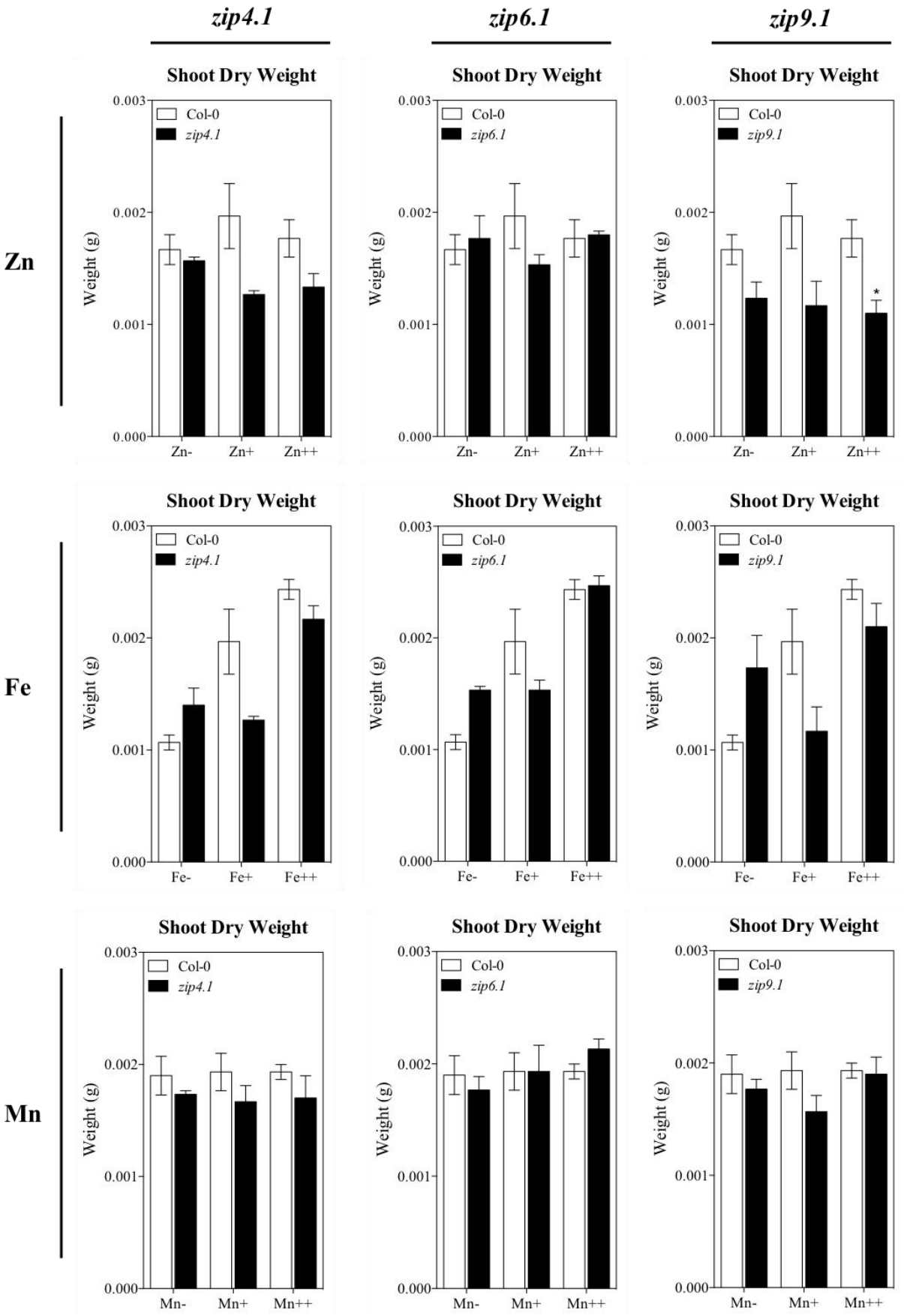

Figure 4.7: Shoot dry weight of *zip4.1*, *zip6.1* and *zip9.1* knockout mutant lines and wild-type plants at different Zn, Fe and Mn concentrations. Values are means ± SEM (n=3).

A

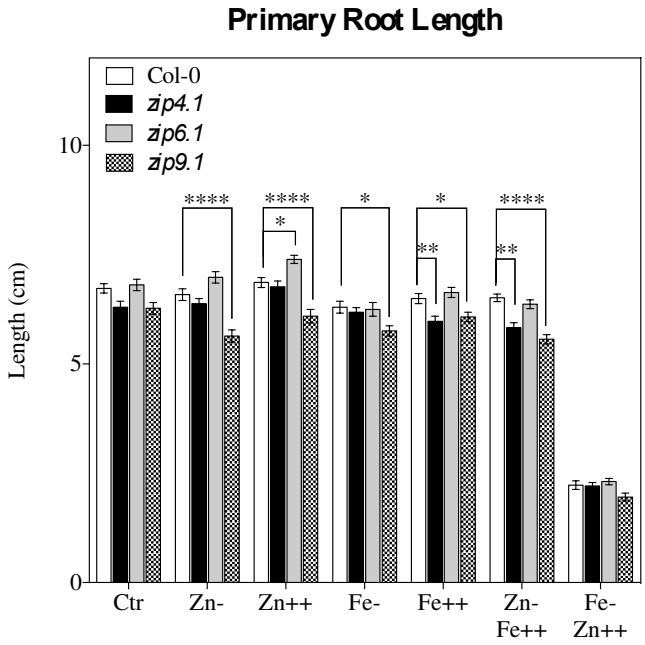

B

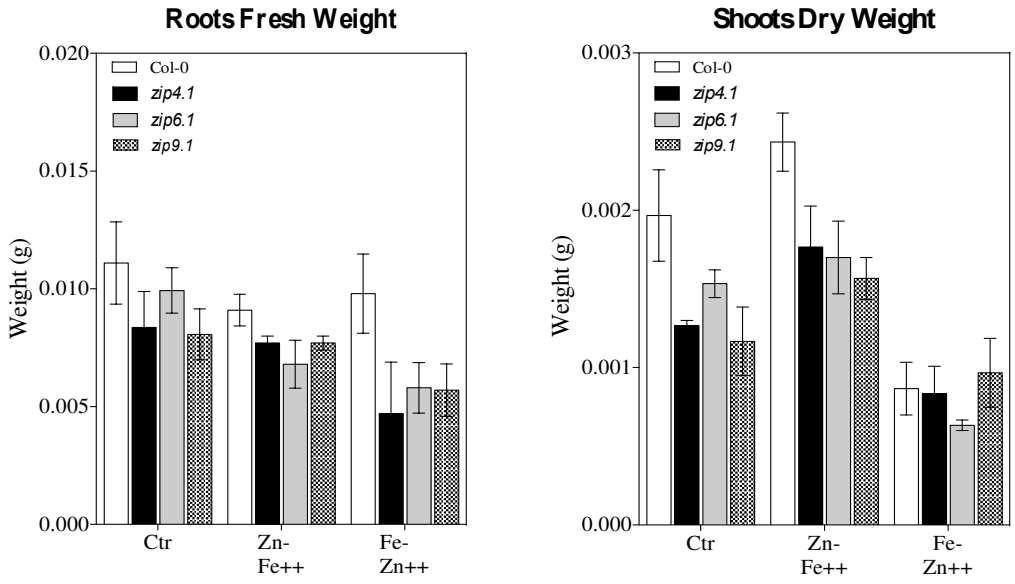

Figure 4.8: Primary root length and the weight of roots and shoots in wild-type controls and single knockout mutant lines. A) Summarized results relative to primary root length for plants grown in the absence (-) or presence of excess (++) Zn and Fe, or after Fe-/Zn++ and Zn-/Fe++ treatments. B) Roots fresh and shoots dry weight in wild-type controls and single knockout mutants in the absence of Zn and presence of excess Fe (Zn-Fe++) and in the absence of Fe and presence of excess Zn (Fe-Zn++). Values are means ± SEM (n=3).

Conversely, the single mutant *zip9.1* displays a significantly shorter primary root when grown in the absence or presence of excess amounts of either Zn or Fe, and also when the treatment provides for low Zn and high Fe availability contemporaneously (Figure 4.6). These results seem to suggest a key role in maintaining the homeostasis of these two metals, although *AtZIP9* expression analysis only revealed a strong up-regulation under conditions of Zn starvation (Figure 4.1). The susceptibility of the *AtZIP9* knockout mutant to different Zn concentrations confirmed what described by Inaba *et al.,* (2015). A similar lower primary root length under excess of Zn was observed in two T-DNA insertional mutants of *AtHMA1* and also in an *AtHMA3* single knock-out mutant (Kim *et al.,* 2009; Morel *et al.,* 2009). These two transporters seems to be involved in the Zn detoxification regulating its transport into the vacuole and into plastids, respectively (Kim *et al.,* 2009; Morel *et al.,* 2009). The seedlings of these mutants were also sampled to analyze the dry weight of shoots (Figure 4.7). Significant results were only found for the single *zip9.1* knockout mutant, which displayed reduced shoot weight at excess levels of Zn, even though lower concentrations also had an impact on plant weight. Interestingly, *zip9.1* seems to be influenced by low Fe at root level (Figure 4.6), displaying under these conditions a greater shoot biomass than the wild-type (Figure 4.7), and suggesting a possible role in Fe transport. Moreover, the effect of a combination of low Fe and excess Zn (Figure 4.8B) on leaf biomass is more similar to that observed under conditions of excess Zn alone.

4.4 *AtZIP4*, *AtZIP6* AND *AtZIP9* OVER-EXPRESSING LINES:

The analysis of metal accumulation in plants that over-express *AtZIP4*, *AtZIP6* and *AtZIP9* transporters can be helpful to integrate the data collected on knockout mutants, obtaining a clearer view on the function of these two membrane transporters. *AtIRT1*, a key ZIP transporter involved in Fe uptake, when over-expressed mediates a reduced accumulation of Zn and Cd under conditions of Fe deficiency (Vert *et al.,* 2002; Connolly *et al.,* 2002; Nishida *et al.,* 2011), but when it is not expressed, a smaller amount of Fe is accumulated in the shoots. Thus, constructs for the overexpression of ZIP4, ZIP6 and ZIP9 were prepared for plant transformation, harboring the strong promoter CaMV35S fused upstream the coding sequence of the three genes (Figure 4.9). *A. thaliana* plants were transformed by floral dipping and different transformants were checked by PCR on the entire 35S promoter fused to the CDS of each gene and on the kanamycin-resistant *nptII* gene. Single copy homozygous lines were obtained, and their transcript levels were analyzed by RT-PCR (data not shown). The homozygous single copy lines over-expressing *AtZIP4* and

AtZIP6 were first analyzed to assess their growth at different concentrations of Zn and Fe. As shown in Figure 4.10, all three over-expressing lines for *AtZIP4* have longer primary roots when grown under conditions of low Zn availability, suggesting a key role in Zn transport, although only two of the three lines displayed a significant difference.

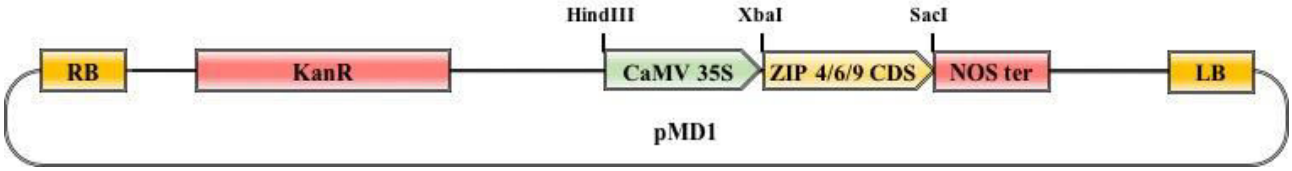

Figure 4.9: Diagram of the constructs for the over-expression of *AtZIP4*, *AtZIP6* and *AtZIP9*.

Interestingly, when ZIP4 is over-expressed, the transgenic lines display a shorter primary root under conditions of Fe starvation, whereas the *zip4.1* knockout mutant seems to be more affected by excess Fe (Figure 4.6). These results, coupled with the complementation of Zn uptake in the *zrt1/zrt2*Δ yeast mutant (Section 4.9), suggest that *AtZIP4* is involved in Zn transport. The reason for the shorter root length of *AtZIP4* over-expressing lines observed at low Fe availability is not as clear: it too may have a role in Fe transport, although it was incapable of complementing a yeast mutant defective for Fe uptake (Section 4.9). Another possible explanation is that the removal of Fe systematically provokes a secondary excess of other metals such Zn or Mn in the medium. Moreover, no significant differences were observed in shoot dry weight at the various Zn and Fe concentrations tested (Figures 4.10-11). Three lines over-expressing *AtZIP6* were also phenotypically tested at different concentrations of Zn (Figure 4.12) and Fe (Figure 4.13), measuring the length of the primary root and the weight of shoots. *AtZIP6ox* lines grew better at excess amounts of both Zn and Fe, but also thrived under standard conditions (Figure 4.12-13). The third *AtZIP6ox* line differed from the first two, suggesting that the insertion of the construct may have occurred in a critical genomic region, thus interfering with the regulation of other metabolic pathways. No significant differences were observed at low Zn availability but interestingly, the primary root of the *AtZIP6ox* lines was shorter, like that of *AtZIP4ox* lines under Fe-deficient conditions. Although *AtZIP6* is not regulated at transcript level by changes in Zn and Fe concentrations, these results suggest that it may be involved in their transport. Many authors believe that *AtZIP6* has a key role in the Zn hyperaccumulation trait, based on micro-array analyses (Filatov *et al.,* 2006). Moreover, the vascular tissues localization (Section 4.7; Figures 4.23, 4.26) of *AtZIP6* expression together with its constitutive expression at different metal concentrations, (Figure 4.1)

confirms the idea that it may be involved in roots to shoots translocation. As observed for *AtZIP4*, the overexpression of *AtZIP6* did not affect the shoot dry weight of these plants (Figure 4.12-13).

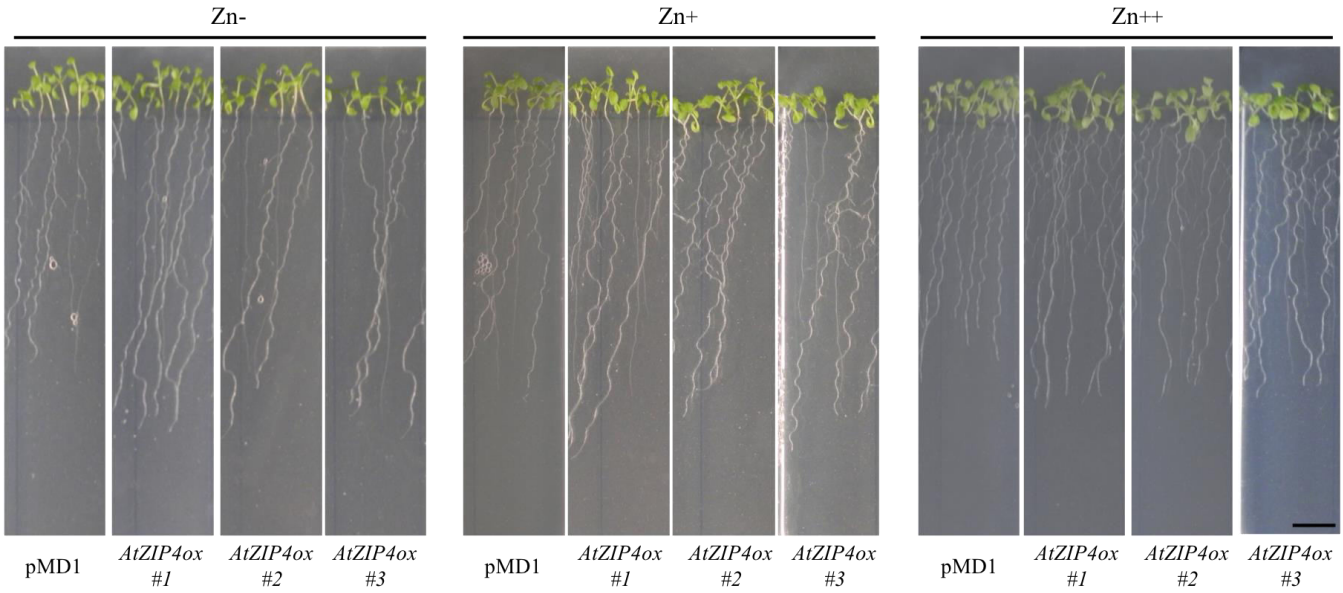

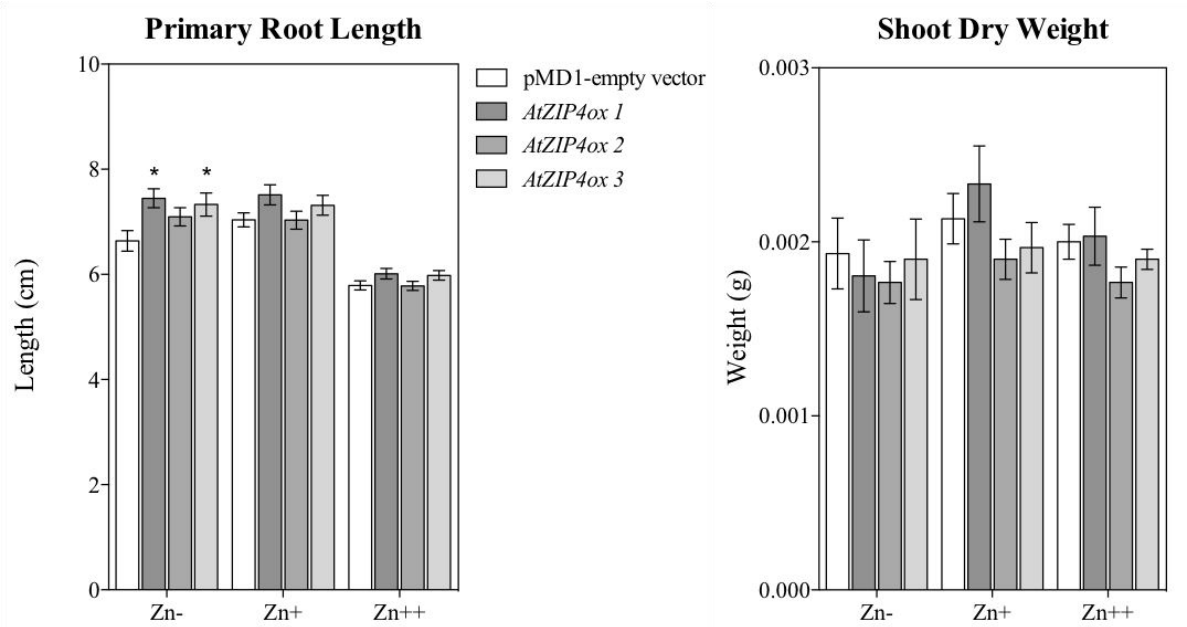

Figure 4.10: Primary root length, root fresh weight and shoot dry weight in three single-copy lines overexpressing *AtZIP4* and the wild-type at different Zn concentrations. Values are means ± SEM (n=30). Scale bars = 1 cm.

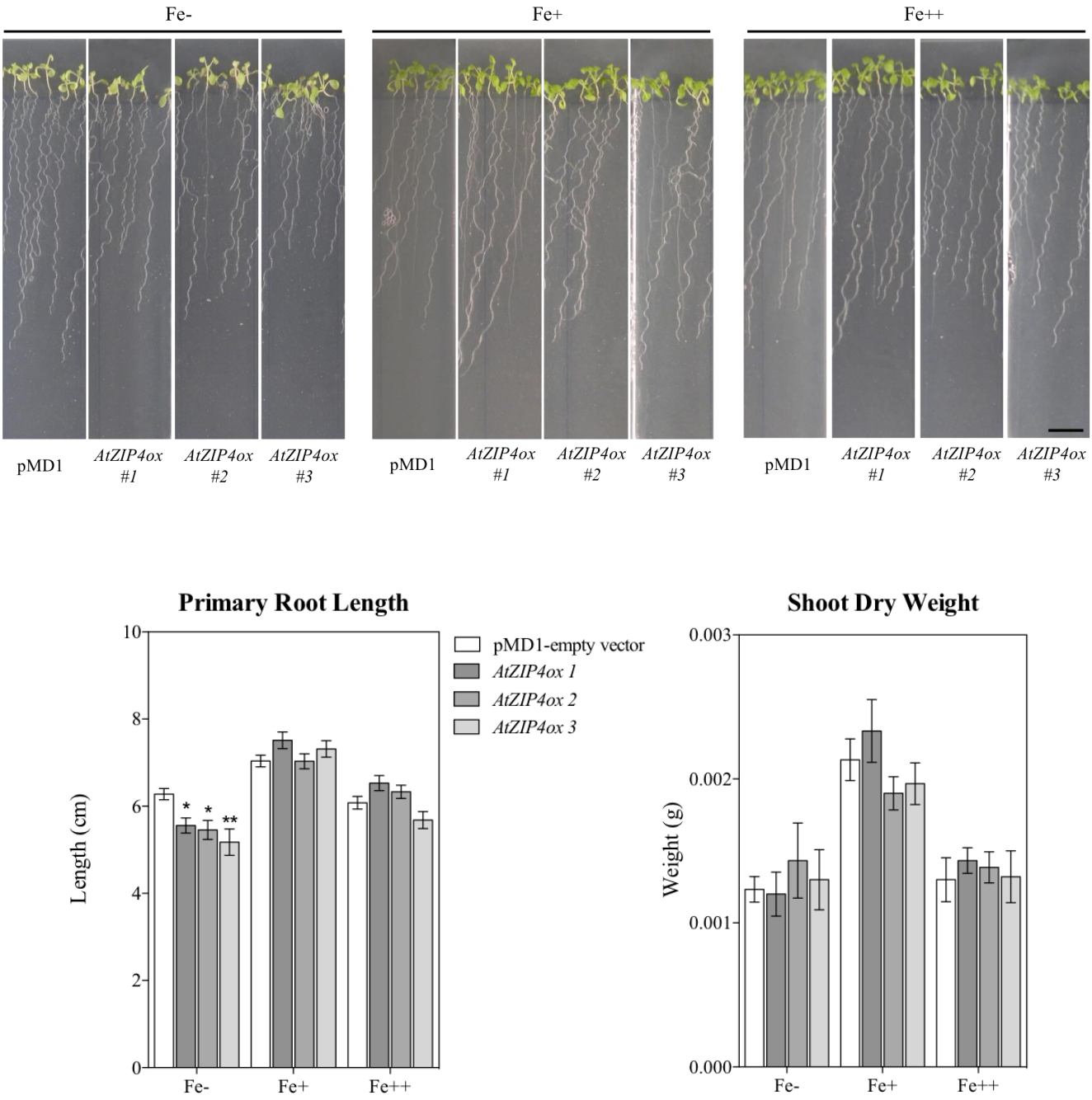

Figure 4.11: Primary root length, root fresh weight and shoot dry weight in three single-copy lines overexpressing *AtZIP4* and the wild-type at different Fe concentrations. Values are means ± SEM (n=30). Scale bars = 1 cm.

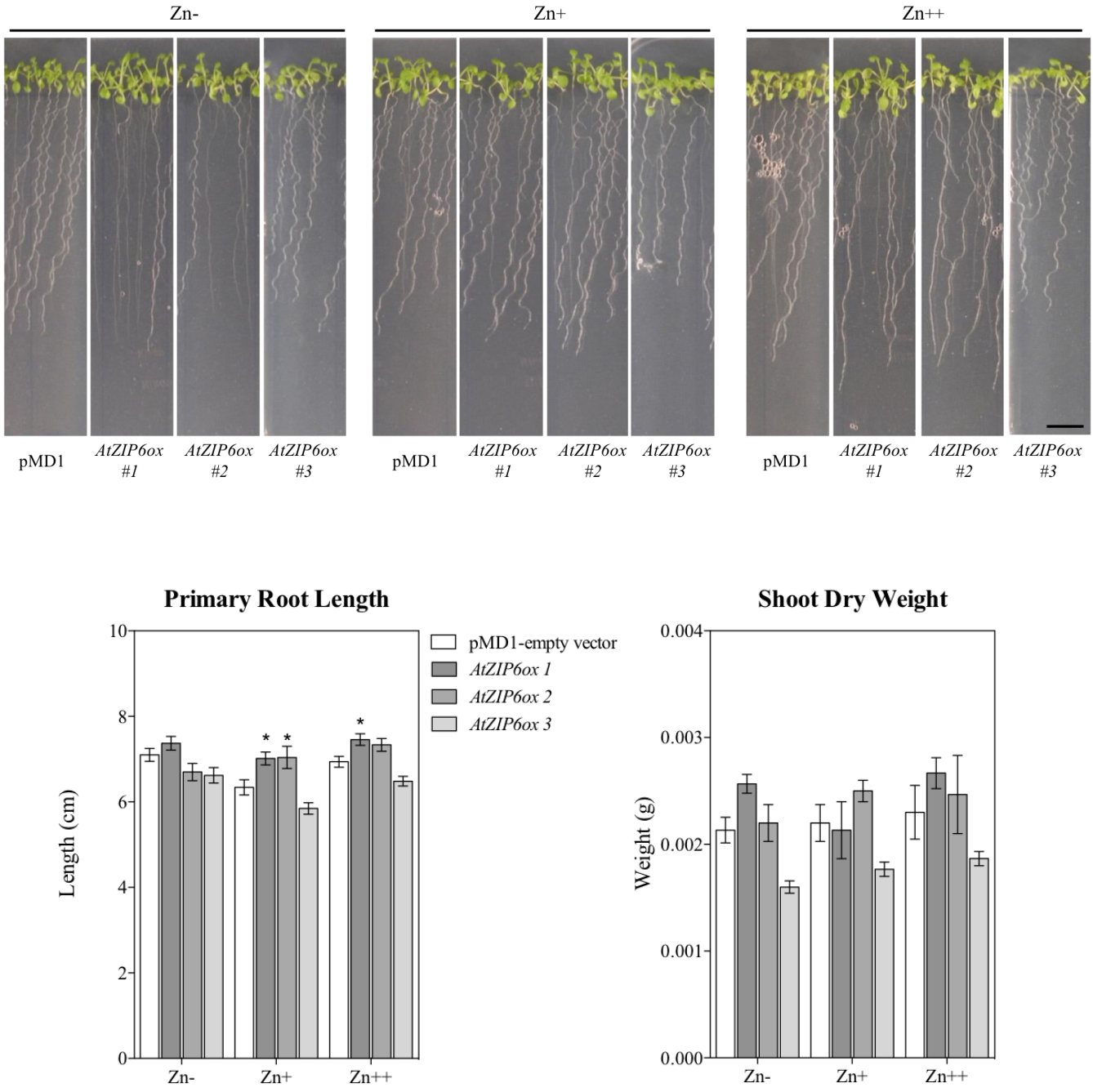

Figure 4.12: Primary root length, root fresh weight and shoot dry weight in three single-copy lines overexpressing *AtZIP6* and the wild-type at different Zn concentrations. Values are means ± SEM (n=30). Scale bars = 1 cm.

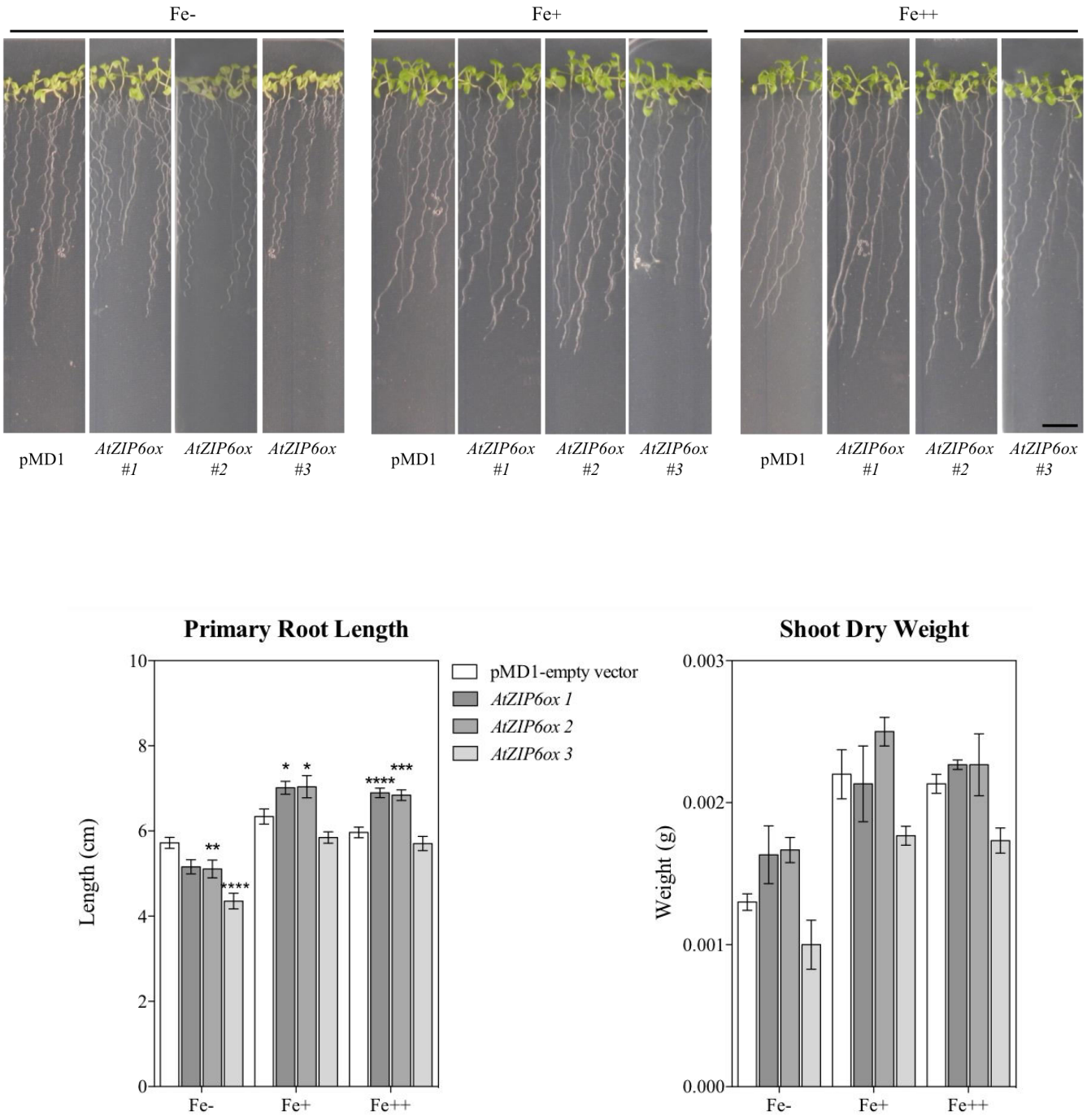

Figure 4.13: Primary root length, root fresh weight and shoot dry weight in three single-copy lines overexpressing *AtZIP6* and the wild-type at different Fe concentrations. Values are means ± SEM (n=30). Scale bars = 1 cm.

AtZIP9 over-expressing lines have not been yet phenotypically characterized at different Zn and Fe concentrations. Moreover, the accumulation analysis on these over-expressing lines has not yet been done, but will be fundamental to clarify the effects on the inorganic ion profile and find what metals are transported by ZIP4, ZIP6 and ZIP9.

4.5 DOUBLE AND TRIPLE KNOCK-OUT MUTANTS:

AtZIP4 and *AtZIP9* share a 60% identity and 77% similarity at protein level, and according to Maser *et al.* (2001) are phylogenetically clustered together (Figure 4.14). Moreover, expression analyses revealed that both genes are highly induced by Zn deficiency in the roots and shoots of the plants, suggesting a possible functional redundancy between these two transporters (Figure 4.1). To avoid the risk that a transporter could be replaced by a similar one carrying out its activity, we produced a *zip4/zip9* double knockout mutant in the traditional way, i.e. by the crossing *zip4.1* (SALK_ 145371C) with *zip9.1* (SALK_ 090000) (Figure 4.14B). *AtZIP6* expression did not seem to respond to changes in metal concentrations, but preliminary analyses suggest that *AtZIP6* and *AtZIP9* are expressed in different tissues (Section 4.7). Furthermore, *AtZIP4* is expressed in the vascular tissues of the roots and has no clear localization in the pericycle (Milner and Kochian, 2008; Lin *et al.,* 2016), hence displaying a very similar expression pattern to that of *AtZIP6* (Section 4.6). We therefore decided to also take into consideration the double *zip4/zip6, zip6/zip9* and triple *zip4/zip6/zip9* knockout mutants. The *zip4/zip6* mutant (Figure 4.14A) was obtained from crossing *zip4.1* (SALK_ 145371C) with *zip6.1* (SALK_116013), and *zip6/zip9* (Figure 4.15A) by crossing *zip6.1* with *zip9.*1; crossing of this latter double mutant with the insertional *zip4.1* line was used to obtain the triple *zip4/zip6/zip9* (Figure 4.15B) knockout mutant. All the double and the triple mutants were checked by PCR (data not shown). Although ZIP6 and ZIP9 are different proteins that only share a 48% similarity at amino acidic level, the study of the double mutant could be useful to reveal differences at phenotypic level, and in metal accumulation and translocation brought about by changes in the metal homeostasis.

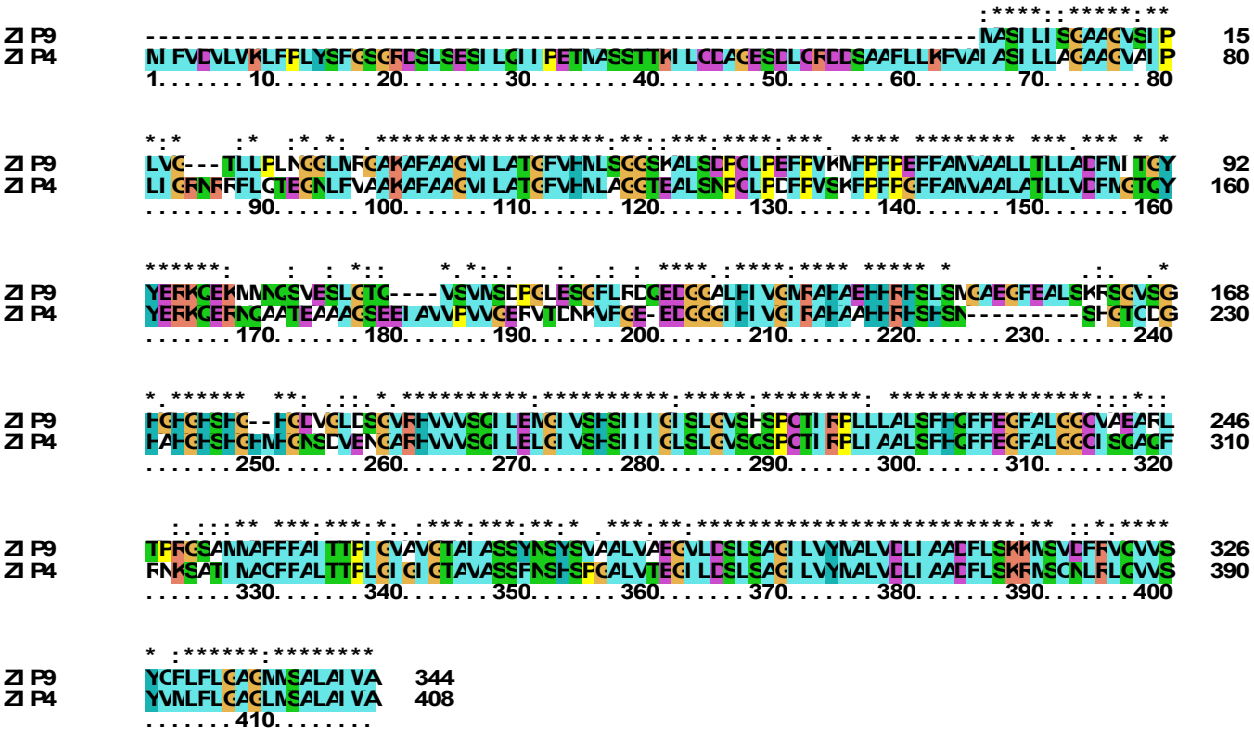

Figure 4.14: Sequence alignments for ZIP4 and ZIP9. Amino acid sequences were aligned using CLUSTAL X v 2.1 (Larkin *et al.,* 2007).

4.6 ANALYSIS OF METAL CONTENT:

Ionome studies aimed at characterizing the inorganic composition of an organism are considered an essential tool for gene functional characterization (Lahner *et al.,* 2003). Investigating the ionome of single, double and triple mutants is therefore fundamental in order to understand whether the lack of these genes leads to changes in the inorganic ion profiles or tissue distribution, and to better focus the role of these genes in metal transport and homeostasis. Inductively coupled plasma mass spectrometry (ICP-MS) is an ideal tool for ionomics, better for small-sized sample analysis than other instruments such as ICP-OES (Inductively coupled optical emission spectrometry) (Lahner *et al.,* 2008). The *zip6/zip9, zip4/zip9*, *zip4/zip6* double knockout mutants and a *zip4/zip6/zip9* triple knockout line, obtained by traditional crossing, were grown under standard growth conditions and at different Zn concentrations together with the single mutants to appraise their accumulation of multiple elements. The ionome analysis was performed at the University of Nottingham with the collaboration and under the supervision of Prof. David Salt, using two different systems: *in vitro* on plates and *in vivo* in hydroponic culture. The *in vitro* experiment was taken into consideration to analyze if the different mutants present the same behavior compared with the hydroponic treatment, even though the accessibility of nutrients into the agar plates is not as uniform as the hydroponic

system. For the *in vitro* experiments, the plants were grown vertically for 2 weeks in solid 1/10 modified Hoagland's medium at four Zn concentrations: 0, 0.07, 5 and 50 µM $ZnSO_4$. For the hydroponic treatment, plants were treated for 2 weeks in liquid 1/10 Hoagland's at three Zn concentrations: 0, 2 and 10 µM $ZnSO_4$. Roots and shoots were collected and a total of 192 samples for the *in vitro* on agar-plates experiment and 224 samples for the hydroponics experiment were analyzed by inductively coupled plasma mass spectrometry (ICP-MS). The complete ionomic profiles of the mutant lines are reported in the Supplementary data (Figure S1). The *in vitro* experiment gave no significant differences for Zn, Fe, Mn, S and P among the various lines, neither in their roots (Figure S2) or shoots (Figure S3). Conversely, in the *in vivo* experiment on hydroponic culture, the double *zip4/zip6*, *zip6/zip9* and the triple *zip4/zip6/zip9* knockout mutants exhibited lower levels of Zn in their shoots (Figure 4.16A) than the other lines, whereas no differences were observed at root level (Figure 4.15A). All the mutants lacking the ZIP9 transporter had higher levels of Zn in their roots than the wild-type under conditions of excess Zn (Figure 4.15A), although statistically, the difference was not significant. Inaba *et al.* (2015) on the other hand, observed that two *AtZIP9* mutants were characterized by significantly smaller amounts of Zn when this metal was present in excess and surprisingly, the mutant that was not completely knocked out displayed the lowest levels of Zn. The phenotypic characterization of these mutants at different Zn concentrations was very similar to what we obtained with *zip9.1* (Figure 4.6). Thus, we ordered from NASC (Nottingham Arabidopsis Stock Centre) the same knock-out mutant used by Inaba et al., (2015) (*zip9*.2; SALK_090345 – NASC ID: N590345) that will be tested to better investigate the differences observed in the Zn accumulation of the single *zip9.1* mutant. The accumulation analysis performed on shoots of plants grown in hydroponics also revealed a reduced level of Fe under conditions of Zn deficiency in all the double knockout mutants, as well as the triple *zip4/zip6/zip9* and the single *zip6.1* knockout one, suggesting a possible role for ZIP6 in Fe roots-to-shoots translocation (Figure 4.16B). The correlation between Zn and Fe is poorly understood even though some studies on the ZIP transporter IRT1 seem to indicate some sort of regulation between the transport of these two metals. It is known that excess Zn induces a physiological reduction in the amounts of Fe (Briat *et al.,* 2015), as confirmed by our accumulation analysis on wild-type plants (Figure 4.16B).

Despite the fact that IRT1 is strongly accumulated under Fe starvation conditions, Fukao et al., (2011) have shown that the abundance of this protein increased also in the presence of high levels of Zn suggesting that plants suffer of Fe deficiency under Zn excess. Mn does not seem to compete for the transport of Zn in the mutants analyzed, as witnessed by the absence of significant differences in Mn accumulation in either shoots or roots under both experimental conditions (Figure

S2C, S3C, 4.15C, 4.16C). Jain *et al.* (2013) observed that high Zn treatments on *A. thaliana*Col-0 plants did not affect the amount of S at root level but increased its concentration in the shoots (Fukao *et al.,* 2011). These observations were confirmed by our analyses, as shown in Figures 4.15D and 4.16D. From a chemical point of view, the interaction between Fe and S producing the Fe–S clusters, which are fundamental for respiration and photosynthesis, is extremely well documented in the literature (Briat *et al.,* 2015). Forieri *et al.* (2013) for example described a reduction in IRT1 expression under S deficiency conditions, and transcriptome analysis on Fe-depleted *A. thaliana* plants showed a correlation between genes involved in S-metabolism and ones responsive to Fe starvation (Schuler *et al.,* 2011). Also in graminaceous plants such as barley, the release of Fe chelators into the rhizosphere is greatly reduced under low S conditions (Kobayashi and Nishizawa, 2012). In our work, the mutant lines exhibiting significant lower levels of Fe under conditions of Zn deficiency also accumulated significantly higher amounts of S, except for the double *zip6/zip9* knockout mutant (Figure 4.16B, 4.16D). Conversely, the double *zip6/zip9* and the triple knockout mutants displayed very low levels of S when Zn was present in excess. Little information is available in the literature on the correlation between S and Zn homeostasis; it is possible that variations in the levels of S among the various mutants is a response to the Fe stress induced by the higher Zn concentrations. There is a strong interaction between P and Zn homeostasis, but to date, the molecular bases behind this interaction are still unclear (Briat *et al.,* 2015). It is known that Zn deficiency induces P accumulation and likewise, P starvation induces greater Zn accumulation (Khan *et al.,* 2014; Misson *et al.,* 2005). These results were confirmed by transcriptome analysis: Zn and P deficiency cause an over-expression of the genes involved in the homeostasis of P and Zn, respectively (van de Mortel *et al.,* 2006; Misson *et al.,* 2005). The ICP-MS analysis performed on the shoots of the mutants grown in hydroponics confirmed the P distribution pattern in the wild-type plants, with a slight accumulation at increasing concentrations of Zn (Figure 4.16E). Interestingly, *zip6.1*, double *zip4/zip6*, *zip4/zip9* and triple *zip4/zip6/zip*9 knock-out mutants displayed significantly higher levels of P when Zn-starved and except for *zip4/zip9*, their P accumulation rate seemed to follow a completely different pattern than that of the wild-type, which decreases at rising concentrations of Zn, with the lowest amounts measured in the triple knockout mutant (Figure 4.16E).

Hydroponic culture - Roots

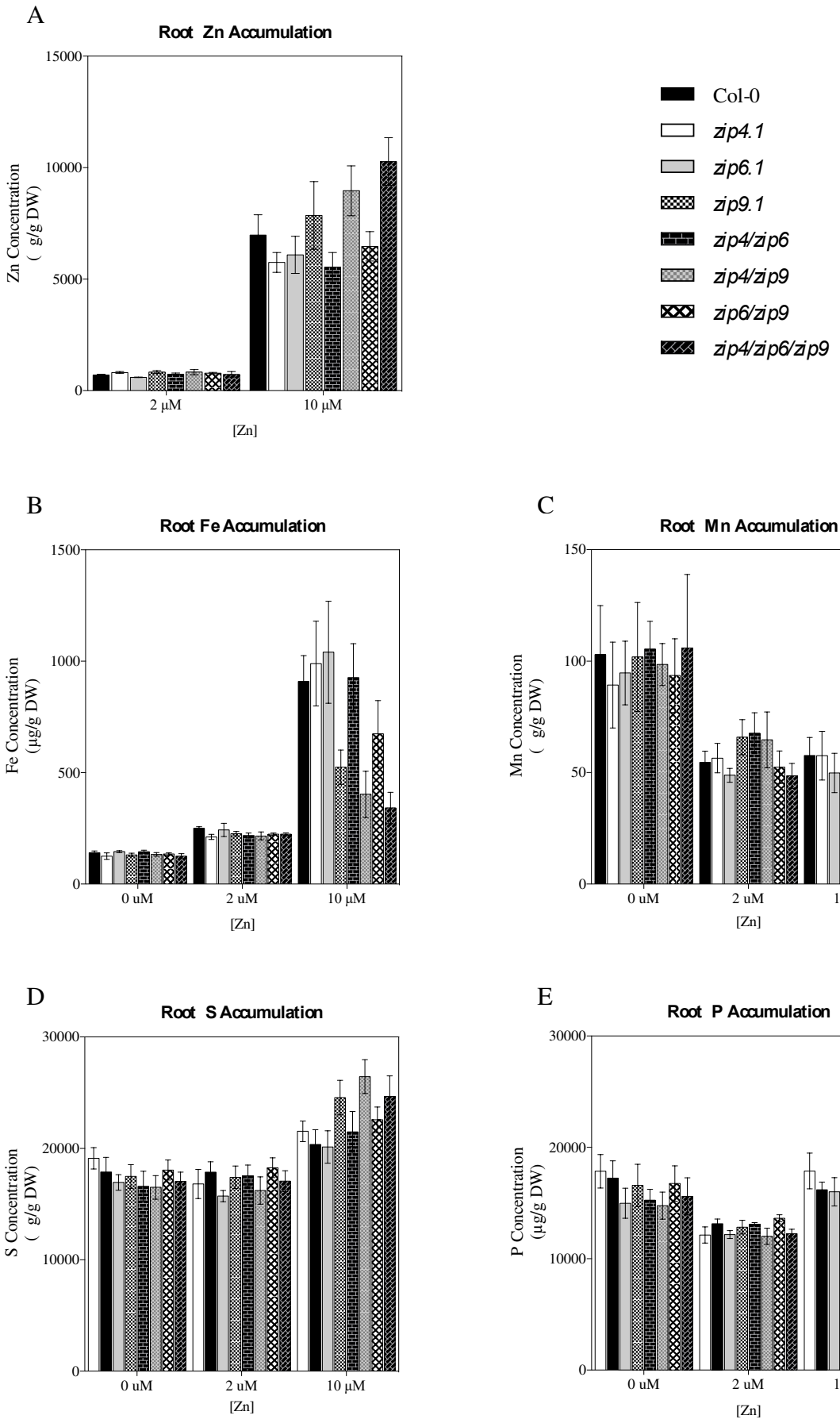

Figure 4.15: ICP-MS analysis for A) Zn, B) Fe, C) Mn, D) S and E) P accumulation in roots of single *zip4.1*, *zip6.1*, *zip9.1,* double *zip4/zip6, zip4/zip9*, *zip6/zip9* and triple *zip4/zip6/zip9* knockout mutants and wild-types grown in hydroponics at different Zn concentrations. Values are means ± SEM (n=3).

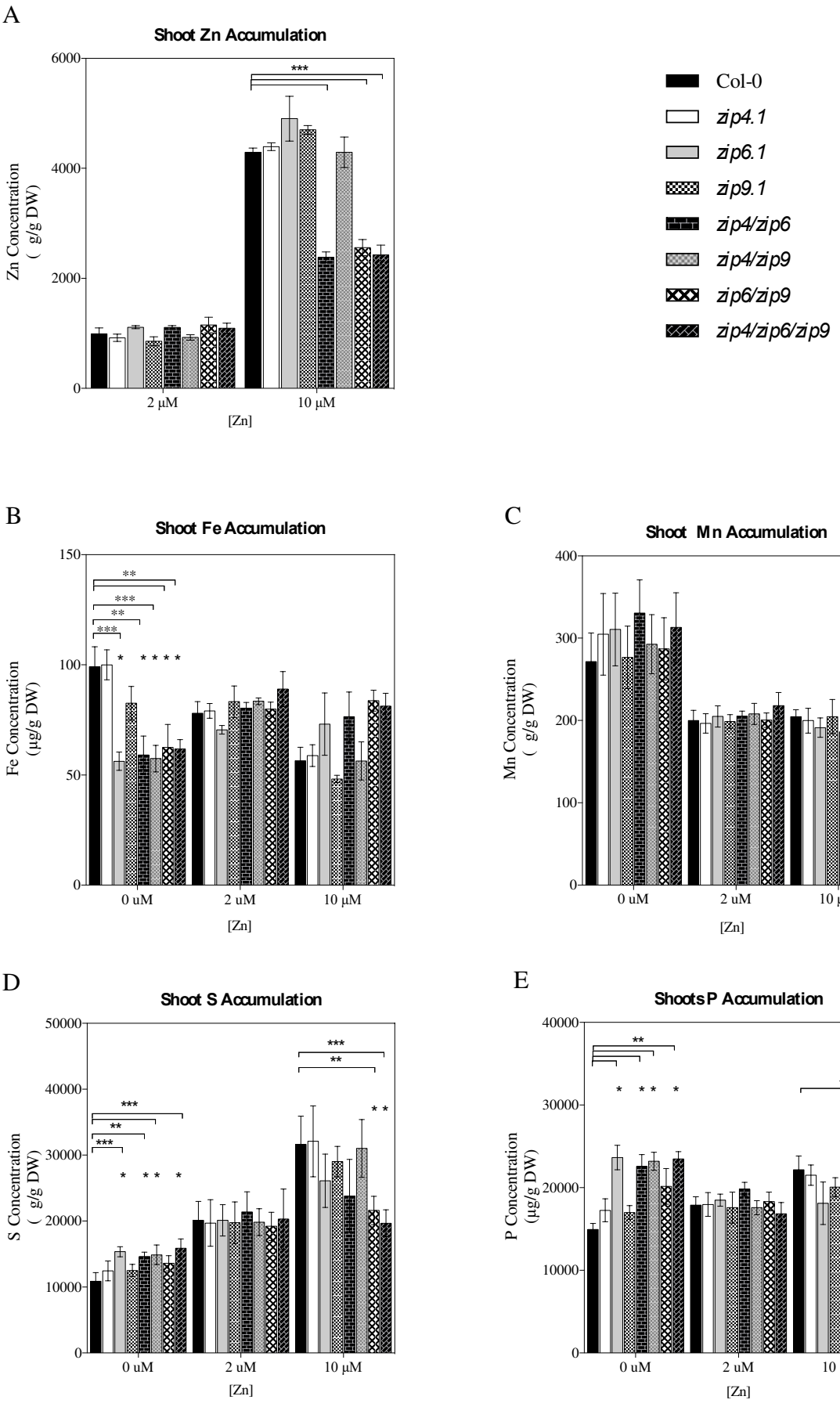

Figure 4.16: ICP-MS analysis of A) Zn, B) Fe, C) Mn, D) S and E) P accumulation in shoots of single *zip4.1*, *zip6.1*, *zip9.1,* double *zip4/zip6, zip4/zip9*, *zip6/zip9* and triple *zip4/zip6/zip9* knockout mutants and wild-type grown in hydroponics at different Zn concentrations. Values are means ± SEM (n=3).

4.7 TISSUE LOCALIZATION of *AtZIP4*, *AtZIP6* AND *AtZIP9*:

Identification of tissue specific localization of *AtZIP4*, *AtZIP6* and *AtZIP9* is a fundamental aspect to better investigate the role of these transporters in the metal homeostasis. The tissue localization of *AtZIP4* expression has been already partly investigated (Lin *et al.,* 2016; Milner and Kochian, 2008). In the roots, Lin *et al.* (2016) observed an endodermis and perycicle localization for *AtZIP4* whereas Milner and Kochian (2008) previously suggested a different cell-specific expression, located in the root stele and not the endodermis. The GUS signal of transgenic pAtZIP4::GUS plants was localized in the leaf edges, trichomes, young buds and the stamen filaments of older ones (Lin *et al.,* 2016). In flowers, a strong signal was observed in the distal ends of siliques and pedicels (Lin *et al.,* 2016). Moreover, the GUS signal for pAtZIP4::GUS transgenic lines was only observed in Zn starved plants (Lin *et al.,* 2016). The exact localization of *AtZIP4* at root level is not as clear at the endodermis layer, due to the absence of root cross sections confirming these results. Moreover, a more recent work seems to indicate that the signal is located in all the tissues of the roots (Sinclair *et al.,* 2018). To better understand the tissue localization of *AtZIP4* expression, we decided to amplify 2000 bp (Figure 4.17) upstream its coding sequence, cloning it with the GUS gene (Figure 4.18) to produce *A. thaliana* pAtZIP4::GUS reporter lines. Differently from what reported by Lin et al., (2016), we amplified 2000 bp instead of 1048 bp before the starting codon, to take into consideration further regulating elements of the promoter. Although the promoter analysis of *AtZIP4* has already been performed (Lin *et al.,* 2016), we wanted to study in greater detail its tissue localization in the root layers by analyzing root cross-sections of these lines. Different pAtZIP4::GUS transgenic *A. thaliana* plants were thus obtained and checked by PCR but the GUS staining analysis has not yet been performed. To analyze the expression pattern of *AtZIP6* and *AtZIP9* we produced two constructs by fusing the *AtZIP6* and *AtZIP9* promoter sequences to the *GUS* reporter gene (Figure 4.20). 1971 bp and 2002 bp upstream of the coding sequence of *AtZIP6* (Figure 4.19) and *AtZIP9* (Figure 4.20), respectively, were amplified by PCR and cloned upstream the GUS coding region in a suitable vector (pMD1 expression vector). Regulatory elements can be hundreds of bp far from the start codon, so we chose to select a region of about 2000 bp. These constructs were used to transform *A. thaliana* by floral dipping. *A. thaliana* pAtZIP6::GUS and pAtZIP9::GUS transformants were analyzed by PCR and a GUS assay was performed on the whole plantlets to understand where the promoter drives the GUS expression. Moreover, the promoter of these transporters was analyzed for the presence of putative cis-regulating elements (Assunção *et al.,* 2010; Jain *et al.,* 2013). The promoters of various ZIP transporters contain one or more Zinc Deficient Response Elements (ZDRE) with the sequence (RTGTCGACAY) as core consensus,

which are the targets of basic-region leucine zippers (bZIP) such as *AtbZIP19* and *AtbZIP23*, regulating the response to Zn starvation (Assunção *et al.,* 2010). Among the various members of the ZIP family, ZIP1, ZIP3, ZIP4, ZIP5, ZIP9, ZIP12 and IRT3 have one or two copies of these *cis* elements (Assunção *et al.,* 2010). ZIP2, which has no ZDRE element, is not up-regulated by Zn deficiency (Assunção *et al.,* 2010), although Jain *et al.* (2013) observed that it is induced in both roots and shoots. ZIP4 has two ZDRE elements (Figure 4.17) -245 and -117 bp upstream of the starting site for transcription, respectively, and is strongly induced by Zn shortage (Figure 4.1).

Nucleotidic sequence of the promoter of *AtZIP4* (pZIP4)

5'_GGAAGAACAGAGGTGGCTATTTACAGGGAGAGAAAGCTCCTTTGAAGAAGTTCTACGCCTCCATGCTTTTGGCTTACGTGGTTC
TTGGCCTAGTTTGGTTTCCACAAGTTGCTCAGTATTGGAAAGATGGAATCCAGTTGCATAGTCATATCAACTTTGTAATTGCATTTA
CCATGGGTGAATTGGCCTTCCTCTACCTTGACTTCGTTTATCTCGACTCAGCTGGTACAAGTCCTATGGAGGTTACAGTATGGGCAA
TAACCCTTTCTTCCATGAGGAAGGCACTCTCCCGGCTTCTACTGTTGGTCATATCTTCAGGGTTTGGGATAGTGAGACCTACCCTAG
GTGGCATAACATTGAAGATGCTTCTTATTGGTGTCTTATGCTTTGTTATAAGTGAATCCCTCGGGTTGGCTATGCAATTTGGGAACA
TCTCTGAAAATGGAATGAATTACTTAATGCTCTCTTGGGCTATACTGGAAACTTGCTTTATCCAGTGGATTTTCAGATCCTTGTCGA
AAACGCTTAAGAAGCTCAAGGTAAGAGAAACATACAATCCTCCTTTTCTTTTGATTATTGATATAACAGGTTAGGCACACTGATTGC
TACATGTTTCTAACATATCACTTGTAAATATATCTTTCTTGTTAATTGTTGAAAGTTGCAGAAAAGCCATTTATAAAGATCCATTTC
TTCTTAGATTATTCATCCCTGCTAATCCCATATTTTTCTTATGTAGCTGAATAAGAGGAACATTACTAAGCTGCAGCTCTACAAGAT
GTTTGCAACTGTGCTTGTAATCATGGTTGTGCTCAGTTTTGCCTGGATTTATGTGGAGGTAACATCTCAACAGTCTAGTGATAACTC
TGGGGAATCACTTGAAAAAAGTCATATGATTGTGTGACTGAAATTGTTTTCTGAATCAGGTATATCTCTACAGCTCCTTGAGTCAGT
TTTGGAAAGTGAAGTGGATTGTTCCAACACTTTGGTACATCCTTTCTTATGCAATGTTGGTACTGATTTGCCTCTTTTGGCCTCCAT
CGGAAAAACCAATGAGGTATGGTATCAATCTTTCTGTACTTGCCCTTTATCAATCGGGTGCTTATGTGGCCTGTTTTAAGTTCCACA
CTAAGATCTTGTCTGTTTTGTACTAACATGTTTGAACTTTGTATATCTGATCTTCTCTGCTGCTAGTTACACATTTTTCTGATGTAT
ATATACTGGTTTGAAATTGCAGGTACCTATACGTAGCTGACATGGAGGAAGAGACTGAAGAAGAAGATGATCTCTCCACTGCAGAAA
CCGGTATGAACGCAACAAAGGCTGAATACGAGAGGAGTGAAAGGAAGACCCTGCTGGAAGCATTCATCCTATTGCTTGGGAATATAC
CAGGGGAGAAGTGAAACTCCCCATCTTACAAAGTTACCGTCCTTTTAGCTTAAGCTGCCTACTTCTCATCCTTTTTCAGCTTAAGCT
ACTCCTAATCATCCTTTTAAACCTACGGCTTTAAGTTTTTTTTTAACTCATATAATCTTCTGCAGTAGACTTGACTTAATCGGATTT
TCTGTTTCATGAACTTGTTGGTAGTGTGGAACAAATGGGAAAATGAATATTTTTGGAACAAATTGATTTTCTGTTTCATATTAAGTT
AAATCATTCTGTTTCCACTGAAATAAATTGTTTTCCAAAAATCACTCCGTTTATTATGTCTTTGTTTTTAAGAAATAAAAGTGAGAA
AACAGAATAACGCGAAAATGTCGACATATTTGGCTAAGTATAGACAAGATTGGGAAGCTCTGTTTAGTTATGCGTCAGTCTCTCATC
AGTGTTCAACTGCCACGGAGCGAACCGATTCCTAATTGCAACGTCCCGAGTCCATAGAATGTCGACACTCTTTCACTCTTTCTCCAA
GTTGCCTCCTTTGAGTCCTTTCTCATATTTTATAGACTCACTTTCTGTTTCTTGATCCCGAGGAAGAAGAAGAATAAACTCTTGTTC
CC-**ATG_3'**

Figure 4.17: Nucleotide sequence of the *AtZIP9* promoter. In red, an iron-dependent regulatory sequence (IDRS)-(CATGC) positioned at -1939 bp from the ATG, and in green, two Zinc Deficiency Response Elements (ZDRE)- (RTGTCGACAY) positioned at -245 and -117 bp from the ATG.

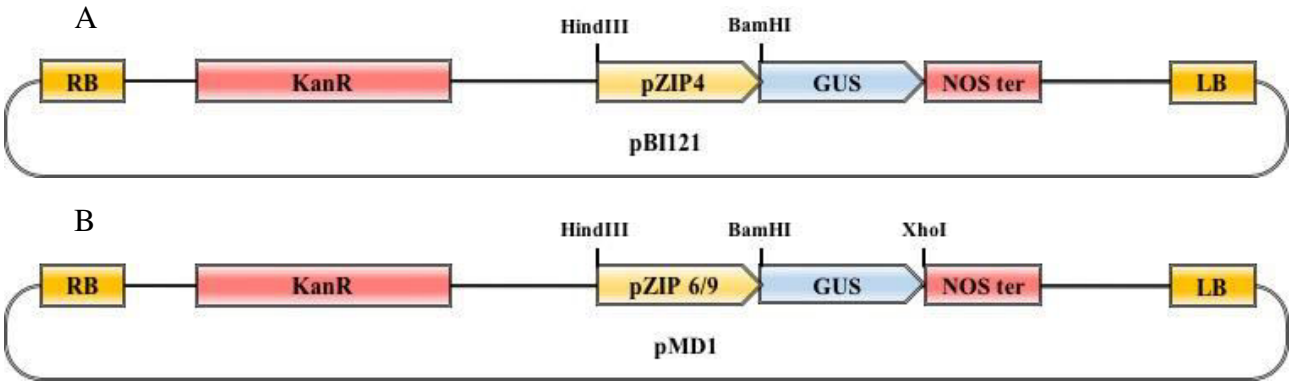

Figure 4.18: Diagram of the constructs obtained for the tissue localization of the expression driven by A) pAtZIP4::GUS and B) pAtZIP6::GUS and pAtZIP9::GUS.

Nucleotidic sequence of the promoter of *AtZIP6* (pZIP6)

5′_CTTGGTTACAAAGTAGCTCCATCTCTGTAGTCCACTCACTGATAATTTACTTCATTTTTTTCATTCTTTTAAACAACTGATAAT
TTACTTCACATGTTAGGAACATGTCAACTTCATTAGCAGTATGAAGTTGAATAACATATCTAATGAAATGTTAATCATGCAATCATT
AGATATAAAATCCACAGTTATTAAATACTTACTAATCACACAATCGTTCAATTGTGTTTATGTGAGAGGATTCAAATCAGTAGTCAT
AGTCTGAGTACCTTAGAAAGATAAAGCAGCCCCCAGTTAGGTGTTGATGTCCTCTTGCCAAACTAGGAAGCTGATGAGTGTACTTTA
TCTGCCCCCATCTTTCTGCATAAGTCGAACCAATTATTGGTTCATTTTTCTCATTTTTTTATTTTTATTTTCAAATAGTTTGGGGCA
AAATATTAAGTGGTGACACAATAAAATGTGGTGCATTGCCGTGTGTTTCAACCGTACGATCCGAAGTGTTTTTTTCACCATTCTCAA
AATTTTGTGGTATTTGTTTTAGGTGGTGCTGCGTTGCAGGACGGTGATATTTTCTTTTTTATATGTTTTGTGAAACGCATTTTTAAA
ATTGTACATGTTAACTTTTATCAATCAATATAAGATTTTGGAAAGATATAATTGTTTTGGCCATTTAAAATGATAAGAAAAAAACAA
ATATTCAAAGTTTGATAATCATTTATATGTGCACCACATTTTTATAGTTACCGTTTAACTTTTGTTTCACCTGCTGGTTGACAGACG
GCACTATCCAACATATGTTAGCTTGTTTCACTTGACATCTCGTTTGTTTCATCAACATATATCGACTATGGGCGAACCTCGAACCCA
AACTAATCTTTTCGGTGAGTATATCTTTTGAATTCCATGTTCATAATGGGTTAATGGGTCTAAAACGTGATACAATTTCGACTTAGA
TAAATAGAAATGAAACGGTAGGAATCAAAATTGAAAGGGAGCAAATTGACGTCATATCTTTTAGTATTTTACATCACTACTACTTCG
TTACTTTTCAATTTTACATTATAAATAAATTACTTTTTCTGAACAAAATAACTTGTTATATTTTTTTCGAGGTATTTTCACGAACAT
AGCAAAAGCCTGCATAGTGGTAATATATACGAACAACTAATGAATTCTCAAACAAAAATCCAAACACTAAGGTTTCGAATAGAGATG
TGCTGTGATAATAACGTATATATATACAGAAAAATTTGTTACTATTGGAACTGCACAGTCTGAACCGCATCGTGCGGTTTGGTCTCC
AAATACTAGATTAAAACGTGAGATCCGCAATACGTGGTAAAAAAAAATATTACAAAGTACGGAACCTATTTTTGCTTTGAATTGATA
TCACTTTTGTTGGGCTTAAAAGTTGAAACTAATTGGTTGGGAAAAGGTCCATAGGGCGATGGTCAAAGCTCAAACACAGAAAGTAAA
AAGGAACACGTACCAGTCTAACTTCATAGAGTGGGCATTGTGTAACCGAACCAAGTAAACCCAAACTGATCACAAATCAAACTGAAC
CACTAATCCACTCTGCTTAGTTGAGTATTGTTAATTAAAAGATGATAACTCCTTTAATTCGATAACTACTAATAAATCCTTTGATGG
TTTGTATTCTGTAAAAATAAATCTAACCGAACTAATAACATCAAGCACAAACATATTTGGGCTCAGGCTACTCAGTCATAATGGGCC
TTTAAACGGCCCATACTAAGTCAGAACAAAGAGCAAGTAATCTCAAAATGTCATCTTCTTCAAAGAAAGCAAAAGAACAAAAACAAA
AAATGGAAAAAGAATAAGTTTCCTTTAAATTTCCCCAATATCAAAAATGGAAGTCTTACTCAACAACGCACTTCTTTTATAACCGTT
TGACGTGTAAGTGGTCCGCGCACTAATCTCTCTCTCCCTCTCTTTCTTCTTCTTCCACAA-**ATG_3′**

Figure 4.19: Nucleotide sequence of the *AtZIP6* promoter. In red, an iron-dependent regulatory sequence (IDRS)-(CATGC) positioned at -1812 bp from the ATG.

Nucleotidic sequence of the promoter of *AtZIP9* (pZIP9)

5′_GGGTGGTGCTTGTTGGGTTATAGGTACAGCAGTTGCTCTGAAAACGCAGCTTTTTCTCGGTTTCTTCTCTTGGAAGAGAAGTCC
TTTGAGAGAAGATCTTGAAAGAAGCTGAGCATTGAAGAAGGTCTGCCCTGAAACAAACGGCTTAACTGAATTCTTGCTGCTGCTGCT
GCTAAGTGAGATAACTGAAGGGCATGAAGCTGAAAGTAGATGCGCCATTTTAAAGGTTTGTTCTTGATTCTATCAAACAAATTCACC
TGCAAAAACAAAAGCAGCTAAGATTTCAAGACATAATTTGGTTCAGCAGAACAAGACATATCAAGTAGATGTTTCATACCATATAAC
AAGTAAGGATTCAGCTGATTTTCTCTAGTTTAACTTCAAATTCAAATCAAAATCCAAAAAGACATGAATAGAAATCGAAACTTTATC
TTCACACCCCCCCCCCTAAATCAGCTACGTCCATAACAAGAGAAGAATCAAAACACACGAAATTTGAAGTCTTTTATCGAATCTGAA
AATCAGCTATTGTCAAAGACTGGATATTTATTTGATCAACTAAAGTAAATGTAAGAAAGAAGTACATTGATGAAATTCAGAGAAAAC
CCAACTGAATGAAAACTCTGTGAATTTTGATTTCCTATCATATTCAGAGTTTCTTCAAAACGAAATCACTCAACTTACAAAACCGGA
GAAATGAAATTCATTAGAAGAAACGATTGCTTACCTTTGAAAATTTGGAATCTTGTTTAGAGAGAGTTGGAGAAGATCCTTCGAGAC
TTTGAACTTTGAAGTGAGGGATGGGTCTCTCTTCTCTTCTCCCGGAACGATGAGAGATGAGATGAGACAGATATAAATCATCAGATA
TGCCCAAAGCATATTCTTACTTATTCCCTTCCCAACAAATTATGGCCCAAAGTGTCGCTTTTTTAAGAACGTTGGTTTATTAGTTTT
AAAGTTTTCCGGTTGTGAATGATACAGGTCCGGCCTTTGTGGGCCAGTTTCTCAGTCGCTCATTTAGGCAACTTAAGGAACATTCTT
CCCTTACTGGGCCGGTTGGCCCAAATATATACTTTTTGAATATGTTTGTGGCTATTTTCTAAATTTTAACTTTTAATTATTAAAACA
GAGAATCATGAGATAGGAGAAAAACAAAATCAACTGTAAAATGCAAACCTAACTTACATAATCTTTTGAATGAAATTTTATTAAGAC
GCAAAACATTACTAGTATTTCGCATTGTAATAGTCATTTTTCTGCAAGTTGACCAAACAAGAGTCATACTTCTGATGCAAGATACGA
ACAAAGACTTCAATTATAACAAAACATTCTCATACATCTCATCTCTAATTCTATATTTGTTTTCTCGTAGTTATTATCTTCCAAACT
TTAATATTCTTGTCAATGAGGGTACTAGATGAAAATGACGACATTCTATGGTCATTTGATTCCCGTGAACCTCATGTGACCTTGTTA
ACGTACGTGCACGCACACACAAACCCTCGCACTGATTGACATTCTCCCAATCTTTCTTTATAAAACACACAGACAACTCCATAATAT
TAATAACCCATATATACTTAGCTTGCTGGTTTCCTTGGCAATAATTTATATAATTCTACAAGTTTAATCGCCTAATCGGATTTAGTA
AATGTCTCTCTTACAGGTCTGAAACTTCTTCCACTTCATCTATTTAATGTTATTTTGCTTCTTCAATCCTGTTTCCTCACATAATTT
TGCCTCATAATGTTTTCAGGATTTTTGGCAGTTTCTTCGACCATTATCATCTGGTTTGACAGGTATTGTCACTTCAAATCTCAAAGC
AATTACTTCATTTCGCTCTTAAACACACTTAAATGCAAATTTTGAGATTTTCTTAGCAAAGTTAACTCAATTTATTTTTGCATGTAA
CAAAACAGAGTCGTTCACAACTAGCTGTGACTCGGGCGACTCAGACCCGTGCCGAGATGACGCAGCTGCTCTTACCCTCAAGTTCGC
AGCT-**ATG_3′**

-ATG_3′

Figure 4.20: Nucleotide sequence of the promoter of *AtZIP9*. In green a Zinc Deficiency Response Element (ZDRE)- (RTGTCGACAY) positioned at -579 bp from the ATG.

Conversely, ZIP6 and ZIP11, which have no ZDRE elements, are uninfluenced by the level of Zn (Jain *et al.,* 2013; Figure 4.1). Like ZIP4, ZIP9, which is strongly induced by low Zn availability, has a single ZDRE element (ATGACGACAT) at a distance of -579 bp from the first ATG (Figure 4.20).

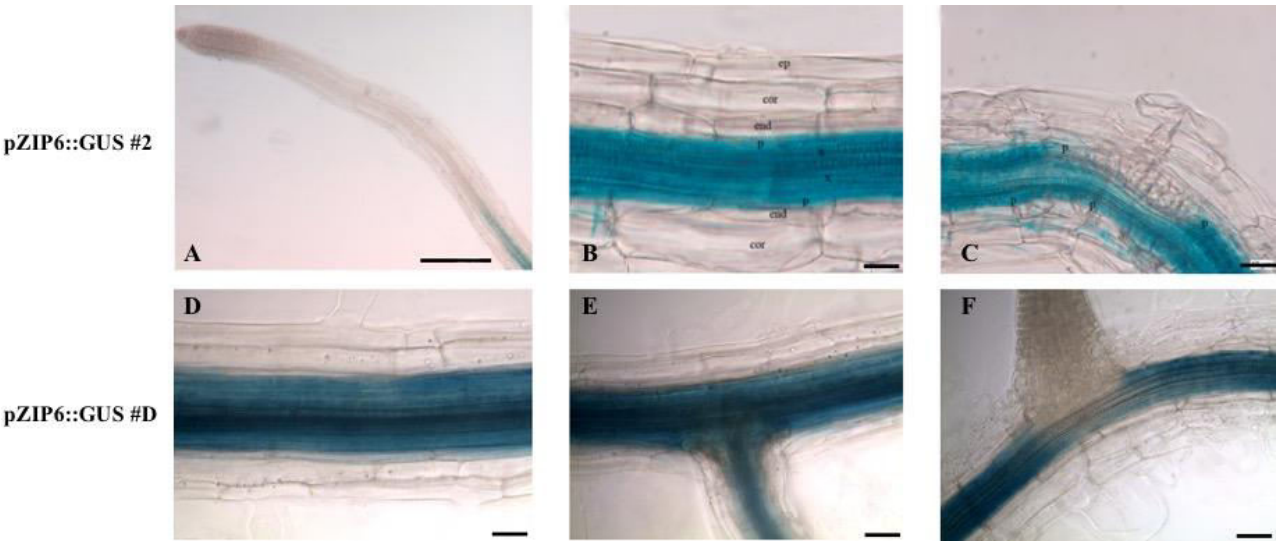

Figure 4.21: GUS expression was analyzed in the roots of transgenic *A. thaliana* pAtZIP6::GUS #2 (A-C) and #D lines (D-F) grown on a standard MS medium. Tissue legenda: xylem (x), pericycle (p), endodermis (end), cortex (cor), epidermis (ep). Scale bars = 40 µm.

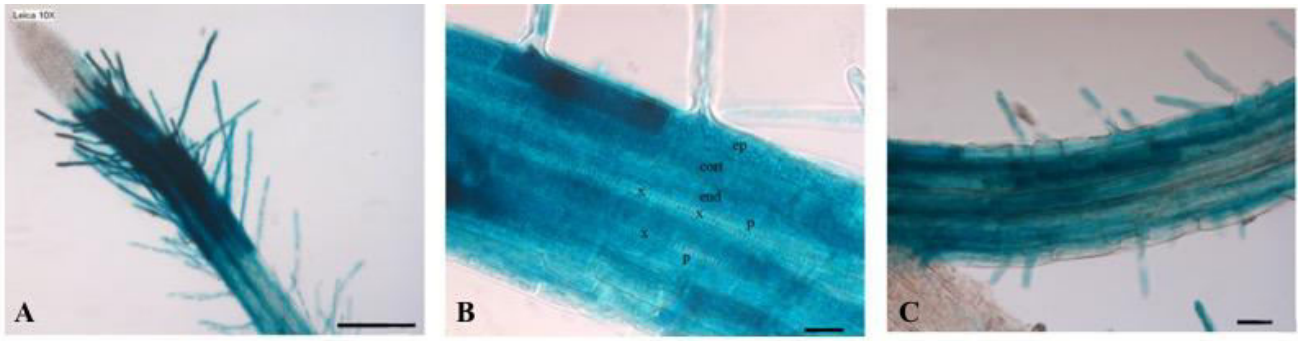

Figure 4.22: GUS expression was analyzed in Zn-deficient roots of transgenic *A. thaliana* roots for pAtZIP9::GUS genes: A) root apex, B) differentiation zone and C) root hairs. Tissue legenda: xylem (x), pericycle (p), endodermis (end), cortex (cor), epidermis (ep). Scale bars = 40 µm.

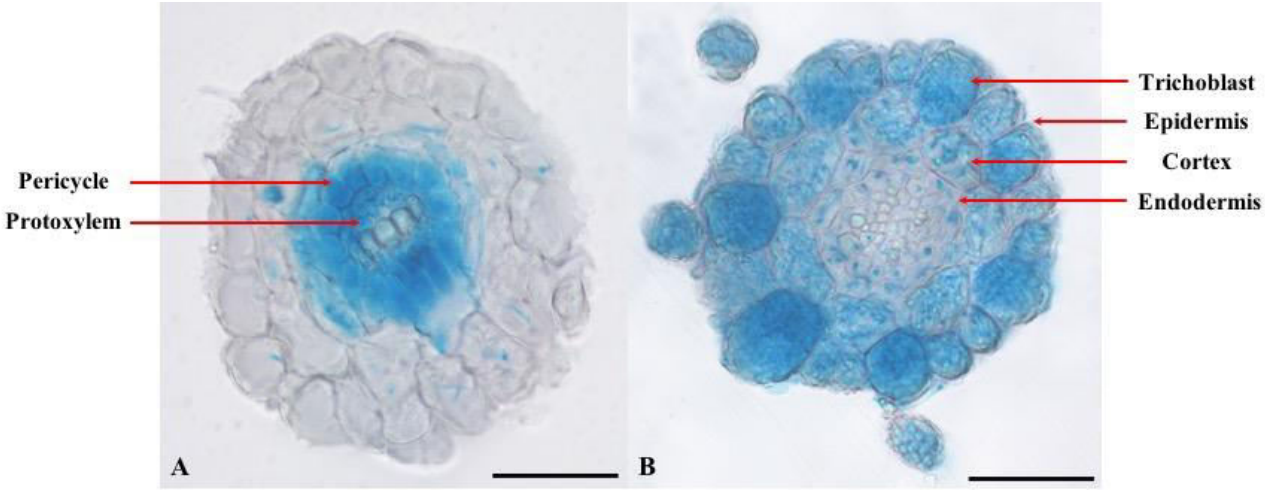

Figure 4.23: GUS Expression was analyzed in transgenic *A. thaliana* root cross-sections for A) pAtZIP6::GUS and B) pAtZIP6::GUS genes. Scale bars = 40 µm.

GUS assays revealed different tissue localizations of *AtZIP6* and *AtZIP9* expression in the roots (Figures 4.21, 4.22). *pAtZIP6::GUS*-transformed *A. thaliana* lines grown on a standard MS medium only displayed GUS expression in the vascular tissues of the roots (Figure 4.21). Interestingly, the GUS signal of *pAtZIP6::GUS* seemed to be reduced in these tissues during lateral roots formation (Figure 4.21C, 4.21F). Milner *et al.* (2013) reported a similar tissue localization for *AtZIP1* and *AtZIP2*. These transporters play an essential role in Zn and Mn translocation from roots to shoots, mediating the mobilization of these metals from the root stele to the xylem parenchyma for the subsequent xylem loading and transport to the shoots (Milner *et al.,* 2013). On the other hand, the *AtZIP9* promoter drives GUS expression in the epidermis, cortex and endodermis (Figure 4.22B) whereas the GUS signal was not detected in the root apexes of either transgenic line (Figure 4.21A, 4.22A). Cross-sections of the roots confirmed these results (Figure 4.25A, 4.25B), and also revealed in the *pAtZIP9::GUS* lines an intense signal in the trichoblast cells, which are involved in the hairy roots formation. As regards the shoots, *AtZIP6* is mainly expressed in the vascular tissues of the stems (Figure 4.24A, 4.24B, 4.24F) and leaves (Figure 4.24E) whereas at floral level the GUS signal was observed in the vasculature of petals (Figure 4.24C). AtZIP6 also seems to be expressed in the style below the stigma (Figure 4.24D), a tissue that forms a cylinder around the tract cells driving pollen tubes from the stigma to the ovary. The GUS signal was also detected in the layer between the vasculature and the endothecium of the stamen (Figure 4.24G) suggesting a role in micronutrient translocation in the pollen maturation organs.

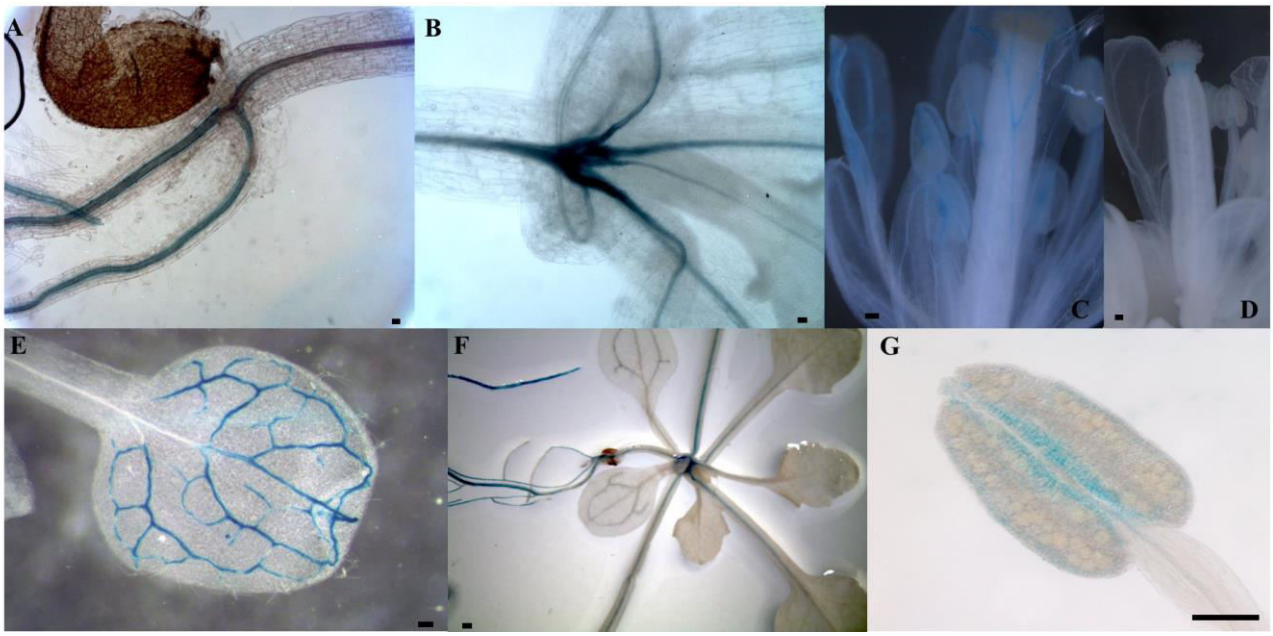

Figure 4.24: GUS expression analyzed in transgenic pAtZIP6::GUS *A. thaliana* plants: A) root/shoot vasculature, B) shoots, C-D) flowers, E-F) leaves and G) anthers. Scale bars = 40

Interestingly, the GUS signal of *pAtZIP9::GUS*-transformed lines was only evident in the roots and shoots of Zn-deficient plants (Figure 4.25B, 4.25E). These results reflect what observed by Lin *et al.* (2016) regarding the promoter analysis of *AtZIP4,* i.e. that the GUS signal was only observed in plants grown at low Zn concentrations. In the shoots, *AtZIP9* expression was slightly detectable in the vasculature, whereas a stronger, diffuse signal was evident in the entire leaf, and at the stomata and hydathodes in particular, suggesting a possible role in stomata formation or regulation (Figure 4.25B). When compared with *AtZIP6*, *AtZIP9* expression displays a different localization within the stamens, more localized at the intersection between vasculature and anther base, instead of specific layers of the anther itself, however further investigations are necessary (Figure 4.25F). In the flowers, the *AtZIP9* promoter also drove GUS expression where valves join together, and both in the style and gynophore regions (Figure 4.25G) with a strong signal at the base of the anther filaments (Figure 4.25G).

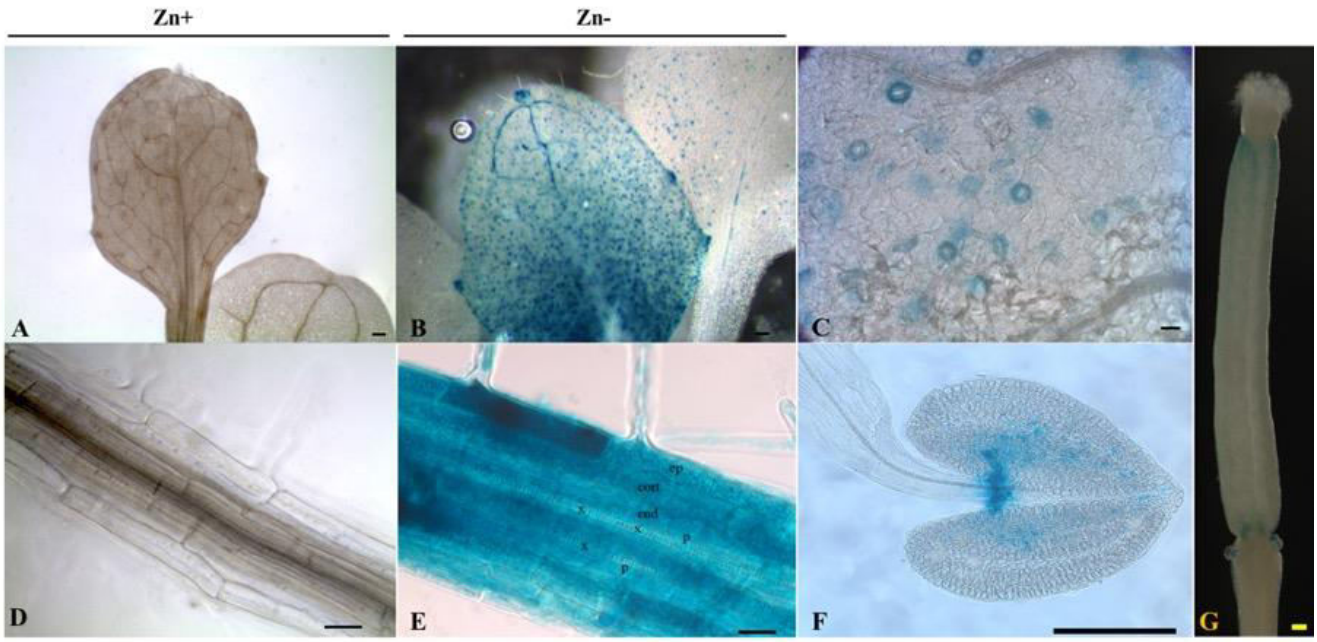

Figure 4.25: GUS expression in transgenic pAtZIP9::GUS *A. thaliana* plants: A-B) leaves, C) stomata, D-E) roots, F) anthers and G) ovary. A and D show leaves and roots of plants grown at standard Zn levels, B and E at low Zn levels. Scale bars = 40 µm.

4.8 SUBCELLULAR LOCALIZATION of *AtZIP4*, *AtZIP6* AND *AtZIP9*:

The analysis of the subcellular protein localization of *AtZIP4*, *AtZIP6* and *AtZIP9* was carried out by producing several constructs fusing the coding sequence of each transporter to the eGFP marker gene, which were then tested through the transient expression in transfected *A. thaliana* protoplasts. At first, we prepared the constructs for the subcellular localization by fusing the eGFP reporter gene at the C-terminus of ZIP4, ZIP6 and ZIP9 (Figure 4.26), in order not to interfere with the presence of a putative signal peptide. Instead of stably transforming *A. thaliana* plants we transiently transfected their isolated protoplast.

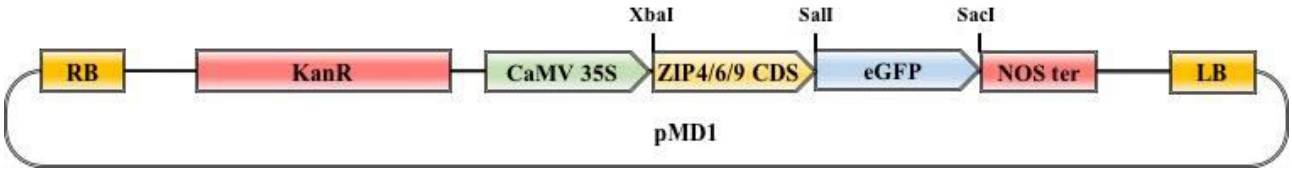

Figure 4.26: Constructs for the subcellular localization of *AtZIP4*, *AtZIP6* and *AtZIP9*. The eGFP reporter gene was inserted downstream the coding sequences of the ZIP transporter using the primers described in Table 3.5 (Materials and Methods).

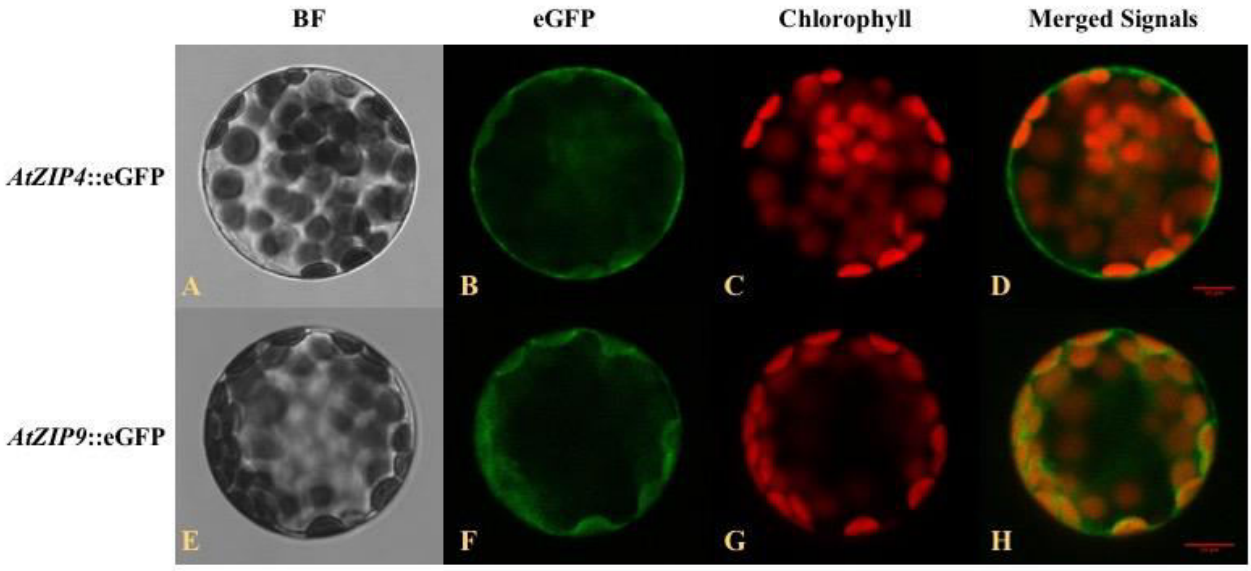

Figure 4.27: Subcellular localization of *AtZIP4*::eGFP (A-D) and *AtZIP9*::eGFP (E-H) proteins transiently expressed in *A. thaliana* protoplasts. From left to right: bright-field image, eGFP fluorescence, chlorophyll fluorescence and a combined image of eGFP and chlorophyll fluorescence. Scale bars = 10 µm.

The signal obtained from protoplasts transfected with *AtZIP4*::eGFP and *AtZIP9*::eGFP genes suggests that ZIP4 could be localized at the plasma membrane and ZIP9 at the tonoplast, although

the eGFP signal was not very strong (Figure 4.27); no results were obtained for the *AtZIP6*::eGFP gene (data not shown).

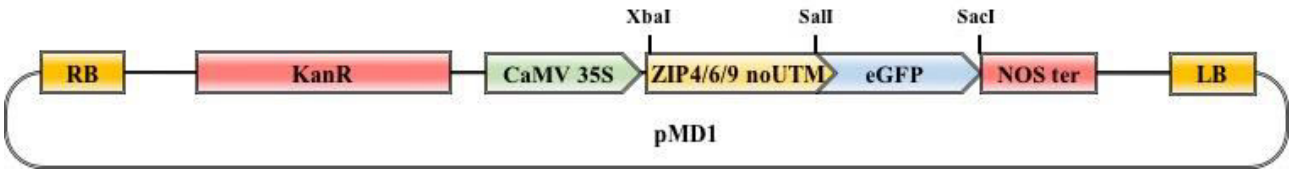

Figure 4.28: Constructs for the subcellular localization of *AtZIP4*, *AtZIP6* and *AtZIP9*. The eGFP gene reporter has been inserted down-stream the coding sequences without the last transmembrane domain of the ZIP transporters using the primers described in the Table 3.5 of Materials and Methods.

A possible explanation for the low eGFP signal could be the proximity of the C-terminus of ZIP4, ZIP6 and ZIP9 to the last transmembrane domain (Figure S4; Supplementary data), which would affect eGFP folding. Moreover, protoplast transfection with eGFP::*AtZIP4,* eGFP::*AtZIP6,* eGFP::*AtZIP9* did not yield any results (data not shown). Hence, to obtain a clearer localization, we removed the last transmembrane domain of each transporter maintaining the eGFP reporter at the C-terminal end obtaining *AtZIP4*noUTM::eGFP, *AtZIP6*noUTM::eGFP and *AtZIP9*noUTM::eGFP genes (Figure 4.28). *A. thaliana* protoplasts were transfected with these constructs obtaining an enhanced fluorescence signal that suggests a plasma membrane and a tonoplast localization for ZIP4 and ZIP9 respectively (Figure 4.29A-D, 4.29I-L). The subcellular localization of ZIP6 (Figure 4.29E-H) was still rather unclear, and we are currently trying to co-localize the signal using different membrane reporters.

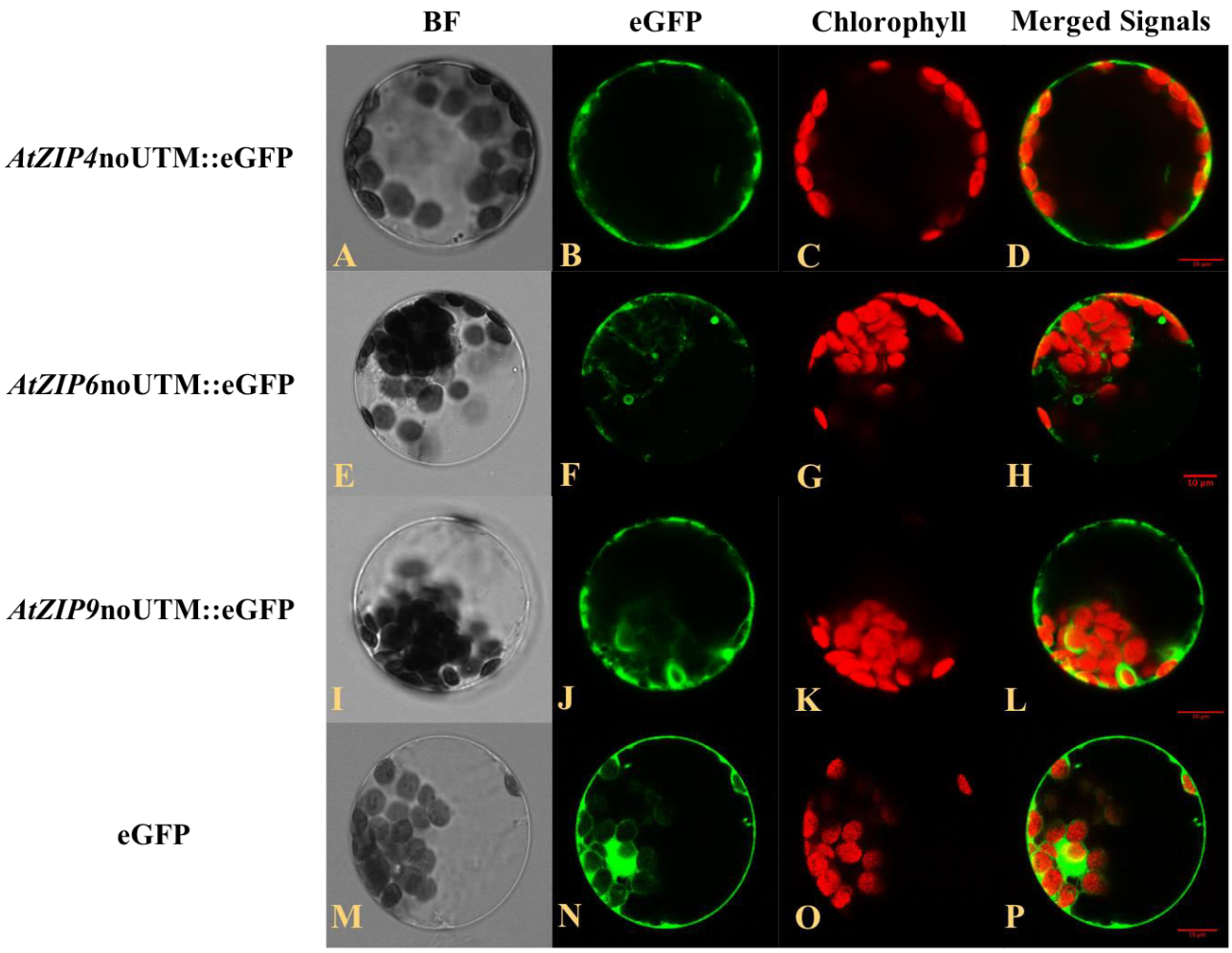

Figure 4.29: Subcellular localization of *AtZIP4*noUTM::eGFP (A-D), *AtZIP6*noUTM::eGFP (E-H), *AtZIP9*noUTM::eGFP (I-L) and eGFP control (M-P) proteins transiently expressed in *Arabidopsis* protoplasts. From left to right: bright-field image, eGFP fluorescence, chlorophyll fluorescence and a combined image of eGFP and chlorophyll fluorescence. Scale bars = 10 µm.

4.9 COMPLEMENTATION OF YEAST METAL UPTAKE MUTANTS:

Previous experiments focusing on the subcellular localization of ZIP4, ZIP6 and ZIP9 suggest that ZIP4 is localized to the plasma membrane and ZIP9 at the tonoplast (Figure 4.29). Assunção *et al.* (2010) observed that ZIP4 complements the *zrt1/zrt2*Δ mutant, suggesting a key role for it in Zn transport, although to date, no research has been carried out to see if it is involved in the mobilization of other metals. The complementation of *zrt1/zrt2*Δ mutant seems to be mediated by ZIP1, ZIP2, ZIP3, ZIP7, ZIP11, and ZIP12, whereas ZIP1, ZIP2, ZIP5, ZIP6, ZIP7, and ZIP9 complementing the *smf1Δ* mutant for Mn transport (Milner *et al.,* 2013). ZIP4 was not investigated, whereas only ZIP7 partially complemented the *fet3/fet4*Δ mutant (Milner *et al.,* 2013). To better understand the role of the ZIP4 and ZIP9 transporters and confirm their subcellular localization, we

performed a complementation assay using yeast mutants lacking Zn (*zrt1/zrt2*Δ) and Fe (*fet3/fet4*Δ) plasma membrane high- and low-affinity transporters for *AtZIP4,* and a Zn (*zrc1/cot1*Δ) tonoplast transporter mutant for *AtZIP9*. The localization of ZIP6 was unclear, so we decided not to take it into account, even though bioinformatics prediction tools suggest a plasma membrane localization for this transporter (Figure S5; Supplementary data) and yeast complementation analyses performed by Milner *et al.* (2013) indicated a role in Mn transport. In our assays, *AtZIP4* complemented the *zrt1/zrt2*Δ (Figure 4.31A) mutant, thus confirming what observed by Assunção *et al.* (2010) but did not complement the *fet3/fet4*Δ (Figure 4.31B) mutant, suggesting it only played a role in Zn transport. We are currently investigating if ZIP4 is involved in Mn transport using the *smf1*Δ yeast mutant (data not shown).

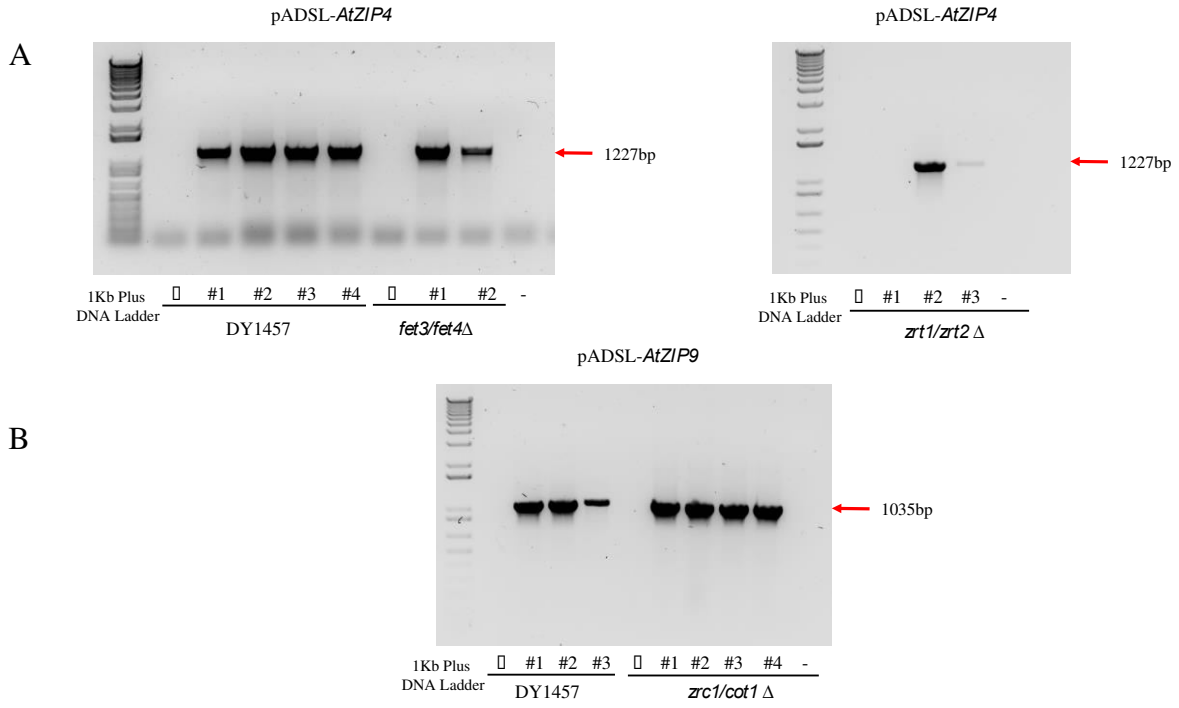

Figure 4.30: A) Colony PCR on yeast Zn and Fe plasma membrane uptake mutants transformed with pADSL-*AtZIP4* and an empty vector (ø). B) Colony PCR on yeast Zn tonoplast uptake mutant transformed with pADSL-*AtZIP9* and an empty vector.

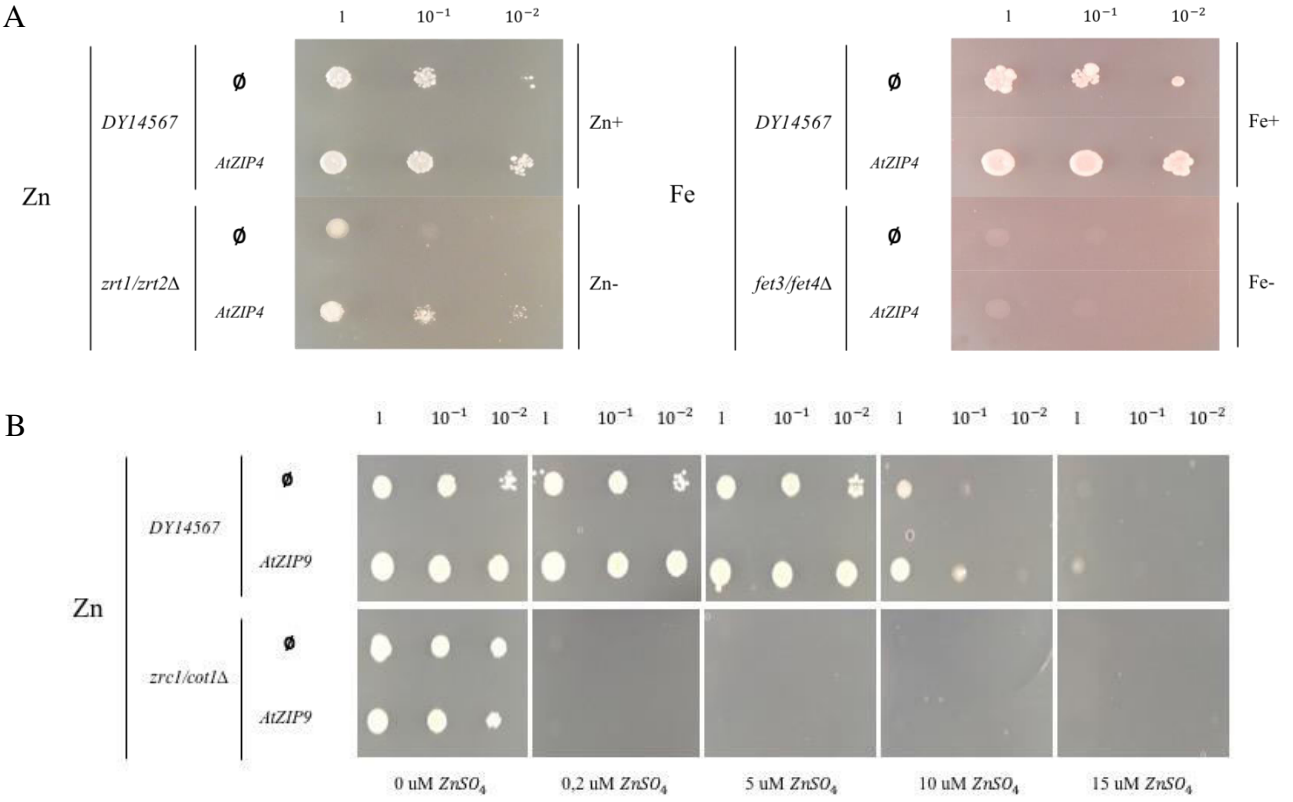

Figure 4.31: Complementation of yeast uptake mutants with ZIP4 and ZIP9. A) Complementation of a yeast mutant defective in the plasma membrane uptake of Zn (*zrt1/zrt2*) and Fe (*fet3/fet4*) using *AtZIP4* and an empty vector as the control (ø). B) Complementation of a yeast mutant defective in the tonoplast uptake of Zn (*zrc1/cot1*) using *AtZIP9* and an empty vector as a control (ø).

ZIP9 cannot complement the *zrc1/cot1*Δ mutant at different concentrations of Zn, suggesting it has no specific role in Zn uptake into the vacuole (Figure 4.31B). Its inability to complement the *zrc1/cot1*Δ and *zrt1/zrt2*Δ mutants (Milner *et al.,* 2013) suggests that it may not be involved in the transport of Zn, although its expression is highly regulated by different concentration of this metal. To verify whether ZIP9 is involved in Zn export instead of import, we transformed the *zrt3*Δ yeast mutant, impaired for Zn extrusion from the tonoplast, but experiments on this mutant are still under way.

4.10 Zinpyr-1 STAINING:

The study of metal localization and accumulation in biological tissues has become of great interest, given the functional role of metal transporters. Various techniques have been appraised to better analyze the specific accumulation and distribution of metals in different plant tissues and organs and the use of ICP-MS, fluorescent dye and X-ray fluorescence-based techniques is very well reported in literature. Zinpyr-1, a fluorescent probe selective for Zn, has recently become popular for the functional analysis of metal transporters (Sinclair *et al.,* 2007; Haydon *et al.,* 2012; Deinlein *et al.,* 2012). Sinclair *et al.* (2007) investigated the use of this fluorescent probe on *Arabidopsis* roots, and found a different Zn distribution between wild-type plants and knockout mutants for *AtHMA2* and *AtHMA4*, two plasma membrane transporters that are expressed in the vascular tissues (Mills *et al.,* 2003; Hussain *et al.,* 2004; Verret *et al.,* 2004). Zn distribution was also analyzed by means of this probe in *A. hallery* RNA interference lines for nicotianamine synthase (NAS), revealing reduced Zn xylem loading due to the lower levels of Nicotianamine (NA), an important Zn-binding agent (Deinlein *et al.,* 2012). When Li *et al.* (2015) produced different *Arabidopsis* lines over-expressing *ZmIRT1* and *ZmZIP3*, two maize ZIP transporters, they confirmed greater Zn accumulation in the roots and shoots by using the Zynpyr-1 dye. To better understand if the absence of expression of single ZIP transporters and their combination can lead to changes in Zn distribution in the roots, we decided to perform a Zinpyr-1 analysis on *zip4.1, zip6.1*, *zip9.1* single, *zip4/zip9*, *zip4/zip6*, *zip6/zip9* double and *zip4/zip6/zip9* triple knockout mutants, as described by Sinclair *et al.* (2007). At first, we tested the effect of the protocol on Col-0 plants, and found that the root tissues were damaged, and the propidium iodide (PI) had stained the nuclei of different cell layers (Figure 4.32E-H). PI staining is localized at the cell wall when the tissues are intact but can also stain the nucleus when the cells are ruptured. We modified the protocol so as not to affect root integrity: the EDTA washes were eliminated and a saline solution was used to prepare the Zinpyr-1 working solution. By removing the EDTA washes, as shown in Figure 4.32A-D, the PI stain was only localized at the cell walls, and no signal was detected at nucleus level. Zinpyr-1 staining of Zn in intact, undamaged Col-0 roots revealed a clear epidermal and cortex localization (Figure 4.35) in the differentiation zone (DZ), unlike the vascular localization observed by Sinclair *et al.* (2007). Using this modified staining protocol, the root tissues remained intact and the Zinpyr-1 signal was very clear, so we proceeded to stain the single *zip4.1*, *zip6.1*, *zip9.1* and the triple *zip4/zip6/zip9* knockout mutants and wild-types (Figure 4.34). All the mutants were characterized by a similar Zn distribution, so we also selected the *hma4-8* mutant as positive control since it showed, according to Sinclair *et al.* (2007), a specific localization at the pericycle.

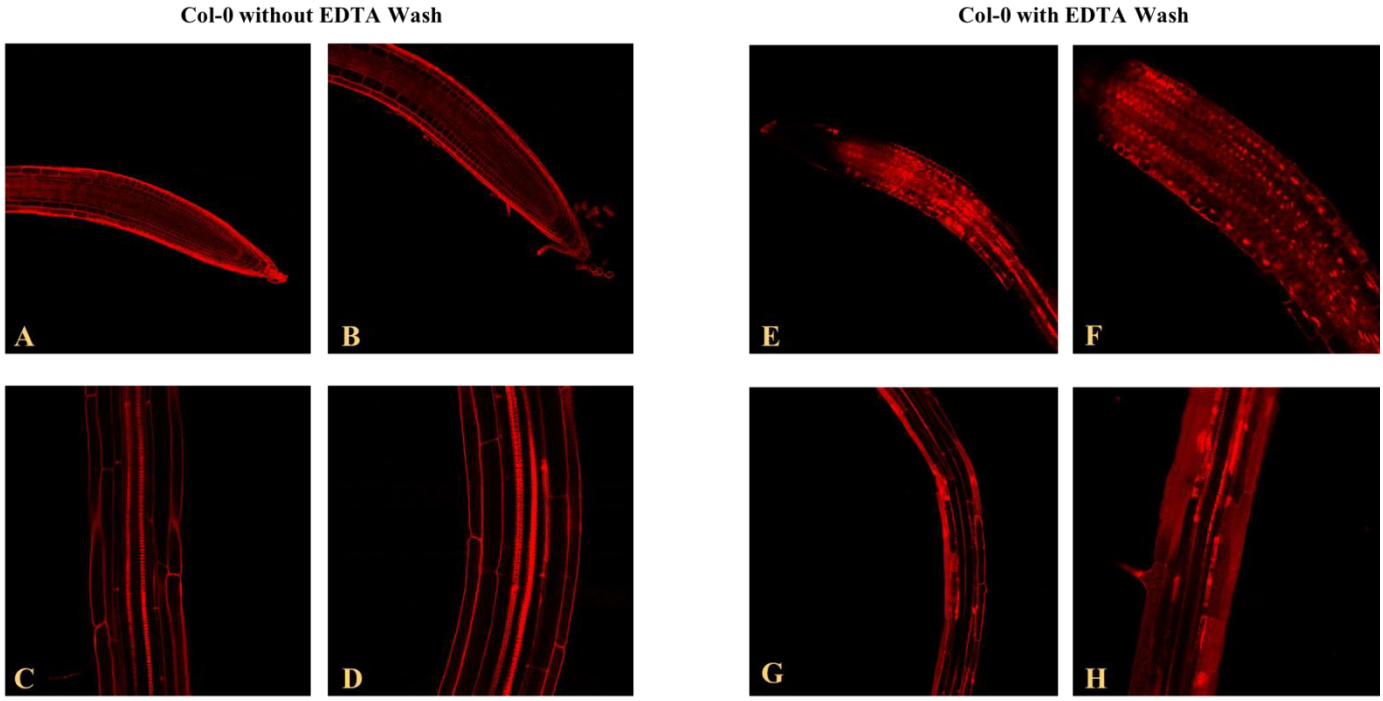

Figure 4.32: Propidium iodide (PI) staining of Col-0 roots without (A-D) and with (E-H) EDTA washes. PI only stains the cell walls of intact tissues, but if cells are damaged, also their nuclei.

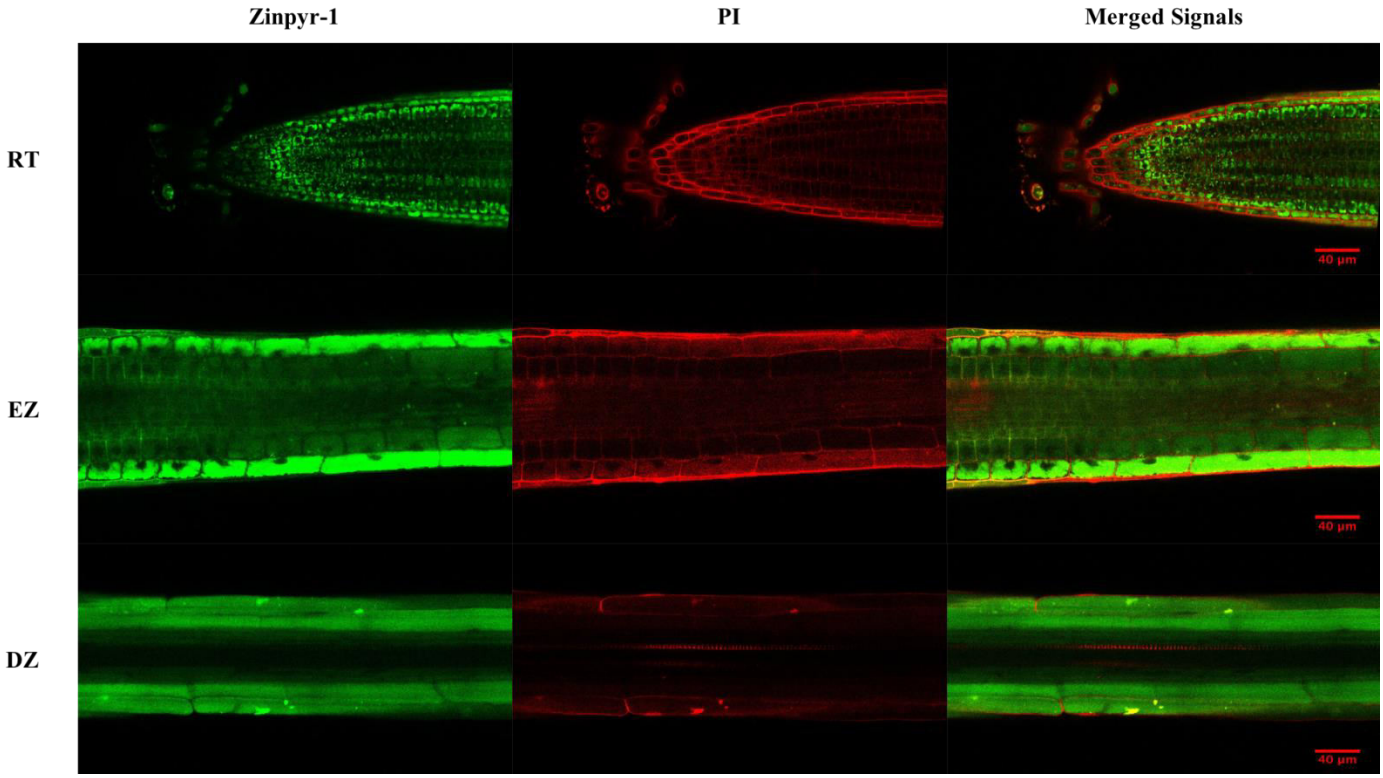

Figure 4.33: Zinpyr-1 staining of different parts of the root of *A. thaliana* cv. Col-0. Propidium iodide staining root cell walls is indicated as (PI). The different zones of the root are indicated: root tip (RT), elongation zone (EZ), and differentiation zone (DZ). Scale bars = 40 µm.

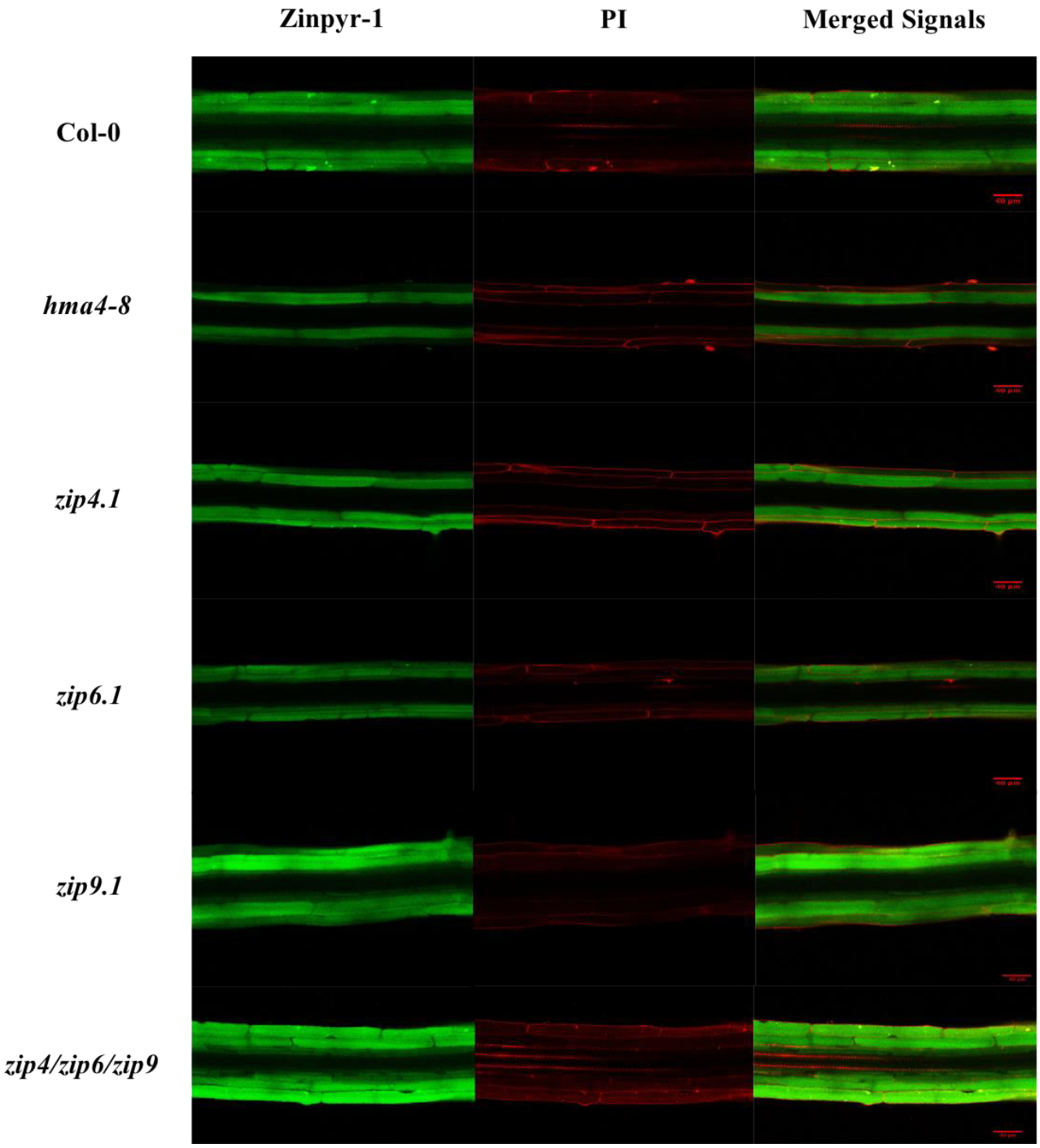

Figure 4.34: Zinpyr-1 staining of the differentiation zone of roots of wild-type plants and single *zip4.1*, *zip6.1*, *zip9.1,* double *zip4/zip6, zip4/zip9*, *zip6/zip9,* triple *zip4/zip6/zip9* and *hma4-8* knockout mutants. Propidium iodide staining cell walls is indicated as (PI). Scale bars = 40 µm.

The *hma4-8* mutant stained with Zinpyr-1 revealed the same endodermal/cortex localization observed in the other mutants, and not the pericycle localization observed by Sinclair *et al.* (2007) (Figure 4.34). Despite the differences in Zn distribution, we observed PI staining at nucleus level in various other works, which confirms that Zinpyr-1 is very invasive for plants. Moreover, we decided to stain directly the root cross-sections of the *hma4-8* positive control coupled with the wild-type and the triple knockout mutant and found a different Zn spatial localization (Figure 4.35).

The Zinpyr-1 dye revealed that Zn was distributed in the stele of both the wild-type and *hma4-8* mutant whereas the signal was more intense and widespread in the tissues of the triple knockout mutant (Figure 4.35). The results obtained from the analysis of Zn distribution using the Zinpyr-1 fluorescent dye suggest that this protocol must be improved, since it was not useful to detect differences among the various mutant lines.

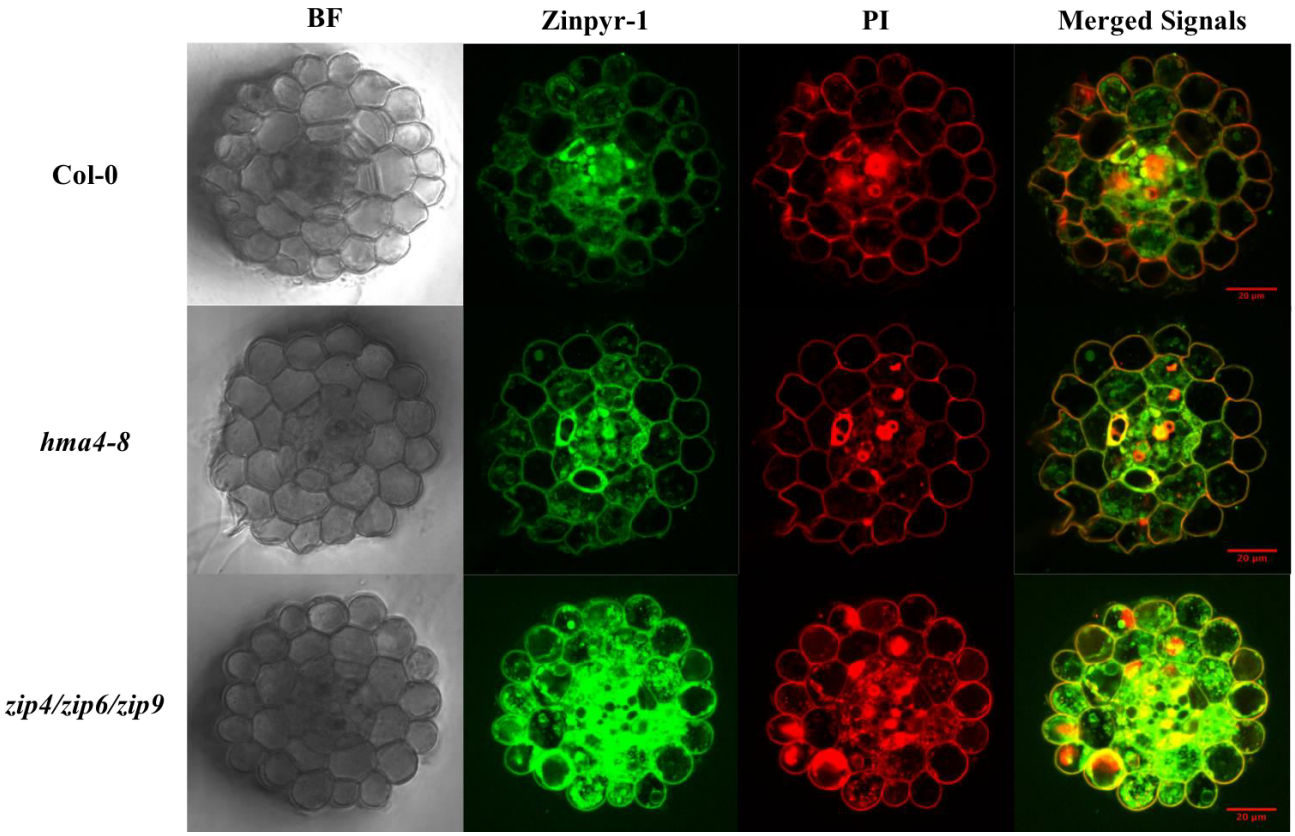

Figure 4.35: Zinpyr-1 staining of the cross sections of the root differentiation zone of wild-type plants and triple *zip4/zip6/zip9* and *hma4-8* knockout mutants. Propidium iodide staining the root cell walls is indicated as (PI). Scale bars = 20 µm.

4.11 TwinMic X-Ray SPECTROMICROSCOPE:

To better improve our knowledge of Zn localization in the plant roots and verify whether the lack of ZIP genes results in a different inorganic ion profile or tissue distribution, we decided to use an X-ray spectromicroscope, hence an alternative technique that requires no fluorescent diffusing dye. X-ray absorption and X-ray fluorescence technologies are characterized by a high spatial resolution and have been widely used to analyze metal distribution in hyper-accumulator plants (Haydon, 2014). The TwinMic X-ray spectromicroscope available at the Elettra-Synchrotron of Trieste is a remarkable facility combining both absorption spectroscopy and low-energy X-ray fluorescence to

transmission imaging and may be an interesting tool to investigate element distribution in plants. Col-0, the triple *zip4/zip6/zip9* knockout mutant and the *hma4-8* control line were grown vertically on Hoagland's medium supplemented with 1 µM Zn, and the roots were subsequently cryo-sectioned 1 cm from the root tip to maintain the spatial distribution of all the elements. The root cryo-sections were made at the University of Ljubljana under the supervision of Prof. Katarina Vogel Mikus.

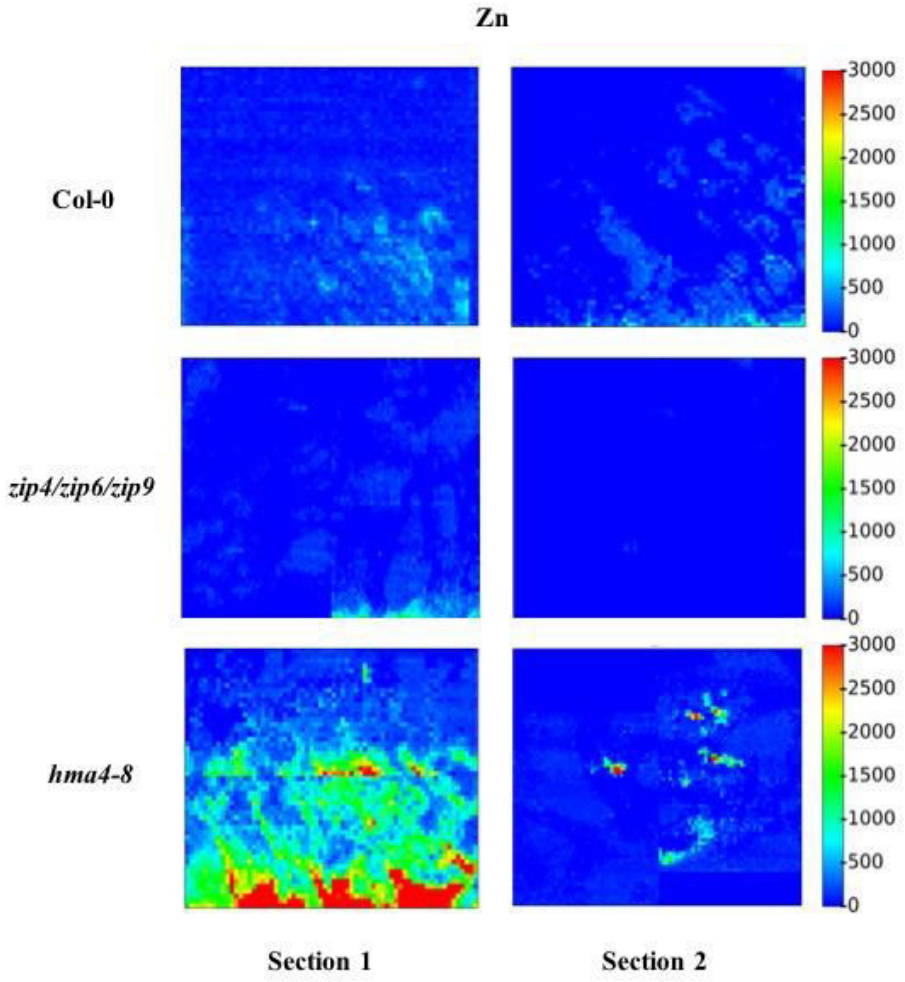

Figure 4.36: Distribution of Zn using LEXRF in root cross sections of wild-type plants and triple *zip4/zip6/zip9* and *hma4-8* knockout mutants. The signal intensity is shown as a color scale, with brighter colors indicating higher concentrations. Zn maps were obtained after scanning with the 1.3 keV beam, yielding 80 x 80 µm scans performed at micrometric

Subsequently the root cross-sections were analyzed by mean of TwinMic X-ray stereomicroscope to obtain information about a possible different distribution among these lines. Unfortunately, the concentrations used in the medium were too low to be clearly characterized with this technique, as evident from Figure 4.38, showing Zn distribution in two different sections of the wild-type, the triple *zip4/zip6/zip9* and the *hma4-8* knock out mutants. The Zn distribution in the root cross

sections of Col-0 and the triple knock-out mutant is very difficult to appreciate, whereas a stronger signal can be seen in the control *hma4-8* mutant lacking the *AtHMA4,* transporter involved in vascular tissue charging of Zn, and confirming the greater accumulation of this element in the roots of this mutant (Mills *et al.,* 2003; Hussain *et al.,* 2004; Verret *et al.,* 2004). Interestingly, Zn distribution seems very widespread and not localized in specific layers, as suggested by Zinpyr-1 staining (Sinclair *et al.,* 2007). Further analyses will be performed increasing the Zn amount in the medium to better improve the effect and the possible different Zn distribution among the root layers.

5. CONCLUSIONS

The transport of nutrients into and inside the plant is an essential mechanism that influences fundamental biological functions in every cell. The correct homeostasis of essential elements such as Zn, Fe and Mn is fundamental for their interaction with all classes of enzymes, for which they act as cofactors or activators. Metal transporters play a key role in the regulation of this mechanism, precisely adjusting this system in response to the various types of stress that plants are subjected to, whether biotic or abiotic. This work focuses on the functional analysis of three members of this transport family, namely *AtZIP4*, *AtZIP6* and *AtZIP9*, the precise role of which is still unclear. Of these, *AtZIP4* has already been partly characterized: previous investigations have shed light on its tissue localization and revealed its ability to complement the *zrt1/zrt2* yeast mutant defective for Zn uptake (Lin *et al.,* 2016; Assunção *et al.,* 2010). The role of these transporters in the metal homeostasis is still rather unclear, so we used different approaches to shed some light on their function in *A. thaliana* plants. At first, we performed an expression analysis on Col-0 plants grown at different Zn, Fe and Mn concentrations, to confirm previous results, also examining their regulation at different Mn levels and under conditions of excess Fe, never previously investigated. The expression of *AtZIP4*, *AtZIP6* and *AtZIP9* at low Fe availability and different Zn concentrations confirmed the results obtained by other authors (Figure 4.1) (Wintz *et al.,* 2003; Join *et al.,* 2013). A shortage of Zn up-regulates the expression of *AtZIP4,* whereas an excess down-regulates it in both roots and shoots; the experimental conditions tested on the other hand appeared to have no effect on the expression of *AtZIP6* (Figure 4.1). *AtZIP9* displays the same behavior as *AtZIP4,* although its expression under conditions of excess Zn does not appear to be so strongly reduced in the shoots (Figure 4.1). Wintz *et al.* (2003) recorded lower *AtZIP4* transcript levels in the roots when Fe availability was limited, and our analyses confirmed these observations (Figure 4.1). Interestingly, a strong reduction in *AtZIP4* was also obtained in excess of Fe, suggesting a possible role in the low-affinity transport of this metal. Decreased *AtZIP4* expression under low Fe conditions suggests that Fe deficiency results in an excess of Zn, hence the plants display a modulation strategy similar to that observed at high Zn levels (Figure 4.1). The lower *AtZIP4* expression at high concentrations of Fe may also be ascribed to its possible role as a low-affinity Fe transporter, hence the need to reduce it to prevent Fe transport into the roots when this metal is too abundant in the external medium. No significant differences were observed in *AtZIP6* and *AtZIP9* expression at different concentrations of Fe (Figure 4.1). *AtZIP4* and *AtZIP9* in the roots were slightly induced by Mn deficiency, although the regulation was not as strong as what observed under different Zn conditions, indicating that Mn is not the main metal transported. The *AtZIP6*

transcript levels did not appear to be modulated by changes in Mn levels, unlike its response to Zn and Fe (Figure 4.1). To analyze the phenotype of plants lacking ZIP4, ZIP6 and ZIP9 we took into consideration single *AtZIP4* (*zip4.1*; SALK_ 145371C - NASC ID: N664252), *AtZIP6* (*zip6.1*; SALK_116013 - NASC ID: N616013) and *AtZIP9* (*zip9.1*; SALK_ 090000 - NASC ID: N590000) knockout mutants that were tested at different Zn, Fe and Mn conditions. The primary root of the *zip4.1* mutant was shorter than that of the wild-type under high Fe conditions, and the difference in length was amplified by removing Zn from the Fe-rich medium (Figure 4.6, 4.12). Conversely, *zip6.1* displayed no differences in primary root length at different Fe and Mn concentrations, except under high Zn conditions, when it was longer than the control (Figure 4.7, 4.12). The absence of Fe coupled with high Zn concentrations did not result in any perceivable difference between the *zip6.1* mutant and the wild-type, which was instead evident when the external medium only contained high levels of Zn (Figure 4.12). *AtZIP9* seems to have a role in Zn transport as suggested by the analysis of its expression (Figure 4.1), and perhaps one in the translocation of Fe, given the shorter root length observed under conditions of deficiency and excess of both Zn and Fe (Figure 4.8, 4.12). Only *zip9.1* exhibited a reduced weight of both roots and shoots in excess of Zn (Figure 4.11) but no differences were observed in the other single mutants (Figure 4.9, 4.10). *AtZIP4* and *AtZIP9* are very similar (77%) at protein level (Figure 4.13), and *AtZIP4* and *AtZIP6* have a comparable tissue localization in roots (Figure 4.23; Lin *et al.,* 2016), so in order to minimize the effects of a possible redundancy of functions, *zip4/zip9*, *zip4/zip6*, *zip6/zip9* double and *zip4/zip6/zip9* triple knockout mutants were prepared by crossing the single *zip4.1*, *zip6.1* an *zip9.1* knockout mutants (Figure 4.14, 4.15). The triple *zip4/zip6/zip9* mutant and the double *zip4/zip6* and *zip6/zip9* ones accumulated less Zn in their shoots when this metal was present in excess in the external medium, suggesting a possible role for *AtZIP6* in Zn translocation from roots to shoots (Figure 4.19A). Moreover, it is plausible that *AtZIP6* may also play a role in Fe translocation, given the lower levels of Fe in the shoots of the single *zip6.1* mutant, as well all the double and triple knockout ones under conditions of Zn deficiency (Figure 4.19B). No significant results were observed at root level, although all the mutants lacking *AtZIP9,* except for the double *zip6/zip9* knockout one, displayed higher Zn levels when this element was present in excess amounts in the external medium (Figure 4.19B). Further analyses on Zn accumulation should be performed on *AtZIP9* knockout mutants to better investigate the lower Zn levels observed by Inaba *et al.* (2015) on two different introgression mutants for this gene in the presence of excess Zn. The tissue localization of *AtZIP4*, *AtZIP6* and *AtZIP9* was also investigated by fusing the promoter sequences upstream to a GUS reporter gene to better visualize where the expression is driven in the plant. *A. thaliana* pAtZIP6::GUS and pAtZIP9::GUS lines were obtained and GUS staining showed a different tissue localization for

these two genes both at root level and in the aerial part of the plant. *AtZIP6* expression is located in the stele of roots and interestingly, the GUS signal was weaker during the lateral root formation (Figure 4.23). The localization of this transporter in the vascular tissues confirmed previous hypotheses about its possible role in xylem loading and Zn and Fe translocation from roots to shoots. Conversely, *AtZIP9* is expressed in the epidermis, cortex and endodermis, and a strong signal was also detected in thrichoblasts (Figure 4.24), the cells involved in root hair formation, suggesting it may play a role in Zn and possibly Fe homeostasis in the outer layers of the roots. In the aerial parts of *A. thaliana*, *AtZIP6* expression was detected in the vascular tissues of leaves and petals, the style above the two carpels and also in the stamen layer adjacent to the vasculature (Figure 4.26). Interestingly, the pAtZIP9::GUS lines displayed a strong GUS signal only when grown under low Zn conditions, hence confirming the expression analysis performed in the early stages of this work (Figure 4.1). The same effect was also reported by Lin *et al.* (2016) in *AtZIP4*::GUS lines. The GUS signal in pAtZIP9::GUS lines was also detected in the stomata and hydathodes, indicating a possible role in plant transpiration, maybe regulated by the transport of other inorganic elements (Figure 4.27B, 4.27C). Furthermore, *AtZIP9* presented a different localization from *AtZIP6* at stamen level (Figure 4.27F), and also exhibited a strong signal at the base of the anther filaments (Figure 4.27G). Although the expression pattern of *AtZIP4* has already been described in a number of articles (Lin *et al.,* 2016; Milner and Kochian, 2008; Sinclair *et al.,* 2018), its endodermis localization is still unclear, so we decided to obtain various pAtZIP4::GUS lines (Figure 4.29B) to confirm this localization by means of cross-sections analysis. Another important aspect regarding the functional analysis of these proteins is their subcellular localization, which was investigated using different constructs. At first, eGFP::*AtZIP4*, eGFP::*AtZIP6* and eGFP::*AtZIP9* genes were analyzed by producing stable lines (Figure 4.31), and also their transient expression was investigated in *A. thaliana* protoplasts (data not shown), but these failed to give clear results. The subcellular localization was subsequently investigated in *Arabidopsis* protoplasts using constructs that harbor the eGFP reporter at the C-terminus of the entire coding sequence of these transporters. The protoplast transfection showed a plasma membrane and tonoplast localization for *AtZIP4* and *AtZIP9* respectively, but the signal was not very strong (Figure 4.33). To overcome problems in the correct folding of the eGFP protein, we decided to design reporter constructs removing the last transmembrane domain of *AtZIP4*, *AtZIP6* and *AtZIP9*. The *AtZIP4*noUTM::eGFP, *AtZIP6*noUTM::eGFP and *AtZIP9*noUTM::eGFP genes thus obtained were analyzed by protoplast transfection, and the results confirmed what observed for *AtZIP4* and *AtZIP9*, whereas the localization of *AtZIP6* remained unclear (Figure 4.35). A co-localization analysis with different membrane reporters is under way to confirm ZIP4 and ZIP9 localization and

clarify in what compartments ZIP6 is driven. The heterologous expression of plant transporters in yeast is a very useful system to understand their function, and verify whether they can complement mutants lacking specific transporters. A complementation analysis was therefore performed for *AtZIP4* using yeast mutants for the uptake of Zn and Fe, since it was believed that this protein was located at the plasma membrane. *AtZIP4* was able to complement the *zrt1/zrt2*Δ yeast mutant lacking low- and high-affinity plasma membrane transporters for Zn, confirming the results obtained by Assunção *et al.* (2010) (Figure 4.37A). Subsequently, we demonstrated that *AtZIP4* is not a high-affinity Fe transporter, given its inability to complement the *fet3/fet4*Δ yeast mutant (Figure 4.37A). The low-affinity Fe transport function has yet to be investigated, but the expression analysis (Figure 4.1) and phenotypic characterization at different Fe concentrations in the *zip4.1* knockout mutant suggests a similar activity. *AtZIP9* is located at the tonoplast and since its expression pattern is consistent with that of a high-affinity Zn transporter, we tested its ability to complement the *zrc1/cot1*Δ yeast mutant, unable to transport Zn into the vacuole, but the results were negative (Figure 4.37B). Further analyses will be needed to test if *AtZIP9* possesses a Zn export activity, and these assays will be done by complementing the yeast *zrt3*Δ mutant, unable to release Zn from the vacuole into the cytosol. In a second stage of our investigations, single copy lines overexpressing these three transporters were produced and a preliminary phenotypic characterization was carried out. The *AtZIP4ox* lines displayed a longer primary root under conditions of Zn deficiency (Figure 4.41), confirming a high affinity for Zn, whereas the shorter length measured in Fe-starved plants (Figure 4.42) excluded a high-affinity transport activity for Fe, suggesting instead that the smaller primary root is a consequence of a perturbation of Fe homeostasis at root level. The overexpression of *AtZIP6* seems on the other hand to mediate a greater tolerance to excessive amounts of both Zn and Fe and a greater susceptibility to Fe deficiency (Figure 4.43, 4.44). The accumulation analysis on *AtZIP4ox*, *AtZIP6ox* and *AtZIP9ox* lines at different Zn, Fe and Mn concentrations has still to be performed and may be fundamental to obtain more information on the functional characterization of these transporters. Finally, during my internationalization project at the University of Nottingham, we tried to investigate Zn distribution in the single *zip4.1*, *zip6.1*, *zip9.1* and the triple *zip4/zip6/zip9* knockout mutants, and see how it differed from that in wild-type plants, using Zinpyr-1, a Zn-specific fluorescent dye, as described by Sinclair *et al.* (2007). The staining protocol was very invasive for the root cells, as confirmed by PI staining (Figure 4.45). We eliminated EDTA rinsing and a saline solution was used to prepare the Zinpyr-1 working solution, but the result was that no differences could be detected among the mutants, even though the root integrity was now preserved (Figure 4.47). The *hma4-8* mutant was used as positive control because according to Sinclair *et al.* (2007), it exhibits a specific Zn

localization at the pericycle that was not evident when we used our modified protocol (Figure 4.47). Additional trials needed to be performed to verify whether this is an adequate technique to analyze Zn distribution in plant tissues without damaging the cells, given that the staining of cross-sections displayed a complete different localization from what expected from prior tests (Figure 4.49). For this reason, we applied for the use of TwinMic X-ray spectromicroscope available at the Elettra-Synchrotron of Trieste. Unfortunately, the Zn level in the root cross-sections analyzed was too low to be detected with this instrument, and we could only confirm a greater accumulation of Zn in the *hma4-8* mutant than the wild-type (Figure 4.49), although its localization appeared to be more widespread than what described by Sinclair *et al.* (2007), who only observed it in the pericycle. Despite the difficulties encountered when investigating Zn distribution in the various ZIP knockout mutants, we managed to gain some information shedding light on the function of *AtZIP4*, *AtZIP6* and *AtZIP9*. Given their comparable tissue localization, *AtZIP4* and *AtZIP6* seem to have a similar role in the translocation of Zn and Fe from roots to shoots, although the expression of *AtZIP4* seems to respond better than *AtZIP6* to variations in metal concentrations, suggesting a more specific role for it in the regulation of endodermis, pericycle and xylem parenchyma metal mobilization. *AtZIP9* may be involved in Zn remobilization from the vacuole in the epidermis, cortex and endodermis tissues under conditions of Zn deficiency, presumably in response to a greater need for this element. Further analyses are required to confirm these results and characterize their real function in the complex network of Zn homeostasis (Figure 4.50).

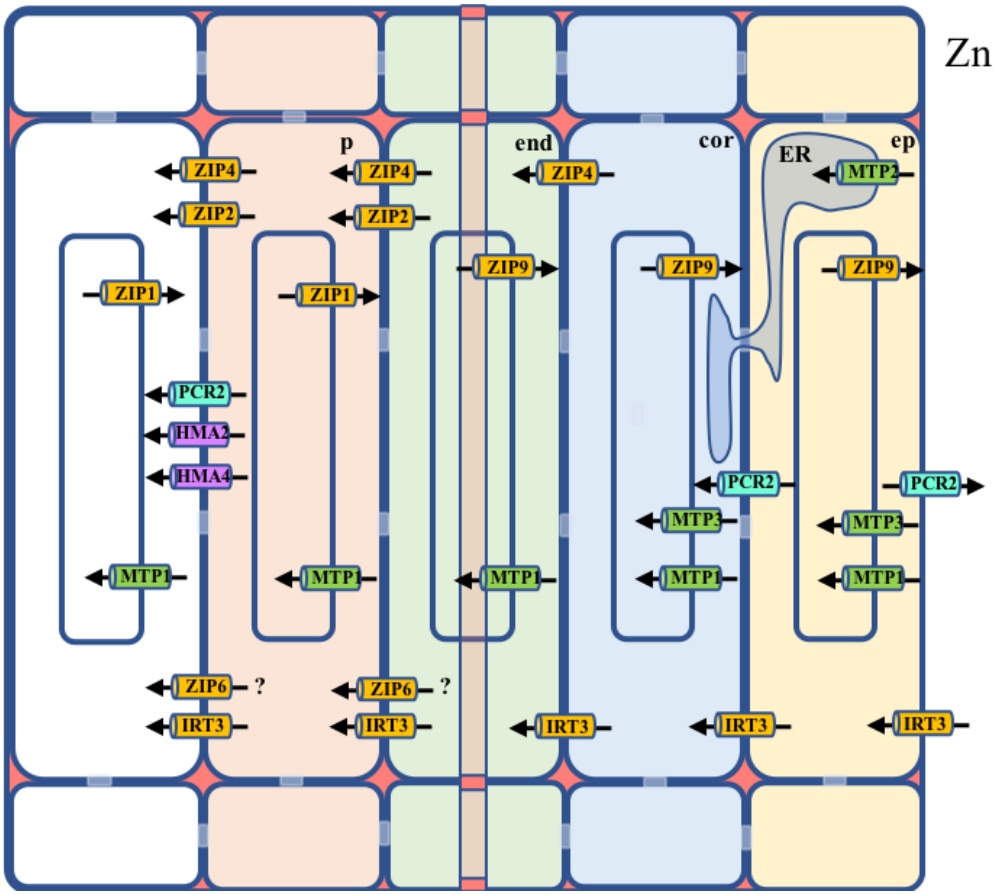

Figure 4.50: Diagram of the distribution of Zn transporters among the different root layers. Tissue legenda: pericycle (p), endodermis (end), cortex (cor), epidermis (ep), endoplasmic reticulum (ER). The localization and distribution of the various transporters are those reported in the literature: MTP1 (Kawachi *et al.,* 2009), MTP2 (Sinclair *et al.,* 2018) and MTP3 (Arrivault *et al.,* 2006) are depicted in green, HMA2 (Hussain *et al.,* 2004) and HMA4 (Verret *et al.,* 2004) in purple, PCR2 (Song *et al.,* 2010) in light blue, IRT3 (Lin *et al.,* 2009), and ZIP1 and ZIP2 (Milner *et al.,* 2013) in orange. The localization of ZIP6 and ZIP9 is that consistent with our results, whereas ZIP4 distribution is that found by Lin *et al.* (2016).

6. SUPPLEMENTARY DATA

In vitro - Roots

Condition	Genotype	B 11	Na 23	Mg 24	P 31	S 34	K 39	Ca 43
Zn 0 µM	wt	nd	6748,63 ± 1580,3	3179,73 ± 313,57	12525,39 ± 999,14	14230,42 ± 1548,86	37169,83 ± 7255,17	9177,13 ± 5714,79
	zip4.1	nd	5960,95 ± 1022,25	3243,16 ± 367,23	12492,76 ± 956,47	13184,08 ± 209,14	38262,81 ± 5592,99	7995,21 ± 1863,26
	zip6.1	nd	6351,24 ± 501,37	3397,34 ± 143,26	12623,68 ± 778,41	13556,07 ± 710,74	43138,53 ± 2172,83	6637,02 ± 586,2
	zip9.1	nd	7711,37 ± 1072,69	3360,84 ± 178,63	12468,16 ± 817,22	13989,15 ± 682,67	38423,34 ± 788,72	5980,94 ± 640,86
	zip4/zip6	nd	6578,38 ± 380,27	3308,28 ± 55,99	12777,87 ± 844,49	13418,64 ± 206,69	41547,06 ± 3153,24	7315,49 ± 983,37
	zip4/zip9	nd	6206,01 ± 336,43	3277,59 ± 400,48	13312,12 ± 714,96	13186,68 ± 546,62	41978,93 ± 3969,59	9097,62 ± 3677,03
	zip6/zip9	nd	7359,68 ± 966,46	3328,31 ± 266,63	12551,93 ± 667,95	13066,55 ± 705,9	39808,03 ± 2741,77	6634,01 ± 1099,51
	zip4/zip6/zip9	nd	6687,35 ± 365,74	3417,89 ± 274,54	12406,19 ± 448,5	13619,93 ± 339,12	42708,14 ± 2024,37	6494,52 ± 123,24
Zn 0,07 µM	wt	nd	6305,25 ± 571,03	3566,3 ± 93,37	12238,55 ± 957,77	14181,57 ± 654,49	36461,75 ± 3511,64	8173,62 ± 3169,11
	zip4.1	nd	6312,78 ± 738,96	3853,79 ± 161,31	11865,81 ± 943,03	13449,15 ± 720,6	40408,76 ± 384,53	6219,17 ± 467,3
	zip6.1	nd	7131,29 ± 723,92	3778,25 ± 172,09	12172,81 ± 974,46	13258,37 ± 265,96	38193,98 ± 1070,62	5884,28 ± 993,39
	zip9.1	nd	6415,96 ± 981,69	3778,7 ± 291,016	12734,1 ± 1363,87	14087,66 ± 1761,42	36444,26 ± 4110,47	6197,79 ± 789,29
	zip4/zip6	nd	6147,66 ± 1117,36	3746,88 ± 88,48	11964,74 ± 960,69	13435,34 ± 859,43	40966,49 ± 1070,62	6420,27 ± 520,4
	zip4/zip9	nd	6274,3 ± 459,08	3614,19 ± 213,73	12254,04 ± 750,17	14129,19 ± 944,07	38726,31 ± 1855,61	6196,47 ± 491,88
	zip6/zip9	nd	5842,25 ± 830,41	3833,66 ± 218,66	11953,44 ± 1068,023	13657,88 ± 353,85	38032,15 ± 5020,94	6783,24 ± 950,9
	zip4/zip6/zip9	nd	6053,98 ± 1094,82	3852,17 ± 265,36	11547,78 ± 290,08	13538,93 ± 519,99	40513,52 ± 1820,98	6301,67 ± 971,64
Zn 5 µM	wt	nd	6321,7 ± 516,41	3913,51 ± 204,69	11363,87 ± 677,94	13691,59 ± 495,63	38706,66 ± 1750,46	6837,76 ± 865,74
	zip4.1	nd	7371,16 ± 738,82	4176,39 ± 228,54	11512,43 ± 615,07	13735,9 ± 763,75	34893,93 ± 292,97	5461,51 ± 810,05
	zip6.1	nd	5999,88 ± 742,72	4255,16 ± 110,06	11340,26 ± 459,71	13618,73 ± 508,17	39534,12 ± 2683,54	6387,12 ± 138,61
	zip9.1	nd	6530,14 ± 689,16	4214,46 ± 117,38	11485,43 ± 562,3	12953,54 ± 474,39	38679,37 ± 3006,93	6291,94 ± 442,38
	zip4/zip6	nd	6732,96 ± 1148,3	4366,34 ± 106,91	11368,47 ± 382,17	13192,41 ± 145,99	37986,51 ± 1945,75	6153,44 ± 1036,5
	zip4/zip9	nd	6534,878 ± 221,39	4018,37 ± 107,37	11489,71 ± 804,33	13526,91 ± 508,45	39738,41 ± 936,61	5942,39 ± 517,99
	zip6/zip9	nd	6007,37 ± 1191,65	4214 ± 221,79	11497,01 ± 862,55	13459,53 ± 325,81	38551,58 ± 1988,14	6230,34 ± 671,02
	zip4/zip6/zip9	nd	6607,98 ± 564,19	4099,31 ± 201,34	11519,15 ± 1034,87	13801,66 ± 845,17	38517,17 ± 711,062	6136,57 ± 1144,23
Zn 50 µM	wt	nd	8792,92 ± 878,77	2872,96 ± 117,29	11995,09 ± 861,23	15743,58 ± 357,61	26719,17 ± 1394,27	6774,54 ± 495,39
	zip4.1	nd	7306,27 ± 1413,19	3152,91 ± 136,39	12368,1 ± 815,54	15482,81 ± 386,76	27925,54 ± 4118,5	7938,21 ± 634,45
	zip6.1	nd	8073,33 ± 3302,11	3314,22 ± 183,03	12214,46 ± 1989,09	16441,67 ± 1757,43	27792,44 ± 2846,92	7498,38 ± 1813,39
	zip9.1	nd	7916,25 ± 1598,49	3332,56 ± 31,79	11830,79 ± 560,46	14990,23 ± 1459,49	26435,38 ± 2912,05	7719,57 ± 1011,77
	zip4/zip6	nd	7659,68 ± 736,09	3123,71 ± 82,38	11625,59 ± 887,61	14948,04 ± 650,92	28109,04 ± 1547,58	10007,71 ± 3255,95
	zip4/zip9	nd	6454,89 ± 745,18	3264,29 ± 289,54	11610,81 ± 776,78	14299,45 ± 647,94	30089,53 ± 2723,63	8869,15 ± 535,46
	zip6/zip9	nd	7326,42 ± 1449,77	3097,98 ± 247,45	11969,13 ± 1212,41	15003,17 ± 590,79	28575,94 ± 1725,89	7702,83 ± 1241,14
	zip4/zip6/zip9	nd	6253,83 ± 244,14	3153,48 ± 374,43	11785,98 ± 720,53	14638,07 ± 2005,19	30019,40 ± 1313,32	10097,55 ± 1384,22

Figure S1: Ionome in roots of single *zip4.1*, *zip6.1*, *zip9.1,* double *zip4/zip6, zip4/zip9*, *zip6/zip9* and triple *zip4/zip6/zip9* knockout mutants and wild-type grown in plates at different Zn concentrations. Values are means ± SEM (n=3). Significant results compared to wild-type are marked in red. nd = not detectable.

In vitro - Roots

Condition	Genotype	Mn 55	Fe 56	Co 59	Ni 60	Cu 63	Zn 66	Mo 98
Zn 0 µM	wt	43,02 ± 8,31	61,49 ± 4,22	0,39 ± 0,38	8,58 ± 12,06	17,86 ± 8,69	nd	0,64 ± 0,05
	zip4.1	42,72 ± 10,24	61 ± 4,15	0,18 ± 0,07	2,64 ± 2,85	15,17 ± 5,26	nd	0,61 ± 0,05
	zip6.1	38,66 ± 1,74	61,22 ± 10,69	0,09 ± 0,01	1,35 ± 0,28	14,76 ± 9,62	nd	0,63 ± 0,02
	zip9.1	38,46 ± 6,05	66,66 ± 9,97	0,13 ± 0,02	1,70 ± 0,84	14,36 ± 6,84	nd	0,62 ± 0,02
	zip4/zip6	34,77 ± 1,96	57,63 ± 8,89	0,16 ± 0,09	4,57 ± 6,07	12,46 ± 7,89	nd	0,58 ± 0,03
	zip4/zip9	35,09 ± 8,71	63,26 ± 11,8	0,15 ± 0,07	1,09 ± 0,31	13,01 ± 7,26	nd	0,61 ± 0,01
	zip6/zip9	35,18 ± 5,46	65,64 ± 9,43	0,17 ± 0,09	2,25 ± 1,19	17,19 ± 13,03	nd	0,63 ± 0,01
	zip4/zip6/zip9	35,66 ± 2,61	66,04 ± 16,45	0,09 ± 0,01	0,84 ± 0,32	17,22 ± 13,78	nd	0,61 ± 0,03
Zn 0,07 µM	wt	40,04 ± 3,69	59,51 ± 2,21	0,20 ± 0,14	3,01 ± 3,16	13,61 ± 3,05	258,87 ± 165,58	0,68 ± 0,02
	zip4.1	39,34 ± 4,21	59,52 ± 2,89	0,13 ± 0,04	3,27 ± 4,29	15,32 ± 10,93	54,14 ± 25,33	0,68 ± 0,04
	zip6.1	31,59 ± 2,71	61,81 ± 7,66	0,12 ± 0,06	2,33 ± 1,34	14,61 ± 5,72	119,09 ± 105,19	0,67 ± 0,03
	zip9.1	36,36 ± 1,14	67,2 ± 1,4	0,1 ± 0,01	1,80 ± 1,51	17,30 ± 11,75	55,31 ± 14,51	0,68 ± 0,06
	zip4/zip6	32,96 ± 6,37	56,14 ± 4,22	0,11 ± 0,05	1,10 ± 0,21	12,33 ± 3,66	167,49 ± 84,75	0,71 ± 0,01
	zip4/zip9	35,69 ± 7,17	65,82 ± 9,36	0,16 ± 0,1	1,06 ± 0,32	12,18 ± 3,77	122,14 ± 51,2	0,71 ± 0,08
	zip6/zip9	29,94 ± 1,84	61,27 ± 8,67	0,11 ± 0,04	1,07 ± 0,23	15,08 ± 4,55	102,89 ± 55,65	0,74 ± 0,05
	zip4/zip6/zip9	32,78 ± 1,85	63,63 ± 11,47	0,1 ± 0,01	1,06 ± 0,43	13,68 ± 4,61	172,09 ± 141,97	0,71 ± 0,06
Zn 5 µM	wt	22,13 ± 0,99	66,89 ± 6,57	0,17 ± 0,11	5,47 ± 7,71	15,91 ± 7,43	991,33 ± 207,08	0,63 ± 0,02
	zip4.1	25,71 ± 3,27	74,58 ± 10	0,11 ± 0,06	1,74 ± 1,01	17,04 ± 9,63	1279,98 ± 254,01	0,68 ± 0,03
	zip6.1	18,81 ± 0,24	64,21 ± 4,96	0,09 ± 0,06	1,31 ± 0,24	17,67 ± 11,83	848,31 ± 123,34	0,66 ± 0,04
	zip9.1	21,57 ± 0,33	67,96 ± 11,11	0,07 ± 0,01	0,93 ± 0,09	14,68 ± 9,62	947,82 ± 86,55	0,66 ± 0,03
	zip4/zip6	18,66 ± 1,65	67,68 ± 10,66	0,08 ± 0,01	1,13 ± 0,15	13,1 ± 4,12	864,52 ± 50,25	0,66 ± 0,02
	zip4/zip9	20,66 ± 2,89	74,51 ± 7,63	0,11 ± 0,06	1,61 ± 1,06	13,22 ± 3,69	1313,50 ± 634,18	0,69 ± 0,09
	zip6/zip9	19,76 ± 1,23	71,18 ± 11,23	0,13 ± 0,06	1,37 ± 0,57	14,99 ± 4,32	1026,38 ± 219,3	0,71 ± 0,02
	zip4/zip6/zip9	18,69 ± 2,56	65,31 ± 8,15	0,11 ± 0,08	1,55 ± 0,23	11,49 ± 3,78	939,09 ± 256,24	0,67 ± 0,03
Zn 50 µM	wt	18,1 ± 2,24	547,75 ± 45,13	0,11 ± 0,04	1,63 ± 0,5	27,13 ± 18,13	16404,62 ± 1895,82	0,57 ± 0,01
	zip4.1	17,25 ± 4,59	567,02 ± 151,52	0,09 ± 0,03	1,43 ± 0,19	32,89 ± 26,94	17280,82 ± 1792,28	0,57 ± 0,04
	zip6.1	18,56 ± 4,75	480,36 ± 129,34	0,07 ± 0,01	1,92 ± 1,52	39,22 ± 41,43	15298,32 ± 4229,29	0,62 ± 0,01
	zip9.1	18,04 ± 1,55	462,19 ± 57,39	0,07 ± 0,18	1,65 ± 0,94	19,13 ± 11,67	13533,87 ± 2566,75	0,62 ± 0,03
	zip4/zip6	19,09 ± 0,43	555,89 ± 71,04	0,22 ± 0,02	3,86 ± 4,29	32,25 ± 17	15170,35 ± 2841,56	0,58 ± 0,04
	zip4/zip9	19,61 ± 1,84	460,21 ± 29,48	0,12 ± 0,02	4,04 ± 4,03	30,65 ± 23,38	14745,93 ± 1758,76	0,60 ± 0,03
	zip6/zip9	18,29 ± 1,13	585,94 ± 42,74	0,08 ± 0,01	1,93 ± 0,85	37,27 ± 16,28	16307,48 ± 2578,56	0,62 ± 0,02
	zip4/zip6/zip9	20,58 ± 2,82	570,62 ± 166,96	0,23 ± 0,08	12,27 ± 11,7	28,63 ± 13,36	17711,93 ± 5565,84	0,59 ± 0,03

Figure S1: Ionome in roots of single *zip4.1*, *zip6.1*, *zip9.1,* double *zip4/zip6, zip4/zip9*, *zip6/zip9* and triple *zip4/zip6/zip9* knockout mutants and wild-type grown in plates at different Zn concentrations. Values are means ± SEM (n=3). Significant results compared to wild-type are marked in red. nd = not detectable.

In vitro - Shoots

Condition	Genotype	B 11	Na 23	Mg 24	P 31	S 34	K 39	Ca 43
Zn 0 µM	wt	26,85 ± 3,38	21914,45 ± 562,74	7151,13 ± 366,42	31735,98 ± 882,37	30528,91 ± 1546,46	57003,43 ± 2242,35	15501,73 ± 222,31
	zip4.1	28,46 ± 1,51	21141,89 ± 765,87	7143,49 ± 62,84	32535,66 ± 323,67	30659,38 ± 2414,18	60606,9 ± 1900,6	15183,53 ± 610,13
	zip6.1	36,15 ± 9,26	21154,02 ± 928,05	7250,25 ± 218,22	32213,81 ± 1039,11	31368,92 ± 349,44	58483,73 ± 1472,19	15437,52 ± 801,59
	zip9.1	36,88 ± 13,03	20208,05 ± 1269,26	7141,6 ± 369,38	28035 ± 5495,71	28602,22 ± 3994,15	58464,99 ± 4052,27	15846,74 ± 731,12
	zip4/zip6	39,62 ± 8,13	21037,7 ± 1613,17	7320,89 ± 419,81	31366,74 ± 935,33	29386,01 ± 1569,3	55771,33 ± 3807,36	20963,67 ± 7276,33
	zip4/zip9	38,8 ± 12	20067,44 ± 200,21	7352,37 ± 75,19	30177,75 ± 2862,35	28167,45 ± 1654,49	58008,07 ± 4218,75	16277,85 ± 723,04
	zip6/zip9	35,12 ± 2,99	20124,28 ± 672,78	7268,38 ± 107,86	32555,96 ± 589,25	30912,34 ± 3048,06	59345,65 ± 2364,26	15786,98 ± 527,3
	zip4/zip6/zip9	33,79 ± 4,82	21063,12 ± 1280,46	7228,32 ± 151,53	31246,4 ± 1935,74	31833,03 ± 2357,31	60701,77 ± 682,63	15404,74 ± 554,33
Zn 0,07 µM	wt	38,59 ± 12,45	23607,43 ± 467,62	6445,03 ± 99,61	32588,33 ± 4714,11	31544,77 ± 3421,56	61907,14 ± 3269,04	14205,73 ± 363,1
	zip4.1	49,71 ± 16,71	22103,26 ± 1045,01	6508,17 ± 153,72	29887,01 ± 4113,21	29944,52 ± 2621,02	63434,2 ± 1739,35	15012,84 ± 371,91
	zip6.1	45,84 ± 8,39	22417,26 ± 305,28	6632,37 ± 52,92	29465,41 ± 6188,99	29087,86 ± 2477,21	62144,02 ± 5931,4	15451,18 ± 667,67
	zip9.1	47,02 ± 8,44	22331,02 ± 2057,83	6694,26 ± 144,48	29950,6 ± 7169,05	30270,08 ± 5177,48	63056,47 ± 3818,82	15049,12 ± 242,01
	zip4/zip6	39,59 ± 7,32	23287,65 ± 2036,27	6604,45 ± 43,79	33986,43 ± 375,11	33570,74 ± 658,64	58753,91 ± 7181,43	15325,37 ± 478,21
	zip4/zip9	38,7 ± 7,72	22051,37 ± 1023,11	6445,54 ± 252,62	34089,37 ± 652,93	33359,72 ± 3110,01	59171,33 ± 3678,58	14903,09 ± 623,19
	zip6/zip9	51,46 ± 19,01	21635,26 ± 1354,31	6602,88 ± 76,58	33551,46 ± 2487,27	32717,95 ± 4000,19	61253,1 ± 2955,7	15757,85 ± 861,47
	zip4/zip6/zip9	39,03 ± 9,03	22143,85 ± 1819,75	6507,02 ± 112,11	30902,01 ± 3796,74	32209,92 ± 1548,65	61531,59 ± 697,12	15165,12 ± 329,61
Zn 5 µM	wt	43,77 ± 16,25	22957,42 ± 892,56	5840,48 ± 245,59	34725,24 ± 3302,94	33405,65 ± 2331,47	63340,14 ± 2270,87	14882,38 ± 929,92
	zip4.1	43,65 ± 11,67	22863,78 ± 743,27	5818,12 ± 106,87	35458,31 ± 1268,02	34780,57 ± 252,8	63602,33 ± 2112,33	15030,62 ± 1156,65
	zip6.1	45,51 ± 13,49	21565,17 ± 178,33	6173,19 ± 265,04	36269,45 ± 376,32	34440,49 ± 866,97	65126,04 ± 2664,28	15740,38 ± 180,75
	zip9.1	42,76 ± 12,2	22335,91 ± 1787,79	5929,56 ± 194,06	34530,91 ± 2163,68	33790,04 ± 1265,41	64780,47 ± 1788,93	15386,51 ± 650,79
	zip4/zip6	51,04 ± 12,21	22995,11 ± 1904,25	6136,64 ± 124,1	31042,10 ± 5449,77	31155,71 ± 3494,42	62286,98 ± 8097,21	15823,56 ± 863,67
	zip4/zip9	46,91 ± 11,61	23747,05 ± 817,13	6069,41 ± 23,49	33608,26 ± 2200,51	34986,18 ± 2856,21	61968,95 ± 4556,31	15829,42 ± 210,78
	zip6/zip9	52,2 ± 13,89	22548,13 ± 2276,72	6109,45 ± 244,48	31869,82 ± 5092,43	34000,48 ± 3671,58	61224,99 ± 5412,86	15907,38 ± 1174,49
	zip4/zip6/zip9	52,86 ± 16,02	23732,23 ± 2078,15	6051,07 ± 109,37	30456,65 ± 7465,53	33320,82 ± 3309,08	63472,3 ± 4110,22	15916,91 ± 718,92
Zn 50 µM	wt	14,63 ± 9,68	26215,06 ± 1540,69	5777,21 ± 150,93	38215,66 ± 1754,04	48043,19 ± 1018,6	51318,54 ± 1322,77	16256,19 ± 547,37
	zip4.1	18,44 ± 19,86	23862,68 ± 1105,98	5497,16 ± 166,37	38326,63 ± 848,45	46381,04 ± 2549,6	53298,87 ± 8129,96	16176,38 ± 1150,02
	zip6.1	32,37 ± 6,12	25667,61 ± 1675,29	5328,61 ± 137,47	39834,99 ± 1830,09	45109,66 ± 696,83	60176,15 ± 4037,78	14962,59 ± 1084,99
	zip9.1	28,34 ± 14,98	22129,39 ± 1816,29	5355,37 ± 74,43	38972,42 ± 1055,34	43110,42 ± 1709,62	64304,13 ± 1376,69	14949,53 ± 438,37
	zip4/zip6	25,98 ± 25,53	23910,52 ± 304,06	5440,91 ± 262,95	35220,68 ± 5315,21	43490,34 ± 4130,13	59525,83 ± 5059,07	15743,66 ± 660,03
	zip4/zip9	33,24 ± 20,57	23015,5 ± 1175,43	5395,13 ± 56,73	36637,52 ± 2862,52	43578,85 ± 1352,77	62665,76 ± 1005,27	15203,47 ± 268,48
	zip6/zip9	26,07 ± 14,17	24143,69 ± 3616,63	5445,31 ± 153,79	35490,85 ± 2822,89	45877,18 ± 2587,09	57324,11 ± 5438,71	15770,79 ± 827,45
	zip4/zip6/zip9	21,1 ± 0,36	22499,36 ± 626,25	5458,11 ± 89,36	36420,64 ± 1057,02	45632,72 ± 902,57	59365,52 ± 6749,93	16169,42 ± 645,24

Figure S1: Ionome in shoots of single *zip4.1*, *zip6.1*, *zip9.1,* double *zip4/zip6, zip4/zip9*, *zip6/zip9* and triple *zip4/zip6/zip9* knockout mutants and wild-type grown in plates at different Zn concentrations. Values are means ± SEM (n=3). Significant results compared to wild-type are marked in red. nd = not detectable.

In vitro - Shoots

Condition	Genotype	Mn 55	Fe 56	Co 59	Ni 60	Cu 63	Zn 66	Mo 98
Zn 0 µM	wt	144,72 ± 6,16	79,53 ± 10,20	0,09 ± 0,02	0,42 ± 0,17	3,24 ± 0,42	nd	2,14 ± 0,17
	zip4.1	144,49 ± 1,16	79,12 ± 3,21	0,08 ± 0,01	0,38 ± 0,13	3,18 ± 0,85	nd	2,19 ± 0,07
	zip6.1	140,29 ± 6,85	75,16 ± 6,71	0,08 ± 0,004	0,26 ± 0,01	2,94 ± 0,46	nd	2,28 ± 0,03
	zip9.1	145,64 ± 1,13	87,31 ± 4,17	0,08 ± 0,01	0,24 ± 0,01	3,04 ± 0,48	nd	2,22 ± 0,1
	zip4/zip6	140,865 ± 5	71,41 ± 10,24	0,26 ± 0,31	3,65 ± 5,83	3,2 ± 0,71	nd	2,15 ± 0,05
	zip4/zip9	141,94 ± 3,21	83,78 ± 1,68	0,08 ± 0,01	0,6 ± 0,63	3,13 ± 0,58	nd	2,15 ± 0,05
	zip6/zip9	139,83 ± 5,74	73,40 ± 2,61	0,08 ± 0,002	0,44 ± 0,11	3,19 ± 0,05	nd	2,24 ± 0,05
	zip4/zip6/zip9	139,53 ± 0,48	75,81 ± 4,03	0,09 ± 0,03	0,36 ± 0,24	3,4 ± 0,41	nd	2,23 ± 0,09
Zn 0,07 µM	wt	137,25 ± 4,27	82,69 ± 11,91	0,07 ± 0,01	0,55 ± 0,33	4,06 ± 0,99	290,34 ± 166,22	2,13 ± 0,02
	zip4.1	133,71 ± 5,86	83,52 ± 5,23	0,08 ± 0,01	0,42 ± 0,12	3,23 ± 0,14	264,03 ± 101,74	2,21 ± 0,07
	zip6.1	133,86 ± 8,8	80,80 ± 7,03	0,08 ± 0,01	0,42 ± 0,17	3,46 ± 0,25	261,72 ± 37,66	2,11 ± 0,02
	zip9.1	133,64 ± 4,96	82,64 ± 9,43	0,06 ± 0,01	0,23 ± 0,05	3,5 ± 0,28	95,94 ± 41,61	2,18 ± 0,01
	zip4/zip6	134,66 ± 1,33	78,89 ± 3,4	0,08 ± 0,01	0,55 ± 0,29	3,36 ± 0,69	276,55 ± 91,80	2,13 ± 0,01
	zip4/zip9	133,15 ± 1,17	82,67 ± 2,46	0,08 ± 0,01	0,3 ± 0,05	3,57 ± 0,57	238,03 ± 80,12	2,18 ± 0,09
	zip6/zip9	131,89 ± 5,77	71,62 ± 9,5	0,09 ± 0,01	0,59 ± 0,23	3,44 ± 0,34	414,21 ± 226,60	2,22 ± 0,15
	zip4/zip6/zip9	133,33 ± 1,92	80,39 ± 2,99	0,09 ± 0,01	0,37 ± 0,25	3,63 ± 0,53	225,67 ± 140,11	2,270,06
Zn 5 µM	wt	108,69 ± 3,86	79,56 ± 2,38	0,06 ± 0,005	0,56 ± 0,21	5,26 ± 1,15	1422,63 ± 598,02	2,12 ± 0,04
	zip4.1	114,09 ± 1,77	73,83 ± 3,6	0,06 ± 0,01	0,38 ± 0,05	4,72 ± 0,36	1245,20 ± 118,59	2,14 ± 0,06
	zip6.1	111,26 ± 8,33	64,96 ± 8,05	0,06 ± 0,003	1,36 ± 1,76	4,69 ± 0,46	1251,74 ± 32,67	2,12 ± 0,12
	zip9.1	110,03 ± 2,16	72,72 ± 0,83	0,06 ± 0,001	0,41 ± 0,03	4,8 ± 0,94	1166,42 ± 40,09	2,15 ± 0,09
	zip4/zip6	110,72 ± 6,15	73,19 ± 8,48	0,06 ± 0,01	0,30 ± 0,05	4,71 ± 0,22	1000,11 ± 250,13	2,11 ± 0,04
	zip4/zip9	111,29 ± 6,3	67,98 ± 11,39	0,08 ± 0,02	0,49 ± 0,04	5,28 ± 0,45	1248,53 ± 134,69	2,15 ± 0,07
	zip6/zip9	112,02 ± 2,45	70,44 ± 6,27	0,06 ± 0,01	0,32 ± 0,07	4,72 ± 0,16	1168,54 ± 272,01	2,25 ± 0,11
	zip4/zip6/zip9	109,09 ± 3,72	71,42 ± 12,06	0,06 ± 0,01	0,43 ± 0,16	4,83 ± 0,46	1108,72 ± 295,40	2,21 ± 0,03
Zn 50 µM	wt	68,89 ± 3,95	45,38 ± 2,94	0,05 ± 0,01	0,63 ± 0,19	4,86 ± 0,39	9291,90 ± 248,91	2,56 ± 0,06
	zip4.1	66,11 ± 6,04	38,75 ± 9,47	0,05 ± 0,014	0,65 ± 0,23	4,39 ± 0,14	8875,78 ± 1152,48	2,54 ± 0,11
	zip6.1	66,47 ± 0,95	44,03 ± 3,2	0,04 ± 0,005	0,49 ± 0,12	4,51 ± 0,61	7928,33 ± 482,07	2,41 ± 0,05
	zip9.1	70,49 ± 1,28	48,62 ± 6,95	0,04 ± 0,004	0,53 ± 0,07	4 ± 0,73	7353,18 ± 503,96	2,38 ± 0,04
	zip4/zip6	67,97 ± 3,66	53,09 ± 7,27	0,06 ± 0,03	0,52 ± 0,15	4,13 ± 0,67	7656,92 ± 2137,20	2,44 ± 0,03
	zip4/zip9	73,16 ± 1,24	53,57 ± 2,12	0,05 ± 0,01	0,68 ± 0,05	4,2 ± 0,49	7502,58 ± 440,83	2,4 ± 0,01
	zip6/zip9	67,08 ± 3,16	44,84 ± 4,15	0,06 ± 0,03	0,49 ± 0,04	4,04 ± 0,65	7955,36 ± 463,78	2,55 ± 0,16
	zip4/zip6/zip9	71,52 ± 2,76	51,91 ± 1,54	0,05 ± 0,003	2,31 ± 3,07	4,19 ± 0,47	8776,01 ± 1172,62	2,5 ± 0,05

Figure S1: Ionome in shoots of single *zip4.1*, *zip6.1*, *zip9.1,* double *zip4/zip6, zip4/zip9*, *zip6/zip9* and triple *zip4/zip6/zip9* knockout mutants and wild-type grown in plates at different Zn concentrations. Values are means ± SEM (n=3). Significant results compared to wild-type are marked in red. nd = not detectable.

Hydroponic culture - Roots

Condition	Genotype	B 11	Na 23	Mg 24	P 31	S 34	K 39	Ca 43
Zn 0 µM	wt	43,91 ± 6,56	3420,94 ± 2204,72	1874,92 ± 150,79	17856,78 ± 2996,82	19111,00 ± 1924,61	82619,93 ± 8429,83	6231,63 ± 1550,43
	zip4.1	41,67 ± 5,97	2636,52 ± 990,93	1691,28 ± 48,03	17228,42 ± 3132,06	17886,11 ± 2611,48	81036,25 ± 6323,94	7575,23 ± 703,97
	zip6.1	43,17 ± 5,27	2387,28 ± 318,63	1832,38 ± 122,40	14985,03 ±2697,81	16946,81 ± 1391,62	81567,31 ± 7127,39	6962,77 ± 814,03
	zip9.1	45,11 ± 11,08	1909,10 ± 847,84	1692,36 ± 83,16	16588,05± 3790,30	17488,22 ± 2132,83	79565,96 ± 3077,51	8643,04 ± 2451,47
	zip4/zip6	41,94 ± 4,73	1683,68 ± 870,75	1698,06 ± 234,25	15256,10 ± 1960,82	16602,32 ± 2691,95	76753,72 ± 7495,63	7524,08 ± 1010,37
	zip4/zip9	43,37 ± 10,18	1021,18 ± 457,86	1600,89 ± 146,29	14763,07 ± 2427,86	16507,05 ± 2112,31	82015,30 ± 2541,35	7476,25 ± 608,50
	zip6/zip9	46,18 ± 9,30	1827,31 ± 530,19	1645,14 ± 127,30	16755,29 ± 3172,90	18062,58 ± 1783,38	82713,52 ± 3669,99	7807,39 ± 1503,13
	zip4/zip6/zip9	39,49 ± 4,29	1698,11 ± 735,79	1604,25 ± 117,78	15596,52 ± 3337,04	17039,19 ± 1667,78	76382,61 ± 7274,57	9554,45 ± 2839,53
Zn 2 µM	wt	50,07 ± 7,26	1784,05 ± 328,21	1958,13 ± 109,90	12132,30 ± 1626,80	16809,42 ± 2917,44	72545,62 ± 3628,46	7863,01 ± 2161,05
	zip4.1	57,43 ± 11,38	2595,88 ± 657,98	1886,03 ± 79,40	13135,01 ± 950,63	17872,96 ± 2075,11	73785,35 ± 3614,98	8852,47 ± 2946,11
	zip6.1	67,06 ± 18,37	1987,23 ± 861,11	1936,78 ± 154,79	12163,69 ± 778,70	15721,66 ± 1124,50	73387,63 ± 3954,01	7846,37 ± 2026,59
	zip9.1	56,16 ± 9,96	1672,11 ± 420,91	1889,06 ± 179,06	12833,35 ± 1364,75	17411,33 ± 2249,02	75479,06 ± 3879,76	7261,48 ± 1086,03
	zip4/zip6	68,58 ± 15,13	1581,66 ± 938,34	1964,37 ± 165,98	13095,69 ± 239,54	17558,01 ± 2144,33	79179,94 ± 3753,14	6692,03 ± 1007,77
	zip4/zip9	68,04 ± 15,81	1373,87 ± 406,90	1933,59 ± 146,26	12012,58 ± 1629,54	16217,94 ± 2749,70	75542,87 ± 6014,47	6860,13 ± 1479,61
	zip6/zip9	67,72 ± 16,27	2090,14 ± 657,38	1990,81 ± 167,83	13637,73 ± 714,57	18267,12 ± 1973,52	76746,90 ± 3881,25	6385,04 ± 1020,69
	zip4/zip6/zip9	62,36 ± 19,14	1705,73 ± 790,34	1971,15 ± 211,05	12248,90 ± 893,25	17060,24 ± 2092,33	75052,80 ± 4647,03	6393,86 ± 511,09
Zn 10 µM	wt	45,90 ± 4,78	738,57 ± 236,06	1955,79 ± 66,92	17874,21 ± 3591,60	21537,10 ± 2071,87	66326,31 ± 5337,44	6591,44 ± 678,26
	zip4.1	44,52 ± 5,12	656,09 ± 181,06	1839,60 ± 183,40	16194,87 ± 1560,95	20358,41 ± 2966,17	67221,73 ± 8637,11	6717,13 ± 270,48
	zip6.1	42,05 ± 6,82	495,63 ± 176,48	1908,30 ± 175,76	16005,07 ± 2832,22	20127,10 ± 3250,52	68763,89 ± 7874,93	6845,38 ± 727,03
	zip9.1	43,86 ± 6,95	712,77 ± 195,71	1920,27 ± 122,74	21082,63 ± 2635,23	24562,69 ± 3476,07	64835,48 ± 12967,55	6656,40 ± 663,41
	zip4/zip6	44,06 ± 11,07	599,90 ± 96,48	1922,58 ± 172,98	17520,75 ± 5392,97	21486,73 ± 4114,58	58583,63 ± 16699,00	8864,08 ± 4595,00
	zip4/zip9	36,21 ± 3,43	866,29 ± 131,14	2021,91 ± 214,37	22875,70 ± 3617,80	26443,43 ± 3391,27	63548,80 ± 14480,30	6456,49 ± 812,13
	zip6/zip9	48,96 ± 11,77	781,36 ± 192,50	1963,86 ± 220,65	18071,37 ± 2312,48	22564,45 ± 2571,44	60840,78 ± 9391,55	7210,38 ± 1532,26
	zip4/zip6/zip9	49,27 ± 7,10	618,94 ± 208,62	1861,18 ± 192,72	19917,29 ± 4452,59	24668,41 ± 4135,20	61850,59 ± 12737,98	6654,21 ± 451,71

Figure S1: Ionome in roots of single *zip4.1*, *zip6.1*, *zip9.1,* double *zip4/zip6, zip4/zip9*, *zip6/zip9* and triple *zip4/zip6/zip9* knockout mutants and wild-type grown in hydroponics at different Zn concentrations. Values are means ± SEM (n=3). Significant results compared to wild-type are marked in red. nd = not detectable.

Hydroponic culture - Roots

Condition	Genotype	Mn 55	Fe 56	Co 59	Ni 60	Cu 63	Zn 66	Mo 98
Zn 0 µM	wt	102,96 ± 37,99	140,97 ± 13,23	0,08 ± 0,04	0,56 ± 0,08	11,70 ± 11,57	nd	5,30 ± 1,97
	zip4.1	89,27 ± 33,36	125,29 ± 24,48	0,0824 ± 0,04	0,53 ± 0,12	14,43 ± 7,95	nd	4,88 ± 0,55
	zip6.1	94,68 ± 24,76	145,59 ± 7,08	0,09 ± 0,03	0,55 ± 0,11	11,06 ± 10,49	nd	5,00 ± 1,35
	zip9.1	101,87 ± 42,33	130,97 ± 12,69	0,09 ± 0,05	0,60 ± 0,14	9,61 ± 10,87	nd	4,56 ± 0,98
	zip4/zip6	105,46 ± 21,43	145,00 ± 12,07	0,08 ± 0,02	0,61 ± 0,11	8,29 ± 7,06	nd	4,33 ± 1,73
	zip4/zip9	98,52 ± 16,26	133,23 ± 14,59	0,07 ± 0,03	0,58 ± 0,14	13,79 ± 10,98	nd	5,02 ± 0,77
	zip6/zip9	93,54 ± 28,58	134,76 ± 8,56	0,08 ± 0,02	0,50 ± 0,01	9,56 ± 10,52	nd	5,05 ± 0,78
	zip4/zip6/zip9	105,89 ± 57,19	124,97 ± 19,32	0,10 ± 0,006	0,63 ± 0,18	9,48 ± 11,15	nd	4,55 ± 0,36
Zn 2 µM	wt	54,58 ± 11,29	250,61 ± 14,50	0,06 ± 0,05	0,56 ± 0,06	3,46 ± 0,32	690,10 ± 109,33	3,83 ± 0,39
	zip4.1	51,31 ± 10,44	211,29 ± 25,70	0,05 ± 0,02	0,47 ± 0,06	3,34 ± 0,25	804,31 ± 95,93	3,94 ± 0,63
	zip6.1	48,81 ± 6,92	243,19 ± 66,62	0,03 ± 0,01	0,58 ± 0,18	3,47 ± 0,38	599,08 ± 18,57	3,81 ± 0,59
	zip9.1	61,10 ± 16,05	226,22 ± 22,46	0,02± 0,01	0,54 ± 0,1	3,27 ± 0,34	832,36 ± 139,90	3,98 ± 0,57
	zip4/zip6	59,71 ± 11,49	217,76 ± 25,00	0,03 ± 0,01	0,48 ± 0,05	3,26 ± 0,45	735,84 ± 116,89	3,86 ± 0,68
	zip4/zip9	55,75 ± 22,50	215,75 ± 39,38	0,04 ± 0,03	0,51 ± 0,13	3,33 ± 0,34	829,60 ± 254,12	4,20 ± 0,63
	zip6/zip9	45,70 ± 7,40	223,98 ± 10,57	0,03 ± 0,006	0,51 ± 0,05	3,65 ± 0,29	785,85 ± 67,77	4,44 ± 0,56
	zip4/zip6/zip9	48,54 ± 11,28	224,48 ± 12,10	0,04 ± 0,02	0,56 ± 0,07	4,11 ± 0,73	733,30 ± 276,72	4,17 ± 0,53
Zn 10 µM	wt	57,68 ± 16,20	909,52 ± 231,08	0,05 ± 0,01	0,44 ± 0,05	4,79 ± 0,89	8773,30 ± 4311,75	5,15 ± 0,55
	zip4.1	49,63 ± 19,29	836,54 ± 293,42	0,05 ± 0,02	0,46 ± 0,15	3,94 ± 0,33	5854,78 ± 813,65	5,38 ± 0,87
	zip6.1	49,83 ± 17,63	861,87 ± 368,57	0,06 ± 0,02	0,5 ± 0,16	4,30 ± 0,61	7257,01 ± 2984,69	6,97 ± 1,02
	zip9.1	54,36 ± 34,24	524,78 ± 154,13	0,04 ± 0,02	0,42 ± 0,04	3,96 ± 0,97	9359,10 ± 2784,23	5,78 ± 1,45
	zip4/zip6	40,66 ± 7,70	926,19 ± 341,42	0,06 ± 0,02	1,3 ± 1,85	4,10 ± 0,60	5533,69 ± 1330,89	5,79 ± 1,31
	zip4/zip9	40,60 ± 8,99	402,79 ± 207,62	0,05 ± 0,01	0,8 ± 0,38	6,34 ± 2,10	11955,75 ± 4469,53	5,81 ± 1,55
	zip6/zip9	42,95 ± 14,51	674,58 ± 296,46	0,08 ± 0,03	0,46 ± 0,09	5,53 ± 2,01	7149,01 ± 1896,77	5,67 ± 2,07
	zip4/zip6/zip9	46,93 ± 16,72	341,41 ± 140,67	0,06 ± 0,02	0,48 ± 0,05	3,52 ± 0,76	10357,05 ± 5099,42	5,38 ± 2,03

Figure S1: Ionome in roots of single *zip4.1*, *zip6.1*, *zip9.1,* double *zip4/zip6, zip4/zip9*, *zip6/zip9* and triple *zip4/zip6/zip9* knockout mutants and wild-type grown in hydroponics at different Zn concentrations. Values are means ± SEM (n=3). Significant results compared to wild-type are marked in red. nd = not detectable.

Hydroponic culture - Shoots

Condition	Genotype	B 11	Na 23	Mg 24	P 31	S 34	K 39	Ca 43
Zn 0 µM	wt	111,80 ± 16,33	26,36 ± 1,49	9247,05 ± 997,72	14946,39 ± 1636,68	10871,50 ± 1316,25	26883,96 ± 10060,88	60012,52 ± 3273,34
	zip4.1	103,12 ± 8,53	27,73 ± 9,21	10823,12 ± 2679,93	17257,37 ± 3114,61	12447,88 ± 1506,59	27640,82 ± 4983,47	68977,38 ± 618,24
	zip6.1	106,79 ± 4,73	19,40 ± 2,49	10940,23 ± 1879,36	**23638,93 ± 3312,33**	**15359,34 ± 764,71**	26399,08 ± 2127,90	72969,65 ± 2169,48
	zip9.1	102,78 ± 11,75	23,08 ± 0,49	9541,69 ± 1221,53	16988,91 ± 1866,15	12501,84 ± 938,94	29557,87 ± 5546,40	59824,85 ± 9479,00
	zip4/zip6	108,94 ± 10,83	18,13 ± 4,75	10559,62 ± 983,97	**22573,63 ± 3172,25**	**14589,75 ± 681,28**	24585,04 ± 4214,54	70667,24 ± 4218,54
	zip4/zip9	106,63 ± 21,03	19,08 ± 3,77	9603,73 ± 1119,32	**23186,90 ± 2433,56**	**14885,68 ± 1471,55**	24970,31 ± 3644,92	64307,81 ± 1887,73
	zip6/zip9	113,90 ± 13,75	20,65 ± 2,25	9876,17 ± 1174,27	20154,24 ± 4802,93	13597,60 ± 1151,88	25444,78 ± 6901,02	69431,13 ± 979,62
	zip4/zip6/zip9	99,82 ± 21,37	20,03 ± 5,77	10047,50 ± 1161,84	**23477,49 ± 1958,27**	**15877,07 ± 1417,58**	23759,02 ± 3381,32	67954,39 ± 3546,93
Zn 2 µM	wt	113,14 ± 2,80	21,64 ± 5,92	9353,84 ± 654,47	17883,74 ± 2261,02	20118,04 ± 2869,66	47073,63 ± 3400,89	55920,94 ± 2479,86
	zip4.1	103,12 ± 5,06	27,28 ± 11,05	8925,44 ± 761,85	17967,55 ± 3212,95	19710,38 ± 3514,88	47160,76 ± 6608,01	53236,39 ± 6178,96
	zip6.1	107,19 ± 6,03	17,94 ± 5,65	9939,49 ± 956,22	18474,94 ± 1626,00	20125,38 ± 2381,07	40542,57 ± 3699,99	59884,96 ± 5544,71
	zip9.1	106,38 ± 9,43	20,69 ± 1,54	9395,91 ± 510,96	17582,14 ± 4177,82	19758,63 ± 3174,19	47354,29 ± 7348,01	55855,47 ± 2817,63
	zip4/zip6	101,01 ± 8,75	24,01 ± 7,84	9739,37 ± 535,96	19806,86 ± 1839,65	21368,46 ± 3034,76	49885,76 ± 9487,17	56707,08 ± 4714,09
	zip4/zip9	119,65 ± 4,57	18,68 ± 2,72	9354,48 ± 1063,15	17576,23 ± 1916,87	19842,49 ± 2040,76	46202,34 ± 6310,71	56228,35 ± 3915,85
	zip6/zip9	107,61 ± 8,91	22,13 ± 4,94	9669,12 ± 621,55	18319,73 ± 2557,70	19201,47 ± 2140,13	47105,35 ± 3974,81	58219,29 ± 3927,62
	zip4/zip6/zip9	114,13 ± 12,55	19,42 ± 4,50	9953,42 ± 1460,85	16831,76 ± 3043,37	20302,82 ± 4551,36	47118,67 ± 11229,02	60664,65 ± 8962,40
Zn 10 µM	wt	105,31 ± 12,81	36,43 ± 11,44	8718,33 ± 281,09	22166,01 ± 3719,47	31636,20 ± 4291,19	65775,55 ± 6511,84	51613,04 ± 2432,04
	zip4.1	104,03 ± 8,31	36,20 ± 9,34	8679,37 ± 1026,36	21508,43 ± 2762,47	32107,82 ± 5378,57	64007,72 ± 9497,88	52543,54 ± 4613,77
	zip6.1	97,27 ± 8,19	36,32 ± 5,96	8147,38 ± 625,04	18109,83 ± 5763,77	26098,76 ± 4038,75	59616,73 ± 3298,73	50275,00 ± 3568,32
	zip9.1	101,88 ± 9,90	27,73 ± 9,07	8762,28 ± 942,25	20054,40 ± 2570,54	29026,86 ± 2299,68	62072,60 ± 3565,99	54101,58 ± 6490,23
	zip4/zip6	96,38 ± 7,79	29,73 ± 8,29	8047,73 ± 284,88	14893,35 ± 5981,48	23793,38 ± 5528,37	58871,51 ± 8554,68	50911,82 ± 2722,59
	zip4/zip9	109,71 ± 9,74	25,06 ± 1,16	8817,26 ± 428,65	22387,56 ± 1295,49	31023,42 ± 4364,65	60983,73 ± 7460,02	53959,44 ± 2790,76
	zip6/zip9	103,89 ± 9,56	28,08 ± 5,92	7834,79 ± 710,92	14857,45 ± 407,56	**21609,54 ± 2160,09**	52930,01 ± 5193,31	49051,59 ± 4875,21
	zip4/zip6/zip9	123,41 ± 15,55	**111,24 ± 27,04**	7801,45 ± 213,63	**12892,69 ± 3115,30**	**19668,45 ± 2060,67**	**51225,21 ± 4920,18**	50406,25 ± 2201,66

Figure S1: Ionome in shoots of single *zip4.1*, *zip6.1*, *zip9.1,* double *zip4/zip6, zip4/zip9*, *zip6/zip9* and triple *zip4/zip6/zip9* knockout mutants and wild-type grown in hydroponics at different Zn concentrations. Values are means ± SEM (n=3). Significant results compared to wild-type are marked in red. nd = not detectable.

Hydroponic culture - Shoots

Condition	Genotype	Mn 55	Fe 56	Co 59	Ni 60	Cu 63	Zn 66	Mo 98
Zn 0 µM	wt	302,78 ± 38,29	99,12 ± 15,81	0,11 ± 0,01	0,07 ± 0,02	5,07 ± 2,53	nd	2,52 ± 0,41
	zip4.1	346,97 ± 63,52	99,93 ± 11,68	0,13 ± 0,05	0,07 ± 0,04	5,99 ± 2,51	nd	2,76 ± 0,15
	zip6.1	346,79 ± 62,28	**56,25 ± 7,20**	0,12 ± 0,01	0,10 ± 0,09	5,47 ± 2,24	nd	2,59 ± 0,05
	zip9.1	311,09 ± 40,08	82,54 ± 13,18	0,12 ± 0,01	0,08 ± 0,03	5,52 ± 2,80	nd	2,46 ± 0,36
	zip4/zip6	362,67 ± 59,30	**59,08 ± 14,87**	0,12 ± 0,01	0,05 ± 0,01	5,14 ± 2,30	nd	2,49 ± 0,43
	zip4/zip9	323,22 ± 46,43	**57,42 ± 10,37**	0,16 ± 0,07	0,05 ± 0,01	5,42 ± 3,11	nd	2,38 ± 0,08
	zip6/zip9	321,33 ± 39,57	**62,48 ± 18,16**	0,12 ± 0,01	0,05 ± 0,01	5,38 ± 1,89	nd	2,66 ± 0,08
	zip4/zip6/zip9	353,31 ± 29,95	**61,82 ± 7,29**	0,11 ± 0,01	0,07 ± 0,02	5,11 ± 2,34	nd	2,55 ± 0,20
Zn 2 µM	wt	199,86 ± 28,12	78,03 ± 11,73	0,07 ± 0,002	0,1 ± 0,02	3,40 ± 0,51	1093,40 ± 76,68	2,27 ± 0,22
	zip4.1	196,48 ± 26,26	79,05 ± 7,48	0,07 ± 0,008	0,1 ± 0,02	3,23 ± 0,54	917,98 ± 150,42	2,31 ± 0,32
	zip6.1	205,02 ± 28,72	70,50 ± 4,33	0,07 ± 0,006	0,1 ± 0,01	3,15 ± 0,46	1111,80 ± 63,17	2,18 ± 0,19
	zip9.1	198,85 ± 18,50	83,30 ± 15,95	0,09± 0,03	0,11 ± 0,02	3,26 ± 0,38	855,53 ± 180,18	2,18 ± 0,27
	zip4/zip6	205,38 ± 13,72	80,37 ± 5,75	0,07 ± 0,006	0,1 ± 0,02	2,83 ± 0,27	1104,42 ± 71,77	2,20 ± 0,36
	zip4/zip9	208,11 ± 28,72	83,47 ± 3,36	0,07 ± 0,007	0,09 ± 0,02	3,51 ± 0,28	926,02 ± 110,70	2,33 ± 0,24
	zip6/zip9	200,43 ± 19,57	79,90 ± 7,12	0,08 ± 0,01	0,12 ± 0,01	3,18 ± 0,40	1151,98 ± 310,52	2,48 ± 0,20
	zip4/zip6/zip9	218,02 ± 35,69	88,99 ± 17,78	0,09 ± 0,02	**0,17 ± 0,07**	3,30 ± 0,41	1092,30 ± 206,84	2,16 ± 0,25
Zn 10 µM	wt	204,64 ± 18,68	56,49 ± 12,25	0,07 ± 0,01	0,18 ± 0,04	3,28 ± 0,80	4691,62 ± 905,71	2,18 ± 0,42
	zip4.1	199,84 ± 33,74	58,76 ± 10,95	0,07 ± 0,01	0,26 ± 0,15	2,93 ± 0,67	4393,05 ± 156,26	2,31 ± 0,32
	zip6.1	191,40 ± 26,30	73,12 ± 31,58	0,08 ± 0,01	0,24 ± 0,03	2,69 ± 0,47	3754,07 ± 1650,85	2,34 ± 0,58
	zip9.1	204,73 ± 46,28	48,18 ± 3,24	0,07 ± 0,01	0,16 ± 0,03	3,28 ± 0,69	4592,50 ± 770,00	2,44 ± 0,68
	zip4/zip6	186,30 ± 21,73	76,42 ± 25,07	0,08 ± 0,02	0,18 ± 0,06	2,69 ± 0,39	**2377,22 ± 198,11**	2,54 ± 0,42
	zip4/zip9	199,43 ± 20,20	56,39 ± 17,27	0,07 ± 0,006	0,13 ± 0,04	2,91 ± 0,71	4618,05 ± 871,71	2,40 ± 0,32
	zip6/zip9	178,35 ± 24,41	83,73 ± 9,57	0,08 ± 0,02	0,14 ± 0,03	2,94 ± 0,35	**2708,65 ± 422,54**	2,48 ± 0,48
	zip4/zip6/zip9	188,14 ± 26,66	81,25 ± 11,75	0,08 ± 0,02	0,15 ± 0,04	2,83 ± 0,43	**2691,22 ± 669,02**	2,33 ± 0,35

Figure S1: Ionome in shoots of single *zip4.1*, *zip6.1*, *zip9.1,* double *zip4/zip6, zip4/zip9*, *zip6/zip9* and triple *zip4/zip6/zip9* knockout mutants and wild-type grown in hydroponics at different Zn concentrations. Values are means ± SEM (n=3). Significant results compared to wild-type are marked in red. nd = not detectable.

In vitro - Roots

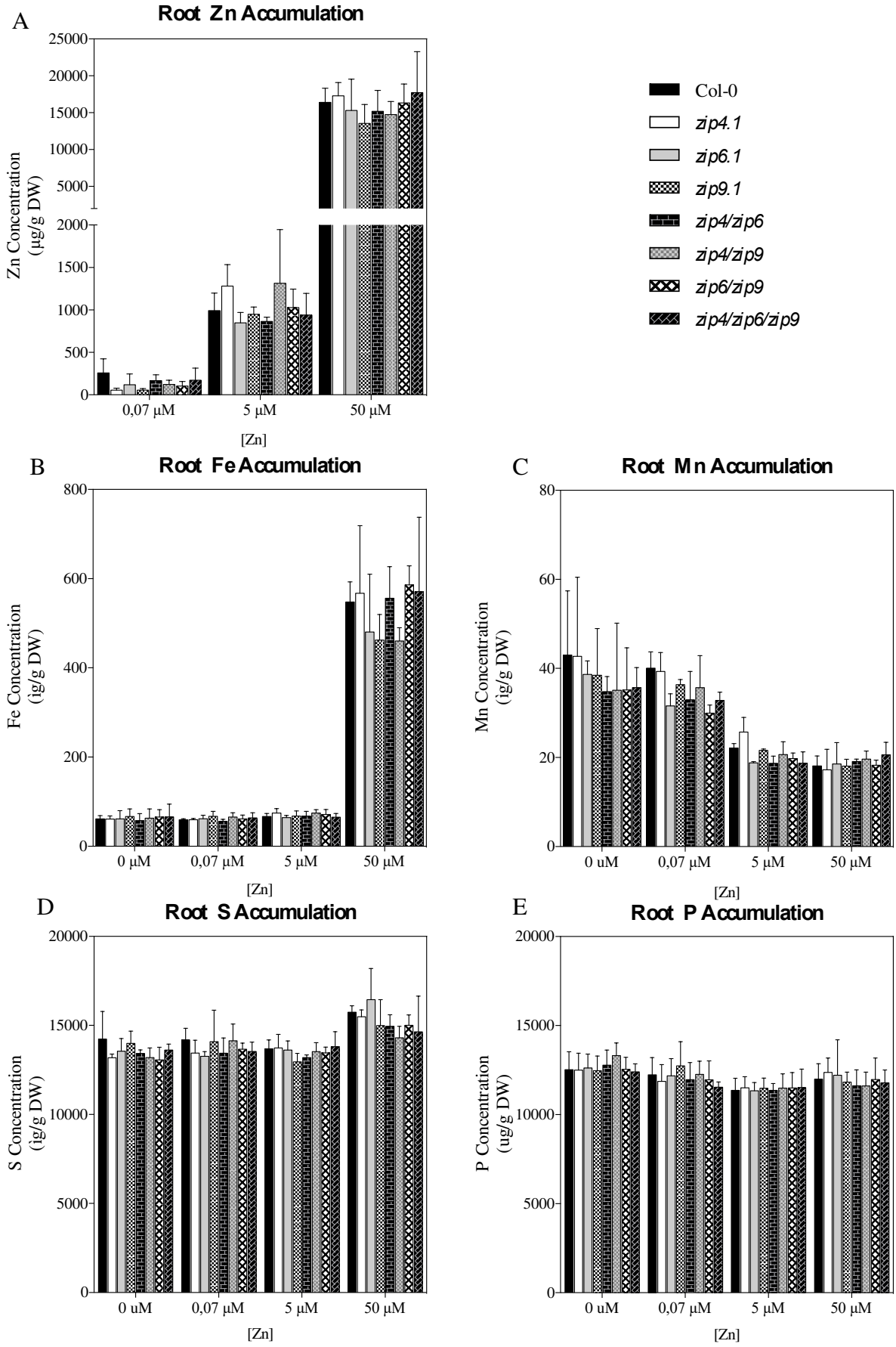

Figure S2: ICP-MS analysis for A) Zn, B) Fe, C) Mn, D) S and E) P accumulation in roots of single *zip4.1*, *zip6.1*, *zip9.1,* double *zip4/zip6, zip4/zip9*, *zip6/zip9* and triple *zip4/zip6/zip9* knockout mutants and wild-types grown on plates at different levels of Zn. Values are means ± SEM (n=3).

In vitro - Shoots

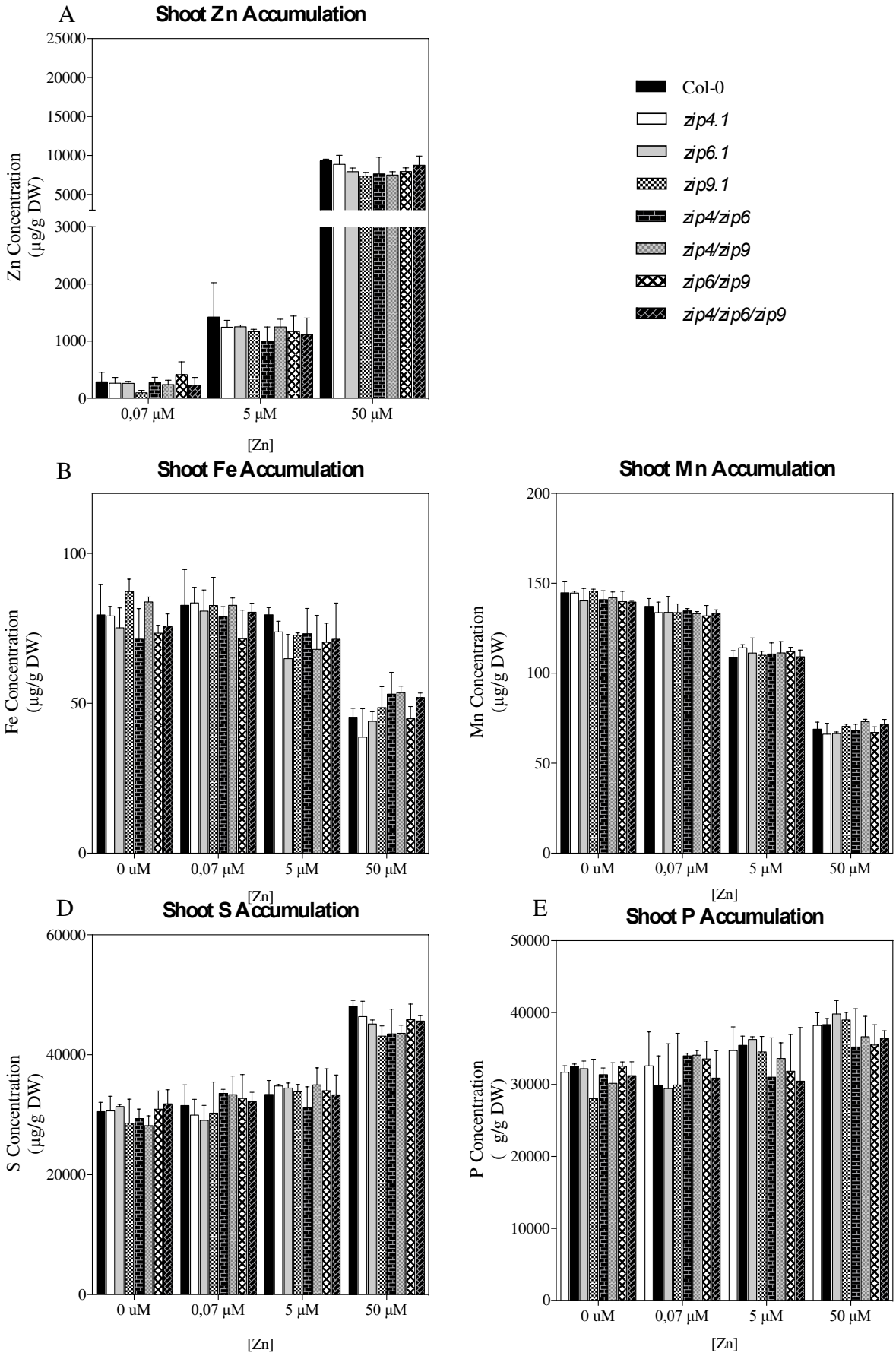

Figure S3: ICP-MS analysis for A) Zn, B) Fe, C) Mn, D) S and E) P accumulation in shoots of single *zip4.1*, *zip6.1*, *zip9.1,* double *zip4/zip6, zip4/zip9*, *zip6/zip9* and triple *zip4/zip6/zip9* knockout mutants and wild-types grown on plates at different levels of Zn. Values are means ± SEM (n=3).

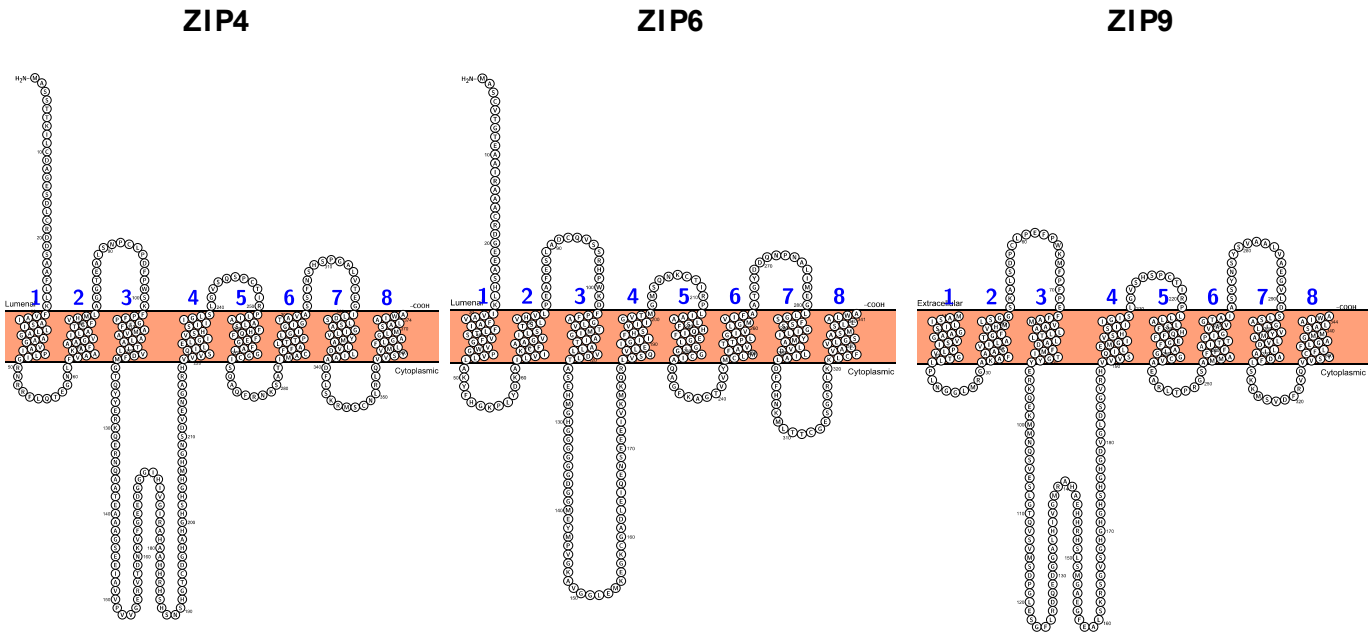

Figure S4: Secondary structure of ZIP4, ZIP6 and ZIP9 obtained using the Protter tool: an interactive protein feature visualization and integration with experimental proteomic data (Omasits *et al.,* 2014).

ZIPs	Protein Length (aa)	Prediction in Protein Databases				
		WoLF PSORT	MultiLoc	EpiLoc	SwissProt	YLoc
ZIP4	408	PM	PM	TP	CL	PM
ZIP6	341	PM	PM	PM	CL	PM
ZIP9	344	PM/TP	PM	TP	PM	PM

Figure S5: Prediction of the subcellular localization of ZIP4, ZIP6 and ZIP9 according to different databases. Plasma membrane (PM), Endoplasmic reticulum (ER), Tonoplast (TP), Chloroplast (CL). WoLF PSORT (Horton *et al.,* 2007); MultiLoc (Höglund *et al.,* 2006); EpiLoc (Brady and Shatkav, 2008); YLoc (Briesemeister *et al.,* 2010);

7. REFERENCES

- Abdel-Ghany S.E., Muller-Moule P., Niyogi K.K., Pilon M., Shikanai T. (2005) Two P-type ATPases are required for copper delivery in *Arabidopsis thaliana* chloroplasts. *The Plant Cell*, 17(4): 1233–1251.
- Aller S.G., Eng E.T., De Feo C.J., Unger V.M. (2004) Eukaryotic CTR copper uptake transporters require two faces of the third transmembrane domain for helix packing, oligomerization, and function. *The Journal of Biological chemistry,* 279(51): 53435-53441.
- Aller S.G., Unger V.M. (2006). Projection structure of the human copper transporter CTR1 at 6-A resolution reveals a compact trimer with a novel channel-like architecture. *Proceedings of the National Academy of Sciences of the United States of America*, 103(10): 3627–3632.
- Alonso J.M., Hirayama T., Roman G., Nourizadeh S., Ecker J.R. (1999) EIN2, a bifunctional transducer of ethylene and stress responses in Arabidopsis. *Science*, 284(5423): 2148-52.
- Andres-Colas N., Sancenon V., Rodriguez-Navarro S., Mayo S., Thiele D.J., Ecker J.R., Puig S., Penarrubia L. (2006) The Arabidopsis heavy metal P-type ATPase HMA5 interacts with metallochaperones and functions in copper detoxification of roots. *The Plant Journal: for cell and molecular biology,* 45(2): 225–236.
- Appenroth K.J. (2010) Definition of "Heavy Metals" and Their Role in Biological Systems. In: *Soil Heavy Metals*. Soil Biology, vol 19. Springer, Berlin, Heidelberg, pp 19-29.
- Argüello J.M. (2003) Identification of ion-selectivity determinants in heavy-metal transport P1B-type ATPases. *The Journal of Membrane Biology*, 195(2): 93-108.
- Arrivault S., Senger T., Krämer U. (2006) The Arabidopsis metal tolerance protein *AtMTP3* maintains metal homeostasis by mediating Zn exclusion from the shoot under Fe deficiency and Zn oversupply. *The Plant Journal: for cell and molecular biology,* 46(5): 861–879.
- Assunção A.G.L., Da Costa Martins P., De Folter S., Vooijs R., Schat H., Aarts M.G.M. (2001) Elevated expression of metal transporter genes in three accessions of the metal hyperaccumulator *Thlaspi caerulescens*. *Plant, Cell & Environment*, 24(2): 217–226.
- Assunção A.G.L, Herrero E., Lin Y.F., Huettel B., Talukdar S., Smaczniak C., Immink R.G.H., van Eldik M., Fiers M., Schat H., Aarts M.G.M. (2010) *Arabidopsis thaliana* transcription factors bZIP19 and bZIP23 regulate the adaptation to zinc deficiency. *Proceedings of the National Academy of Sciences of the United States of America*, 107(22): 10296-10301.
- Aufsatz W., Nehlin L., Voronin V., Schmidt A., Matzke A., Matzke M. (2009) A novel strategy for obtaining kanamycin resistance in *Arabidopsis thaliana* by silencing an endogenous gene encoding a putative chloroplast transporter. *Biotechnology Journal*, 4(2): 224–229.
- Auld D.S. (2001) Zinc coordination sphere in biochemical zinc sites. *Biometals*, 14(3-4):271-313.
- Axelsen K.B., Palmgren M.G. (2001) Inventory of the superfamily of P-type ion pumps in Arabidopsis. *Plant Physiology,* 126(2): 696-706.
- Baker A.J.M. (1981) Accumulators and excluders -strategies in the response of plants to heavy metals. *Journal of Plant Nutrition,* 3(1-4): 635-642.
- Baker A.J.M. (1987) Metal Tolerance. *New Phytologist*, 106: 93–111.
- Baker A.J.M., Walker P.L. (1990) Ecophysiology of metal uptake by tolerant plants. In: Shaw A.J. (ed) Heavy metal tolerance in plants: evolutionary aspects. CRC Press, Boca Raton, pp 155–177.
- Baker A.J.M., Reeves R.D., Hajar A.S.M. (1994) Heavy metal hyperaccumulation and tolerance in British populations of the metallophyte *Thlaspi caerulescens* J. & C. Presl (Brassicaceae). *New Phytologist*, 127:61–68.

- Baker A.J.M., Ernst W.H.O., van der Ent A., Malaisse F., Ginocchio R. (2010) Metallophytes: the unique biological resource, its ecology and conservational status in Europe, central Africa and Latin America. *In* LC Batty, KB Hallberg, eds, Ecol. Ind. Pollut., Cambridge. Cambridge, UK, pp 7–40.
- Basu C., Kausch A.P., Luo H., Chandlee J.M. (2003) Promoter analysis in transient assays using a GUS reporter gene construct in creeping bentgrass (*Agrostis palustris*). *Journal of Plant Physiology,* 160(10): 1233–1239.
- Becher M., Talke I.N., Krall., Krämer U. (2004) Cross-species microarray transcript profiling reveals high constitutive expression of metal homeostasis genes in shoots of the zinc hyperaccumulator Arabidopsis halleri. *The Plant Journal: for cell and molecular biology,* 37(2): 251–268.
- Bernal M., Casero D., Singh V., Wilson G.T., Grande A., Yang H., Dodani S.C., Pellegrini M., Huijser P., Connolly E.M., Merchant S.S., Krämer U. (2012) Transcriptome sequencing identifies SPL7-regulated copper acquisition genes FRO4/FRO5 and the copper dependence of iron homeostasis in Arabidopsis. *Plant Cell,* 24(2): 738–761.
- Brady S., Shatkay H. (2008) EpiLoc: a (working) text-based system for predicting protein subcellular location. *Pacific Symposium of Biocomputing*: 604-615.
- Briat J.F., Rouached H., Tissot N., Gaymard F., Dubos C. (2015) Integration of P, S, Fe, and Zn nutrition signals in *Arabidopsis thaliana*: potential involvement of PHOSPHATE STARVATION RESPONSE 1 (PHR1). *Frontiers in Plant Science,* 6:290.
- Briesemeister S., Rahnenführer J., Kohlbacher O. (2010) YLoc--an interpretable web server for predicting subcellular localization. *Nucleic Acids Reserch*, 38 (Web Server issue): W497-502.
- Broadley M.R., White P.J., Hammond J.P., Zelko I., Lux A. (2007) Zinc in plants. *The New Phytologist,* 173(4): 677-702.
- Brooks R.R.., Lee J, Reeves R.D., Jaffre´ T. (1977) Detection of nickeliferous rocks by analysis of herbarium specimens of indicator plants. *Journal of Geochemical Exploration*, 7: 49–57.
- Bughio N., Yamaguchi H., Nishizawa N.K., Nakanishi H., Mori S. (2002) Cloning an iron-regulated metal transporter from rice. *Journal of Experimental Botany*, 53(374): 1677-1682.
- Cailliatte R., Schikora A., Briat J.F.., Mari S, Curie C. (2010) High-affinity manganese uptake by the metal transporter NRAMP1 is essential for Arabidopsis growth in low manganese conditions. *The Plant Cell,* 22(3): 904-917.
- Cheng N.H., Pittman J.K., Barkla B.J., Shigaki T., Hirschi K.D. (2003) The Arabidopsis cax1 mutant exhibits impaired ion homeostasis, development, and hormonal responses and reveals interplay among vacuolar transporters. *The Plant Cell,* 15(2): 347-364.
- Cheng N.H., Pittman J.K., Shigaki T., Lachmansingh J., LeClere S., Lahner B., Salt D.E., Hirschi K.D. (2005) Functional association of Arabidopsis CAX1 and CAX3 is required for normal growth and ion homeostasis. *Plant Physiology,* 138(4): 2048-2060.
- Chu H.H., Chiecko J., Punshon T., Lanzirotti A., Lahner B., Salt D.E., Walker E.L. (2010) Successful reproduction requires the function of Arabidopsis Yellow Stripe-Like1 and Yellow Stripe-Like3 metal-nicotianamine transporters in both vegetative and reproductive structures. *Plant Physiology,* 154(1): 197-210.
- Chu H.H., Car S., Socha A.L., Hindt M.N., Punshon T1, Guerinot M.L. (2017) The Arabidopsis MTP8 transporter determines the localization of manganese and iron in seeds. *Scientific reports,* 7(1): 11024.
- Clemens S., Palmgren M.G., Krämer U. (2002) A long way ahead: understanding and engineering plant metal accumulation. *Trends in plant Science,* 7(7): 309-315.
- Clough S.J., Bent A.F. (1998) Floral dip: a simplified method for Agrobacterium-mediated transformation of *Arabidopsis thaliana*. *The Plant Journal: for cell and molecular biology,* 16(6): 735–743.

- Cobbett C.S., Hussain D., Haydon M.J. (2003) Structural and functional relationships between type 1_B heavy metal-transporting P-type ATPases in *Arabidopsis*. *The New Phytologist,* 159(2): 315-321.
- Cohen C.K., Fox T.C., Garvin D.F., Kochian L.V. (1998) The Role of Iron-Deficiency Stress Responses in Stimulating Heavy-Metal Transport in Plants. *Plant Physiology,* 116(3): 1063–1072.
- Cohen C.K., Garvin D.F., Kochian L.V. (2004) Kinetic properties of a micronutrient transporter from *Pisum sativum* indicate a primary function in Fe uptake from the soil. *Planta,* 218(5): 784-792.
- Connolly E.L., Fett J.P., Guerinot ML. (2002) Expression of the IRT1 metal transporter is controlled by metals at the levels of transcript and protein accumulation. *Plant Cell*, 14(6): 1347-1357.
- Conte S., Stevenson D., Furner I., Lloyd A. (2009) Multiple antibiotic resistance in Arabidopsis is conferred by mutations in a chloroplast-localized transport protein. *Plant Phisiology*, 151(2): 559-573.
- Conte S.S., Chu H.H., Rodriguez D.C., Punshon T., Vasques K.A., Salt D.E., Walker E.L. (2013) Arabidopsis thaliana Yellow Stripe1-Like4 and Yellow Stripe1-Like6 localize to internal cellular membranes and are involved in metal ion homeostasis. *Frontiers in Plant Science,* 4: 283.
- Curie C., Alonso J..M, Le Jean M., Ecker J.R., Briat J.F. (2000) Involvement of NRAMP1 from Arabidopsis thaliana in iron transport. *The Biochemical Journal,* 347(Pt 3): 749-755.
- Curie C., Panaviene Z., Loulergue C., Dellaporta S.L., Briat J.F., Walker E.L. (2001) Maize yellow stripe1 encodes a membrane protein directly involved in Fe(III) uptake. *Nature,* 409(6818): 346-349.
- Curie C., Cassin G., Couch D., Divol F., Higuchi K., Le Jean M., Misson J., Dchikora A., Czernic P., Mari S. (2008) Metal movement within the plant: contribution of nicotianamine and yellow stripe 1-like transporters. *Annals of Botany,* 103(1), 1–11.
- Curie C., Cassin G., Couch D., Divol F., Higuchi K., Le Jean M., Misson J., Schikora A., Czernic P., Mari S. (2009) Metal movement within the plant: contribution of nicotianamine and yellow stripe 1-like transporters. *Annals of Botany,* 103(1): 1-11.
- Chrispeels M.J., Crawford N.M., Schroeder J.I. (1999) Proteins for transport of water and mineral nutrients across the membranes of plant cells. *Plant Cell,* 11(4): 661-676.
- Deinlein U., Weber M., Schmidt H., Rensch S., Trampczynska A., Hansen T.H., Husted S., Schjoerring J.K., Talke I.N., Krämer U., Clemens S. (2012) Elevated nicotianamine levels in *Arabidopsis halleri* roots play a key role in zinc hyperaccumulation. *The Plant Cell*, 24(2): 708-723.
- Delhaize E., Gruber B.D., Pittman J.K., White R.G., Leung H., Miao Y., Jiang L., Ryan P.R., Richardson A.E. (2007) A role for the AtMTP11 gene of Arabidopsis in manganese transport and tolerance. *The Plant Journal: for cell and molecular biology*, 51(2), 198–210.
- Desbrosses-Fonrouge A.G., Voigt K., Schröder A., Arrivault S., Thomine S., Krämer U. (2005) *Arabidopsis thaliana* MTP1 is a Zn transporter in the vacuolar membrane which mediates Zn detoxification and drives leaf Zn accumulation. *FEBS Lett*ers 579: 4165–4174.
- DiDonato R.J. Jr, Roberts L.A., Sanderson T., Eisley R.B., Walker E.L. (2004) Arabidopsis Yellow Stripe-Like2 (YSL2): a metal-regulated gene encoding a plasma membrane transporter of nicotianamine-metal complexes. *The Plant Journal: for cell and molecular biology,* 39(3): 403-414.
- Divol F., Couch D., Conéjéro G., Roschzttardtz H., Mari S., Curie C. (2013) The Arabidopsis YELLOW STRIPE LIKE4 and 6 transporters control iron release from the chloroplast. *The Plant Cell,* 25(3): 1040-1055.
- Dräger D.B., Desbrosses-Fonrouge A.G., Krach C., Chardonnens A.N., Meyer R.C., Saumitou-Laprade P., Krämer U. (2004) Two genes encoding *Arabidopsis halleri* MTP1 metal transport proteins co- segregate with zinc tolerance and account for high MTP1 transcript levels. *The Plant Journal: for cell and molecular biology,* 39(3): 425–439.
- Duffus J.H. (2002) ‘‘Heavy metal’’—a meaningless term? (IUPAC Technical Report). *Pure and Applied Chemistry*, 74(5): 793–807.

- Eckhardt U., Mas Marques A., Buckhout T.J. (2001) Two iron-regulated cation transporters from tomato complement metal uptake-deficient yeast mutants. *Plant Molecular Biology,* 45(4):437-448.
- Ehrnstorfer I.A., Geertsma E.R., Pardon E., Steyaert J., Dutzler R. (2014). Crystal structure of a SLC11 (NRAMP) transporter reveals the basis for transition-metal ion transport. *Nature Structural & Molecular Biology,* 21(11): 990–996.
- Eide D., Broderius M., Fett J., Guerinot M.L. (1996) A novel iron-regulated metal transporter from plants identified by functional expression in yeast. *Proceedings of the National Academy of Sciences of the United States of America*, 93(11): 5624-5628.
- Eng B.H., Guerinot M.L., Eide D., Saier M.H. Jr. (1998) Sequence analyses and phylogenetic characterization of the ZIP family of metal ion transport proteins. *The Journal of Membrane Biology,* 166(1): 1-7.
- Englbrecht C.C., Schoof H., Böhm S. (2004) Conservation, diversification and expansion of C2H2 zinc finger proteins in the Arabidopsis thaliana genome. *BMC Genomics,* 5(1): 39.
- Epstein E. (1972) Mineral nutrition of plants: principles and perspectives. New York: John Wiley and Sons Inc., 44.
- Fasani E., DalCorso G., Varotto C., Li M., Visioli G., Mattarozzi M., Furini A. (2017) The MTP1 promoters from *Arabidopsis halleri* reveal cis-regulating elements for the evolution of metal tolerance. *The New Phytologist*, 214(4): 1614-1630.
- Filatov V., Dowdle J., Smirnoff N., Ford-Lloyd B., Newbury H.J., Macnair M.R. (2006) Comparison of gene expression in segregating families identifies genes and genomic regions involved in a novel adaptation, zinc hyperaccumulation. *Molecular Ecology*, 15(10): 3045-3059.
- Forieri I., Wirtz M., Hell R. (2013). Toward new perspectives on the interaction of iron and sulfur metabolism in plants. *Frontiers in Plant Science,* 4:357.
- Fu X.Z., Zhou X., Xing F., Ling L.L., Chun C.P., Cao L., Aarts M.G.M., Peng L.Z. (2017) Genome-Wide Identification, Cloning and Functional Analysis of the Zinc/Iron-Regulated Transporter-Like Protein (ZIP) Gene Family in Trifoliate Orange (*Poncirus trifoliata* L. Raf.). *Frontiers in Plant Science,* 8: 588.
- Fukao Y., Ferjani A., Tomioka R., Nagasaki N., Kurata R., Nishimori Y., Fujiwara M., Maeshima M. (2011) iTRAQ analysis reveals mechanisms of growth defects due to excess zinc in *Arabidopsis*. *Plant Physiology*, 155(4): 1893-1907.
- Gaither L. A., Eide D. J. (2000). Functional expression of the human hZIP2 zinc transporter. *The Journal of Biological Chemistry*, 275(8): 5560–5564.
- García-Molina A., Andrés-Colás N., Perea-García A., del Valle-Tascón S., Peñarrubia L., Puig S. (2011) The intracellular Arabidopsis COPT5 transport protein is required for photosynthetic electron transport under severe copper deficiency. *The Plant Journal: for cell and molecular biology,* 65(6): 848–860.
- Gollhofer J., Schläwicke C., Jungnick N., Schmidt W., Buckhout T.J. (2011) Members of a small family of nodulin-like genes are regulated under iron deficiency in roots of Arabidopsis thaliana. *Plant Physiology and Biochemistry: PPB,* 49(5): 557- 564.
- Gollhofer J., Timofeev R., Lan P., Schmidt W., Buckhout T.J. (2014) Vacuolar-Iron-Transporter1-Like proteins mediate iron homeostasis in *Arabidopsis*. *PLoS One*, 9(10): e110468.
- González-Guerrero, M., and Argüello, J. M. (2008). Mechanism of Cu+ transporting ATPases: soluble Cu+ -chaperones directly transfer Cu+ to transmembrane transport sites. *Proceedings of the National Academy of Sciences of the United States of America*, 105(16): 5992–5997.
- González-Guerrero M., Escudero V., Saéz Á., Tejada-Jiménez M. (2016) Transition Metal Transport in Plants and Associated Endosymbionts: Arbuscular Mycorrhizal Fungi and Rhizobia. *Frontiers in Plant Science,* 7:1088.

- Grotz N., Fox T., Connolly E., Park W., Guerinot M.L., Eide D. (1998) Identification of a family of zinc transporter genes from Arabidopsis that respond to zinc deficiency. *Proceedings of the National Academy of Sciences of the United States of America*, 95(12): 7220-7224.
- Guerinot M.L. (2000) The ZIP family of metal transporters. *Biochimica et Biophysica Acta*, 1465 (1-2): 190-198.
- Gunshin H., Mackenzie B., Berger U.V., Gunshin Y., Romero M.F., Boron W.F., Nussberger S., Gollan J.L, Hediger M.A. (1997). Cloning and characterization of a mammalian proton- coupled metal-ion transporter. *Nature,* 388(6641): 482–488.
- Gustin J.L, Zanis M.J., and Salt D.E. (2011) Structure and evolution of the plant cation diffusion facilitator family of ion transporters. *BMC Evolutionary Biology,* 11: 76-89.
- Hafeez B., Khanif I.M., Saleem M. (2013) Role of Zinc in Plant Nutrition – A Review. *American Journal of Experimental Agricolture*, 3(2):374-391.
- Hall J.L., Williams L.E. (2003) Transition metal transporters in plants. *Journal of Experimental Botany,* 54(393): 2601-2613.
- Hammond, J.P., Bowen H.C., White P.J., Mills V., Pyke K.A., Baker A.J., Whiting S.N., May S.T., Broadley M.R. (2006) A comparison of the *Thlaspi caerulescens* and *Thlaspi arvense* shoot transcriptomes. *New Phytologist* 170(2), 239–260.
- Haydon M.J., Kawachi M., Wirtz M., Hillmer S., Hell R., Krämer U. (2012) Vacuolar nicotianamine has critical and distinct roles under iron deficiency and for zinc sequestration in *Arabidopsis*. *The Plant Cell,* 24(2): 724-737.
- Haydon M.J. (2014) Getting a sense for zinc in plants. *The New Phytologist,* 202(1): 10-12.
- Henriques R., Jásik J., Klein M., Martinoia E., Feller U., Schell J., Pais M.S., Koncz C. (2002) Knock-out of Arabidopsis metal transporter gene IRT1 results in iron deficiency accompanied by cell differentiation defects. *Plant Molecular Biology,* 50(4-5): 587-597.
- Hirayama T., Kieber J.J., Hirayama,N., Kogan M., Guzman P., Nourizadeh S., Alonso J.M., Dailey W.P., Dancis A., Ecker J.R. (1999). Responsive-to-antagonist1, a Menkes/Wilson disease-related copper transporter, is required for ethylene signaling in Arabidopsis. *Cell,* 97(3): 383–393.
- Hirschi K.D., Zhen R.G., Cunningham K.W., Rea P.A., Fink G.R. (1996) CAX1, an H+/Ca2+ antiporter from *Arabidopsis*. *Proceedings of the National Academy of Sciences of the United States of America,* 93(16):8782-8786.
- Höglund A., Dönnes P., Blum T., Adolph H.W., Kohlbacher O. (2006) MultiLoc: prediction of protein subcellular localization using N-terminal targeting sequences, sequence motifs and amino acid composition. *Bioinformatics (Oxford, England)*, 22(10):1158-1165.
- Horton P., Park K.J., Obayashi T., Fujita N., Harada H., Adams-Collier C.J., Nakai K. (2007) WoLF PSORT: protein localization predictor. *Nucleic Acids Research*, 35(Web Server issue): W585-587.
- Huang D., Dai W. (2015) Two iron-regulated transporter (IRT) genes showed differential expression in poplar trees under iron or zinc deficiency. *Journal of Plant Physiology,* 186-187: 59-67.
- Hussain D., Haydon M.J., Wang Y., Wong E., Sherson S.M., Young J., Camakaris J., Harper J.F., Cobbett C.S. (2004) P-type ATPase heavy metal transporters with roles in essential zinc homeostasis in Arabidopsis. *The Plant Cell*, 16 (5): 1327–1339.
- Inaba S., Kurata R., Kobayashi M., Yamagishi Y., Mori I., Ogata Y., Fukao Y. (2015) Identification of putative target genes of bZIP19, a transcription factor essential for Arabidopsis adaptation to Zn deficiency in roots. *The Plant Journal: for cell and molecular biology*, 84(2): 323-334.
- Ishimaru Y., Suzuki M., Kobayashi T., Takahashi M., Nakanishi H., Mori S., Nishizawa N.K. (2005) *OsZIP4*, a novel zinc-regulated zinc transporter in rice. *Journal of Experimental Botany,* 56(422): 3207-3214.
- Ishimaru Y., Suzuki M., Tsukamoto T., Suzuki K., Nakazono M., Kobayashi T., Wada Y., Watanabe S., Matsuhashi S., Takahashi M., Nakanishi H., Mori S., Nishizawa N.K. (2006) Rice plants take up iron as an Fe3+-phytosiderophore and as Fe2+. *The Plant Journal: for cell and molecular biology*, 45(3): 335-346.

- Ishimaru Y., Masuda H., Suzuki M., Bashir K., Takahashi M., Nakanishi H., Mori S., Nishizawa N.K. (2007) Overexpression of the OsZIP4 zinc transporter confers disarrangement of zinc distribution in rice plants. *Journal of Experimental Botany,* 58(11): 2909-2915.
- Jain A., Sinilal B., Dhandapani G., Meagher R.B., Sahi S.V. (2013) Effects of deficiency and excess of zinc on morphophysiological traits and spatiotemporal regulation of zinc-responsive genes reveal incidence of cross talk between micro- and macronutrients. *Environmental science & technology,* 47(10): 5327-5335.
- Jaquinod M., Villiers F., Kieffer-Jaquinod S., Hugouvieux V., Bruley C., Garin J., Bourguignon J. (2007) A proteomics dissection of *Arabidopsis thaliana* vacuoles isolated from cell culture. *Molecular & Cellular Proteomics: MCP*, 6(3): 394-412.
- Jung H., Gayomba S.R., Rutzke M.A., Craft E., Kochian L.V., Vatamaniuk O.K. (2012) COPT6 is a plasma membrane transporter that functions in copper homeostasis in Arabidopsis and is a novel target of SQUAMOSA promoter-binding protein-like7. *The Journal of Biological chemistry*, 287(40): 33252–33267.
- Kabata-Pendias A., Pendias, H. (1984) Trace Elements in Soils and Plants. CRC Press, Inc., Florida.
- Kampfenkel K., Kushnir S., Babiychuk E., Inzé D., Van Montagu M. (1995) Molecular characterization of a putative Arabidopsis thaliana copper transporter and its yeast homologue. *The Journal of Biological Chemistry*, 270(47):28479-28486.
- Kang J., Park J., Choi H., Burla B., Kretzschmar T., Lee Y., Martinoia E. (2011) Plant ABC Transporters. *The Arabidopsis Book,* 9: e0153.
- Kavitha P.G., Kuruvilla S., Mathew M.K. (2015) Functional characterization of a transition metal ion transporter, *OsZIP6* from rice (*Oryza sativa L.*). *Plant Physiology & Biochemistry: PPB,* 97: 165-174.
- Kawachi M., Kobae Y., Mimura T., Maeshima M. (2008) Deletion of a histidine-rich loop of AtMTP1, a vacuolar Zn(2+)/H(+) antiporter of *Arabidopsis thaliana*, stimulates the transport activity. *The Journal of Biological Chemistry*, 283(13): 8374-8383.
- Khan G.A., Bouraine S., Wege S., Li Y., de Carbonnel M., Berthomieu P., Poirier Y., Rouached H. (2014). Coordination between zinc and phosphate homeostasis involves the transcription factor PHR1, the phosphate exporter PHO1, and its homologue PHO1;H3 in Arabidopsis. *Journal of Experimental Botany*, 65(3): 871–884.
- Kim D.Y., Bovet L., Kushnir S., Noh E.W., Martinoia E., Lee Y. (2006) *AtATM3* is involved in heavy metal resistance in Arabidopsis. *Plant Physiology,* 140(3): 922-932.
- Kim D.Y., Bovet L., Maeshima M., Martinoia E., Lee Y. (2007) The ABC transporter AtPDR8 is a cadmium extrusion pump conferring heavy metal resistance. *The Plant Journal: for cell and molecular biology,*50(2): 207-218.
- Kim S.A., Punshon T., Lanzirotti A., Li L., Alonso J.M., Ecker J.R., Kaplan J., Guerinot M.L. (2006) Localization of iron in Arabidopsis seed requires the vacuolar membrane transporter VIT1. *Science,* 314(5803): 1295-1298.
- Kim Y.Y., Choi H., Segami S., Cho H.T., Martinoia E., Maeshima M., Lee Y. (2009) AtHMA1 contributes to the detoxification of excess Zn(II) in Arabidopsis. *The Plant Journal: for cell and molecular biology,* 58(5): 737-753.
- Klein M., Burla B., Martinoia E. (2006) The multidrug resistance-associated protein (MRP/ABCC) subfamily of ATP-binding cassette transporters in plants. *FEBS Letters*, 580(4):1112-1122.
- Kobayashi T., Nishizawa N.K. (2012) Iron uptake, translocation, and regulation in higher plants. *Annual Review of Plant Biology*, 63: 131-152.
- Koike S., Inoue H., Mizuno D., Takahashi M., Nakanishi H., Mori S., Nishizawa N.K. (2004) OsYSL2 is a rice metal-nicotianamine transporter that is regulated by iron and expressed in the phloem. *The Plant Journal: for cell and molecular biology,* 29(3): 415-424.
- Krämer U., Talke I.N., Hanikenne M. (2007) Transition metal transport. *FEBS Letters*, 581:2263–2272.
- Lahner B., Gong J., Mahmoudian M., Smith E.L., Abid K.B., Rogers E.E., Guerinot M.L., Harper J.F., Ward J.M., McIntyre L., Schroeder J.I., Salt D.E. (2003) Genomic scale profiling of nutrient and trace elements in *Arabidopsis thaliana*. *Nature Biotechnology,* 21(10): 1215–1221.

- Lanquar V., Lelièvre F., Bolte S., Hamès C., Alcon C., Neumann D., Vansuyt G., Curie C., Schröder A., Krämer U., Barbier-Brygoo H., Thomine S. (2005) Mobilization of vacuolar iron by AtNRAMP3 and AtNRAMP4 is essential for seed germination on low iron. *The EMBO Journal,* 24(23): 4041-4051.
- Larkin M.A., Blackshields G., Brown N.P., Chenna R., McGettigan P.A., McWilliam H., Valentin F., Wallace I.M., Wilm A., Lopez R., Thompson J.D., Gibson T.J., Higgins D.G. (2007) Clustal W and Clustal X version 2.0. *Bioinformatics (Oxford, England)*, 23(21): 2947-2948.
- Lee S., An G. (2009) Over-expression of *OsIRT1* leads to increased iron and zinc accumulations in rice. *Plant, Cell & Environment,* 32(4): 408-416.
- Lee S., Kim S., Lee J., Guerinot M., An G. (2010) Zinc deficiency-inducible *OsZIP8* encodes a plasma membrane-localized zinc transporter in rice. *Molecules and cells*, 29(6): 551-558.
- Lehn H., Bopp M. (1987) Prediction of heavy-metal concentrations in mature plants by chemical analysis of seedlings. *Plant Soil,* 101: 9–14.
- Li L., Chen O.S., McVey Ward D., Kaplan J. (2001) CCC1 is a transporter that mediates vacuolar iron storage in yeast. *The Journal of Biological Chemistry,* 276(31): 29515-29519.
- Li S., Zhou X., Huang Y., Zhu L., Zhang S., Zhao Y., Guo J., Chen J., Chen R. (2013) Identification and characterization of the zinc-regulated transporters, iron-regulated transporter-like protein (ZIP) gene family in maize. *BMC Plant Biology,* 13: 114.
- Li S., Zhou X., Li H., Liu Y., Zhu L., Guo J., Liu X., Fan Y., Chen J., Chen R. (2015) Overexpression of ZmIRT1 and ZmZIP3 Enhances Iron and Zinc Accumulation in Transgenic *Arabidopsis*. *PloS One,* 10(8): e0136647.
- Lin W., Chai J., Love J., Fu D. (2010). Selective electrodiffusion of zinc ions in a Zrt-. Irt-like Protein, ZIPB. *The Journal of Biological Chemistry,* 285(50), 39013–39020.
- Lin Y.F., Liang H.M., Yang S.Y., Boch A., Clemens S., Chen C.C., Wu J.F., Huang J.L., Yeh K.C. (2009) Arabidopsis IRT3 is a zinc-regulated and plasma membrane localized zinc/iron transporter. *The New Phytologist*, 182(2): 392-404.
- Lin Y.F., Hassan Z., Talukdar S., Schat H., Aarts M.G. (2016) Expression of the ZNT1 Zinc Transporter from the Metal Hyperaccumulator Noccaea caerulescens Confers Enhanced Zinc and Cadmium Tolerance and Accumulation to Arabidopsis thaliana. *PLoS One*, 11(3): e0149750.
- Liu Z., Li H., Soleimani M., Girijashanker K., Reed J. M., He L., Dalton T.P., Nebert D.W. (2008) Cd2+ versus Zn2+ uptake by the ZIP8 -dependent symporter: kinetics, electrogenicity and trafficking. *Biochemical and Biophysical Research Communications*, 365(4):814-820.
- Livak K.J., Schmittgen T.D. (2001). Analysis of relative gene expression data using real- time quantitative PCR and the 2(-delta delta C(T)) method. *Methods*, 25(4): 402–408.
- López-Millán A.F., Ellis D.R., Grusak M.A. (2004) Identification and characterization of several new members of the ZIP family of metal ion transporters in *Medicago truncatula*. *Plant Molecular Biology,* 54(4): 583-596.
- Lu M., Fu D. (2007). Structure of the zinc transporter YiiP. *Science*, 317(5845): 1746–1748.
- Marschner H. (1995) Mineral Nutrition of Higher Plants, (Press Academic, Boston), 2nd Ed.
- Maser P., Thomine S., Schroeder J.I., Ward J.M., Hirschi K., Sze H., Talke I.N., Amtmann A., Maathuis F.J.M., Sanders D., Harper J.F., Tchieu J., Gribskov M., Persans M.W., Salt D.E., Kim S.A., Guerinot M.L. (2001) Phylogenetic Relationships within Cation Transporter Families of Arabidopsis. *Plant Physiology,* 126(4): 1646–1667.
- McKie A.T., Marciani P., Rolfs A., Brennan K., Wehr K., Barrow D., Miret S., Bomford A., Peters T.J., Farzaneh F., Hediger M.A., Hentze M.W., Simpson R.J. (2000) A novel duodenal iron-regulated transporter, IREG1, implicated in the basolateral transfer of iron to the circulation. *Molecular Cell,* 5(2): 299-309.
- Mei H., Cheng N.H., Zhao J., Park S., Escareno R.A., Pittman J.K., Hirschi K.D. (2009) Root development under metal stress in Arabidopsis thaliana requires the H+/cation antiporter CAX4. *The New Phytologist,* 183(1): 95-105.
- Mengel K., Kirkby E.A., Kosegarten H., Appel T. (2001) The Soil as a Plant Nutrient Medium. In: Mengel K., Kirkby E.A., Kosegarten H., Appel T. (eds) *Principles of Plant Nutrition*. Springer, Dordrecht.

- Mills R.F., Krijger G.C., Baccarini P.J., Hall J.L., Williams L.E. (2003) Functional expression of AtHMA4, a P1B-type ATPase of the Zn/Co/Cd/Pb subclass. *The Plant Journal: for cell and molecular biology,* 35(2): 164-176.
- Milner M.J., Kochian L.V. (2008) Investigating heavy-metal hyperaccumulation using *Thlaspi caerulescens* as a model system. *Annals of Botany,* 102(1): 3-13.
- Milner M.J., Craft E., Yamaji N., Koyama E., Ma J.F, Kochian L.V. (2012) Characterization of the high affinity Zn transporter from *Noccaea caerulescens*, *NcZNT1*, and dissection of its promoter for its role in Zn uptake and hyperaccumulation. *The New Phytologist,* 195(1):113-123.
- Milner M.J., Seamon J., Craft E., Kochian L.V. (2013) Transport properties of members of the ZIP family in plants and their role in Zn and Mn homeostasis. *Journal of Experimental Botany*, 64(1): 369-381.
- Minguzzi C., Vergnano O. (1948) Il contenuto del nichel nelle ceneri di *Alyssum bertolonii* Desv. *Atti della Società Toscana di Scienze Naturali*, Serie A. 55: 49–77.
- Misson J., Raghothama K.G., Jain A., Jouhet J., Block M.A., Bligny R., Ortet P., Creff A., Somerville S., Rolland N., Doumas P., Nacry P., Herrerra-Estrella L., Nussaume L., Thibaud M.C. (2005). A genome-wide transcriptional analysis using *Arabidopsis thaliana* Affymetrix gene chips determined plant responses to phosphate deprivation. *Proceedings of the National Academy of Sciences of the United States of America,* 102(33): 11934–11939.
- Mizuno T., Usui K., Horie K., Nosaka S., Mizuno N., Obata H. (2005) Cloning of three ZIP/Nramp transporter genes from a Ni hyperaccumulator plant *Thlaspi japonicum* and their Ni2+-transport abilities. *Plant Biology and Biochemistry: PPB*, 43(8): 793-801.
- Mizuno T., Hirano K., Kato S., Obata H. (2008) Cloning of ZIP family metal transporter genes from the manganese hyperaccumulator plant *Chengiopanax sciadophylloides*, and its metal transport and resistance abilities in yeast. *Soil Science & Plant Nutrition,* 54(1): 86-94.
- Montanini B., Blaudez D., Jeandroz S., Sanders D., Chalot M. (2007) Phylogenetic and functional analysis of the cation diffusion facilitator (CDF) family: improved signature and prediction of substrate specificity. *BMC Genomics,* 8: 107.
- Morel M., Crouzet J., Gravot A., Auroy P., Leonhardt N., Vavasseur A., Richaud P. (2009) AtHMA3, a P1B-ATPase allowing Cd/Zn/Co/Pb vacuolar storage in Arabidopsis. *Plant Physiology,* 149(2): 894-904.
- Morrissey J., Guerinot M.L. (2009) Iron uptake and transport in plants: the good, the bad, and the ionome. *Chemical Reviews,* 109(10): 4553-4567.
- Murashige T., Skoog F. (1962) A revised medium for rapid growth and bio assays with tobacco tissue cultures. *Physiologia Plantarum,* 15: 473–497.
- Nishida S., Mizuno T., Obata H. (2008) Involvement of histidine-rich domain of ZIP family transporter TjZNT1 in metal ion specificity. *Plant Physiology & Biochemistry*, 46(5-6): 601-606.
- Nishida S., Tsuzuki C., Kato A., Aisu A., Yoshida J., Mizuno T. (2011) AtIRT1, the primary iron uptake transporter in the root, mediates excess nickel accumulation in Arabidopsis thaliana. *Plant & Cell Physiology*, 52(8): 1433-1442.
- Nishida S., Kato A., Tsuzuki C., Yoshida J., Mizuno T. (2015) Induction of Nickel Accumulation in Response to Zinc Deficiency in *Arabidopsis thaliana*. *International Journal of Molecular Sciences*, 16(5): 9420-9430.
- Nose Y., Rees E.M., Thiele D.J. (2006). Structure of the Ctr1 copper trans“PORE”ter reveals novel architecture. *Trends in Biochemical Sciences,* 31(11): 604–607.
- Noulas C., Tziouvalekas M., Karyotis T. (2018) Zinc in soils, water and food crops. *Journal of Trace Elements in Medicine and Biology,* 49: 252-260.

- Ó Lochlainn S., Bowen H.C., Fray R.G., Hammond J.P., King G.J., White P.J., Graham N.S., Broadley M.R. (2011) Tandem quadruplication of HMA4 in the zinc (Zn) and cadmium (Cd) hyperaccumulator *Noccaea caerulescens*. *Plos One,* 6(3): e17814.
- Olsen L.I., Palmgren M.G. (2014) Many rivers to cross: The journey of zinc from soil to seed. *Frontiers in Plant Science*, 5: 30.
- Omasits U., Ahrens C.H., Müller S., Wollscheid B. (2014) Protter: interactive protein feature visualization and integration with experimental proteomic data. *Ioinformatics (Oxford, England)*, 30(6): 884-886.
- Palmer C.M., Guerinot M.L. (2009) Facing the challenges of Cu, Fe and Zn homeostasis in plants. *Nature Chemical Biology,* 5(5): 333-340.
- Papoyan A., Kochian L.V. (2004) Identification of *Thlaspi caerulescens* genes that may be involved in heavy metal hyperac- cumulation and tolerance. Characterization of a novel heavy metal transporting ATPase. *Plant Physiology,* 136(3): 3814-3823.
- Park J., Song W.Y., Ko D., Eom Y., Hansen T.H., Schiller M., Lee T.G., Martinoia E., Lee Y. (2012) The phytochelatin transporters *AtABCC1* and *AtABCC2* mediate tolerance to cadmium and mercury. *The Plant Journal: for cell and molecular biology,* 69(2): 278-288.
- Paulsen I.T., Saier M.H. (1997). A novel family of ubiquitous heavy metal ion transport proteins. *The Journal of Membrane Biology,* 156(2): 99–103.
- Pedas P., Ytting C.K., Fuglsang A.T., Jahn T.P., Schjoerring J.K., Husted S. (2008) Manganese efficiency in barley: identification and characterization of the metal ion transporter HvIRT1. *Plant Phiysiology,* 148(1): 455-466.
- Pedas P., Schjoerring J.K., Husted S. (2009) Identification and characterization of zinc-starvation-induced ZIP transporters from barley roots. *Plant Physiology & Biochemistry: PPB,* 47(5): 377-383.
- Peiter E., Montanini B., Gobert A., Pedas P., Husted S., Maathuis F.J.M., Blaudez D., Chalot M., Sanders D. (2007) A secretory pathway-localized cation diffusion facilitator confers plant manganese tolerance. *Proceedings of the National Academy of Sciences of the United States of America*, 104(20): 8532–8537.
- Pence N.S., Larsen P.B., Ebbs S.D., Lasat M.M., Letham D.L.D., Garvin D.F., Eide D., Kochian L.V. (2000) The molecular basis for heavy metal hyperaccumulation in *Thlaspi caerulescens*. *Proceedings of the National Academy of Sciences of the United States of America*, 97(9): 4956–4960.
- Perea-García A., García-Molina N., Andrés-Colás N., Vera-Sirera F., PérezAmador M.A., Puig S., Peñarrubia L. (2013) Arabidopsis copper transport protein COPT2 participates in the cross talk between iron deficiency responses and low-phosphate signaling. *Plant Physiology,* 162(1): 180–194.
- Pittman J.K., Shigaki T., Marshall J.L., Morris J.L., Cheng N.H., Hirschi K.D. (2004) Functional and regulatory analysis of the *Arabidopsis thaliana* CAX2 cation transporter. *Plant Molecular Biology,* 56(6): 959-971.
- Pittman J.K., Hirschi K.D. (2016) CAX-ing a wide net: Cation/H(+) transporters in metal remediation and abiotic stress signalling. *Plant Biology (Stuttgart, Germany),* 18(5): 741-749.
- Puig S., Lee J., Lau M., Thiele D.J. (2002) Biochemical and genetic analyses of yeast and human high affinity copper transporters suggest a conserved mechanism for copper uptake. *The Journal of Biological chemistry,* 277(29): 26021-26030.
- Rea P.A. (2007) Plant ATP-binding cassette transporters. *Annual Review of Plant biology,* 58: 347-375.
- Ricachenevsky F.K., Menguer P.K., Sperotto R.A., Williams L.E., Fett, J.P. (2013). Roles of plant metal tolerance proteins (MTP) in metal storage and potential use in biofortification strategies. *Frontiers in plant Sciences*, 4: 144.
- Robinson B., Schulin R., Nowack B., Roulier S., Menon M., Clothier B., Green S., Mills T. (2006) Phytoremediation for the management of metal flux in contaminated sites. *Forest Snow and Landscape Research*, 80(2): 221–234.

- Rogers E.E, Eide D.J., Guerinot M.L. (2000) Altered selectivity in an *Arabidopsis* metal transporter. *Proceedings of the National Academy of Sciences of the United States of America*, 97(22): 12356-12360.
- Roschzttardtz H., Conéjéro G., Divol F., Alcon C., Verdeil J.L., Curie C., Mari S. (2013) New insights into Fe localization in plant tissues. *Frontiers in Plant Sciences,* 4:350.
- Ruzin S.E. (1999) Plant microtechnique and microscopy, Oxford University. New York
- Sachs J. (1865) Handbuch der Experimentalphysiologie der Pflanzen. In *Handbuch der Physiologischen Botanik*, ed. W Hofmeister, Leipzig: Engelmann:153-154.
- Salt D.E., Blaylock M., Kumar N.P., Dushenkov V., Ensley B.D., Chet I., Raskin I. (1995) Phytoremediation: a novel strategy for the removal of toxic metals from the environment using plants. *Bio/technology (Nature Publishing Company)*, 13(5): 468-474.
- Sancenón V., Puig S., Mira H., Thiele D.J., Peñarrubia L. (2003) Identification of a copper transporter family in Arabidopsis thaliana. *Plant Molecular Biology,* 51(4): 577–587.
- Sancenón V., Puig S., Mateu-Andrés I., Dorcey E., Thiele D.J., Peñarrubia L. (2004) The Arabidopsis copper transporter COPT1 functions in root elongation and pollen development. *The Journal of Biological chemistry,* 279(15): 15348–15355.
- Santi S., Schmidt W. (2009) Dissecting iron deficiency-induced proton extrusion in Arabidopsis roots. *The New Phytologist,* 183(4): 1072-1084.
- Sasaki A., Yamaji N., Mitani-Ueno N., Kashino M., Ma J.F. (2015) A node-localized transporter *OsZIP3* is responsible for the preferential distribution of Zn to developing tissues in rice. *The Plant Journal*, 84(2): 374-384.
- Schaaf G., Ludewig U., Erenoglu B. E., Mori S., Kitahara T., Wiren N. (2004) ZmYS1 functions as a proton-coupled symporter for phytosiderophore- and nicotianamine-chelated metals. *The Journal of Biochemical Chemistry,* 279(10): 9091–9096.
- Schaaf G., Schikora A., Häberle J., Vert G., Ludewig U., Briat J.F., Curie C., von Wirén N. (2005) A putative function for the arabidopsis Fe-Phytosiderophore transporter homolog *AtYSL2* in Fe and Zn homeostasis. *Plant & Cell Phisiology*, 46(5): 762-774.
- Schaaf G., Honsbein A., Meda A.R., Kirchner S., Wipf D., von Wirén N. (2006) AtIREG2 encodes a tonoplast transport protein involved in iron-dependent nickel detoxification in Arabidopsis thaliana roots. *The Journal of Biological chemistry,* 281(35): 25532-25540.
- Schuler M., Keller A., Backes C., Philippar K., Lenhof H.P., and Bauer P. (2011). Transcriptome analysis by GeneTrail revealed regulation of functional categories in response to alterations of iron homeostasis in *Arabidopsis thaliana*. *BMC Plant Biology,* 11:87.
- Shanmugam V., Lo J.C., Wu C.L., Wang S.L., Lai C.C., Connolly E.L., Huang J.L., Yeh K.C. (2011) Differential expression and regulation of iron-regulated metal transporters in *Arabidopsis halleri* and *Arabidopsis thaliana* - the role in zinc tolerance. The New Phytologist, 190(1): 125-137.
- Shikanai T., Müller-Moulé P., Munekage Y., Niyogi K.K., Pilon M. (2003) PAA1, a P-Type ATPase of Arabidopsis, functions in copper transport in chloroplasts. *The Plant Cell,* 15(6): 1333–1346.
- Song W.Y., Park J., Mendoza-Cózatl D.G., Suter-Grotemeyer M., Shim D., Hörtensteiner S., Geisler M., Weder B., Rea P.A., Rentsch D., Schroeder J.I., Lee Y., Martinoia E. (2010) Arsenic tolerance in Arabidopsis is mediated by two ABCC-type phytochelatin transporters. *Proceedings of the National Academy of Sciences of the United States of America*, 107(49): 21187-21192.
- Sinclair S.A., Sherson S.M., Jarvis R., Camakaris J., Cobbett C.S. (2007) The use of the zinc-fluorophore, Zinpyr-1, in the study of zinc homeostasis in Arabidopsis roots. *The New Phytologist,* 174(1):39-45.
- Sinclair S.A., Senger T., Talke I.N., Cobbett C.S., Haydon M.J., Krämer U. (2018) Systemic Upregulation of MTP2- and HMA2-Mediated Zn Partitioning to the Shoot Supplements Local Zn Deficiency Responses. *The Plant Cell*, 30(10): 2463-2479.

- Smith S., De Smet I. (2012) Root system architecture: insights from *Arabidopsis* and cereal crops. *Philosophical Transactions of the Royal Society B: Biological Sciences,* 367(1595): 1441-1452.
- Suzuki M., Bashir K., Inoue H., Takahashi M., Nakanishi H., Nishizawa N.K. (2012) Accumulation of starch in Zn-deficient rice. *Rice*, 5: 9.
- Talke I.N., Hanikenne M., Krämer U. (2006) Zinc-dependent global transcriptional control, transcriptional deregulation, and higher gene copy number for genes in metal homeostasis of the hyperaccumulator Arabidopsis halleri. *Plant Physiology,* 142(1): 148-167.
- Thomine S., Wang R., Ward J.M., Crawford N.M., Schroeder J.I. (2000) Cadmium and iron transport by members of a plant metal transporter family in Arabidopsis with homology to Nramp genes. *Proceedings of the National Academy of Sciences of the United States of America*, 97(90): 4991–4996.
- Thomine S., Lanquar V. (2011) Iron Transport and Signaling in Plants. In: Geisler M., Venema K. (eds) Transporters and Pumps in Plant Signaling. *Signaling and Communication in Plants*, vol 7. Springer, Berlin, Heidelberg.
- Tiong J., McDonald G., Genc Y., Shirley N., Langridge P., Huang C.Y. (2015) Increased expression of six ZIP family genes by zinc (Zn) deficiency is associated with enhanced uptake and root-to-shoot translocation of Zn in barley (*Hordeum vulgare*). *New Phytologist*, 207(4): 1097-1109.
- van de Mortel, J.E., Almar Villanueva L., Schat H., Kwekkeboom J., Coughlan S., Moerland P.D., Ver Loren van Themaat E., Koornneef M., Aarts M.G. (2006) Large expression differences in genes for iron and zinc homeostasis, stress response, and lignin biosynthesis distinguish roots of *Arabidopsis thaliana* and the related metal hyperaccumulator *Thlaspi caerulescens*. *Plant Physiology,* 142(3): 1127–1147.
- Varotto C., Maiwald D., Pesaresi P., Jahns P., Salamini F., Leister D. (2002) The metal ion transporter IRT1 is necessary for iron homeostasis and efficient photosynthesis in Arabidopsis thaliana. *The Plant Journal: for cell and molecular biology,* 31(5): 589-599.
- Verbon E.H., Trapet P.L., Stringlis I.A., Kruijs S., Bakker P.A.H.M., Pieterse C.M.J. (2017) Iron and Immunity. *Annual Review of Phytopathology*, 55: 355-375.
- Verret F., Gravot A., Auroy P., Leonhardt N., David P., Nussaume L., Vavasseur A., Richaud P. (2004) Overexpression of AtHMA4 enhances root-to-shoot translocation of zinc and cadmium and plant metal tolerance. *FEBS Letters,* 576(3): 306-312.
- Vert G., Briat J.F., Curie C. (2001) Arabidopsis IRT2 gene encodes a root-periphery iron transporter. *The Plant Journal: for cell and molecular biology,* 26(2): 181-189.
- Vert G., Grotz N., Dédaldéchamp F., Gaymard F., Guerinot M.L., Briat J.F, Curie C. (2002) IRT1, an Arabidopsis transporter essential for iron uptake from the soil and for plant growth. *The Plant Cell,* 14(6): 1223-1233.
- Vert G., Barberon M., Zelazny E., Séguéla M., Briat J.F., Curie C. (2009) Arabidopsis IRT2 cooperates with the high-affinity iron uptake system to maintain iron homeostasis in root epidermal cells. *Planta,* 229(6): 1171-1179.
- Waters B.M., Chu H.H., Didonato R.J., Roberts L.A., Eisley R.B., Lahner B., Salt D.E., Walker E.L. (2006) Mutations in Arabidopsis yellow stripe-like1 and yellow stripe-like3 reveal their roles in metal ion homeostasis and loading of metal ions in seeds. *Plant Physiology,* 141(4): 1446-1458.
- Waters B.M., Sankaran R.P. (2011) Moving micronutrients from the soil to the seeds: Genes and physiological processes from a biofortification perspective. *Plant Science: a International Journal of Experimental Plant Biology*, 180(4): 562-574.
- Weber, M., Harada, E., Vess, C., von Roepenack-Lahaye, E. and Clemens, S. (2004) Comparative microarray analysis of Arabid- opsis thaliana and Arabidopsis halleri roots identifies nicotian- amine synthase, a ZIP transporter and other genes as potential metal hyperaccumulation factors. *The Plant Journal: for cell and molecular biology,* 37(2): 269–281.

- White P.J., Whiting S.N., Baker A.J.M., Broadley M.R. (2002) Does zinc move apoplastically to the xylem in roots of *Thlaspi caerulescens*? *The New Phytologist*, 153: 201–207.
- White P.J., Broadley M.R. (2011) Physiological limits to zinc biofortification of edible crops. *Frontiers in Plant Science*, 2: 80.
- Williams L., Salt D.E. (2009) The plant ionome coming into focus. *Current Opinion in Plant Biology,* 12(3): 247-249.
- Williams L.E., Pittman J.K., Hall J.L. (2000) Emerging mechanisms for heavy metal transport in plants. *Biochimica et Biophysica Acta,* 1465(1-2): 104-126.
- Williams L.E., Mills R.F. (2005) P(1B)-ATPases--an ancient family of transition metal pumps with diverse functions in plants. *Trends in Plant Science,* 10(10): 491-502.
- Wintz H., Fox T., Wu Y.Y., Feng V., Chen W., Chang H.S., Zhu T., Vulpe C. (2003) Expression profiles of Arabidopsis thaliana in mineral deficiencies reveal novel transporters involved in metal homeostasis. *The Journal of Biological Chemistry*, 278(48): 47644–47653.
- Woeste K.E., Kieber J.J. (2000). A strong loss-of-function mutation in RAN1 results in constitutive activation of the ethylene response pathway as well as a rosette-lethal phenotype. *The Plant Cell*, 12(3): 443–455.
- Yamasaki H., Hayashi M., Fukazawa M., Kobayashi Y., Shikanai T. (2009) SQUAMOSA promoter binding protein-like7 is a central regulator for copper homeostasis in Arabidopsis. *Plant Cell*, 21(1): 347–361.
- Yang T.J., Perry P.J., Ciani S., Pandian S., Schmidt W. (2008) Manganese deficiency alters the patterning and development of root hairs in Arabidopsis. *Journal of Experimental Botany,* 59(12): 3453-3464.
- Yang X., Huang J., Jiang Y., Zhang H.S. (2009) Cloning and functional identification of two members of the ZIP (Zrt, Irt-like protein) gene family in rice (*Oryza sativa L.*). *Molecular Biology Reports*, 36(2): 281-287.
- Yeh K.Y., Yeh M., Glass, J. (2011). Interactions between ferroportin and hephaestin in rat enterocytes are reduced after iron ingestion. *Gastroenterology,* 141(1): 292–299.
- Yoo S.D., Cho Y.H., Sheen J. (2007) *Arabidopsis* mesophyll protoplasts: a versatile cell system for transient gene expression analysis. *Nature Protocols*, 2(7):1565-1572.
- Zhang X., Henriques R., Lin S.S., Niu Q.W., Chua N.H. (2006) *Agrobacterium*-mediated transformation of Arabidopsis thaliana using the floral dip method. *Nature Protocols*, 1(2): 641-646.
- Zhao H., Eide D. (1996a) The yeast ZRT1 gene encodes the zinc transporter protein of a high-affinity uptake system induced by zinc limitation. *Proceedings of the National Academy of Sciences of the United States of America*, 93(6): 2454-2458.
- Zhao H., Eide D. (1996b) The ZRT2 Gene Encodes the Low Affinity Zinc Transporter in *Saccharomyces cerevisiae*. *The Journal of Biological Chemistry*, 271(38): 23203-23210.

Chapter 2:

Expression of *Saccharomyces cerevisiae* ZRC1 in different plant species.

1. INTRODUCTION

1.1 BIOFORTIFICATION AND PHYTOREMEDIATION:

In recent years, environmental pollution has rapidly increased due to anthropogenic activities that include industrial processes, smelting and mining, as well as the use of pesticides and fertilizers. Contamination of soils by heavy metals is of particular concern due to their long persistence in the environment and their effects on human health (Jia et al., 2018). On the other hand, under-nutrition is a very serious problem and more than half the world population has an inadequate diet, lacking vitamins, proteins and minerals, especially zinc (Zn), iron (Fe) and iodine (I) (White and Broadley, 2005). Developing countries are particularly affected by this problem: the diet of the local populations offers little or no variety, and derives from crops grown on deplete, exhausted soils. In this context, phytoremediation of contaminated soils and biofortification of the plants' edible organs to reduce micronutrients deficiency may offer some aid. Both applications share the same background, i.e. the study of mineral uptake and transport mechanisms of plants.

1.1.1BIOFORTIFICATION:

Biofortification is a process that increases the mineral content in the edible organs of staple food crops, thus producing enriched foods that can help reduce malnutrition in developing countries where this problem is most serious (Zhao and McGrath, 2009). In recent years, breeders have mostly focused on improving crop productivity, but have obtained a reduction in mineral contents at grain level (Fan *et al.,* 2008). Biofortification can be achieved by using an agricultural approach (agronomic biofortification), consisting in applying specific fertilizers to improve the mineral concentration in the soils, or by using biotechnological tools such as genetic engineering (Zhao and McGrath, 2009). Increasing the food crops levels of Zn and Fe, the most important micronutrients for our diet, is a fundamental cost-effective approach to decrease malnutrition. In recent years, various genetic engineering approaches have been tested to improve the concentrations of Zn and Fe in the receiving crops, from increasing the amount of chelating agents to the expression of specific metal transporters (Sperotto *et al.,* 2012). Suzuki *et al.* (2008) observed, for example, that the introgression of a barley dioxygenase, the *IDS3* (Fe- deficiency specific clone no. 3) gene involved in phytosiderophore biosynthesis, into the rice genome increases the amount of Fe and Zn by 25% and 37% respectively. Other approaches investigated include the overexpression of high-affinity Fe transporters in rice such as *AtIRT1* (Connolly *et al.,* 2002) under the control of the

Cauliflower mosaic virus 35S promoter and *OsIRT1*(Lee *et al.,* 2009), under the control of the maize *ubiquitin* gene promoter. In both cases, greater accumulations of Zn, Fe and other metals were observed, together however with a marked reduction in plant yield. Another approach aimed at the biofortification of rice grains consists in the expression of chelating agents or metal transporters directly in the endosperm using specific promoters. For example, the introgression of the recombinant human lactoferrin (rHLF) (Nandi *et al.,* 2002) and the soyben ferritin (Vasconcelos *et al.,* 2003) under the control of the endosperm-specific glutelin promoter yielded a 2- to 3-fold increase in Fe concentration in rice grains. Zn and Mn contents have been also improved in finger millet seeds by expressing the metal transporter *OsZIP1* driven by the *Bx17* endosperm specific promoter (Ramegowda *et al.,* 2013). The aleurone and the embryo scutellum are the main Fe storage layers in rice, but they can also contain high levels of phytate, an anti-nutrient that reduces the bioavailability of Zn and Fe. Instead of only increasing the endosperm concentration of these micronutrients, an alternative strategy could be to enhance their bioavailability. Drakakaki *et al.* (2005) introduced a phytase from *Aspergillus niger* into rice, since is involved in phytate digestion, driving the expression specifically in the endosperm. The presence of this enzyme, both alone and coupled with soybean ferritin, increased the Fe content in the seeds and also its bioavailability (Drakakaki *et al.,* 2005).

1.1.2 PHYTOREMEDIATION:

In recent decades, anthropic activities have released huge amounts of toxic elements, threatening both ecosystems and human health (Wijnhoven *et al,* 2007). The remediation techniques currently employed, i.e. excavation, soil washing and landfilling, are both very expensive and destructive for the soil structure. An emerging technology aimed at reducing the environment contamination of polluted soils relies on plants and their ability to take up these toxic elements. Plants can be exploited in a wide array of phytoremediation strategies such as:

1. Phytoextraction: plants take up the elements from the soil and translocate them in the aerial organs where they are sequestered into specific organelles (Lampis *et al.,* 2015). The contaminants are then removed from the polluted site by harvesting the plants and subsequently incinerating them.
2. Rhizofiltration: plants are grown in hydroponics and their roots are used to take up and concentrate metals from metal-polluted effluents (Dimitroula *et al.,* 2015).
3. Phytostabilization: the bioavailability of toxic elements is prevented by reducing their migration and mobility along the soil profile (Guo *et al.,* 2014), and therefore lowering the

risk of leaching to groundwater.

4. Phytodegradation: Toxic organic compounds can be directly degraded by plants through internal metabolic processes or by the secretion into the soil of specific enzymes (de Farias *et al.,* 2009). The major goals of this strategy are the reduction of explosives such as TNT (2,4,6-trinitrotoluene) (Hannink *et al.,* 2001) or halocarbon solvents such as TCE (trichloroethylene) (Newman *et al.,* 1997) in contaminated soils.
5. Phytovolatilization: Plants can remove volatile elements from soil such as selenium (Se) (de Souza *et al.,* 2000) and mercury (Hg) (Rugh *et al.,* 1998), releasing them into the atmosphere through the transpiration flow (Marr *et al.,* 2006).
6. Phytostimulation: Plants can stimulate the degradation of toxic organic compounds by enhancing the microbial activity at the rhizosphere; this is accomplished by secreting phyto-stimulators such as acetates, enzymes, carbohydrates and amino acids (Dzantor, 2007).

Phytoremediation is therefore a more sustainable and cost-effective strategy than the invasive physical and chemical approaches currently employed. The main problems of this approach are the long remediation times of the plants considered suitable for this technique, which in turn depend on the physiological limits in the uptake and accumulation of contaminants. The improvement of the plants' uptake and accumulation ability has become a topic of great interest; thus, plant biologists are looking for new biotechnological approaches to produce plants able to storage higher amounts of toxic compounds and completely degrade the toxic forms (Krämer *et al.,* 2007).

1.2 TRANSGENIC POPLAR PLANTS AND PHYTOREMEDIATION:

In recent times, the heavy metal accumulation trait in plants has also been improved through genetic engineering of model species. The production of genetically engineered trees has been appraised as an approach to improve the phytoremediation of contaminated soils (Kärenlampi *et al.,* 2000). The ideal plant should tolerate high levels of accumulated metals, storing them preferably in aerial parts. Furthermore, they should grow rapidly, producing large amounts of biomass for an effective metal accumulation (Kärenlampi *et al.,* 2000). Hyperaccumulator plants are able to accumulate and tolerate high levels of heavy metals in their shoots, but their limited biomass and slow growth rate makes them unsuitable for phytoremediation. High-biomass plants engineered to accumulate and tolerate heavy metals represent an innovative approach to enhance soil decontamination. In a recent work, poplar was engineered to improve Cd phytoremediation by introducing a metal resistance yeast gene (Shim *et al.,* 2013). Poplar is naturally resistant to heavy metals, grows rapidly and

produces great aerial biomass that can effectively accumulate higher metal levels than herbaceous plants. It needs to undergo years of vegetative growth before it can flower, and this obviously prevents any risk of genetic spreading. Moreover, it is not a source of food for animals and develops an extended root system useful for phytostabilization. Shim *et al.* (2013) produced transgenic poplar lines engineered with the yeast vacuolar Cd-transporter ScYCF1, using the non-flowering genotype Bonghwa (Populus alba × P. tremula var. glandulosa) to avoid genetic spreading. The engineered poplar plants tested under greenhouse conditions using a contaminated soil from a mine site in South Korea displayed greater tolerance to Cd and their shoots contained five times more Cd than the wild-type plants (Shim *et al.,* 2013). When these lines were grown in the field on the same soil, their root dry weight was higher than the wild-type and accumulated more Cd, Pb and Zn, whereas no differences were observed at shoot level (Shim *et al.,* 2013). The ability to accumulate high level of metals in the roots and produce a more complex root system in the field suggest that these lines could be used for phytostabilization, without excluding a long-term phytoextraction approach for the phytoremediation of heavy metal-contaminated soils (Shim *et al.,* 2013). Previous investigations (Song *et al.,* 2003) had already revealed a greater tolerance and accumulation of Cd in transgenic *A. thaliana* plants expressing ScYCF1.

Poplar lines overexpressing enzymes involved in glutathione synthesis were investigated by Koprivova *et al.* (2002) as a possible strategy for Cd phytoremediation. The glutathione (GSH) pathway plays an essential role in the detoxification of reactive oxygen species (ROS) and the heavy metal detoxification by chelation, since GSH is the precursor of phytochelatins (PCs), a class of metal-chelating peptides rich in cysteine residues. Hybrid poplars (*Populus tremula* × *P. alba*) were genetically engineered by introducing the *E. coli* γ-glutamylcysteine synthetase (*γ-ECS*) gene. When tested in hydroponics, the root tissues of the transgenic lines displayed higher levels of Cd than the over-expressing glutathione synthetase (GS) lines and wild-type plants (Koprivova *et al.,* 2002). The Cd tolerance observed and its increased accumulation in the aerial tissues of γ-*ECS* overexpressing poplar lines could be ascribed to the induction of genes involved in Cd detoxification mediated by GSH (He *et al.,* 2015).

Poplars have also been engineered for phytoremediation introducing bacterial *merA* (mercuric ion reductase) and *merB* (organomercury lyase) genes to improve soil Hg decontamination through a process of phytovolatilization. *merB* converts methylmercury in ionic mercury Hg(II) which in turn is reduced by *merA* to elemental mercury Hg(0), the gaseous form of Hg. Che *et al.* (2003) introduce *merA* in the Eastern cottonwood (*Populus deltoides*), and observed a 2-4 fold greater production of Hg (0) than the wild-type. Moreover, when grown on Hg-contaminated soil, the

transgenic *merA* plants accumulated more biomass than the controls (Che *et al.,* 2003). Both *merA* and *merB* have been introduced in *Populus deltoids* by Lyyra *et al.* (2008), yielding a significant Hg tolerance and volatilization.

1.3 THE ZINC HOMEOSTASIS IN *Saccharomyces cerevisiae*:

All organisms regulate their intracellular Zn by means of various transporters that can be regulated by a complex homeostatic network. Zn uptake across the *Saccharomyces cerevisiae* plasma membrane is regulated by two transporters: ZRT1 (Zhao and Eide, 1996a) and ZRT2 (Zhao and Eide, 1996b), involved in high- and low-affinity transport respectively (Figure 1). These two transporters belong to the ZIP super family and are up-regulated in Zn limited cells (Zhao and Eide, 1996a, b). The activation of the expression of these two transporters is mediated by the transcriptional factor ZAP1, which is able under low Zn conditions to induce its own expression (Zhao and Eide, 1997).

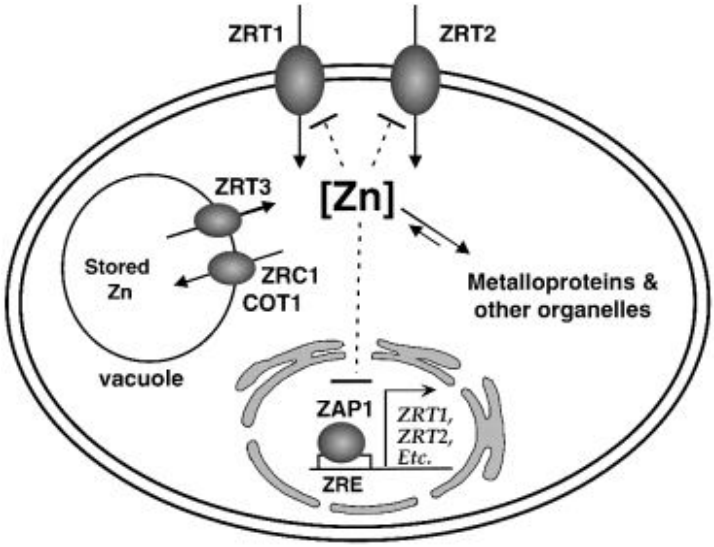

Figure 1: Model of the Zn homeostasis in yeast (MacDiarmid *et al.*, 2000).

In the promoters of ZRT1, ZRT2 and ZAP1, there are cis-acting elements, i.e. 11-bp-long conserved sequences called zinc-responsive elements (ZRE), which are recognized by ZAP1 and regulate the gene expression (Zhao *et al.,* 1998). 5'-ACCYYNAAGGT-3' is one of sequences derived from ZRE elements (MacDiarmid *et al.,* 2000). At tonoplast level, two members of the CDF family of proteins are involved in Zn transport, i.e. COT1 and ZRC1 (Li and Kaplan, 1998). COT1 is a Co (Conklin *et al.,* 1992) and Zn (Conklin *et al.,* 1994) transporter sharing a 78%

similarity with ZRC1 at protein level (Lin *et al.,* 2008). The substitution of asparagine at position 45 with isoleucine improved the ability of COT1 to transport Fe, but reduced that of Co (Lin *et al.,* 2008). ZRC1 is a tonoplast transporter (Miyabe *et al.,* 2001) involved in the sequestration of Zn into the vacuole. ZRC1 also seems to be involved in Ni and Cd transport but not in that of Fe and Mn (MacDiarmid *et al.,* 2002). The ability of ZRC1 to transport Fe and Mn was observed by Lin *et al.* (2008) by substituting asparagine at position 44 with isoleucine, a mutation that nullified its Zn transport ability. The ZRC1 promoter contains the ZRE and is up-regulated by ZAP1 under conditions of Zn deficiency (Miyabe *et al.,* 2001). ZRC1 presents six transmembrane domains (TMs) with three predicted cytoplasm histidine motifs between the IV and V TM (141-HSHSH-145; 163-HSHSH-167; and 216-HDHSH-220) involved in Zn binding (Eide, 1998). MacDiamrmid *et al.* (2000) also revealed the presence of ZRT3, a tonoplast efflux ZIP transporter involved in the remobilization of the Zn stored into the vacuole (Figure 1).

3. AIM OF THE WORK

With regard to environmental pollution, of particular concern is the accumulation of inorganic compounds in the soil that cannot be degraded by any biological or chemical reaction (Meagher, 2000). The raising amount of heavy metals such as Zn, Cd, As, Hg and Pb, elements that are extremely persistent in the soil, is becoming very dangerous for both the environment and human health (Gisbert *et al*., 2003). The use of plants for remediation of polluted soils and waters, referred as phytoremediation, is an environmental-friendly emerging technology that takes advantage of the ability of plants to absorb pollutants and store them in cellular compartments (Pilon-Smits, 2005). Poplar appears to be an excellent candidate for phytoremediation thanks to its high biomass production and rapid growth (Shim *et al.,* 2013). Moreover, poplar is naturally resistant to pollutants and produces an extended root system which widens the surface area involved in metal absorption. Poplar can be easily propagated by cuttings and its long flowering season reduces the possibility of genetic spreading. Finally, it does not enter the food chain, since it is not a source of food for any animal (Shim *et al.,* 2013). In recent years, this plant species has been engineered to increase its ability to tolerate Cd, for example through the improved biosynthesis of chelating agents (Arisi *et al.,* 2000; Koprikova *et al.,* 2002). Tong *et al.* (2004) suggested that the sequestration of pollutants into the vacuole could be a good target to promote the phytoremediation strategy. The introduction of a yeast tonoplast-localized Cd transporter in poplar showed indeed a higher Cd accumulation in the shoots of transgenic lines than in the wild-type controls (Shim *et al.,* 2013). Therefore, this research work focuses on the effect of heterologous yeast genes in *A. thaliana* and poplar plants, analyzing their impact on heavy metal accumulation. We have selected the ZRC1 gene, a Zn/Cd resistance protein found in *Saccharomyces cerevisiae. ScZRC1* is a vacuolar high-affinity Zn transporter belonging to the CDF transporter family primarily involved in the uptake of Zn into the vacuole (MacDiarmid *et al.,* 2003), and, to a lesser extent, Cd and Ni (MacDiarmid *et al.,* 2002). Various transgenic *A. thaliana* and poplar lines with the *ScZRC1* gene driven by a 35S constitutive promoter or by a light inducible one (prbcS) were obtained to mediate the accumulation of this metal in the whole plant or mainly at above-ground level, respectively. The subcellular localization was tested on *A. thaliana* protoplasts to evaluate if this heterologous transporter is functionally expressed in plants, thus confirming its position at tonoplast level. Finally, Zn accumulation was measured on transgenic *A. thaliana* and poplar lines cultivated in hydroponics, revealing higher Zn levels in their shoots as compared to those of their wild-type counterparts

3. MATERIALS AND METHODS

3.1 PLANT MATERIAL AND GROWTH CONDITIONS:

In this study, different plant species were engineered:

- *A. thaliana* ecotype Columbia (Col-0)
- *Populus alba* cv. Villafranca

Arabidopsis was cultured on a MS (Murashige and Skoog, 1962) medium whereas poplar on a WPM medium (Lloyd and McCown, 1981) under 16-h light/8-h dark regime at 22 °C/18 °C (light intensity of 80 to 120 μmol $m^{-2}s^{-1}$). Alternatively, plants were grown in hydrophonic culture or in soil, and kept in greenhouse, under controlled conditions.

3.2 AMPLIFICATION OF *ScZRC1* AND THE PROMOTER OF THE SMALL SUBUNIT OF RUBISCO (prbcS):

The *ScZRC1* gene was amplified from the genomic DNA of *S. cerevisiae* using the primers reported in the Table 3.1 and cloned into the pMD1 vector, under the control of the CaMV35S promoter. In order to induce the expression of ZRC1 in the aerial part of the plant alone, the 35S promoter was substituted with that for the Rubisco small subunit (prbcS), which was amplified from tobacco, thus obtaining a light-inducible cassette. The prbcS promoter was amplified using the HindIII-prbcS-For - XbaI-prbcS-Rev primer starting from *N. tabacum* L. cv. Petit Havana SR1 genomic DNA. All the sequences inserted into the pMD1 vector were checked by sequencing. pMD1-35S::*ScZRC1* and pMD1-prbcS::*ScZRC1* constructs were inserted into *A. tumefaciens* strain EHA105 for the genetic transformation of *A. thaliana* (Zhang *et al.,* 2006) and poplar.

Table 3.1

Gene	Primer Name	Primer Sequence	Tm(°C)	Length(bp)
ZRC1	XbaI-ZRC1-For SacI-ZRC1-Rev	5'-TCTAGAATGATCACCGGTAAAGAATTGA-3' 5'-CTCGAGTTACAGGCAATTGGAAGTATTG-3'	60 60	22 22
prbcS	HindIII-prbcS-For XbaI-prbcS-Rev	5'-AAGCTTAAGCTTGTGGGAACGAGATAA-3' 5'-TCTAGATGTTAATTACACTTAGACAGAAAG-3'	60 60	21 24

3.3 POPLAR TRANSFORMATION:

Leaves of *Populus alba* cv. Villafranca were excised from plantlets cultured *in vitro* and cut into discs that were then dipped into an *Agrobacterium* culture for 8-10 min. After co-cultivation for 2 days in the dark on a WPM medium, they were transferred on the same medium to which however 2 mg/L zeatin, 1 mg/L NAA, 25 mg/L kanamycin, 400 mg/L cefotaxime and 0.8% agar were added, to induce callus formation. The explants with the induced calli were transferred onto a similar medium, but with a reduced NAA content (0.1 mg/L) to induce adventitious buds which were cultured in the WPM rooting medium (0.1 mg /l NAA, 400 mg/L cefotaxime, 25 mg/L kanamycin) as previously described (Fan *et al.,* 2015). The plantlets were subsequently acclimatized at 25°C with a 16 h photoperiod.

3.4 EVALUATION OF TRANSGENIC LINES:

Arabidopsis and poplar transgenic lines were checked by PCR on genomic DNA and by RT-PCR on retro transcribed RNA using specific primers for *A. thaliana* (Table 3.2).

Table 3.2

Gene	Primer Name	Primer Sequence	Tm(°C)	Length(bp)
ZRC1	ZRC1-RT-For ZRC1-RT-Rev	5'-AGCTCCGCCAAGCTGATAAG-3' 5'-TCTGCGAATATCCTCATTAACA-3'	60 60	20 22
Actin	AtACT-RT-For AtACT-RT-Rev	5'-GAACTACGAGCTACCTGATG-3' 5'-CTTCCATTCCGATGAGCGAT-3' 5'-ATCCCAGTTGCTGACAATTC-3' 5'-GACCCGCCATACTGGTGTGAT-3	60 60 60 60	20 20 20 21

3.5 ANALYSIS OF METALS CONTENT:

Accumulation experiments using a hydroponic system were performed on *A. thaliana* and poplar plants using three independent transgenic lines for both the 35S::*ScZRC1* and prbcS::*ScZRC1* constructs. Ten plants for each transgenic *A. thaliana* line were germinated and grown in half-strength Hoagland's solution. After two weeks of acclimatization, the plants were treated for a further two weeks with 0.7 and 20 μM $ZnSO_4$. Four plants for each poplar transgenic line were propagated *in vitro* on WPM medium for two weeks and then transferred to a hydroponic culture on half-strength Hoagland's solution for two more weeks. The plants were treated with 500 μM $ZnSO_4$ for three weeks, changing the solution every week. The shoots and roots of *A. thaliana* plants, and

the apical, basal leaves and roots of poplars were harvested, respectively. The samples were oven-dried at 60°C for 48 h and the dry weight was determined. 200 mg of dried material were digested with 6 mL of Suprapur® quality concentrated (30%) hydrochloric acid and 3 mL of Suprapur® quality concentrated (65%) nitric acid (Merck Chemicals GmbH, Darmstadt, Germany) for 15 min at 25-200°C, 18 min at 200°C and 25 min at 200-35°C using an Ethos 1600 Advanced Microwave Digestion Labstation (Milestone S.r.l., Sorisole, BG, Italy). The samples were diluted to 50 mL with sterile deionized water and analyzed using an Arcos EOP ICP-OES analyzer (Spectro Analytical Instruments GmbH, Kleve, Germany). Calibration standards were prepared using multi-element and single-element standard solutions (Inorganic Ventures Inc. Christiansburg, VA, USA) in 12% hydrochloric and 6% nitric Suprapur® acid (Merck Chemicals) as the samples.

3.7 SUBCELLULAR LOCALIZATION OF *ScZRC1* IN *A. thaliana* PROTOPLASTS:

The coding sequences of *ScZRC1* was fused in frame to the N- terminus of the reporter eGFP by using the primers listed in Table 3.3 and cloned into the pMD1 expression vector under the control of 35S promoter. *A. thaliana* protoplasts were then isolated and transfected with pMD1-p35S::*ScZRC1*::eGFP and pMD1-p35S::eGFP was used as reporter control (Yoo *et al.,* 2007).

Table 3.3

Gene	Primer Name	Primer Sequence	Tm(°C)	Length(bp)
ZRC1	XbaI-ZRC1-For SalI-ZRC1-Rev	5'-TCTAGAATGATCACCGGTAAAGAATTGA-3' 5'-GTCGACCAGGCAATTGGAAGTATTGCA-3'	60 60	22 22
GFP	SalI-GFP-For SacI-GFP-Rev	5'-GTCGACGTGAGCAAGGGCGAGGAGC-3' 5'-GAGCTCTTACTTGTACAGCTCGTCCATG-3'	64 64	19 22

3.8 STATISTICAL ANALYSIS:

Statistical analysis of data was analyzed using the one-way analysis of variance (ANOVA) followed by a post hoc Tukey's test using the GraphPad Prism 7 (GraphPad Software). Statistical significant variations are marked by asterisks (*P<0.05; **P<0.01; ***P<0,001; ****P<0,0001).

4. RESULTS AND DISCUSSION

4.1 AMPLIFICATION of *ScZRC1* AND THE PROMOTER OF THE SMALL SUBUNIT OF RUBISCO:

The coding sequence of *ScZRC1* was amplified from *Saccharomyces cerevisiae* and cloned into two separate expression vectors: 1) under the control of the CaMV35S constitutive promoter and 2) under the control of the ligh-inducible Rubisco promoter (prbcS) isolated from tobacco genome (Figure 4.1). In the latter case, the 1050 bp sequence upstream of the ATG of the rubisco small subunit prbcS (GenBank: X02353.1) was considered and amplified by PCR. A comparison between the sequence of the amplified prbcS promoter and that obtained from the GenBank database (Figure 4.2) revealed three single nucleotide insertions in position -295, -300, -390 bp upstream the start codon, but these mutations are also conserved in the promoter sequence of the Rubisco small subunit of other plant species, such as *Lactuca sativa*. The tobacco prbcS sequence was also analyzed *in silico* using PlantCare (Plant Cis-acting Regulatory Element) to verify the presence of light responsive elements and check whether the identified mutations affect promoter responsive elements and transcription factor binding sites.

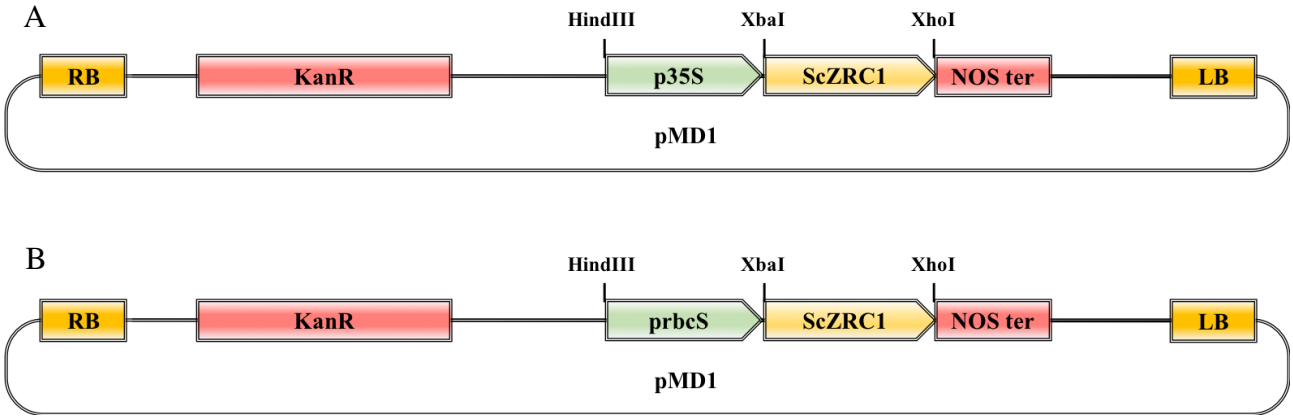

Figure 4.1: Schematic representation of the constructs for the expression in plants of *ScZRC1* in plants driven by A) the constitutive 35S promoter and B) the light inducible promoter of the Rubisco small subunit (prbcS).

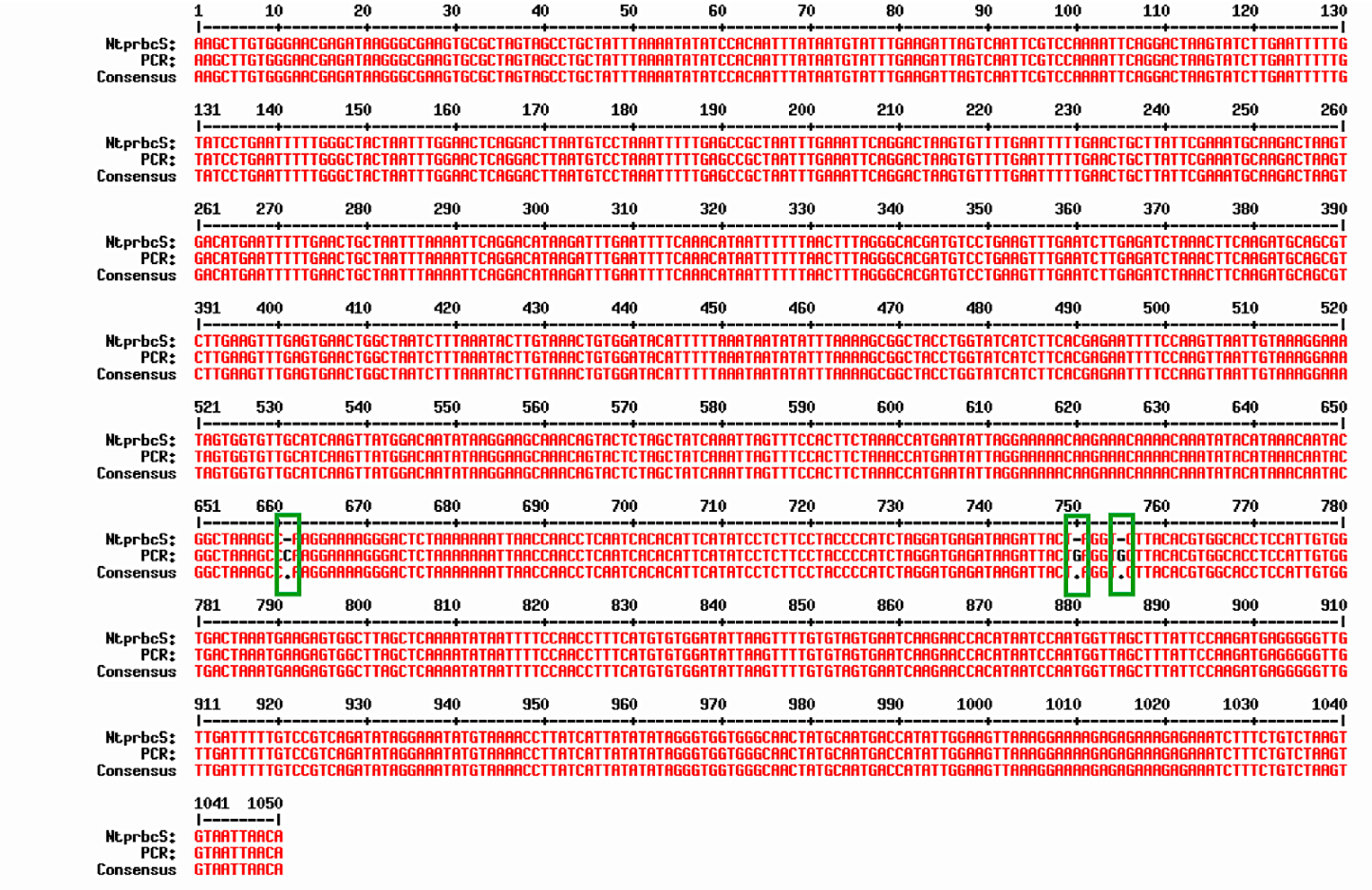

Figure 4.2: Comparison of the promoter of the small subunit of Rubisco (prbcS) obtained from *Nicotiana tabacum* L. cv. Petit Havana SR1 genome and the accession obtained from the literature (GenBank: X02353.1). The single nucleotide insertions are marked by the green boxes. The alignment was performed using MultAlin (http://multalin.toulouse.inra.fr/multalin).

Nucleotidic sequence of the promoter of the small subunit of Rubisco promoter (prbcS)

5′ AAGCTTGTGGGAACGAGATAAGGGCGAAGTGCGCTAGTAGCCTGCTATTTAAAATATATCCACAATTTATAATGTATTTGAAGA
TTAGTCAATTCGTCCAAAATTCAGGACTAAGTATCTTGAATTTTTGTATCCTGAATTTTTGGGCTACTAATTTGGAACTCAGGACTT
AATGTCCTAAATTTTTGAGCCGCTAATTTGAAATTCAGGACTAAGTGTTTTGAATTTTTGAACTGCTTATTCGAAATGCAAGACTAA
GTGACATGAATTTTTGAACTGCTAATTTAAAATTCAGGACATAAGATTTGAATTTTCAAACATAATTTTTTAACTTTAGGGCACGAT
GTCCTGAAGTTTGAATCTTGAGATCTAAACTTCAAGATGCAGCGTCTTGAAGTTTGAGTGAACTGGCTAATCTTTAAATACTTGTAA
ACTGTGGATACATTTTTAAATAATATATTTAAAAGCGGCTACCTGGTATCATCTTCACGAGAATTTTCCAAGTTAATTGTAAAGGAA
ATAGTGGTGTTGCATCAAGTTATGGACAATATAAGGAAGCAAACAGTACTCTAGCTATCAAATTAGTTTCCACTTCTAAACCATGAA
TATTAGGAAAAACAAGAAACAAAACAAATATACATAAACAATACGGCTAAAGCCAAGGAAAAGGGACTCTAAAAAAATTAACCAACC
TCAATCACACATTCATATCCTCTTCCTACCCCATCTAGGATGAGATAAGATTACTAGGTCTTACACGTGGCACCTCCATTGTGGTGA
CTAAATGAAGAGTGGCTTAGCTCAAAATATAATTTTCCAACCTTTCATGTGTGGATATTAAGTTTTGTGTAGTGAATCAAGAACCAC
ATAATCCAATGGTTAGCTTTATTCCAAGATGAGGGGGTTGTTGATTTTTGTCCGTCAGATATAGGAAATATGTAAAACCTTATCATT
ATATATAGGGTGGTGGGCAACTATGCAATGACCATATTGGAAGTTAAAGGAAAAGAGAGAAAGAGAAATCTTTCTGTCTAAGTGTAA
TTAACA-**ATG_3′**

Figure 4.3: Nucleotide sequence of the Rubisco small subunit promoter (prbcS) from the tobacco genome. In green, different cis-acting regulatory elements involved in light responsiveness, in yellow the TATA-box, in red the CAAT-box, in purple the GT-1 element and in light blue the I-box obtained using the PlantCARE database (Lescot *et al.,* 2002).

4.2 SUBCELLULAR LOCALIZATION OF *ScZRC1* IN *A. thaliana* PROTOPLAST:

ZRC1 is a *Saccharomyces cerevisiae* high-affinity Zn transporter localized at tonoplast level, and involved in the storage of excess Zn into the vacuole (Miyabe *et al.,* 2001). To confirm that in the heterologous system *ScZRC1* is also localized at the tonoplast, reporter lines were obtained by fusing the eGFP protein at the C- terminus of ZRC1. The subcellular localization of *ScZRC1*::eGFP protein was thus tested on *Arabidopsis* protoplasts using the PEG-mediated transfection method (Yoo *et al.,* 2007).

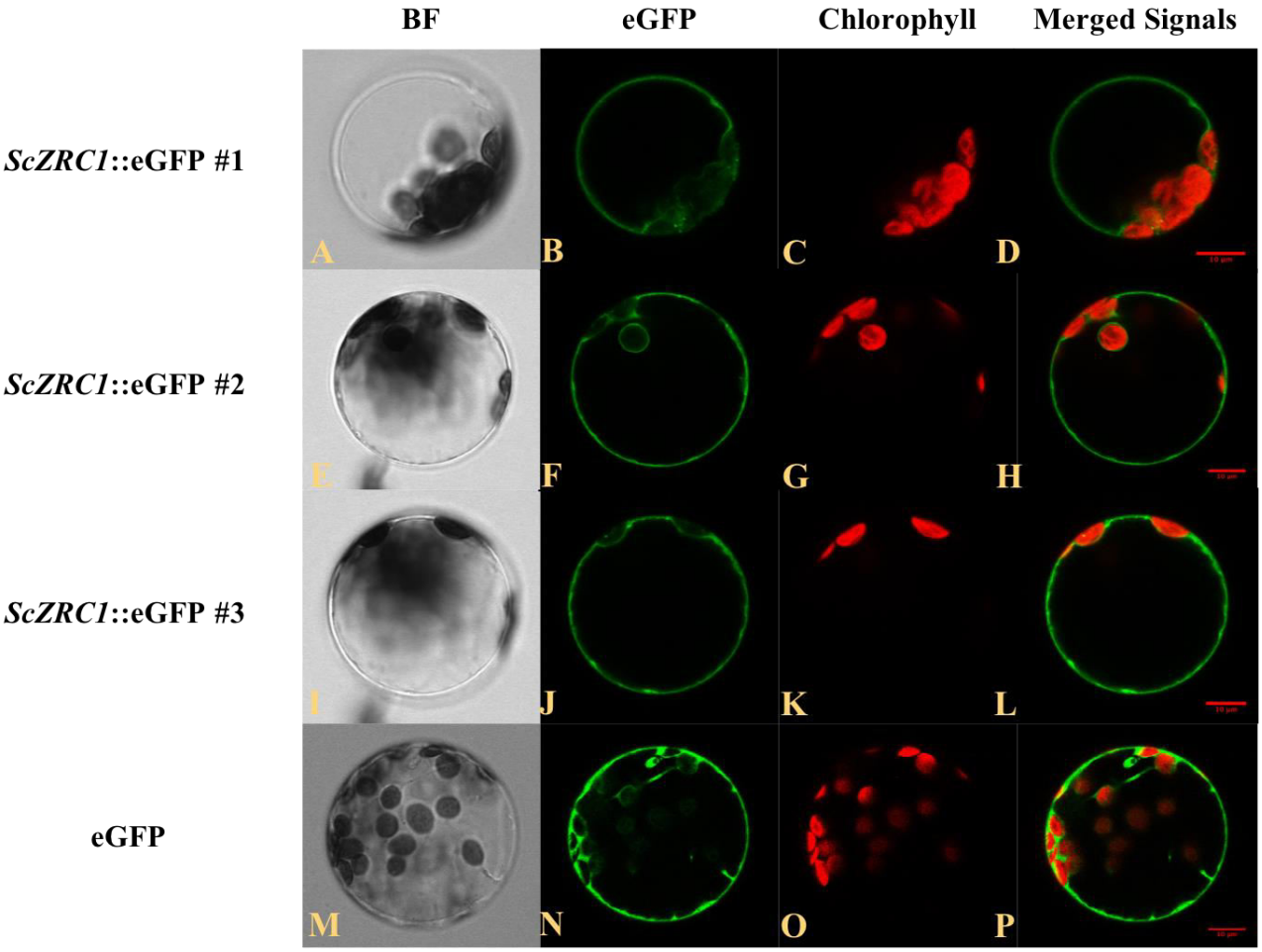

Figure 4.4: Subcellular localization of the *ScZRC1*::eGFP protein transiently expressed in *Arabidopsis* protoplasts. *ScZRC1*::eGFP #1(A-D), *ScZRC1*::eGFP #2 (E-H) and *ScZRC1*::eGFP #3(I-L) are three different protoplasts transfected with *ScZRC1*::eGFP, whereas the eGFP control (M-P) proteins were transiently expressed in *Arabidopsis* protoplasts. The panels show, from left to right: bright-field image, eGFP fluorescence, chlorophyll fluorescence and a combined image of eGFP and chlorophyll fluorescence. Scale bars = 20 µm.

ScZRC1 was positively expressed in the protoplast of *A. thaliana* (Figure 4.4), confirming not only the active protein folding in plants but also its conserved tonoplast localization.

4.3 TRANSGENIC *ScZRC1 A. thaliana* LINES:

The confirmation of the heterologous expression of *ScZRC1* in plant cells prompted us to introduce this gene controlled by the CaMV 35S and prbcS promoters into different plant backgrounds. Various *A. thaliana* p35S::*ScZRC1* and prbcS::*ScZRC1* transgenic lines were obtained, which were checked by PCR and their expression by RT-PCR (Figure 4.5). Moreover, we tested if light induced the transcription of *ScZRC1* in prbcS::*ScZRC1* lines. As shown in Figure 4.5, even though the expression is not high, the *ScZRC1* transcript was only detected in the shoots, and not in the roots.

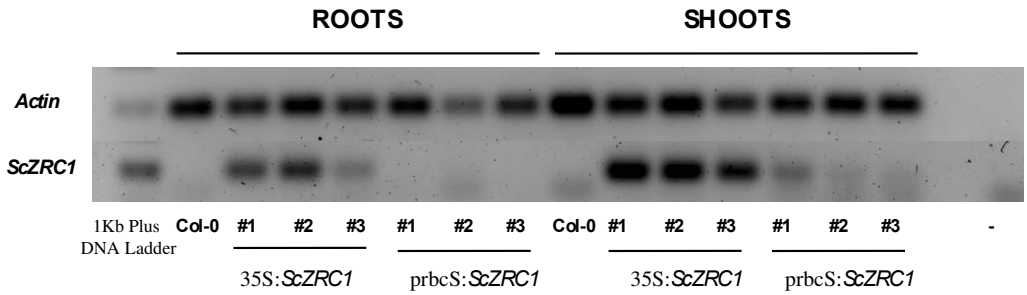

Figure 4.5: RT-PCR was performed on the roots and shoots of three *A. thaliana* transgenic lines for p35S::*ScZRC1* and prbcS::*ScZRC1* to test the expression of *ScZRC1* and the light-inducible activity of the prbcS promoter.

4.4 ACCUMULATION ANALYSIS ON *ScZRC1* TRANSGENIC *A. thaliana* LINES:

In *Saccharomyces cerevisiae, ScZRC1* is involved in Zn detoxification by accumulating it into the vacuole (Miyabe *et al.,* 2001). The aim of this project is to improve the accumulation ability of model plants which could be then used in various phytoremediation strategies for the decontamination of soils and waters polluted by heavy metals. The heterologous expression of *ScZRC1* in *A. thaliana* plants induced an increased Zn accumulation in shoots, when the genes driven by both the 35S constitutive promoter and the light-inducible one (Figure 4.7B). Only the second prbcS::*ScZRC1* line failed to reveal any significant accumulation (Figure 4.7B), despite the fact that the amount of Zn was higher than in the control.

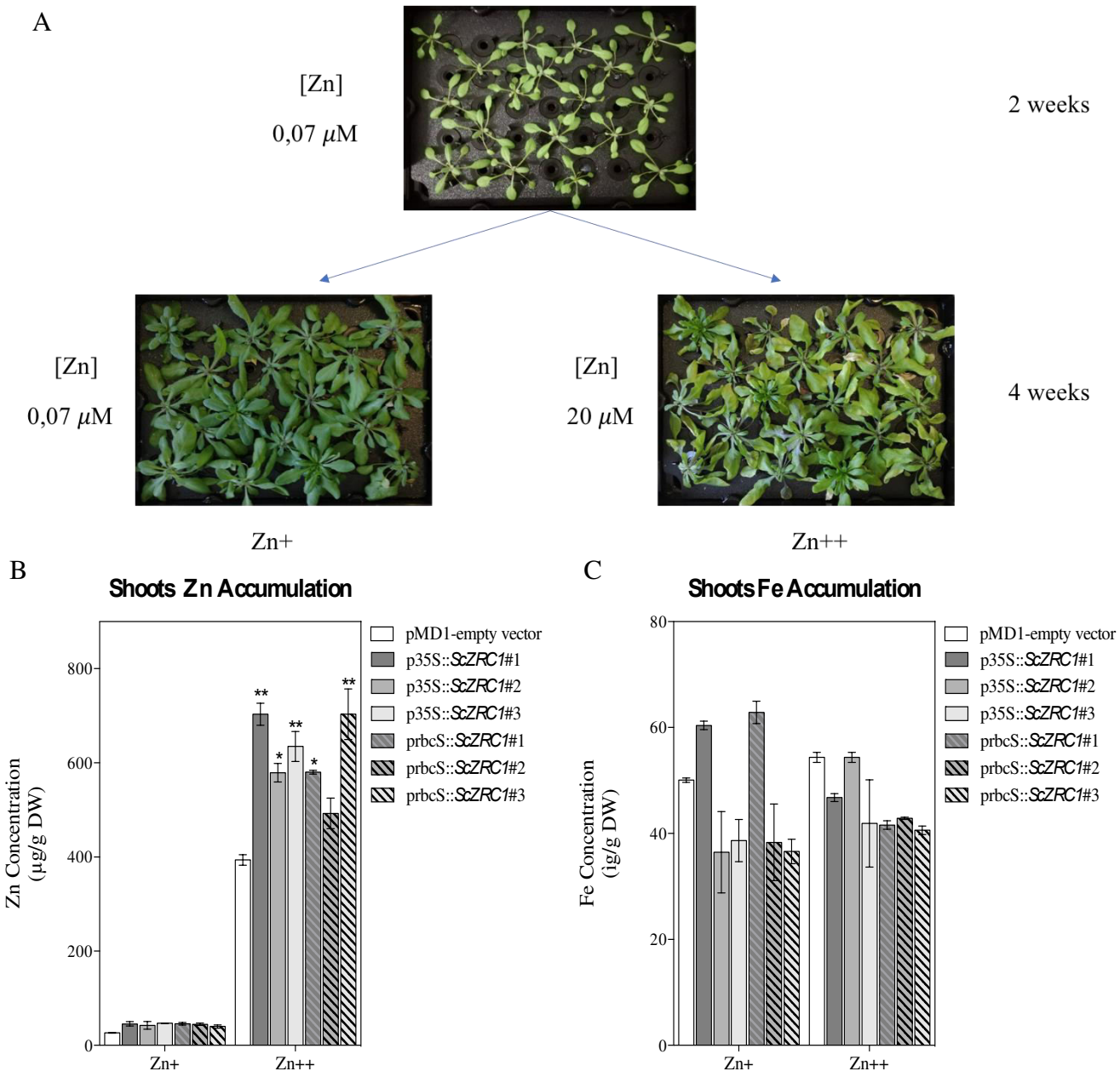

Figure 4.6: ICP-MS analysis on hydroponics-grown *A. thaliana* transgenic lines for p35S::*ScZRC1* and prbcS::*ScZRC1* compared to an empty vector control line at different Zn concentrations. A) Hydroponic system and Zn concentration used for the first two weeks of acclimatization and the following two weeks of Zn treatment whereas B) and C) depict Zn and Fe levels respectively, in the shoots of the transgenic lines tested. Values are means ± SEM (n=3).

The p35S::*ScZRC1* #1 and prbcS::*ScZRC1* #3 lines displayed the peak levels of accumulation which were 0.8 fold greater than the control line carrying the pMD1 empty vector (Figure 4.6B). The amount of Fe detected was lower in almost all p35S::*ScZRC1* and prbcS::*ScZRC1* transgenic lines under excess Zn (Figure 4.6C), a fact that can be presumably ascribed to competition for the transport of these two metals, and furthermore suggests that *ScZRC1* is not involved in Fe transport.

4.5 TRANSGENIC *ScZRC1* POPLAR LINES AND ACCUMULATION ANALYSIS:

Poplar has been suggested as an ideal model for metal accumulation thanks to its natural tolerance to heavy metals and its high biomass production. This plant species can store large amounts of both inorganic elements and organic toxic compounds. Poplar genetic engineering has therefore been proposed as a new approach to improve its ability to remove contaminants from polluted soils. In recent years, it has been genetically modified to increase the production of chelating peptides, introducing for example enzyme such as γ-glutamylcysteine synthetase (*γ-ECS*) and glutathione synthetase (GS), which are involved in the production of glutathione (Koprivova *et al.,* 2002). Hg decontamination was also improved by introducing into the plant's background bacterial proteins that can convert methylmercury into a volatile form, thus increasing Hg volatilization (*merA* and *merB*) (Che *et al.,* 2003; Lyyra *et al.,* 2008). Shim *et al.* (2013) were the first to engineer poplars with a yeast metal transporter located at the vacuole, thus improving the plant's ability to tolerate and accumulate Cd. In this work, *ScZRC1* was introgressed into *Populus alba* cv. Villafranca using the available transformation protocol (Confalonieri *et al.,* 2000), assessing its ability to tolerate high concentrations of Zn (Romeo *et al.,* 2014).

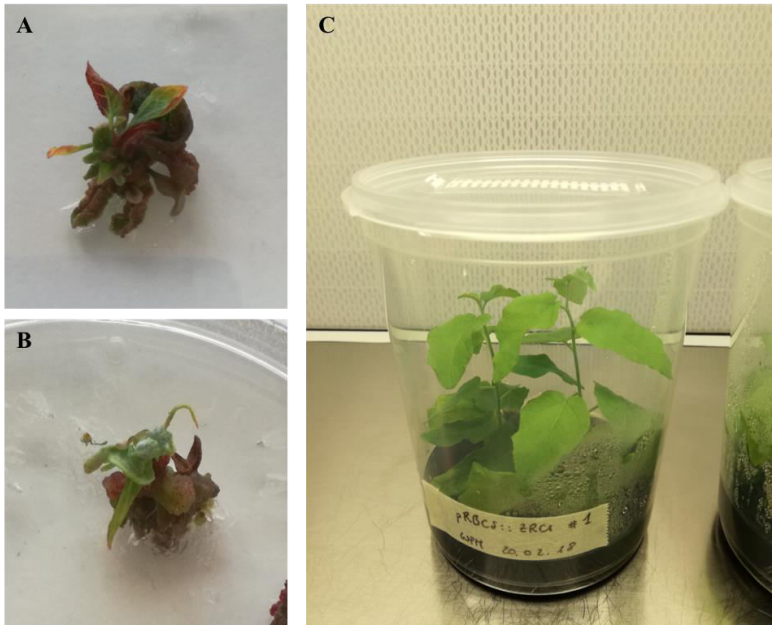

Figure 4.7: *P.alba* cv. Villafranca transformation with *A. tumefaciens* strain EHA 105 carrying the p35S::*ScZRC1* and prbcS::*ScZRC1* genes, starting from leaf explants. A, B) shoot regeneration and C) transgenic poplar plants propagated *in vitro.*

In comparison to other poplar clones such as Baldo (*Populous deltoids*), I-214 (*Populus x euramericana*) and Jean Pourtet (*Populus nigra*), *Populus alba* cv. Villafranca appeared to be the

least susceptible to Zn, displaying the greatest accumulation rate when grown for four weeks in the presence of high concentrations of this metal (Romeo *et al.,* 2014). The I-214 clone produced the largest amount of biomass under high Zn conditions but Villafranca appeared to be the most tolerant, with the least reduction in leaf Chl-a content (Romeo *et al.,* 2014).

A

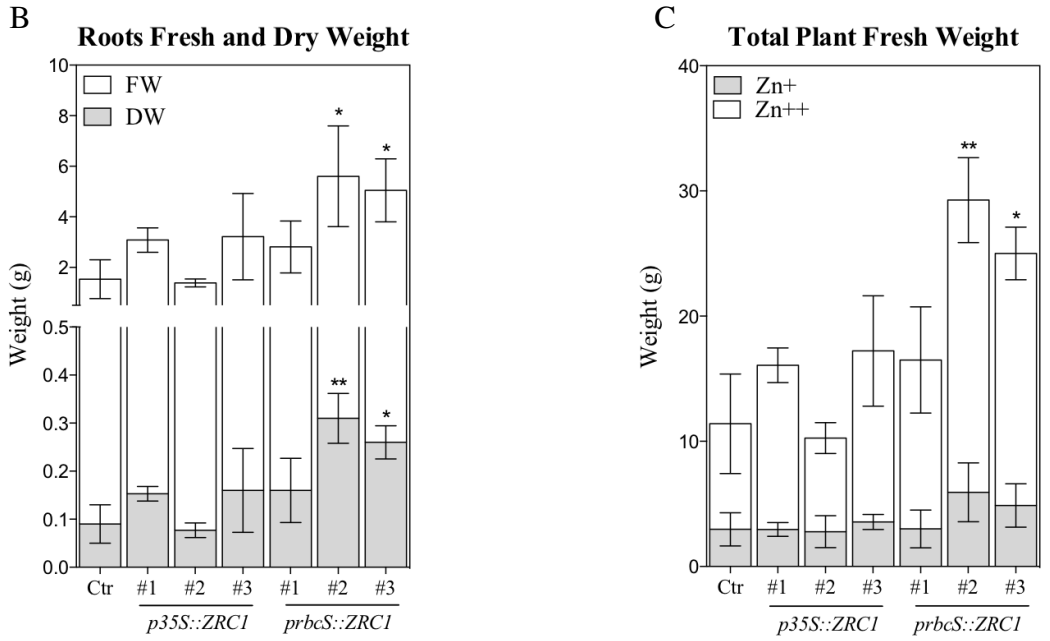

Figure 4.8: Phenotype characterization of hydroponics-grown *P. alba* cv. Villafranca transgenic lines for p35S::*ScZRC1* and prbcS::*ScZRC1*genes and wild-type controls after three weeks of 500 µM $ZnSO_4$ treatment. A) p35S::*ScZRC1*, prbcS::*ScZRC1* and wild-type plants at the end of the experiment, B) Root fresh and dry weight after the Zn treatment and C) Total fresh weight before and at the end of the treatment. Values are mean ± SEM (n=3).

The cultivar Villafranca was obtained by crossing a male parent *P. alba* from Lucca (Tuscany, Italy) with a female parent *P. alba* from Villafranca Piemonte (Piedmont, Italy) and registered for commercial use in Italy in 1989 (Confalonieri *et al.,* 2000). The aim of this project is to improve the accumulation rate of a model species such as poplar for phytoremediation purposes, increasing both its resistance and translocation ability. The prbcS::*ScZRC1* gene has been deliberately designed to enhance the *P. alba* cv. Villafranca translocation factor, which is the lowest among the various clones investigated by Romeo *et al.* (2014). In order to obtain poplar introgression lines we used two different transformation protocols: one starting from internode stem segments, as described by Confalonieri *et al.* (2000) and the other starting from leaf explants, as described by Fan *et al.* (2015). The *Material and Methods* section only describes the latter protocol, because it yielded the highest transformation rate (Figure 4.7). 5 transgenic p35S::*ScZRC1* and 3 prbcS::*ScZRC1* poplar lines were obtained starting from 76 and 73 explants respectively, obtaining a transformation rate of 6,5% and 4,1%. Subsequently, three independent lines for each construct were transferred into a hydroponic system and acclimated for two weeks in half-strength Hoagland's solution. The plants were then treated for three weeks with half strength Hoagland's medium with the addition of 500 µM $ZnSO_4$. After three weeks of Zn treatment, two of the three prbcS::*ScZRC1* lines displayed greater total plant weight and fresh and dry root weight at the root level than the wild-type (Figure 4.8).

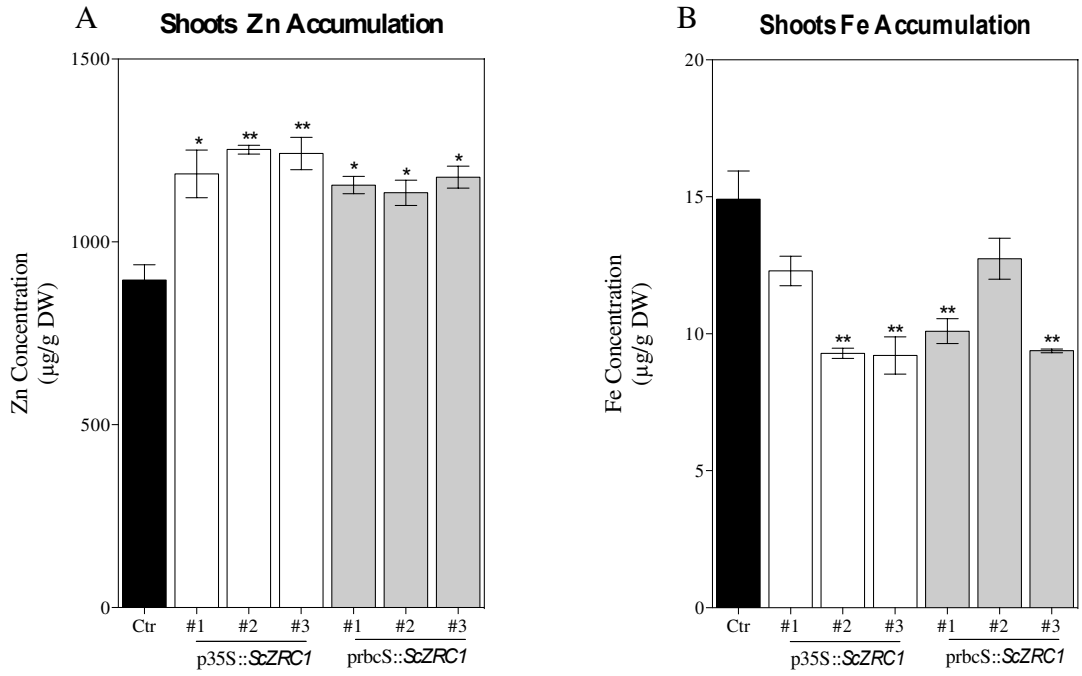

Figure 4.9: ICP-MS analysis on the shoots of hydroponics-grown *P. alba* cv. Villafranca transgenic lines for p35S::*ScZRC1* and prbcS::*ScZRC1* and the wild-type control after three weeks of 500 µM $ZnSO_4$treatment. A) Zn and B) Fe levels, respectively, in the transgenic lines tested. Values are means ± SEM (n=3).

Moreover, all the transgenic lines, regardless of the promoter inserted, contained significantly higher levels of Zn in their shoots than the control (Figure 4.9A). Fe accumulation in the leaves of almost all these lines was lower than in wild-types under conditions of excess Zn (Figure 4.9B). As regards the roots, p35S::*ScZRC1* and prbcS::*ScZRC1* poplar lines did not display significantly higher amounts of Zn than the wild-type; on the contrary, several lines had lower Zn concentrations than the control plants (Figure 4.10), but the difference was not significant. These results suggest that a higher sequestration in the shoots (Figure 4.9) leads to an enhanced translocation factor that does not significantly affect the Zn levels in roots. Moreover, Fe accumulation observed in all the p35S::*ScZRC1* and prbcS::*ScZRC1* roots was lower than the wild-type counterparts, but once again, the difference was not significant (Figure 4.10).

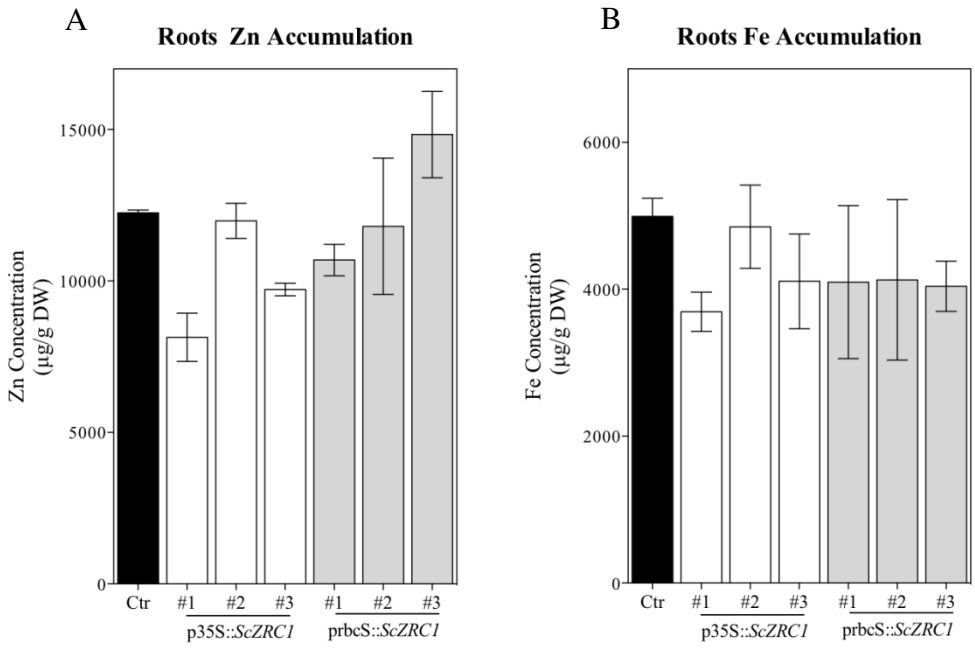

Figure 4.10: ICP-MS analysis on the roots of hydroponics-grown *P. alba* cv. Villafranca transgenic lines for p35S::*ScZRC1* and prbcS::*ScZRC1* and wild-type counterpart after three weeks of 500 µM $ZnSO_4$ treatment. A) Zn and B) Fe levels, respectively, in the transgenic lines tested. Values are means ± SEM (n=3).

The heterologous expression of yeast *ScZRC1* in the poplar background leads to a greater Zn accumulation in shoots (Figure 4.9) of both the p35S::*ScZRC1* and prbcS::*ScZRC1* lines, although no significant results were evident at root level (Figure 4.10). This effect was also observed in the shoots of *A. thaliana ScZRC1* lines (Figure 4.6). Further analyses need to be performed to confirm

these results, increasing the duration of the treatment to evaluate both the accumulation and tolerance rates of these transgenic lines compared to their wild-type. Kamizono *et al.* (1989) isolated this gene from a library of yeast genomic DNA for its ability to confer resistance to both Zn and Cd ions, although the ability of poplar *ScZRC1* lines to tolerate and accumulate this latter heavy metal has not yet been tested.

5. CONCLUSIONS

The transport of contaminants into the vacuole has been suggested as a promising strategy for the genetic engineering of model plant species (Tong *et al.,* 2004). Shim *et al.* (2013) were the first to observe that the heterologous expression of a yeast tonoplast Cd transporter in the poplar background improved the accumulation and sequestration of this heavy metal in the aerial part of the transgenic lines.

We decided to focus on Zn, and with a view to possible applications in soil and water decontamination, we attempted to improve the ability of various plant species to sequester it by means of a heterologous expression of the *S. cerevisiae ScZRC1* gene, a high-affinity Zn tonoplast transporter (Miyabe *et al.,* 2001). At first, we tested if the *ScZRC1* heterologous expression leads to a full protein expression and if the sub-cellular localization was maintained. *ScZRC1*::eGFP reporter construct was analyzed in *A. thaliana* protoplasts, and the results confirmed the *ScZRC1* tonoplast localization in plant cells (Figure 4.4). Therefore, *A. thaliana* was engineered driving the *ScZRC1* expression under the control of either a constitutive CaMV 35S promoter or the light-inducible one of the Rubisco small subunit in tobacco (prbcS; GenBank: X02353.1) (Figure 4.2). The sequence of the prbcS promoter was analyzed in silico using the PlantCARE database (Figure 4.3; Lescot *et al.,* 2002) and the light induction of *ScZRC1* expression was confirmed in prbcS::*ScZRC1 Arabidopsis* lines by the presence of transcripts in the shoots alone, and not in roots (Figure 4.5). In order to test their ability to accumulate Zn, the *ScZRC1 A. thaliana* transgenic lines for both constructs were grown in hydroponics, at standard (0.07 µM) and excess concentrations of Zn (20 µM) for two weeks. All the p35S::*ScZRC1* and prbcS::*ScZRC1* lines, with the exception of prbcS::*ScZRC1*#2, revealed an enhanced Zn accumulation in the shoots, suggesting that *ScZRC1* is functionally active in these plants and could be used to improve species that are more suitable for phytoremediation purposes (Figure 4.6). Among the various poplar clones available, we chose to genetically engineer *P. alba* cv. Villafranca, since it is characterized by a naturally high tolerance to Zn and a marked ability to accumulate metals (Romeo *et al.,* 2014). The plants were transformed using two protocols, starting from the internode tissues (Confalonieri *et al.,* 2000) and leaves (Fan *et al.,* 2015), respectively. Various transgenic poplar p35S::*ScZRC1* and prbcS::*ScZRC1* lines (Figure 4.7) were obtained and their Zn accumulation ability was tested by growing them hydroponically and treating them for three weeks with 500 µM Zn. All the poplar lines revealed an enhanced Zn accumulation in the shoots tissues, and most also a significant reduction in the Fe levels (Figure 4.9), confirming what observed in the *Arabidopsis* plants. By contrast, no differences were observed in the roots of p35S::*ScZRC1* and prbcS::*ScZRC1* poplar lines (Figure 4.10). The absence of

differences in the accumulation of Zn between prbcS::*ScZRC1* and wild-type roots was not surprising, since the expression of *ScZRC1* is only driven in the shoots, but the lack of higher levels of Zn in the roots of p35S::*ScZRC1* lines deserves to be better investigated. A possible explanation is that the overexpression of *ScZRC1* across the entire plant improved the translocation factor from roots to shoots, thus preventing Zn accumulation at root level. Further aspects need to be investigated to understand what heavy metals are transported by *ScZRC1*, since it has been suggested that it may also play a role in the regulation of Cd and Ni (Kamizono *et al.,* 1989; MacDiarmid *et al.,* 2002). The aim of this work was to use biotechnological tools to develop plants that are more suitable for phytoremediation. The transgenic poplar lines obtained show an increased Zn accumulation and tolerance, and can be considered promising candidates for this type of application. However, further analyses are needed to test and validate these lines in pilot experiments.

6. REFERENCES

- Arisi A.C.M., Mocquot B., Lagriffoul A., Mench M., Foyer C. H., Jouanin L. (2000) Responses to cadmium in leaves of transformed poplars overexpressing Γ-glutamylcysteine synthetase. *Physiologia Plantarum*, 109(2): 143-149.
- Brown S.L., Angle J.S., Chaney R.L., Baker A.J.M. (1995) Zinc and Cadmium Uptake by Hyperaccumulator Thlaspi caerulescens Grown in Nutrient Solution. *Soil Science Society of America Journal,* 59(1); 125-133.
- Che D., Meagher R.B., Heaton A.C., Lima A., Rugh C.L. & Merkle S.A. (2003) Expression of mercuric ion reductase in Eastern cottonwood (Populus deltoides) confers mercuric ion reduction and resistance. *Plant Biotechnology Journal* 1(4); 311–319.
- Confalonieri M., Belenghi B., Balestrazzi A., Negri S., Facciotto G., Schenone G., Delledonne M. (2000) Transformation of elite white poplar (*Populus alba* L.) cv. 'Villafranca' and evaluation of herbicide resistance. *Plant Cell Reports*, 19(10): 978-982.
- Confalonieri M., Balestrazzi A., Bisoffi S., Carbonera D. (2003). In vitro culture and genetic engineering of *Populus* spp.: synergy for forest tree improvement. *Plant Cell Tissue and Organ Culture*, 72(2): 109–138.
- Conklin D.S., McMaster J.A., Culbertson M.R., Kung C. (1992) COT1, a gene involved in cobalt accumulation in *Saccharomyces cerevisiae*. *Molecular and Cellular Biology,* 12(9): 3678-3688.
- Conklin D.S., Culbertson M.R., Kung C. (1994) Interactions between gene products involved in divalent cation transport in *Saccharomyces cerevisiae*. *Molecular and General Genetics*, 244(3): 303-311.
- Connolly E.L., Pand F.J., Guerinot M.L. (2002) Expression of the IRT1 Metal Transporter is Controlled by Metals at the Levels of Transcript and Protein Accumulation. *The Plant Cell*, 14(6): 1347–1357.
- Dimitroula H., Syranidou E., Manousaki E., Nikolaidis N.P., Karatzas G.P. & Kalogerakis N. (2015) Mitigation measures for chromium-VI contaminated groundwater – the role of endophytic bacteria in rhizofiltration. *Journal of Hazardous Materials*, 281: 114–120.
- Dix M.E., Klopfenstein N.B., Zhang J.W., Workman S.W., Kim M.S. (1997) Potential use of Populus for phytoremediation of environmental pollution in riparian zones. USDA Forest Service General Technical Report. RM-GTR-297: 206-211.
- Drakakaki G., Marcel S., Glahn R.P., Lund E.K., Pariagh S., Fischer R., Christou P., Stoger E. (2005) Endosperm-specific co-expression of recombinant soybean ferritin and *Aspergillus* phytase in maize results in significant increases in the levels of bioavailable iron. *Plant Molecular Biology,* 59(6): 869-880.
- Dzantor E.K. (2007) Phytoremediation: the state of rhizosphere engineering for accelerated rhizodegradation of xenobiotic contaminants. *Journal of Chemical Technology and Biotechnology*, 82(3): 228- 232.
- Eide, D. J. (1998) The molecular biology of metal ion transport in *Saccharomyces cerevisiae*. *Annual Review of Nutrition,* 18: 441–469.
- Fan M.S., Zhao F.J., Fairweather-Tait S.J., Poulton P.R., Dunham S.J., McGrath S.P. (2008) Evidence of decreasing mineral density in wheat grain over the last 160 years. *Journal of Trace Elements in Medicine and Biology*, 22(4): 315-324.
- Fan D., Liu T., Li C., Jiao B., Li S., Hou Y., Luo K. (2015) Efficient CRISPR/Cas9-mediated Targeted Mutagenesis in *Populus* in the First Generation. *Scientific Reports*, 5:12217.

- de Farias V., Maranho L.T., de Vasconcelos E.C., da Silva Carvalho Filho M.A., Lacerda L.G., Azevedo J.A., Pandey A., Soccol C.R. (2009) Phytodegradation potential of *Erythrina crista-galli* L., Fabaceae, in petroleum-contaminated soil. *Applied Biochemistry and Biotechnology*, 157(1): 10–22.
- Gisbert C., Ros R., De Haro A., Walker D.J., Pilar Bernal M., Serrano R., Navarro-Aviñó J. (2003) A plant genetically modified that accumulates Pb is especially promising for phytoremediation. *Biochemical and biophysical research communications,* 303(2): 440-445.
- Guo P., Wang T., Liu Y., Xia Y., Wang G., Shen Z. & Chen Y. (2014) Phytostabilization potential of evening primrose (*Oenothera glazioviana*) for copper-contaminated sites. *Environmental Science and Pollution Research International*, 21(1): 631–640.
- Hannink N., Rosser S.J., French C.E., Basran A., Murray J.A., Nicklin S., Bruce N.C. (2001) Phytodetoxification of TNT by transgenic plants expressing a bacterial nitroreductase. *Nature Biotechnology,* 19(12): 1168-1172.
- He J., Li H., Ma C., Zhang Y., Polle A., Rennenberg H., ... Luo Z.B. (2015) Overexpression of bacterial γ-glutamylcysteine synthetase mediates changes in cadmium influx, allocation and detoxification in poplar. *New Phytologist*, 205(1); 240–254.
- Jia Z., Li S., Wang L. (2018) Assessment of soil heavy metals for eco-environment and human health in a rapidly urbanization area of the upper Yangtze Basin. *Scientific reports,* 8: 3256.
- Kamizono A., Nishizawa M., Teranishi Y., Murata K., Kimura A. (1989) Identification of a gene conferring resistance to zinc and cadmium ions in the yeast *Saccharomyces cerevisiae*. *Molecular & General Genetics: MGG*, 219(1-2):161-167.
- Kärenlampi S., Schat H., Vangronsveld J., Verkleij J.A., van der Lelie D., Mergeay M., Tervahauta A.I. (2000) Genetic engineering in the improvement of plants for phytoremediation of metal polluted soils. *Environmental Pollution,* 107(2): 225-231.
- Koprivova A., Kopriva S., Jäger D., Will B., Jouanin L. & Rennenberg H. (2002) Evaluation of transgenic poplars over-expressing enzymes of glutathione synthesis for phytoremediation of cadmium. *Plant Biology,* 4(6); 664–670.
- Krämer U., Talke I.N., Hanikenne M. (2007) Transition metal transport. *FEBS Letters*, 581: 2263–2272.
- Lampis S., Santi C., Ciurli A., Andreolli M., Vallini G. (2015) Promotion of arsenic phytoextraction efficiency in the fern *Pteris vittata* by the inoculation of As-resistant bacteria: a soil bioremediation perspective. *Frontiers in Plant Science*, 6; 80.
- Lee S., An G. (2009) Over-expression of *OsIRT1* leads to increased iron and zinc accumulations in rice. *Plant, Cell & Environment,* 32(4): 408-416.
- Lescot M., Déhais P., Thijs G., Marchal K., Moreau Y., Van de Peer Y., Rouzé P., Rombauts S. (2002) PlantCARE, a database of plant cis-acting regulatory elements and a portal to tools for in silico analysis of promoter sequences. *Nucleic Acids Research,* 30(1): 325-327.
- Li L., Kaplan J. (1998) Defects in the yeast high affinity iron transport system result in increased metal sensitivity because of the increased expression of transporters with a broad transition metal specificity. *The Journal of Biological Chemistry,* 273(35): 22181-22187.
- Lin H., Kumánovics A., Nelson J.M., Warner D.E., Ward D.M., Kaplan J. (2008) A single amino acid change in the yeast vacuolar metal transporters ZRC1 and COT1 alters their substrate specificity. *The Journal of Biological Chemistry,* 283(49): 33865-33873.
- Lloyd G., McCown B.H. (1981) Commercially feasible micropropagation of mountain laurel, *Kalmia latifolia*, by use of shoot-tip culture. *Combined Proceedings, International Plant Propagators' Society*, 30: 421–427.
- Lyyra S., Meagher R.B., Kim T., Heaton A., Montello P., Balish R.S. & Merkle S. A. (2007) Coupling two mercury resistance genes in Eastern cottonwood enhances the processing of organomercury. *Plant Biotechnology Journal* 5(2): 254–262.
- MacDiarmid C.W., Gaither L.A., Eide D. (2000) Zinc transporters that regulate vacuolar zinc storage in *Saccharomyces cerevisiae*. *The EMBO Journal,* 19(12): 2845–2855.
- MacDiarmid C.W., Milanick M.A., Eide D.J. (2002) Biochemical properties of vacuolar zinc transport systems of *Saccharomyces cerevisiae*. *The Journal of Biological Chemistry,* 277(42): 39187-39194.

- MacDiarmid C.W., Milanick M.A., Eide D.J. (2003) Induction of the ZRC1 metal tolerance gene in zinc-limited yeast confers resistance to zinc shock. *The Journal of Biological Chemistry,* 278(17): 15065-15072.
- Marr L.C., Booth E.C., Andersen R.G., Widdowson M.A. Novak J.T. (2006) Direct volatilization of naphthalene to the atmosphere at a phytoremediation site. *Environmental Science and Technology*, 40(17): 5560–5566.
- Miyabe S., Izawa S., Inoue Y. (2001) The Zrc1 is involved in zinc transport system between vacuole and cytosol in *Saccharomyces cerevisiae*. *Biochemical and Biophysical Research Communications,* 282(1): 79-83.
- Murashige T., Skoog F. (1962) A revised medium for rapid growth and bio assays with tobacco tissue cultures. *Physiologia Plantarum*, 15: 473–497.
- Nandi S., Suzuki Y.A., Huang J.M., Yalda D., Pham P., Wu L.Y., Bartley G., Huang N., Lönnerdal B. (2002) Expression of human lactoferrin in transgenic rice grains for the application in infant formula. *Plant Science,* 163(4): 713-722.
- Newman L.A., Strand S.E., Choe N., Duffy J., Ekuan G., Ruszaj M., Shurtleff B. B., Wilmoth J., Heilman P., Gordon M.P. (1997) Uptake and Biotransformation of Trichloroethylene by Hybrid Poplars. *Environmental Science & Technology,* 31(4): 1062-1067.
- Pilon-Smits E. (2005) Phytoremediation, *Annual Review of Plant Biology,* 56:15-39.
- Ramegowda Y., Venkategowda R., Jagadish P., Govind G., Hanumanthareddy R.R., Makarla U., Guligowda S.A. (2013) Expression of a rice Zn transporter, *OsZIP1*, increases Zn concentration in tobacco and finger millet transgenic plants. *Plant Biotechnology Reports*, 7(3): 309-319.
- Romeo S., Francini A., Ariani A., Sebastiani L. (2014) Phytoremediation of Zn: Identify the Diverging Resistance, Uptake and Biomass Production Behaviours of Poplar Clones Under High Zinc Stress. *Water, Air, & Soil Pollution*, 225: 1813.
- Rugh C.L., Senecoff J.F., Meagher R.B., Merkle S.A. (1998) Development of transgenic yellow poplar for mercury phytoremediation. *Nature Biotechnology,* 16(10): 925-928.
- Shim D., Kim S., Choi Y.I., Song W.Y., Park J., Youk E.S., Jeong S.C., Martinoia E., Noh E.W., Lee Y. (2013) Transgenic poplar trees expressing yeast cadmium factor 1 exhibit the characteristics necessary for the phytoremediation of mine tailing soil. *Chemosphere,* 90(4), 1478-1486.
- Song W.Y., Sohn E.J., Martinoia E., Lee Y.J., Yang Y.Y., Jasinski M., Forestier C., Hwang I., Lee Y. (2003) Engineering tolerance and accumulation of lead and cadmium in transgenic plants. *Nature Biotechnology,* 21(8): 914-919.
- de Souza M.P., Pilon-Smits E.A.H., Terry N. (2000) The physiology and biochemistry of selenium volatilization by plants. In: Raskin I, Ensley BD, editors., eds Phytoremediation of toxic metals: using plants to clean-up the environment. New York: John Wiley and Sons, 171–190.
- Sperotto R.A., Ricachenevsky F.K., Waldow Vde A., Fett J.P. (2012) Iron biofortification in rice: it's a long way to the top. *Plant Science,* 190: 24-39.
- Suzuki M., Morikawa K., Nakanishi H., Takahashi M., Saigusa M., Mori S., Nishizawa N.K. (2008) Transgenic rice lines that include barley genes have increased tolerance to low iron availability in a calcareous paddy soil. *Soil Science and Plant Nutrition,* 54(1): 77–85.
- Tong Y.P., Kneer R., Zhu Y.G. (2004) Vacuolar compartmentalization: a second- generation approach to engineering plants for phytoremediation. Trends in Plant Science, 9(1): 7–9.
- Vasconcelos M., Datta K., Oliva N., Khalekuzzaman M., Torrizo L., Krishnan S., Oliveira M., Goto F., Datta S.K. (2003) Enhanced iron and zinc accumulation in transgenic rice with the ferritin gene. *Plant science,* 164(3): 371-378.
- White P.J., Broadley M.R. (2005) Biofortifying crops with essential mineral elements. *Trends in Plant Science,* 10(12): 586-593.
- Wijnhoven S., Leuven R.S., van der Velde G., Jungheim G., Koelemij E.I., de Vries F.T., Eijsackers H.J., Smits A.J. (2007) Heavy-metal concentrations in small mammals from a diffusely polluted floodplain: importance of species-and location-specific characteristics. *Archives of Environtal Contamination and Toxicology*, 52(4): 603–613.

- Zhao F.J., McGrath S.P. (2009) Biofortification and phytoremediation. *Current Opinion in Plant Biology,* 12(3): 373-380.
- Zhao H., Eide D. (1996a) The yeast ZRT1 gene encodes the zinc transporter protein of a high-affinity uptake system induced by zinc limitation. *Proceedings of the National Academy of Sciences of the United States of America*, 93(6): 2454-2458.
- Zhao H., Eide D. (1996b) The ZRT2 Gene Encodes the Low Affinity Zinc Transporter in *Saccharomyces cerevisiae*. *The Journal of Biological Chemistry*, 271(38): 23203-23210.
- Zhao H., Eide D.J. (1997) Zap1p, a metalloregulatory protein involved in zinc-responsive transcriptional regulation in Saccharomyces cerevisiae. *Molecular and Cellular Biology*, 17(9); 5044-5052.
- Zhao H., Butler E., Rodgers J., Spizzo T., Duesterhoeft S., Eide D. (1998) Regulation of zinc homeostasis in yeast by binding of the ZAP1 transcriptional activator to zinc-responsive promoter elements. *The Journal of Biological Chemistry*, 273(44); 28713-28720.
- Zhang X., Henriques R., Lin S.S., Niu Q.W., Chua N.H. (2006) *Agrobacterium*-mediated transformation of Arabidopsis thaliana using the floral dip method. *Nature Protocols*, 1(2): 641-646.

AKNOWLEDGEMENTS:

I would like to thank my supervisor, Prof. Antonella Furini, and my lab colleagues, Dr. Giovanni dal Corso, Dr. Elisa Fasani and Dr. Anna Manara for the precious help, the advices about my projects and the support that they gave me during these PhD years.

I thank Prof. David Salt for taking me in his lab and for the help with the Ionomic analysis during the internationalization project. Thanks to Dr. Sina Fischer for the ionomic experimental design, Dr. Paulina Flis for the ICP-MS experiments and Dr. Priya Ramakrishna for the support with the confocal microscope. It has been a very educational work and life experience.
(Insitute of Plant Sciences, University of Nottingham, Sutton Bonington, Nottingham, LE12 5RD, UK)

Thanks to Dr. Katarina Vogel Mikuš for teaching me how to do cryo-sectioning on roots and to Dr. Alessandra Gianoncelli for the help with the TwinMic X-ray microscopy.
(Department of Biology, University of Ljubljana, Večna pot 111, 1000, Ljubljana, Slovenia)
(ELETTRA Sincrotrone di Trieste, Bassovizza, Strada Statale 14, 34149, Trieste, Italy)

Thank to Prof. Giuseppina Falasca and Dr. Edoardo Santucci for the root cross sections of the GUS staining.
(Dipartimento di Biologia Ambientale, Sapienza Università di Roma, Piazzale Aldo Moro 5, Roma, Italy)

I'd like to thank Simone, Gianluca and Alessandro for the moral support, the paints and the jokes that got me over all the difficulties.

I thank Valentina, Mattia, Riccardo, Giorgia, Erica, Fede, Erika, Massimiliano, Davide, Fra, Fedy, Leo, Mezz, Ruggio and all my friends of the University for the advices, the laughter and the adventures that always make me smile.

Thanks to Silvio, Maddy, Luca, Marti, Ciosky, Led, Monica, Ester, Leo, Sara, Vale, Vingé, Grisa, Anna e Fina for being very supportive in every difficulty and always being there for me.

Finally, special thanks to my parents and my family for their patience and for guiding me.

Flavio Martini